Membrane Distillation for Water Recovery from Pretreated High-Strength Brewery Wastewater

Nawrin Anwar

A Thesis

In the Department

Of

Building, Civil, and Environmental Engineering

Presented in Partial Fulfillment of the Requirements

For the Degree of

Doctor of Philosophy (Civil Engineering) at

Concordia University

Montreal, Québec, Canada

July 2021

CONCORDIA UNIVERSITY
SCHOOL OF GRADUATE STUDIES

This is to certify that the thesis prepared

By: Nawrin Anwar

Entitled: Membrane distillation for water recovery from pretreated high-strength brewery wastewater

and submitted in partial fulfillment of the requirements for the degree of

Doctor of Philosophy (Civil Engineering)

complies with the regulations of the University and meets the accepted standards with respect to originality and quality
Signed by the final examining committee:

_____ Chair
Dr. Tiberiu Popa

_____ External Examiner
Dr. Richard G. Zytner

_____ External to Program
Dr. Christian Moreau

_____ Examiner
Dr. Zhi Chen

_____ Examiner
Dr. Chunjiang An

_____ Thesis Supervisor
Dr. Catherine Mulligan

_____ Thesis Co-Supervisor
Dr. Saifur Rahaman

Approved by _____
Dr. Mazdak Nik-Bakht, Graduate Program Director

9/10/2021
` _____
Dr. Mourad Debbabi, Dean
Gina Cody School of Engineering and Computer Science

Abstract

Membrane Distillation for Water Recovery from Pretreated High-Strength Brewery Wastewater

Nawrin Anwar, Ph.D.
Concordia University, 2021

Membrane-based processes are consistently gaining popularity to provide a dependable supply of reusable water from wastewater streams, while simultaneously combatting the water shortage issues and reducing the wastewater load to the environment due to the rising cost of intake water and water shortages experienced around the world. Beer is one of the top five beverages consumed in the world, and brewing industries have high economic value. However, beer production generates a high quantity of wastewater (~3 to 10 L wastewater per 1 L of beer production) containing sugars, ethanol, soluble starch, total suspended solids, volatile fatty acids, and a low concentration of heavy metals. The breweries dispose of 70% of their consumed water to the environment or to the municipal sewage system with or without any treatment. Increasing restrictive environmental regulations and enormous wastewater surcharges related to water consumption and wastewater discharges in the brewery industries have led to the investigation of emerging technologies and their integration with conventional processes for water recovery. The implementation of membrane bioreactor (MBR) technologies has achieved a substantial amount of organic removal for brewery wastewater, as well as showcasing the potential to recover energy through biogas production. The primary goal of this research is to identify suitable membrane-based processes for water reclamation from MBR treated brewery wastewater and to identify the challenges for its implementation. To attain this objective, (i) performance assessment of different effective membrane-based processes for water reclamation were carried out. Here, both the pressure-driven methods (reverse osmosis, RO and nanofiltration, NF), as well as the emerging thermally driven methods (membrane distillation, MD), were explored. Significantly higher water recovery (~ 86%) was obtained with the MD, compared to NF (~16%) and RO (~12%) with a relatively lower water flux drop (~53%) for MD compared to substantial flux drop (~98%) for NF and RO. The physicochemical characterization of the fouled membranes revealed biofouling along with organic and inorganic fouling for both NF and RO membranes whereas the MD membrane was fouled primarily by organic and inorganic species, with no noticeable biofouling. Further

research concerning the effect of operating conditions on membrane fouling was carried out to select optimal condition for water reclamation application. The study identified a 0.45 μm PVDF membrane with 55°C hot feed temperature and 10 gCOD/L/d feed load to MBR to be the optimal condition for stable DCMD implementation for water reclamation with low flux drop and moderate recovery with minimal membrane fouling and excellent contaminant rejection. A techno-economic analysis was conducted to provide a basic understanding regarding the energy and cost associated with membrane distillation process implementation on a larger scale. The study observed a \$2.34/m^3 water price for a 100 m^3/day stand-alone DCMD system. Results suggested that the source of energy is a key parameter for optimizing cost in DCMD application, and waste heat incorporation could lead towards a viable, and cost-effective DCMD application. The understanding of water reclamation performance, membrane fouling tendencies, contaminant rejection, optimal operating conditions, and economic perspective of membrane distillation research will provide insight towards sustainable water recovery in brewery industries leading towards the reduction of the water footprint in beer production and a better understanding of the feasibility of adopting membrane distillation for brewery industries.

This research recommends membrane distillation as an efficient and cost-effective method for water reclamation from membrane bioreactor treated brewery wastewater effluent and enhances the knowledge around the optimal conditions for its water recovery application. The study contributes to the application viability of membrane distillation for water reclamation and advances the knowledge on ideal conditions for membrane performance including high recovery, low flux drop, minimal fouling, high rejection, and membrane reuse along with utilizing alternate energy sources to fulfill the energy requirement of the hot feed. This can further expand to the pilot scale and eventually real scale application of membrane distillation for water reclamation from pre-treated brewery wastewater enhancing the future fresh water supply.

Keyword: Membrane distillation; Water reclamation; Fouling; Contaminant rejection; Membrane recovery; Water Price.

Acknowledgements

I would like to gratefully acknowledge the financial support of Alexander Graham Bell Canada Graduate Scholarship (CGSD) from the Natural Sciences and Engineering Research Council of Canada (NSERC) as well as that of the Fonds de Recherche du Québec-Nature et technologies (FRQNT) for providing me with the opportunity and privilege to pursue my doctoral studies. I would also like to show my sincere gratitude to Concordia University for accepting me as their community member and allowing me to nurture my knowledge, to learn and to grow.

My sincere appreciation and deep gratitude go to my Ph.D. supervisor Dr. Catherine Mulligan for her profound insight, and valuable advice. I would also like to thank Dr. Saifur Rahaman for his constant motivation throughout my graduate studies. I have learnt from their dedication, work ethics, constructive criticism, and valuable advice. I would also take this opportunity to thank my master's supervisor Dr. Clare Robinson who will always have a positive and profound impact in my life. I am sincerely grateful the members of my examination committee, Dr. Richard G. Zytner, Dr. Christian Moreau, Dr. Zhi Chen, and Dr. Chunjiang An. Also, I am thankful to the graduate program director, Dr. Michelle Nokken for all her support. I will always try to embrace all the good virtues that I have learnt from all my professors and apply them in my future life.

I would also like to thank all my Concordia friends and official for making this journey a memorable one. Special thanks to Hong Guan for her continuous support during all the difficulties faced in the lab. I would also like to thank all my research group members who supported me all through my journey. My warm gratitude goes to all my family and friends here in North America, in Bangladesh, and all around the globe for morally supporting and encouraging me during my difficult times.

I am forever grateful to my family members, especially my parents and my husband for believing in me and always being there for me to accomplish this endeavor. I am eternally grateful for my daughter Inaya whose presence makes me work hard and strive to be a better person every day and to pursue my dreams.

Dedication

To her I dedicate: *My daughter "INAYA"*

Co-Authorship Statement

Chapter 2 Fouling and wetting in membrane distillation driven wastewater reclamation process – A review
This chapter is a published article in Advances in Colloids and Interface Science

Author(s): Mahbuboor R. Choudhury[1a], Nawrin Anwar[1a], David Jassby[2], Md. Saifur Rahaman[1,*]
1 Department of Building Civil and Environmental Engineering, Concordia University, Montreal, Quebec, H3G 1M8, Canada
2 Department of Civil and Environmental Engineering, University of California Los Angeles, Los Angeles, California, 90095-1593, United States
[a] Co first-author
** The corresponding author*

Nawrin Anwar and Mahbuboor R. Choudhury contributed equally to writing the manuscript. David Jassby and Md. Saifur Rahaman provided valuable inputs in the manuscript outline and reviewed the article.

Chapter 3 Membrane desalination processes for water recovery from pre-treated brewery wastewater: Performance and fouling
This chapter is a published article in Separation and Purification Technology

Author(s): Nawrin Anwar[1], Md. Saifur Rahaman[1,*]
1 Department of Building Civil and Environmental Engineering, Concordia University, Montreal, Quebec, Canada H3G 1M8,
** The corresponding author*

Nawrin Anwar conducted laboratory investigation, data analysis, and wrote the original draft. Md. Saifur Rahaman supervised the research and reviewed the article.

Chapter 4 Direct contact membrane distillation (DCMD) application for water recovery from pre-treated high strength brewery wastewater: A parametric study (Manuscript ready to submit)

Nawrin Anwar conducted all the laboratory experiments, data analysis, membrane characterization, and wrote the original draft. Mahbuboor R. Choudhury and Md. Saifur Rahaman supervised the research. Catherin Mulligan and Mahbuboor R. Choudhury reviewed the article

Chapter 5 Techno-economic evaluation of DCMD for water recovery from pre-treated brewery wastewater effluent (Manuscript ready to submit)

Nawrin Anwar conceptualized, investigated, analyzed data, and wrote the original draft. Khaled Touati and Md. Saifur Rahaman supervised the research. Catherine Mulligan and Khaled Touati reviewed the article.

Table of Contents

List of Figures

List of Tables

Chapter 1: Introduction

1.1 Problem Statement

Water recovery through membrane-based processes can offer effective means to address the water shortage issues as well as to reduce the volume of wastewater discharge to the environment. Membrane-based processes are consistently gaining popularity for the reclamation of wastewater streams and provide a dependable supply of reusable water [1–7]. Current membrane-based processes used for water recovery are categorized as pressure-driven, such as nanofiltration (NF) or reverse osmosis (RO) and thermal-driven membrane distillation (MD) [1,2,11,3–10]. Membrane Distillation (MD) has gained attention recently as a promising technology to supply freshwater for reuse. MD is a thermally driven process which allows water vapor to pass through a membrane and unlike reverse osmosis (RO) is not pressure driven [12]. MD has larger membrane pore sizes as compared to other membrane separation processes (e.g., RO) [12]. Therefore, MD shows less fouling compared to RO and can theoretically achieve 100% rejection of ions and macromolecules [12,13]. MD operates at much lower temperatures compared to other thermal processes and potentially can use low-grade waste heat and solar or geothermal energy as an energy source [12,14]. For MD, long-term stable permeate flux and salt rejection are significant from the perspective of industrial implementation. However, one of the significant limitations that hinders the widespread application of membrane-based processes is membrane fouling. MD and RO have often been discussed and compared for their desalination applications. However, for the comparison between thermal and pressure-based membrane performances, most literature conducted studies using saline water and synthetic wastewater. RO has demonstrated to be energy efficient compared to MD as the thermal energy requirement of MD is considerably high. On the contrary, MD has proven to be superior in fouling resistance, thus effectively treating highly concentrated wastewater [15–17]. Another challenge in membrane distillation application is membrane wetting which degrades the permeate quality and eventually results in process failure. Hence, in addition to the water recovery performance (both in terms of quality and quantity of reclaimed water), it is also essential to assess the membrane fouling. The pressure requirement of NF is lower than RO, and the NF application may be adequate for wastewater reclamation.

Beer, which is among the top five-beverage category by world market share, is one of the most consumed beverages in the world [18]. The brewing industry has a high economic value (estimated at approximately 593 billion USD in 2017), and the global beer market has a growth projection with a compound annual growth rate of 1.8% between 2019 and 2025 [19]. In Canada, beer is the most popular alcoholic beverage product constituting about 41.5% of total alcohol sales through the liquor boards and other retail outlets. Nearly 85% of the beer sales in 2016 originated from local breweries [20]. Between 2013 and 2018, the number of breweries in Canada increased by 162% (from 380 breweries in 2013 to 995 breweries in 2018) [21]. The beer economy contributed about 13.6 billion CAD to Canada's gross domestic product in 2016 and has generated jobs and economic activities across other sectors as well [21]. However, the production of beer results in discharging high quantity of wastewater (~3 to 10 L wastewater for 1 L of beer production) containing sugars, ethanol, soluble starch, total suspended solids, volatile fatty acids, and a low concentration of heavy metals [22–25]. Discharge of brewery wastewater effluent requires adequate treatment to comply with the regulations along with protecting the environment, aquatic life, and human health. In California, restrictive water consumption as well as high water intake price, and strict wastewater discharge guidelines and high disposal surcharges for breweries have led the brewers to reduce their production capacity, thus reducing their market coverage. Thus, brewers look for alternative options for water intake as well as wastewater discharge by spending millions of dollars for emerging technologies [26]. Along with enhanced financial incentives of intake water and wastewater disposal, the brewers are inclining towards locating sustainable solutions within the industry for the generation of reusable water from the wastewater effluent for production or non-production purposes. The reclaimed water can be used for the primary beer production process water, for the water used in the packaging process, or as cooling water for utilities and cleaning water for the brewery industry. However, to utilize the reclaimed water for human consumption, the water quality needs to be adequate. Thus, proper disinfection and mineralization of reclaimed water needs to be ensured prior to its consumption.

Integration of MD with other separation processes (e.g., ultrafiltration (UF)) [27] proper pre-treatment technologies, prior to the application of membrane distillation for removal of contaminants, can have significant effects on the applicability of MD for treatment of high strength wastewater. Previous studies have explored the potential of water reclamation of membrane

bioreactor treated wastewater effluents through MD, NF, and RO for different types of wastewater, including synthetic water, municipal wastewater, sewage treatment, etc., for various potable and non-potable reuse applications [1,2,5–7,28–31]. The incorporation of membrane-based processes with membrane bioreactor treatment for brewery wastewater has the potential to recover water for reuse within the brewery industries. The primary concern regarding the application of membrane-based processes is membrane fouling, which hinders membrane performances by reducing the permeate flux. Moreover, membrane fouling is a complex phenomenon. The operating conditions of the membrane-based processes, e.g., feed temperature, membrane material, membrane pore sizes, feed pressure, as well as feed loading, may pose a significant influence on the membrane performance in terms of flux and membrane fouling. However, it is difficult to predict the exact effects of membrane fouling and membrane performance with varying operating conditions and different feed characteristics. Thus, before process implementation, it is inevitable to assess the impact of operating conditions to evaluate the optimal conditions better as well as to avoid process failure. A better understanding of the interactions between water quality, operating conditions, and membrane performance can make water recovery sustainable and reduce the water footprint in beer production. For brewery wastewater treated by MBR, the effluent contains a combination of different contaminants (organic and inorganic). The interactions between these various constituents and the membranes may lead to multidimensional fouling with varying loading rates. This variation in fouling provides an impetus for conducting investigations for the reclamation of pre-treated brewery wastewater under varying operating conditions, which, in turn, will help in the effective implementation of the membrane-based technology. Finally, evaluation of the techno-economic viability of the process is necessary to facilitate the transition to widespread industrial application. The detail investigation of membrane-based processes for MBR treated effluent based on this study will lead to process implementation for water reclamation from brewery industries aiding the global freshwater crisis as well as reducing the wastewater load to the environment.

1.2 Research Objective

The water reclamation processes are continuously gaining attention due to stringent wastewater disposal regulations along with the rising cost of the intake water. The breweries dispose ~70% of their intake water [32]. The limiting environmental guidelines related to wastewater disposal as

well as high cost associated with the brewery wastewater consumption and discharge has motivated study of emerging technologies and their integration with conventional processes for brewery wastewater reclamation and reuse.

The global shortage of water is increasing with time and the brewery wastewater recovery and reuse is inevitable [22]. The understanding of the fouling phenomena is crucial for any membrane-based processes, along with their performance for development and implementation of successful membrane technologies. The fouling investigation of the membrane processes provides valuable insight regarding process selection. Furthermore, it can guide potential future research regarding fouling reduction and assist the implementation of industrial applications. Despite numerous studies on fouling mechanisms of membrane processes, further research is critical as it is difficult to predict fouling mechanism for specific process as well as for specific feed water characteristics.

The primary objective of this research is to verify MD as an efficient membrane-based process for water reclamation from brewery wastewater treated by a membrane bioreactor by comparing performances and challenges associated with different treatment scenario. Moreover, a detailed investigation of membrane fouling is crucial to understand the optimal membrane process, which will be included in this research. Finally, a techno-economic analysis will be included. The implementation of membrane distillation processes investigated in this research could provide an effective means for water recovery from pretreated brewery wastewater for reuse in industrial applications, aiding in the mitigation of the global freshwater crisis. A direct contact membrane distillation was implemented for this research. DCMD can employ recovered heat most efficiently though it showed less energy efficiency compared to other configurations in some research. Some researchers observed DCMD to be the most cost-effective whereas other researcher observed DCMD to be the least cost-effective. Moreover, among all the membrane distillation configurations, DCMD is the simplest configuration, and it has been investigated most for MD studies. Thus, to achieve the research goals, the following specific objectives and research plan will be implemented:

- To identify effective membrane-based processes for water recovery from membrane bioreactor treated brewery wastewater. Emerging thermally driven direct contact membrane distillation (DCMD) process will be studied and compared with conventional

pressure driven reverse osmosis (RO) and nanofiltration (NF) in terms of membrane performance, contaminant rejection, and membrane fouling. The altered surface morphologies and chemical compositions of the membranes before and after water recovery operations were evaluated to elucidate the fouling phenomena in these processes. The outcome of the effective membrane cleaning mechanisms for the processes were also explored for possible flux recovery and membrane reuse.

- To study the effect of major parameters, e.g., operational conditions, membrane types and pore sizes, and feed load, on membrane performance and membrane fouling to better elucidate the DCMD application for water reclamation from MBR treated brewery wastewater as well as to find the optimal condition for its application. This study employed DCMD for the reclamation of membrane bioreactor (MBR) treated high-strength brewery wastewater with varying feed temperature, membrane materials and pore sizes as well as with varying strength of wastewater. Commercially available hydrophobic membranes will be implemented to assess the membrane recovery performance through evaluating the membrane permeate flux and contaminant rejections. In addition to that, membrane surface morphologies and chemical compositions before and after the recovery applications will be examined to better comprehend the fouling phenomena.

- To methodically analyze the economic aspect of DCMD system for water reclamation from a pre-treated brewery wastewater effluent. Moreover, to better comprehend the effect of alternate energy sources on the water price, DCMD process will be evaluated with heat recovery within the system as well as with solar energy as an alternate source of energy. Furthermore, effect of varying process parameters on the cost of the DCMD, like; plant capacity, water recovery, and waste heat integration from industry will be explored.

1.3 Thesis Outline

Chapter 1 demonstrates the background stating the problem, research objective, and the thesis outline.

Chapter 2 is a comprehensive literature review for membrane distillation. It introduces the principles of membrane distillation, process configurations, membrane features, membrane fouling and wetting mechanisms and detection techniques, factors affecting membrane fouling, mitigation of membrane fouling and wetting, and economic aspects of membrane distillation. This information helps to understand the fundamentals of fouling and wetting in membrane distillation process during water reclamation application.

Chapter 3 presents a study which applies the pressure-based and thermal-based membrane separation processes for water recovery application from membrane bioreactor treated (MBR) brewery wastewater effluent. Reverse osmosis (RO), nanofiltration (NF), and direct contact membrane distillation (DCMD) were implemented to identify the effective separation process through studying the membrane performance, contaminant rejection, and membrane fouling. It is the first time that the RO, NF, and DCMD performance and fouling comparison with real wastewater effluent has been investigated.

Chapter 4 illustrates optimal condition for direct contact membrane distillation application for water reclamation from pre-treated brewery wastewater for stable and sustainable performance.

Chapter 5 demonstrates a techno-economic analysis of the direct contact membrane distillation process for water reclamation application from pre-treated brewery wastewater effluent. This study considers the utilization of alternate energy sources, including solar power and waste heat. This is the first time that economic analysis of DCMD has been conducted for water recovery application of membrane bioreactor treated brewery wastewater effluent.

Chapter 6 is a summary of the contributions and conclusions of this thesis. The limitations and possible future work identified in this thesis have also been discussed.

Chapter 2: Fouling and Wetting in the Membrane Distillation Driven Wastewater Reclamation Process – A Review

Abstract

Fouling and wetting of membranes are significant concerns that can impede widespread application of the membrane distillation (MD) process during high-salinity wastewater reclamation. Fouling, caused by the accumulation of undesirable materials on the membrane surface and pores, causes a decrease in permeate flux. Whereas membrane wetting, the direct permeation of the feed solution through the membrane pores, results in reduced contaminant rejection and overall process failure. Lately, the application of MD for water recovery from various types of wastewaters has gained increased attention among researchers. In this review, we discuss fouling and wetting phenomena observed during the MD process, along with the effects of various mitigation strategies. In addition, we examine the interactions between contaminants and different types of MD membranes and the influence of different operating conditions on the occurrence of fouling and wetting. We also report on previously investigated feed pre-treatment options before MD, application of integrated MD processes, the performance of fabricated/modified MD membranes, and strategies for MD membrane maintenance during water reclamation. We also discussed energy consumption and economic aspects of MD for wastewater recovery. Finally, we engage in a discussion of research needs for furthering the development of MD: notably the incorporation of MD in the overall wastewater treatment and recovery scheme (including selection of appropriate membrane material, suitable pre-treatment processes, and membrane maintenance strategies), and the application of MD in long-term pilot-scale studies using real wastewater.

Keywords: Membrane distillation; Fouling; Wetting; Wastewater; Reclamation.

2.1 Introduction

The scarcity of clean water has become a significant challenge in today's world, which inevitably has led towards the need to develop novel technologies to help provide a dependable supply of fresh water [33–35]. As of late, Membrane Distillation (MD) has gained significant attention as a promising technology for the production of fresh water via the treatment of high-salinity wastewater. MD is a membrane-based, vapor-driven thermal desalination process, in which water molecules are transported in a vapor phase through a porous and hydrophobic membrane [36–40]. The porous, hydrophobic membrane is used to separate a hot, highly concentrated feed stream, and a cold distillate stream [36,40,41]. The temperature difference between the feed and distillate streams creates a partial vapor pressure difference that drives the water vapor through the membrane from feed side to distillate side, where it condenses to pure water. The hydrophobic membrane prevents direct permeation of feed water, an essential feature for contaminant rejection. Due to reduced sensitivity to concentration polarization and the much high driving force resulting from a temperature difference, MD can operate at high salinities on the feed side [42]. MD demonstrates several distinct advantages such as: a 100% theoretical non-volatile salt rejection, a lower required operating temperature as compared to conventional thermal desalination processes, the ability to utilize low-grade thermal energy, a lower operating hydrostatic pressure, and less stringent mechanical property requirements for the membranes used when compared to conventional pressure-driven membrane processes such as reverse osmosis (RO) [40,41,51,43–50]. MD has the potential to provide sustainable water recovery when heat sources (low-grade or renewable) and waste-heat from industrial processes are readily available [52,53]. Despite these advantages, extensive application of MD still faces uncertainty with respect to its overall sustainability and effectiveness [38]. MD is not efficient in separating volatile and semi-volatile compounds [54,55]. It is a highly energy intensive technology compared to pressure-driven (e.g., RO) desalination processes, which makes it unattractive unless very high-salinity brines (which cannot be treated effectively by RO) require treatment [56]. Though other thermal distillation processes like multi-effect distillation (MED) and multistage flash (MSF) can be used to treat highly saline brine at low temperature, the energetic performance of MD is reported to be superior to MED and MSF for small-scale systems (<1000 m^3 day^{-1}) [56]. A fundamental challenge involved in conventional MD revolves around heat management in the process. Single-pass

recoveries are very low in MD [57], and adoption of a multi-stage approach [50] through the involvement of many heat exchangers can enhance water productivity and energy efficiency [56]. The multi-stage approach moves away from the all-plastic system design and will increase the capital cost of the treatment system. Achieving higher fluxes and thermal efficiencies in the MD process can be reached through the optimization of operating conditions or system configuration. Novel options like self-heating membranes (membranes heated on the feed side by Joule heating or photo-thermal surface heating) have been adopted in MD, which reduces temperature polarization and yields higher single-pass recoveries than conventional MD membranes [52,58,59]. However, these advances have only been demonstrated at the laboratory scale and further pilot-scale testing is necessary to assess their viability.

Wetting and fouling are two interrelated phenomena in MD, which influence each other and pose significant challenges in the application of MD. Membrane wetting is a unique challenge in MD, and it refers to the direct permeation of the feed solution through the membrane pores, resulting in reduced salt rejection and overall process failure [41,60–62]. Wetting has been associated as a problem during the long-term operation of MD systems, provided appropriate operating conditions are maintained [63]. Wetting can also occur in short-term MD operations due to improper operating conditions (e.g., pore size, membrane hydrophobicity, LEP of the system, etc.) in the system. On the other hand, as in other membrane-based processes, membrane fouling is a major drawback of MD, causing a decrease in permeate-flux due to the accumulation of undesirable material on the membrane surface and pores. Both fouling and wetting are time-dependent processes, and long-term effects cannot be easily predicted [64].

MD has been extensively studied for the removal of salts from brackish water, seawater, and high-salinity brines [48,65–69]. Numerous studies have investigated MD for the production of fresh water from seawater/brine water via desalination using varying membranes and operating parameters. These studies have widely indicated the negative impacts of both membrane fouling and wetting on the overall performance of the MD process [46,67,70–74]. MD has also been studied for recovery of heavy metals from water streams [75–77]. There are few review articles focused on membrane fouling and relevant control methods as encountered in different applications of MD [16,40]. A literature search for “membrane distillation”, in Web of Science,

revealed more than 4,300 articles published from January 1991 to December 2018, with an increasing growth in the number of articles published during the past decade (Figure 2.1). However, research concerning application of MD in wastewater treatment and reclamation has gained attention recently. MD has found a niche application, in particular for recovery of hypersaline wastewater in emerging industries (e.g., shale-gas), which conventional membrane desalination such as RO cannot access [78–81]. MD has also received interest as a promising technology to produce high quality freshwater from wastewater through utilization of available waste-heat or low-grade solar or geothermal heat [82–85]. There is a continuous drive to improve energy and process efficiency of MD systems, while recovering freshwater from wastewater, through improvement of MD system configuration, development of novel/modified membrane material, or integration of other processes with MD. It also provides good scalability due to its modular features. Though MD is primarily utilized for water recovery from highly saline/brine water, it showed potential for reclamation of high-strength wastewater in small-scale decentralized systems with available waste/alternative heat sources.

This review discusses the fouling and wetting scenarios in MD as reported in the literature, along with contaminant-membrane interactions, influence of operational conditions, treatment performances, and the effects of different mitigation strategies employed during the recovery of various types of real wastewater. This article also discusses different MD membrane fabrication/modification, integrated MD processes, pre-treatment strategies for feed wastewater streams, and membrane cleaning strategies for wastewater reclamation. This review also contains, as a necessary background for readers, a brief discussion of classical and recent MD module configurations, MD membrane features as well as the mechanisms influencing membrane fouling and wetting. Different invasive and non-invasive membrane fouling and wetting monitoring techniques have also been discussed briefly in this article. The discussions also include future research directions pertaining to the application of MD in wastewater reclamation.

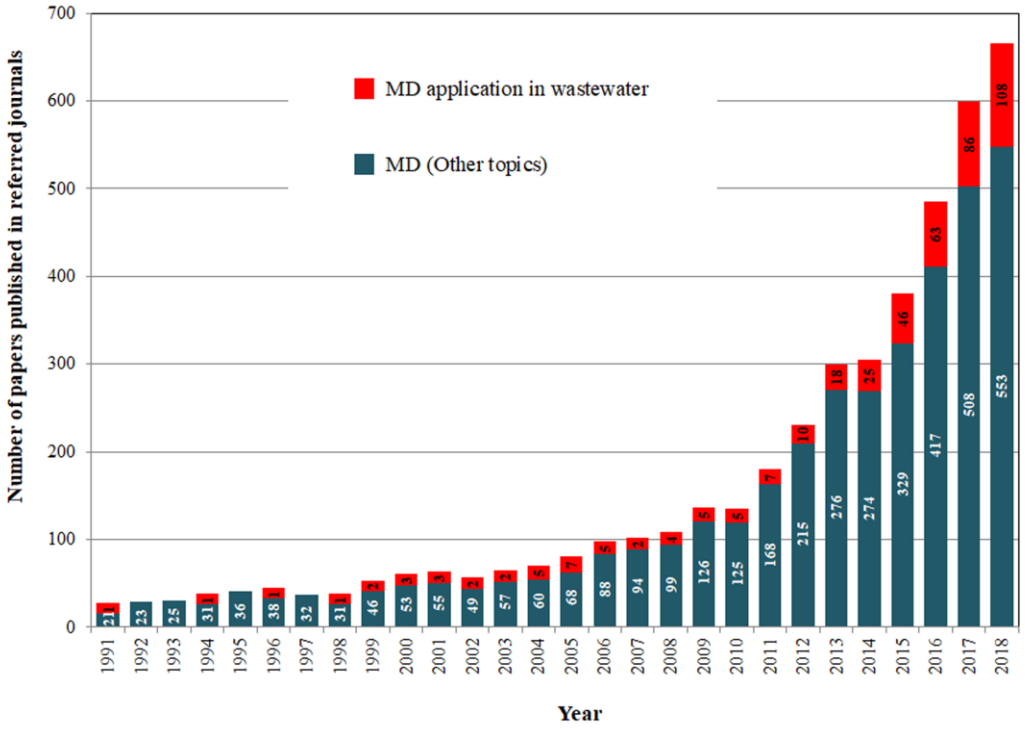

Figure 2.1: The growth in research activity related to MD and application of MD for wastewater reclamation from 1991 to 2018 (Source: Web of Science). Numbers in the stacked columns indicate the number of published papers in each category.

2.2 MD: process configurations and membranes

2.2.1 Process configurations in MD

Subject to the process of stimulating vapor pressure gradient across the membrane and gathering the transported vapors on the permeate side, there are four different classical configurations of MD [38,64]. The basic mechanisms of these classical configurations are briefly described in the following sections and illustrated in Figure 2.2.

Direct contact membrane distillation (DCMD): In DCMD, a hot solution (feed) and a cold solution are in direct contact with the hot feed side surface and the cold permeate side surface of the membrane, respectively. The vapor generated at the hot feed-side membrane surface flows through the membrane pores to the cold permeate-side due to the vapor pressure difference, resulting from the temperature difference, across the membrane. Warm pure water leaving the MD module preheats the feed in a separate external heat exchanger (not shown in Figure 2.2).

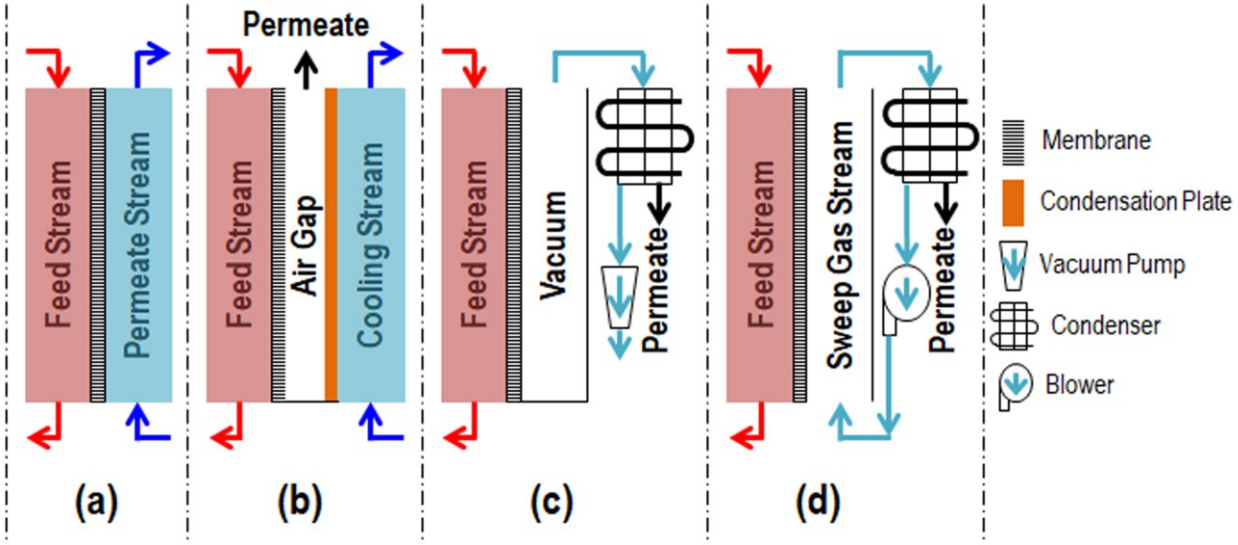

Figure 2.2: Schematic diagrams showing configurations of classical single-stage MD systems: (a) Direct Contact Membrane Distillation (DCMD), (b) Air Gap Membrane Distillation (AGMD), (c) Vacuum Membrane Distillation (VMD), (d) Sweeping Gas Membrane Distillation (SGMD).

The DCMD has been reported as the simplest of MD configurations and has been studied the most in literature for wastewater recovery, and concentration of aqueous solutions [Table 2.1].

Table 2.1: Operational parameters in MD processes applied to different types of wastewater treatment and reclamation.

MD setup	Feed type	Pre-treatment	Membrane Properties					Temperature (°C)		Flow Rate/Velocity		Ref.
			Membrane type (Module: Material)	Mean pore size (µm)	Porosity (%)	Thickness (µm)	In-air contact angle (°)	Feed	Permeate	Feed	Permeate	
DCMD	TDW	Foam fractionation, Conventional (flocculation-biological) treatment	Flat sheet: PTFE	0.5	---	---	---	60	20	0.8 L m^{-1} 45–47 L m^{-1}	0.8 L m^{-1} 45–47 L m^{-1}	[86]
DCMD	TDW	NP, physicochemical-biological (anaerobic-aerobic) treatment	Flat sheet: PTFE	0.22	85.1	180	133.7	50	20	0.35 L m^{-1}	0.25 L m^{-1}	[87]
DCMD	TDW	NP	Hollow fiber: PVDF-Cloisite 15A composite	0.088	83.70 ± 0.67	---	97.7	90±1	25±2	0.023 m s^{-1}	0.002 m s^{-1}	[88]
DCMD	TDW	NP	Flat sheet: PTFE on PET support with Agarose	0.2	85%	130	127	60	21	2 L m^{-1}	2 L m^{-1}	[89]
DCMD	OMW	NP	Flat sheet: PTFE, PVDF	0.199 0.283	---	55 ± 6 118 ± 4	---	30 - 60	20	---	---	[90]
DCMD	OMW	NP, Coagulation/flocculation, MF	Flat sheet: PTFE	0.2	80%	178	---	40	20	---	---	[91]
DCMD	MW	NP, advanced biological treatment	Flat sheet: PTFE, PVDF	0.45, 0.45	---	---	124.9, 123.6	40 - 60	10	---	---	[92]
FO-DCMD	FO feed: sanitary wastewater; DCMD feed: OW+FO permeate	Ultrafiltration for OW	Flat sheet: PTFE	0.45	---	---	120	45.5	25	---	---	[93]
FO-DCMD	FO feed: secondary MW, DCMD feed: 1M NaCl+FO permeate	FO for secondary MW effluent	Flat sheet: PP	0.22	---	130-170	---	50	20	0.4 L m^{-1}	0.4 L m^{-1}	[94]
FO-DCMD	FO feed: secondary MW, DCMD feed: 1M NaCl+FO permeate	FO for secondary MW effluent	Flat sheet: PP	0.22	---	130-170	---	50	20	0.4 L m^{-1}	0.4 L m^{-1}	[95]
FO-DCMD	FO Feed: domestic wastewater, DCMD feed: 35 g/L NaCl+FO permeate	FO for domestic wastewater	Hollow fiber: PVDF	0.073	---	186±5	---	53	20	0.5 m s^{-1}	0.15 m s^{-1}	[96]
FO-DCMD	FO feed: raw sewage, DCMD feed: 1.5M NaCl+FO permeate	FO for raw sewage, MD feed solution was pre-treated using GAC or UV	Flat sheet: PTFE	0.3	---	---	135±15	40	20	1.0 L m^{-1}	1.0 L m^{-1}	[97]
DCMD	RCW	Coagulation-sedimentation, filtration, acidification and degasification	Flat sheet: PVDF	0.18	82	---	---	50	20	0.5 m s^{-1}	0.2 m s^{-1}	[98]

MD setup	Feed type	Pre-treatment	Membrane Properties					Temperature (°C)		Flow Rate/Velocity		Ref.
			Membrane type (Module: Material)	Mean pore size (µm)	Porosity (%)	Thickness (µm)	In-air contact angle (°)	Feed	Permeate	Feed	Permeate	
DCMD	OW: oil, sodium dodecyl sulfonate and sodium chloride	NP	Flat sheet: PVDF	0.22	75	125	111	55	15	0.8 L m^{-1}	0.8 L m^{-1}	[99]
DCMD	OW: 1 wt% NaCl solution with oil	NP	Capillary: PP	0.2	73	---	---	40-80	20	---	---	[100]
DCMD	OW: shale oil and gas produced water	Filtration through 8-µm filter	Flat sheet: PVDF, PVDF-PVA, PVDF-SiO_2-FAS	0.45 (PVDF)	---	125 (PVDF)	119±4, 50±2, 159±2	60	20	0.4 L m^{-1}	0.35 L m^{-1}	[79]
DCMD	LLRW	NP	Hollow fiber: PVDF	0.15	80	---	---	47.5±0.5	27.0±0.5	0.303 m s^{-1}	0.075 m s^{-1}	[101]
DCMD	LLRW	NP	Spiral wound: PTFE	0.2	80	---	---	35-80	5-30	16 L m^{-1}	16 L m^{-1}	[102]
DCMD	LLRW/MLRW	NP	Flat sheet: PS, PES, PTFE	---	---	138.80 – 146.56	92.45 - 113.99	55	21.5	0.0023 L m^{-1}	0.0014 L m^{-1}	[103]
DCMD	ROC	NP, GAC	Flat sheet: PTFE	0.2	70-80	179	139.4±1.5	55	25	0.06 m s^{-1}	0.06 m s^{-1}	[10]
DCMD	ARD	NP, thermal precipitation	Flat sheet: PVDF	---	---	---	122.7±7.7	57.1±1.7	22.5±1.1	3.5 L m^{-1}	3.5 L m^{-1}	[104]
DCMD	PW	NP	Flat sheet: PVDF	0.22	---	104	124.9	60±2	20 ± 2	0.5 L m^{-1}	0.5 L m^{-1}	[105]
AGMD	PW	Pre-filtration	Flat sheet: PTFE with PP	0.2	80	200	---	55-90	15-50	20 L m^{-1}	20 L m^{-1}	[106]
Modified DCMD	LL	NP, MBR (anoxic+aerobic+UF)	Flat sheet: PTFE, PVDF	0.22, 0.45	---	170-240, 120-180	127.61, 124.91; 128.99, 123.59	40 - 60	10	3.5 L m^{-1}	3.5 L m^{-1}	[107]
FO-DCMD	FO feed: LL, DCMD feed: 4.82 M NaCl and FO permeate	FO	Flat sheet: PTFE-PVDF composite with PET	0.45	---	---	---	72.5±0.5 62.5±0.5	15±0.5	0.31 L m^{-1}	0.31 L m^{-1}	[108]
DCMD	FW	NP	Hollow fiber PP	0.46	80	250	---	55-60	30	2 L m^{-1}	2 L m^{-1}	[9]

Note: TDW = textile/dyeing wastewater, OMW = olive mill wastewater, MW = municipal wastewater, RCW = recirculating cooling water, OW = oily wastewater/oil-water emulsion, RW = radioactive wastewater, LLRW = low-level RW, MLRW = mid-level RW, ROC = wastewater reverse osmosis concentrate, ARD = acid rock drainage water, PW = pharmaceutical wastewater, LL = landfill leachate, FW = fermentation wastewater, NP = no pre-treatment, MF = microfiltration, FO = forward osmosis, MBR = membrane bioreactor, DCMD = direct contact membrane distillation (MD), VMD = vacuum MD, AGMD = air gap MD, PP = Polypropylene, PTFE = polytetrafluoroethylene, PVDF = polyvinylidene fluoride, PET = polyester, PS = polysulfone, PES = polyethersulfone, PVA= polyvinyl alcohol, FAS = Heptadecafluoro-1,1,2,2-tetrahydrodecyl triethoxysilane, GAC = granular activated carbon adsorption.

The membrane remains as the only barricade between the recirculating hot feed and cold permeate solution streams. As a result, DCMD experiences the highest heat loss through conduction among the four classical configurations.

Air gap membrane distillation (AGMD): AGMD introduces a thin stagnant air gap between the membrane and a condensation surface on the permeate side, whereas the hot feed solution remains in direct contact with the membrane solution. The vapor passing through the membrane, crosses the air gap and condenses on the cold condensation surface (usually a thin dense polymer or metal layer) [109,110]. AGMD offers reduced heat loss through conduction. However, the enhanced resistance to mass transport, introduced by the air gap, results in lower flux of AGMD than other MD configurations [111].

Vacuum membrane distillation (VMD): A pump is used on the permeate side to create a vacuum and provide driving force lower than the saturation pressure of volatile molecules in the feed water. Condensation may occur inside or outside of the membrane module [112–114]. Conducting heat loss is negligible in VMD [113,114].

Sweeping gas membrane distillation (SGMD): This configuration allows sweeping flow of a cold inert gas to collect vapor molecules from the membrane permeate surface and condense it outside the membrane module [64,115]. There is a moving gas barrier, which enhances mass transport efficiency compared to AGMD and also reduces conductive heat loss [64]. The SGMD requires external condenser to collect a small volume of permeate in a large volume of sweep gas [64,115].

Recent MD Configurations: Recent studies have revealed development of a number of novel variations to the classical AGMD and VMD configurations to enhance energy efficiency of the process and the water vapor flux through the membrane. The different novel configurations with modified gaps are the permeate gap MD (PGMD), the material gap MD (MGMD), and conductive gap MD (CGMD) [116–123]. PGMD, also known as water gap MD or liquid gap MD, is a hybrid of the AGMD and DCMD configurations where a water or liquid is used to fill up the gap between membrane and cold condensation surface [116–118,120,122]. The MGMD configuration uses additional material (such as sand) in the gap between the membrane and the condensation plate [119]. Finally, the CGMD configuration employs a high thermal conductivity spacer (such as a metallic mesh) in the permeate gap to improve the conductance of the gap along the thickness direction [116–118]. Figure 2.3 provides a schematic of different gap MD systems. Energy

efficiency measurement for similar sized systems demonstrated that CGMD can have two times higher energy efficiency than PGMD and PGMD can have about 20% higher energy efficiency than the classical AGMD arrangement [118].

In addition to these gap MD systems, another novel configuration introduced a flashed-feed VMD system where the feed stream was not allowed to touch the MD membrane [124]. The flashed-feed VMD configuration used a throttling valve in the feed line along with a vacuum pump (maintaining a vacuum in the flashing chamber) to regulate the feed flow rate to the flashing chamber (Figure 2.4). The novel flashed-feed VMD system eliminated the temperature polarization effect near the membrane (which can reduce the feed water temperature near the membrane relative to the bulk feed temperature) and provided up to 3.5 times higher flux than conventional VMD under similar operating conditions [124].

Efforts have been carried out to develop new MD process configurations and membrane modules with higher thermal efficiencies [125–133]. Fabrication of hollow fiber (single or multi-bore) membranes have been developed to enable modular design of the MD systems [123,125,126,134,135]. Multi-stage and multi-effect MD (MEMD) configurations for gap MD and VMD systems have been proposed for seawater desalination with internal heat recovery and enhanced flux in the systems [129,131–133,136]. The concept of the MEMD systems involve placing the cold feed solution beneath the condensation surface, as a coolant, to gain some degree of pre-heating as the permeated vapor gets condensed [129,131–133,136]. The internal heat recovery mechanism in the MEMD systems enable better thermal efficiency in the MD process [50,133,136].

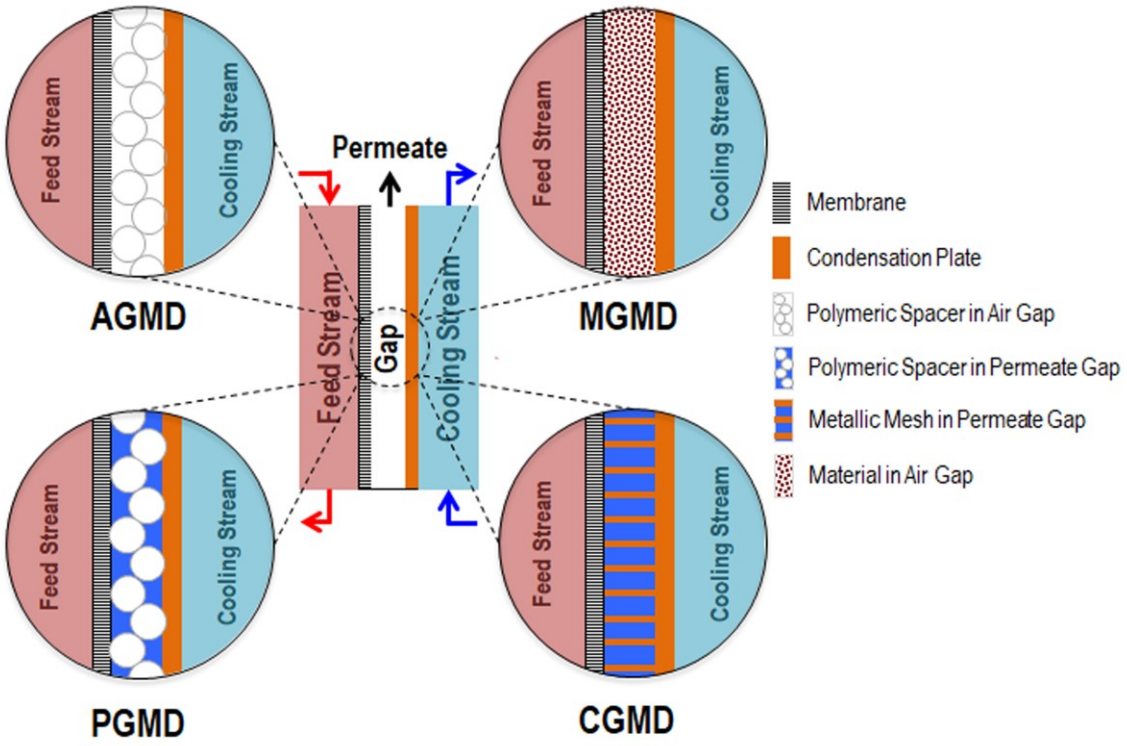

Figure 2.3: Schematic diagrams showing variations in configurations of different types of gap MD systems: Air gap membrane distillation (AGMD), permeate gap membrane distillation (PGMD), conductive gap membrane distillation (CGMD), and material gap membrane distillation (MGMD).

The several recently developed MD configurations have been studied mostly in seawater desalination. The updated versions of traditional gap MD, VMD systems and the modular MEMD systems hold promising traits in terms of demonstrating enhanced flux and energy consumption performances than conventional MD systems during reclamation of high-salinity wastewater. However, high levels of organic contaminants in the wastewater, compared to seawater, might result in the occurrence of excessive organic fouling and biofouling in the updated systems. Similarly, module scale-up with efficient internal heat recovery and satisfactory flux in the MEMD systems will also pose challenges with altered membrane fouling and wetting scenarios. Hence these updated and modular MD systems should be studied for recovery of high-salinity wastewater.

2.2.2 Features of MD membranes

MD membranes should have high porosity, high hydrophobicity, uniform pore size distribution, and low tortuosity [40]. To prevent heat loss across the membrane, microporous membranes employed in MD should possess low mass transfer resistance and low thermal conductivity [36]. Also, suitable thermal stability and resistance to chemicals (e.g., acids and bases), are essential characteristics of membranes used in MD [36]. Optimal membrane pore size must be balanced in terms of high permeate flux and effective pore wetting resistance. High porosity membranes with low mechanical strength tend to degrade under even mild operational pressures, resulting in a decline in membrane performance [137]. The porosity values for different MD membranes, used in high-strength wastewater reclamation, are observed to be in the range between 70-85%. Usually, commercial hydrophobic MD membranes are made of polytetrafluoroethylene (PTFE), polypropylene (PP), or polyvinylidene fluoride (PVDF) active layers with optional support layer materials (e.g., PP, polyester) [36,40,138,139]. Another significant property of MD system is "liquid entry pressure" (LEP), which is the pressure at which the liquid penetrates the membrane pores and causes wetting of the membrane. To prevent the penetration of feed solution through membrane pores, the applied pressure in MD should always be less than the LEP. LEP is an intrinsic property of the system involving the membrane and solution. The major parameters that influence the LEP are: surface tension of the solution, surface energy of membrane material (which controls the membrane hydrophobicity), membrane pore size and geometry, feed concentration, and the presence of organic solutes and surfactants [36,140]. LEP is described by the Laplace-Young equation [36]:

$$LEP = \frac{-4B_g \sigma \cos\theta}{d_{\max}}$$

Where, B_g = pore geometric factor, σ = surface tension of the solution, θ = contact angle between the solution and the membrane surface, and $d_{\max}$ = diameter of the largest membrane pore size.

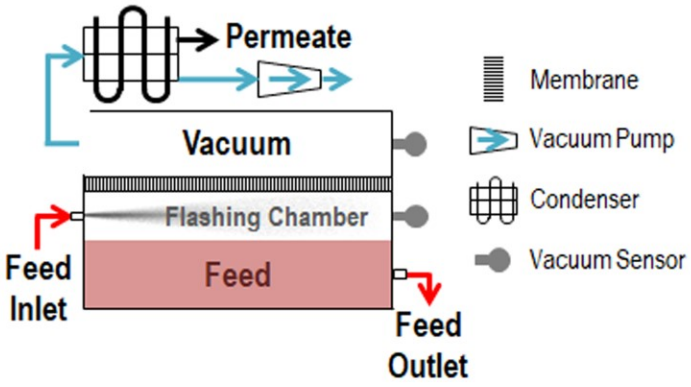

Figure 2.4: Schematic diagram showing configuration of Flashed-feed Vacuum Membrane Distillation. (Redrawn following [124])

Apparently, the Laplace-young equation might indicate that a lower pore size is desirable to prevent the occurrence of membrane wetting. However, too much lowering of the membrane pore size will result in a decrease of trans-membrane flux and overall recovery performance. The membrane pore size thus should be selected in such a way that the trans-membrane flux must be enhanced without increasing the chance of membrane wetting. Fabrication of composite MD membranes with novel materials and architecture, which involve different surface and inner membrane conformations (discussed in a later section), demonstrated enhanced porosity and flux with low wetting potential.

2.3 Fouling and wetting phenomena in MD

2.3.1 Fouling mechanism in MD

Foulants (depositing compounds causing fouling) are usually of inorganic, organic, or biological nature and can interact with each other as well as membrane surfaces. Membrane fouling is affected by the following parameters [40]: i) foulant characteristics (e.g., concentration, molecular size, solubility, diffusivity, hydrophobicity, charge); ii) membrane properties (e.g., hydrophobicity, surface roughness, pore size and its uniformity distribution, membrane structure, surface charge, surface functional groups); iii) operational conditions (e.g., flux, solution temperature, flow velocity, pressure); and iv) feed water characteristics (e.g., pH, ionic strength, presence of organic/inorganic matters, microorganisms). Surface roughness influences the hydrophobicity of a membrane, which in turn impart antifouling and antiwetting property. Higher

surface roughness entraps more air fraction in the micro- and nano-sized pores of the membrane surface [99]. As a result the membrane surface become more hydrophobic with increased solid-gas interface fraction in the overall mix of solid-liquid and solid-gas interfaces on membrane surface. According to the extended DLVO model, three key interfacial interactions for particles in aqueous media are Lifshitz-van der Waals, Lewis acid-base, and electrostatic double layer interactions [141]. Fouling is minimized if the particle and surface have similar charges leading towards repulsion. Also, deposition of particulate matter forms on the membrane surface by agglomeration of particles in aqueous solutions. Higher aggregation occurs because of large attachment coefficients resulting from an extensive degree of collisions [142]. At high ionic strengths, the interaction between particles is dominated by acid-base interactions as electrical double layer forces that are weak in this condition [143,144]; whereas Van der Waals interactions are not susceptible to variations in pH and electrolyte concentrations. Studies have showed that increased ionic strength, in the presence of divalent cations, resulted in more fouling of humic substances on DCMD membranes [145–147]. At high ionic strength, the charges of the membrane surface and humic macromolecules are significantly reduced, which leads to a decrease in the electrostatic repulsion between the membrane surface and humic macromolecules. As a result, the humic macromolecules, which become coiled and spherical in shape, form a more compact fouling layer [147]. The presence of a foulant layer causes additional thermal and hydraulic resistance based on the characteristics (porosity, thickness, etc.) of the fouling layers [43,146]. Feed water foulants can attach to the hydrophobic membrane surface and block membrane pores leading to a decline in permeate flux [140]. Fouling is severe when the feed contains ample hydrophobic contaminants (oil, hydrophobic organics, etc.) as hydrophobic-hydrophobic attraction results in strong bonding between the membrane surface and the contaminants [16,148].

Fouling in MD has been broadly classified into the following groups: (a) inorganic fouling, (b) organic fouling, and (c) biological fouling [42,64,149,150]. Figure 2.5 schematically represents these fouling mechanisms and their combined effect on MD, leading to partial or complete pore blocking and surface fouling.

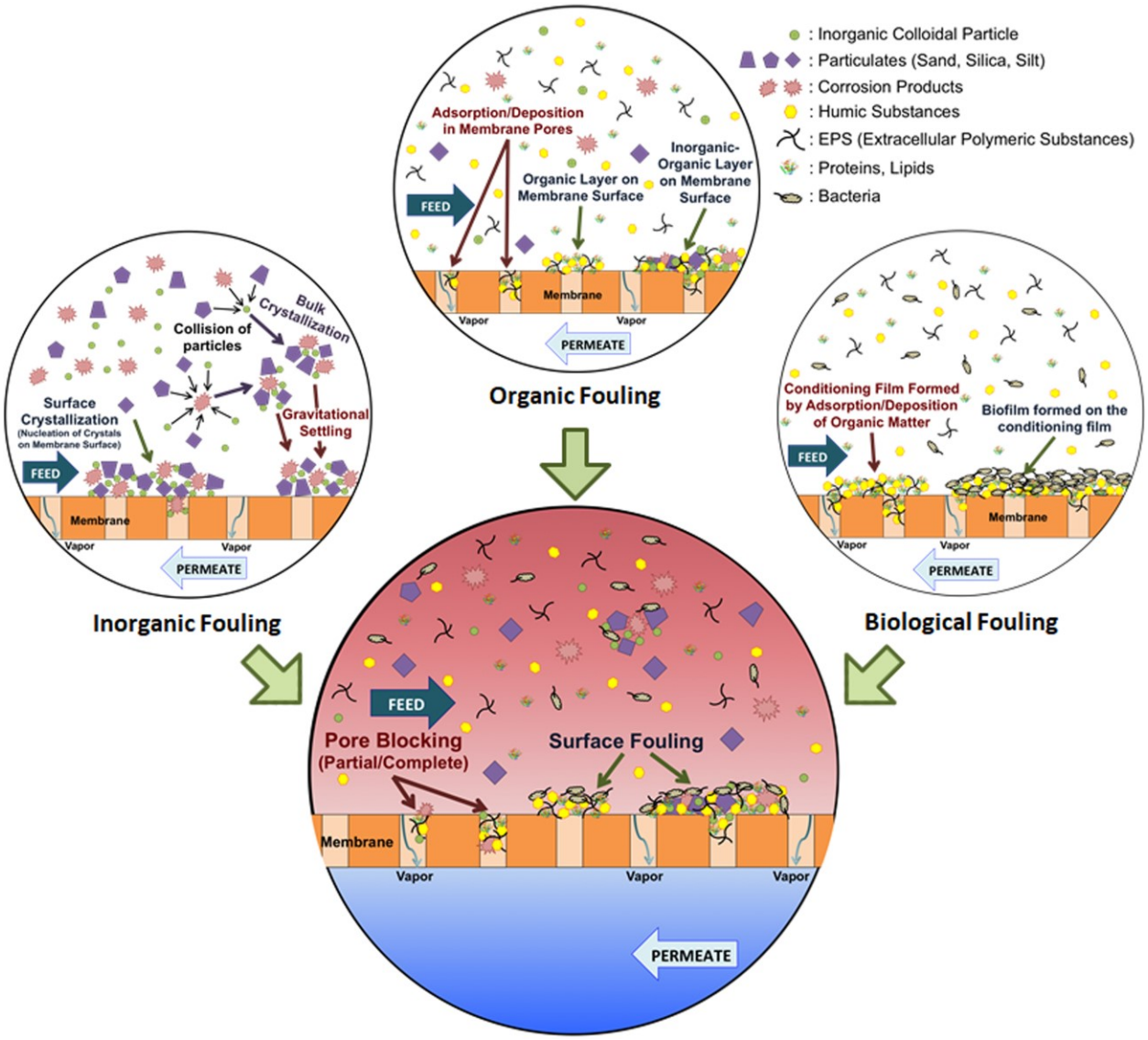

Figure 2.5: Combined effect of different fouling mechanisms (i.e., inorganic fouling, organic fouling, and biological fouling) leading to partial or complete pore blocking (internal fouling) and surface fouling (external fouling) in membrane distillation process.

Inorganic fouling mainly refers to scaling that is comprised of the precipitation of hard salts such as calcium carbonate, calcium sulfate, silicate, sodium chloride, or calcium phosphate. Water evaporation and temperature changes create supersaturation on the feed side that lead to nucleation and crystallization in the feed and on the membrane surface, resulting in inorganic fouling [140]. Colloidal organic matter, (e.g., humic substances, proteins, extracellular polymeric substances (EPS), etc.) are responsible for organic fouling in the MD process [40,151]. Finally, biological fouling or biofouling refers to the accumulation and evolution of microorganisms on the membrane

surface that cause permeate flux decline [40]. Dynamic biofouling experiments (with *Anoxybacillus* sp. as a model bacterium) were carried out to indicate impact of increasing feed water temperatures on biofilm growth and MD performance [152]. The *Anoxybacillus* sp. has been identified as a major bacterial genera in MD bioreactor suspended sludge [153]. Biofouling situation in PVDF MD membranes were studied in the feed side at temperatures of 47°C (temperature below the optimum temperature for thermophilic bacterial growth), 55°C (optimum temperature for thermophilic bacterial growth) and 65°C (temperature above the optimum temperature for thermophilic bacterial growth) [152]. Extensive bio cell growth was observed on the feed side at 55°C, when compared to the same at 47°C. As a result the water flux decline was more (78%) at 55 °C compared to the water flux decline at 47°C (30%) after 3 days of operation. Increasing temperature to 55°C also enhanced biofouling induced membrane wetting and allowed bacterial cells and endosposes through the membrane to the permeate side. Bacterial growth was impaired when feed water temperature was increased to 65°C. However, excessive production of extracellular polymeric substances (EPS) at 65°C caused severe pore wetting and hampered MD function [152]. Bacterial EPS, protein and polysaccharides were observed on the fouling layers of flat-sheet PVDF and PTFE membranes in a submerged MD bioreactor [154]. The polysaccharide concentration on the fouling layer and total amount of fouling on PVDF membranes were more than that observed on PTFE membranes. This indicated that the polysaccharides play a vital role in the initial attachment and subsequent formation of fouling layer [154]. Thus, interaction between membrane material and specific fouling component can enhance overall fouling in the system [154]. It has been suggested that thermophilic bacteria may also survive in the high feed temperature by forming spores, which later settle and accumulate on the membrane surface at a lower temperature zone [155,156]. Small colonies of *S. faecalis* bacteria was observed on the membrane surface on the distillate side in the vicinity of large membrane pores while recovery of wastewater generated from processing animal intestines [155]. The growth of the *S. faecalis* bacteria was restricted due to scarcity of nutrients and organic matters on the distillate side [155]. The biofouling conditions reported across different publications varied in extent due to the different feed water conditions, operational conditions, and duration of experiment. Dynamic biofouling experiments at different temperature, with specific microorganism dosed on the feed side, have generated a better understanding of the biofouling mechanisms [152]. Experiments with other major microorganism groups may indicate how different microorganisms interact with each

other as biofouling takes place on MD membranes. Also, the impact of water quality (i.e., change in nutrient content) and operational conditions should also be assessed in similar dynamic biofouling experiments to achieve a better understanding on MD membrane biofouling process.

2.3.2 Wetting mechanism in MD

Wetting refers to the permeation of water through membrane pores, which degrades permeate quality, especially during long-term MD operation [63]. Membrane wetting is stimulated in MD by the presence of inorganic fouling/scaling, amphiphilic molecules (e.g., surfactants and protein), low surface tension liquids (e.g., alcohol), the use of antiscalants, and chemical degradation of the membrane [16,40]. Wetting can also occur when the pressure on the feed side exceeds the LEP of the membrane [16]. Often, fouling by salt deposition on the membrane surface, as well as in the membrane pores (inorganic fouling), provides hydrophilicity to the membrane, resulting in wetting [16]. Low surface tension contaminants and surfactants, which are commonly found in wastewater streams, can lead to the wetting of conventional hydrophobic membranes in MD [78,157,158]. These contaminants, which have a hydrophobic tail moiety, tend to adsorb on the surface and pore walls of MD membranes through hydrophobic-hydrophobic interactions, and can make the membrane surface and pores more hydrophilic. The wettability of membranes have been classified as (a) non-wetted (with maximum vapor transport through the pores, which obtain highest flux and maximum salt rejection), (b) surface-wetted (gap for vapor transport reduced, but no permeation of feed water towards the permeate), (c) partially-wetted (feed water permeates through some pores, while vapor transport gap reduces in other pores), and (d) fully-wetted (all membrane pores allow permeation of feed water, which extremely deteriorates permeate quality due to contaminants' penetration) [60,159–161]. Some studies have also referred to different stages of MD membrane wetting as (a) non-wetted (refers to the state where maximum vapor pressure exists through the pores to achieve highest flux and maximum salt rejection), (b) surface/partial-wetted (refers to the transition state, where partial penetration of the feed solution occurs, which decreases the average distance between the two liquid−air interfaces, or the thickness of the air gap within the pores), and (c) pore-wetted/wetted (refers to the state where some membrane pores are fully penetrated and the salt in the feed stream can freely move through the wetted pores to the permeate side) membranes [158,162–164]. Studies have observed that operational parameters in MD, (e.g.,

pressure, temperature and flow rate) can affect membrane wettability and salt rejection rates [61,132,133,165].

2.3.3 Fouling and wetting monitoring techniques in MD

The conventional fouling and wetting monitoring techniques in different types of MD processes involves observing the change in flux through the membrane to the permeate side and measuring the conductivity on the permeate side, respectively. The occurrence of fouling on the feed side of the membrane results in a low trans-membrane flux while wetting of the MD membrane effects in an increase in conductivity on the permeate side. Although measurement of trans-membrane flux and permeate conductivity provides information on the occurrence of fouling and wetting in MD, respectively, they do not necessarily provide much insight on the mechanism and kinetics of fouling and wetting occurrences. Many analytical techniques both invasive and non-invasive have been developed to study fouling and wetting in the MD process. These are briefly discussed in the following subsections:

Invasive analytical techniques: The invasive fouling and wetting monitoring methods in MD involve conducting the MD experiments repeatedly over different periods under different operational conditions and then analyzing the membrane after disassembling it outside the MD module. These invasive techniques of membrane surface analysis help in understanding the fouling and wetting characteristics, mechanism and extent on the membranes. The most commonly reported invasive procedures for fouling and wetting assessment involves using direct visualization and/or SEM (scanning electron microscopy) to evaluate the surface morphology of the membrane surface as it is altered by the deposition of inorganic, organic, and biological foulants. SEM and/or optical laser techniques are also employed to measure the membrane thickness.

Additionally, analytical techniques like EDX (energy dispersive x-ray spectroscopy) and/or XPS (x-ray photoelectron spectroscopy) have been used along with SEM to gather elemental composition of the membrane surfaces [37,51,79,158,166–169]. Techniques like AFM (atomic force microscopy) and XRD (x-ray diffraction) have been employed to characterize the surface structure, roughness of the membranes [37,167,170–173] and the crystal composition of the scales formed on the membrane surface, respectively [104,145,172,174,175]. FTIR (Fourier transform

infrared spectrometer) has been used to assess chemical composition of foulants (like functional groups, biopolymers, polysaccharides or humic acids), which helps in understanding the interaction and bonding between the foulants and the membrane surface [88,105,149,174,176,177]. Also, the contact angle (Table 2.1) and the zeta potential [10,105] are measured on the membrane surface to evaluate the change in surface hydrophobicity and charge due to fouling and wetting, respectively. Apart from these primary analytical techniques, many water quality analysis experiments are also carried out in both feed and permeate water to gain an understanding of the feed water constituents influencing the mechanism of fouling and wetting.

Non-invasive analytical techniques: Recent studies have reported novel non-invasive methods, which enable membrane fouling and wetting monitoring while the membrane is held during operation within the MD module. Optical coherence tomography (OCT) has been reported to study in-situ fouling (inorganic fouling, organic fouling, and biofouling) in DCMD systems [105,152,166,178,179]. The OCT device is placed next to the DCMD set up to monitor the feed half, using a special viewing window on the MD module. The cross-sectional image of the foulant on the membrane surface is then captured as a function of time while the MD operation ensues. Recent studies have successfully employed OCD based fouling visualization methods and validated the monitoring method using conventional invasive techniques [105,152,166,179]. Bauer et al. (2019) presented an innovative methodology using OCT, which enables 3D dataset analysis allowing for quantification of scaling on the membrane surface in a DCMD. The generated data from OCT were not only used to describe the structural development of scaling in the MD system, but the data was further processed to formulate and calculate quantitative fouling parameters based on layer volume and coverage, which can allow for process control. The developed methodology was able to assess the fouling condition independent from the flux decrease, and hence it can be used for an early prediction of process efficiency loss due to fouling [178].

An electrochemical impedance-based method has been reported recently to in-situ monitor membrane pore wetting in a DCMD setup [162]. The study provided an impedance-measuring arrangement in a DCMD configuration. Membrane wetting was observed using both single-frequency cross-membrane impedance measurements and distillate conductivity measurements.

The noteworthy response of single-frequency impedance to partial pore wetting before any change in distillate conductivity suggest that the in-situ impedance measurement method can provide early detection of imminent membrane wetting [162].

The novel in-situ fouling and wetting monitoring techniques offer the advantage of linking real-time fouling and wetting mechanisms and kinetics to operating conditions and water quality. As the number of studies concerning the application of MD for wastewater reclamation is increasing in the research community, implementation of these novel-monitoring techniques will provide a better perception on the dynamics of fouling and wetting in the system. However, for the fundamental understanding of the fouling and wetting scenario involving different contaminant groups in the feed stream, the non-invasive methods will be critical.

2.4 Factors affecting the occurrences of fouling and wetting in MD

Several studies have reported operational parameters (Table 2.1) and performance (Table 2.2) of MD process when it is applied either individually or integrated into a more extensive treatment system for the treatment and recovery of different types of wastewaters. The following sections review critical observations concerning influence of wastewater composition and process operating condition on fouling and wetting in MD.

2.4.1 Impact of wastewater composition

Most studies involving the use of MD for wastewater recovery use synthetic wastewater with model contaminants to assess scaling and fouling performance [172,176,180]. Reports describing MD with real wastewater indicates that system performance varies significantly from studies conducted with synthetic wastewater [86,87]. Several studies have observed the occurrence of fouling and wetting in direct contact membrane distillation (DCMD) [87,172,176,181] and vacuum membrane distillation (VMD) [180] of synthetic solutions prepared using dyes specifically found in textile/dyeing wastewater. VMD demonstrated complete rejection of five different dyes in a bench-scale setup during short duration (less than 2 hours) experiments [180]. Fouling performance of treatment via DCMD for four different dyes (methylene blue, crystal violet, acid red 18, and acid yellow 36) reported dye-dye interactions and membrane-dye

interfacial interactions [176]. Negatively charged PVDF/PTFE membrane surfaces performed well in the treatment of acid and azo dyes of the same charge and showed higher fluxes [176].

Similarly, the charge of contaminants in pharmaceutical wastewaters influenced the interaction among the contaminants and the membrane yielding fouling and wetting of MD membranes during treatment/reclamation of pharmaceutical wastewaters [105]. A total of 12 selected antibiotics were mixed with feed solution and treated in DCMD process with a PVDF membrane. The antibiotics were selected on the basis of the charges in them (i.e. positive, negative or neutral). Eight antibiotics with negative charge (Cefazolin, Cefotaxime, Amoxicillin trihydrate, Cephalothin, Ceftazidime hydrate, Piperacillin, Cloxacillin monohydrate, Antimony (III) isopropoxide), two antibiotics with positive charge (Gentamicin sulfate, Tobramycin), and two antibiotics with neutral charge (Ciprofloxacin, Enrofloxacin) were dozed in the range of 1-200 mg/L in DI feed water to produce pharmaceutical wastewater. For a negatively charged PVDF membrane, a significant decline in water flux and wetting was observed during reclamation of pharmaceutical wastewaters containing a positively charged antibiotic, while water flux remained stable in the case of negatively charged and neutral antibiotics with 100% rejection [105]. Rejection of positively charged antibiotics: Gentamicin sulfate and Tobramycin were 86% and 78%, respectively [105]. Air gap membrane distillation (AGMD) pilot trials in pharmaceutical wastewaters recovery witnessed greater removal efficiencies than most other technologies (activated sludge, membrane bioreactors, membrane bioreactors with flocculation and sedimentation, forward osmosis) and comparable removal performances as nanofiltration and RO [106]. A total of nineteen pharmaceutical residues were detected in the effluent from a municipal wastewater treatment plant [106]. Table 2.3 outlines the removal efficiencies (%) for different pharmaceutical residues observed by AGMD, DCMD, and other technologies. A study evaluated rejection of 25 pharmaceutical compounds (Table 2.3) by DCMD process using a PTFE membrane and observed more than 99% rejection for all the pharmaceutical compounds (even in the presence of humic acid) [182]. DCMD experiments were carried out with and without humic acid (0, 20, 40, 60, and 80 mg/L) in DI feed solution, which contains pharmaceuticals (each compound having a concentration of 1 μg/L). It was observed that retention of pharmaceutical compounds predominantly occurred by membrane rejection (which is mainly governed by volatility and to a lesser extent by hydrophobicity) [182].

DCMD was also employed successfully to treat low-level radioactive wastewater using PVDF hollow fiber membranes [101] and spiral wound PTFE membranes [102]. In the study involving treatment of simulated radioactive solutions containing cesium (Cs^{+}), strontium (Sr^{2+}), cobalt (Co^{2+}) in a PVDF hollow fiber membrane module, two solutions were prepared with concentrations of 20 mg/L and 100 mg/L for all the cations. DCMD achieved complete rejection of the cations as no detectable concentrations were observed for Cs^{+}, Sr^{2+}, and Co^{2+} in the permeate solution, which reflected an infinite decontamination factor [101]. A synthetic solution, prepared using inorganic salts (non-active) and radioactive elements, was treated using a spiral wound PTFE membrane module [102]. The non-active inorganic ions in solution were Na^{+} (1060.6 mg/L), NH_4^{+} (207.1 mg/L), K^{+} (21 mg/L), Mg^{2+} (33.7 mg/L), Ca^{2+} (87.2 mg/L), F^{-} (5.7 mg/L), Cl^{-} (744.2 mg/L), NO_3^{-} (1832.9 mg/L), SO_4^{2-} (37.6 mg/L) and the radioisotopes were ^{140}La (<6.53 x 10^{-1} Bq/L), ^{133}Ba (2.99 x 10^{3} Bq/L), ^{170}Tm (5.26 x 10^{2} Bq/L), ^{114m}In (86.2 Bq/L), ^{192}Ir (37.3 Bq/L), ^{110m}Ag (10.4 Bq/L), ^{65}Zn (3.39 x 10^{3} Bq/L), ^{134}Cs (7.84 Bq/L), ^{137}Cs (29.5 Bq/L), and ^{60}Co (4.51 x 10^{3} Bq/L) [102]. All the radioisotopes, except ^{137}Cs and ^{60}Co, displayed infinite decontamination factor, and the decontamination factor of ^{137}Cs and ^{60}Co were 43.8 and 4336.5, respectively [102]. Jia et al. reported treatment of a synthetic feed solution containing 10 mg/L $SrCl_2$ or $Co(NO_3)_2$ in a VMD using a PP hollow fiber membrane and reported very high rejection of Co^{2+} (99.67% – 99.82%) and Sr^{2+} (99.60% – 99.74%) in the membrane [183,184]. Decontamination factors (DF) observed for low- and medium-level radioactive wastewater in other treatment processes, like evaporation, ion exchange (organic), ion exchange (inorganic), chemical precipitation, bioaccumulation, biosorption, and reverse osmosis are 10^{3}-10^{6}, 10-10^{3}, 10-10^{4}, 10-10^{3}, more than 10^{3}, less than 10^{3}, and 10-10^{3}, respectively [101,185]. Membrane distillation with its high DFs (almost infinite with many radioisotopes) is a competitive method in treatment and recovery of radioactive wastewater. However, it has to be mentioned that these high-decontamination factors are achieved from low-volatile solutes after adequate pre-treatment [185].

.

Table 2.2: Performances of treatment processes involving MD applied to different types of wastewater treatment and reclamation.

MD setup	Feed type	Pre-treatment	MD performance		Ref.
			Mean permeate flux, L m^{-2} h^{-1} (Time)	Reported rejections, water recovery	
DCMD	TDW	Foam fractionation, Conventional (flocculation-biological) treatment	~5 (0-40 days) ~2 (66 days) ~ 4 (after caustic cleaning)	Sulphate (>99.9%) Water recovery (91.6%)	[86]
DCMD	TDW	NP, physicochemical-biological (anaerobic-aerobic) treatment	NP: 19.8 (~6 hours); <1 (48 hours) P: ~21 (~6 hours); ~18 (48 hours)	NP: Color (94%); Conductivity (98.78%); COD (90%) P: Color (100%); Conductivity (99.95%); COD (96%)	[87]
DCMD	TDW	NP	37.8 (150 minutes) 13-15 (40 hours)	Rejection in 150-minute experiment: Color (95.3%); Conductivity (93.7%); Turbidity (93.0%); TDS (93.6%); COD (89.6%); BOD_5 (90.8%)	[88]
DCMD	TDW	NP	Bare PTFE (salt solution): 32 (24 hours) Bare PTFE (wastewater): 8 (24 hours) Protected PTFE (wastewater): 20 (24 hours)	---	[89]
DCMD	OMW	NP	PTFE: 7.68 ± 0.22 (9 hours) PVDF: 4.95± 0.14 (9 hours)	Phenolic Compound separation factor: PTFE 99%, PVDF 89% (9 hours)	[90]
DCMD	OMW	NP, Coagulation/flocculation, MF	NP: 5.6, Coagulation/flocculation: 6.9, MicrofiltrationL 7.7 (initial); NP: 3.5, Coagulation/flocculation: 5.5, MicrofiltrationL 7.1 (3 hours); NP: 1.44 L m^{-2} h^{-1} (76 hours)	Phenolic Compound separation factor >99% (8 hours)	[91]
DCMD	MW	NP, advanced biological treatment	NP: PTFE 4.1 – 13.5, PVDF 2.9 – 8.6 (1.5 hours) P: PTFE 6 – 16.4, PVDF 2.2 – 8.16 (1.5 hours) (Maximum and minimum variations in flux results from temperature differences of 30°C and 50°C, respectively, between the feed and permeate side)	PTFE: NP (conductivity 93-96%, COD >98.5%, alkalinity 94%, hardness 98%, ammonia-nitrogen 45-50%); P (conductivity 96-98%, COD 89%, alkalinity 87%, hardness 98.7-99.1%, ammonia-nitrogen 50-60%) PVDF: NP (conductivity 74-76%, COD 97%, alkalinity 53-63%, hardness 66-83%, ammonia-nitrogen 31-50 %); P (conductivity 79-81%, COD 89%, alkalinity 65-78%, hardness 76-82%, ammonia-nitrogen 35-40%)	[92]
FO-DCMD	FO feed: sanitary wastewater; DCMD feed: OW+FO permeate	Ultrafiltration for OW	6-8.5 (salt content = 0.1-0.75 mol/L)	High rejection (~99%) achieved for different organic, nutrient and ionic parameters due to complimentary ultrafiltration and FO pre-treatment.	[93]

MD setup	Feed type	Pre-treatment	MD performance		Ref.
			Mean permeate flux, L m^{-2} h^{-1} (Time)	Reported rejections, water recovery	
FO-DCMD	FO feed: secondary MW, DCMD feed: 1M NaCl+FO permeate	FO for secondary MW effluent	Initial: 14.4 (DCMD), 12.24 (FO) Aftre 48 hours: 6.84 (Both FO-DCMD)	Conductivity rejection >97% in first 6 days, then deteriorated rapidly due to the presence of organic materials in the feed solution.	[94]
FO-DCMD	FO feed: secondary MW, DCMD feed: 1M NaCl+FO permeate	FO for secondary MW effluent	---	Overall 99.9% rejection of combined solutes in the system after 48 hours	[95]
FO-DCMD	FO Feed: domestic wastewater, DCMD feed: 35 g/L NaCl+FO permeate	FO for domestic wastewater	FO-DCMD: 17.60 (120 hours)	FO: TOC>95%, NH_3-N>73%, TN>65%, TP>95%, NO_3^- >70%, SO_4^{2-} >95%, PO_4^{3-} >90% FO-DCMD: TOC>98%, NH_3-N>90%, TN>90%, TP>98%, Cl^- >95%, NO_3^- >95%, SO_4^{2-} >98%, PO_4^{3-} >97%	[96]
FO-DCMD	FO feed: raw sewage, DCMD feed: 1.5M NaCl+FO permeate	FO for raw sewage, MD feed solution was pre-treated using GAC or UV	7 (FO-DCMD) 4.5 (DCMD alone) (Cumulative permeate volume of 4000 mL)	>98% for TOC, TN, and UV_{254} absorbance, >83% for conductivity, >90% for trace organic contaminants. 99.5% trace organic contaminants in FO-MD hybrid system coupled with GAC adsorption or UV oxidation.	[97]
DCMD	RCW	Coagulation-sedimentation, filtration, acidification and degasification	RCW with filtration, acidification, and degassing: normalized flux reduced from 0.964 to 0.664 (30 days) RCW with coagulation-sedimentation, filtration, acidification, and degassing: normalized flux reduced from 0.966 to 0.876 (30 days)	---	[98]
DCMD	OW: oil, sodium dodecyl sulfonate and sodium chloride	NP	Normalized flux reduced to 0.4 (600 min)	TOC rejection 49.1 ± 20.3 %	[99]
DCMD	OW: 1 wt% NaCl solution with oil	NP	For 1000 ppm oil: 4.93 ($\Delta T = 60^oC$); 0.55 ($\Delta T = 40^oC$)	Oil rejection: 99.996% and 99.969% (for oil concentration of 1000 ppm and 2000 ppm, respectively)	[100]
DCMD	OW: shale oil and gas produced water	Filtration through 8-µm filter	PVDF: 30.9, 29.4 (initial), 17.3, 23.52 (after 800 ml permeate collection in 16.4 and 14.9 hrs, respectively); PVDF-PVA: 30.3, 31.5 (initial), 23.3, 24.3 (after 800 ml permeate collection in 14.6 and 14.3 hrs, respectively); PVDF-SiO_2-FAS: 23.4, 26.2 (initial), 15.7, 20.2 (after 800 ml permeate collection in 21.1 and 18.1 hrs, respectively)	Salt removal efficiencies >99.9%, distillate conductivity increased by less than 75 µS/cm (corresponds to an increase in salinity of less than 35 mg/L NaCl). Water recovery achieved 53.33%	[79]
DCMD	LLRW	NP	7.85 (120 min)	100% rejections for Cs^+, Sr^{2+}, and Co^{2+}	[101]

MD setup	Feed type	Pre-treatment	MD performance		Ref.
			Mean permeate flux, L m^{-2} h^{-1} (Time)	Reported rejections, water recovery	
DCMD	LLRW	NP	6.75 (20 hours)	High rejection (>90%) for major anions and cations Most radioisotopes were undetectable in permeate. Only Co-60 and Cs-137 were detected in permeate with high rejection values (97.7% and 99.9%, respectively)	[102]
DCMD	LLRW/MLRW	NP	Thickness normalized permeate flux J_w, (kg m^{-1} h^{-1}): SMM1/PES: 0.143, SMM2/PES: 0.16, SMM1/PS: 0.07, SMM2/PS: 0.08, PTFE: 0.155	Almost 100% rejection of non-radioactive ions (Co^{2+}, Cs^{-}, Sr^{2+}); and radioisotopes (^{60}Co, ^{137}Cs, ^{85}Sr)	[103]
DCMD	ROC	NP, GAC	NP: 16 (initial), 11 (at 85% water recovery) P: 16 (initial), 12.3 (at 85% water recovery)	99% ion rejection, more than 90% rejection of all (with GAC) and majority (with NP) micro-pollutants. For NP condition low rejections of propylparaben (50%), salicylic acid (86%), benzophenone (62%), triclosan (83%), bisphenol A (84%), atrazine (88%)	[10]
DCMD	ARD	NP, thermal precipitation	NP: 38.4 (Initial), 36.4~32.7 (after 13 hours) Thermal precipitation pre-treated ARD: 38.4 (Initial), 36.28~36.25 (after 13 hours)	Salt rejection: 99.88 – 99.93% (NP), 99.96% (thermal precipitation pre-treated ARD)	[104]
DCMD	PW	NP	Cefotaxime: 20.6 (initial), ~18.5 (24 hour) Ciprofloxacin: 20.6 (initial), ~19 (24 hour) Tobramycin: 20.6 (initial), ~16 (24 hour)	100% (for neutral and negatively charged antibiotics) 86% (for positively charged Gentamicin sulfate) 78% (for positively charged Tobramycin)	[105]
AGMD	PW	Pre-filtration	2–6.8 (one week)	Diclofenac 99%, Atenolol 99%, Carbamazepine 99-100%, Ciprofloxacin 37-99%, Estradiol 70-98%, Estriol 76-87%, Estrone 66-86%, Ethinylestradiol 72-90%, Hydrochlorothiazide 99-100%, Ibuprofen 95-98%, Ketoprofen 92-98%, Metoprolol 100%, Naproxen 62-95%, Norfloxacin 60-98%, Progesterone 67-83%, Propranolol 96-100%, Ranitidine 89-100%, Sulfamethoxazole 92-99%, Trimetoprim 80-99%	[106]
Modified DCMD	LL	NP, MBR (anoxic+aerobic+UF)	NP: PTFE (0.45 µm) 4.56-9.87, PVDF (0.45 µm) 4.7-8.1 PTFE (0.22 µm) 4.1-6.1, PVDF (0.22 µm) 3.7-7.9 (2 hours) P: PTFE (0.45 µm) 6.5-15.54, PVDF (0.45 µm) 2.5-7.5 PTFE (0.22 µm) 6.0-13.8, PVDF (0.22 µm) 2.4-4.6 (2 hours)	NP (% Rejection range for PTFE, PVDF): Conductivity (75-85%, 77-84%), COD (99-99.5%, 97.8-99.5%), SO_4 (92-95.5%, 91-95.5%), alkalinity (82-91%, 79-87%), hardness (97-99%, 95-97%), NH_4-N (43-73%, 30-62%) P (% Rejection range for PTFE, PVDF): Conductivity (98-99%, 98-99%), COD (97.5-98.5%, 97-97.5%), SO_4 (90-96%, 90-96%), alkalinity (79-93%, 82-87%), hardness (97-98.5%, 97-98.5%), NH_4-N (85-95%, 90-93%)	[107]

MD setup	Feed type	Pre-treatment	MD performance		Ref.
			Mean permeate flux, L m^{-2} h^{-1} (Time)	Reported rejections, water recovery	
FO-DCMD	FO feed: LL, DCMD feed: 4.82 M NaCl and FO permeate	FO	4.75 – 6.29 (250 minutes)	Salt: 96.70%-98.99%, TOC >98%, TN >98%, NH_4^+-N 100%, Hg 100%, As 100%, Sb 100% (250 min)	[108]
DCMD	FW	NP	8.7 (initial), 4.3 (12 hours), 7.6 (after cleaning by pure water)	COD 95.3%, TOC 95.7%, Protein 98.9%	[9]

Note: TDW = textile/dyeing wastewater, OMW = olive mill wastewater, MW = municipal wastewater, RCW = recirculating cooling water, OW = oily wastewater/oil-water emulsion, RW = radioactive wastewater, LLRW = low-level RW, MLRW = mid-level RW, ROC = wastewater reverse osmosis concentrate, ARD = acid rock drainage water, PW = pharmaceutical wastewater, LL = landfill leachate, FW = fermentation wastewater, NP/P = no pre-treatment/pre-treatment, MF = microfiltration, FO = forward osmosis, MBR = membrane bioreactor, DCMD = direct contact membrane distillation (MD), VMD = vacuum MD, AGMD = air gap MD, PP = Polypropylene, PTFE = polytetrafluoroethylene, PVDF = polyvinylidene fluoride, PET = polyester, PS = polysulfone, PES = polyethersulfone, PVA= polyvinyl alcohol, SMM = surface modifying macromolecule, FAS = Heptadecafluoro-1,1,2,2-tetrahydrodecyl triethoxysilane, GAC = granular activated carbon adsorption, TDS = total dissolved solids, COD = chemical oxygen demand, BOD_5 = biochemical oxygen demand, TOC = total organic carbon, NH_3-N/NH_4^+-N = ammonia/ammonium-nitrogen, TN = total nitrogen, TP = total phosphate, NO_3/NO_3^- = nitrate, SO_4/SO_4^{2-} = sulfate, PO_4/PO_4^{3-} = phosphate, Hg = mercury, As = arsenic, Sb = antimony, Co = cobalt, Cs = caesium, Sr = strontium.

Table 2.3: Removal efficiencies (%) of selected pharmaceutical residues in pharmaceutical wastewater using different treatment technologies. (*Values obtained from graphs.)

Pharmaceutical Compound	Activated Sludge	Membrane Bioreactor	Bioreactors with flocculation and sedimentation	Forward osmosis	Nanofiltration	Reverse Osmosis	Air Gap Membrane Distillation	Direct Contact Membrane Distillation
Diclofenac	-143 – 80	-8 – 87.4	-370	92 – 100*, 92.9 - 96	55 – 101*, 94 – 98.5*	98 – 101*	99	
Atenolol	0 – 97	65.5 – 76.7			48 – 96*		99	93.4 – 99.4
Carbamazepine	-122 – 58	-22 – 23		95 – 98*, 84.7 – 94.4	64 – 98*	75 – 100*	99 – 100	
Ciprofloxacin			90.9	98.7 – 99			37 – 99	
Estradiol			>82.6				70 – 98	
Estriol							76 – 87	
Estrone			-343.9				66 – 86	
Ethinylestradiol							72 – 90	
Hydrochlorothiazide	0 – 76.3	0 – 66.3					99 – 100	
Ibuprofen	52 – 99.7	89 – 99.8	98.9	82 – 97*	47 – 100*, 92 – 98*	96 – 102*, 90 – 100*	95 – 98	
Ketoprofen	9 – 91.1	43.9 – 97					92 – 98	
Metoprolol	-1 – 77	29.5 – 58.7		98.1 – 98.7			100	
Naproxen	-2 – 98	71 – 99.3	92.1	64 – 97*, 90.2 – 97.9	53 – 103*		62 – 95	
Norfloxacin				99.7			60 – 98	94.5 – 99.9

Pharmaceutical Compound	Activated Sludge	Membrane Bioreactor	Bioreactors with flocculation and sedimentation	Forward osmosis	Nanofiltration	Reverse Osmosis	Air Gap Membrane Distillation	Direct Contact Membrane Distillation
Progesterone							67 – 83	
Propranolol	59	65.5 – 77.6		95 – 97.8			96 – 100	
Ranitidine	24.7 – 42.2	29.5 – 95		98.8 – 99.3			89 – 100	99.6
Sulfamethoxazole	-138 – 99	57 – 90		88.2 – 93.9	45 – 100*	90 – 100*	92 – 99	
Trimetoprim	-40 – 40.4	47.5 – 66.7			42 – 101*		80 – 99	99.5
Loratadine	15	0 – 33.5						99.6
Paroxetine	91	90						99
Omeprazole								98.5 – 99.1
Cimetidine								99.5 – 99.6
Fenofibrate								95.4 – 99.6
Phenylbutazone								95.8 – 99.9
Phenazone								87.7 – 99.8
Betamethasone								92.4 – 97.6
Prednisone								98.6 – 99.6
Scopolamine								99.9
Metformin								92 – 95.6
Enrofloxacin								92.7 – 95.8
Enoxacin								91.6 – 99.5
Danofloxacin								100
Caffeine					32 – 88*	86 – 101*		89.8 – 93.3
Atorvastatin								93 – 99.3
Ampicillin				~ 100				99.9
Amoxicillin								99.9
Erythromycin				99.5 – 99.8				94.7 – 99.6
Clarithromycin								95 – 96.4
Fluconazole								95.6 – 99.9
Reference	[186]	[186]	[187]	[188], [189]	[190], [191], [192]	[192], [193]	[106]	[182]

Fermentation wastewater, having high organic content, resulted in a 50.5% reduction in flux after 12-hour DCMD treatment with PP membranes without any pre-treatment of feed water [9]. The fermentation wastewater samples were collected from a yeast factory with initial chemical oxygen demand (COD), total organic carbon (TOC) and protein concentrations as 54,900 mg/L, 20,900 mg/L, and 1,765 mg/L, respectively [9]. Gas chromatography-mass spectrometry analysis revealed 14 major organic compounds including isoamyl; 2-methyl butyric acid; 2,3,5-trimethyl pyrazine; 2-acetyl pyrrole; 2-pyrrolidinone; phenethyl alcohol; benzoic acid; phenylacetic acid; 4-ethenyl-2-methoxyphenol; o-hydroxybenzoic acid; p-hydroxyphenyl ethanol; p-hydroxyphenylcyanide; 4-hydroxy-3-methoxyphenethyl alcohol; and butyl phthalate in the fermentation wastewater [9]. Among the dominant organics present in fermentation wastewater, volatile organic compounds (trimethyl pyrazine, 2-acetul pyrrole, phenethyl alcohol and phenylacetic acid) and a non-volatile (dibutyl phthalate) transferred through the membranes and were detected in permeate water due to membrane wetting, which resulted in 95.3% and 95.7% rejection for COD and TOC, respectively [9]. After 5 hours of DCMD operation, 2,3,5-trimethyl pyrazine, 2-acetyl pyrrole and phenethyl alcohol were detected in the permeate stream [9]. While after 10 hours another organic compound phenylacetic acid was detected in the permeate stream, whose late occurrence was attributed to its complex nature. Finally, dibutyl phthalate, which is not a volatile compound, was observed in the permeate stream after 12 hours due to membrane wetting [9]. The deposited foulants were mostly organic components combined with inorganics, which were hard to remove by only water rinsing (for 60 minutes), while most of them were removed in a sequential wash of water, acid ((HCl solution 0.5 mol/L), base (NaOH solution 0.5 mol/L), and water for 10, 20, 20, and 10 minutes, respectively [9]. Transfer of organic matter to the distillate solution through the membrane has also been associated with an adsorption-desorption mechanism [145,194]. Organic humic acid, which initially adsorb on the membrane surface, forms hydrogen bond with water vapor (between the carboxylic group in the humic acid and the oxygen molecule in water vapor) and moves through the membrane pore space. The hydrogen bond weakens as the water vapor moves through the membrane pore space and re-adsorption of humic acid takes place in downstream membrane pore location [194]. This adsorption-desorption process ensues recurrently until the humic acid reaches and disperse into the permeate [194]. Ammonia (NH_4-N) rejection in MD has been reported to be poor in different types of organic wastewater treatment and reclamation in comparison to other

kinds of contaminants [92,107]. Low NH_4-N rejection may be attributed to the preferential generation of volatile ammonia gas and its permeation through membrane pores during the heating process [107]. Recovery of water from raw and biologically pre-treated municipal wastewater by DCMD using PTFE and PVDF membranes was calculated to yield high (about 87-99% for PTFE and 63-97% for PVDF) rejection of the conductivity, COD, alkalinity, hardness and low rejection (about 50-60% for PTFE and 35-50% for PVDF) of NH_4-N [92]. The experimental operating conditions and rejections of these water quality parameters by PVDF and PTFE membranes are separately mentioned in Table 2.1 and Table 2.2, respectively. Increased wetting of PVDF membrane with raw municipal wastewater when compared to PTFE membrane, resulted in reduced NH_4-N rejection efficiency in PVDF membranes [92]. Also, increase in feed stream temperature resulted in a higher temperature gradient across the membrane, which favored volatilization of ammonia gas and its permeation through the membrane pores [92]. DCMD of raw landfill leachates using PTFE and PVDF membranes (operational conditions in Table 2.1) demonstrated high rejection efficiencies for most of the water quality parameters (conductivity, alkalinity, hardness, COD, sulfate) but a low rejection of NH_4-N (Table 2.2) [107]. The presence of organic biomass in wastewater resulted in observable decrease in vapor pressure (due to the non-volatile fraction of biomass) in feed water and reduced the permeate flux in DCMD system to more than 50% and 75% of initial flux value for 6 and 12 g/L biomass, respectively [195].

Oily wastewater recovery using PVDF membrane in DCMD showed that presence of only oil, with salt or surfactant, caused a gradual decline in flux and increase in permeate conductivity, while the presence of oil and surfactants together, with salt, severely affected MD performance [99]. In general, presence of surfactants promotes wetting, while presence of oil enhances fouling through hydrophobic-hydrophobic interaction with membrane surface and pores. Presence of only oil in feed water eventually led to higher fouling and pronounced flux decline, due to higher affinity between the hydrophobic species (i.e., oil) to the hydrophobic MD membrane [99]. Only oily feed water, with 100 ppm oil concentration, did not show any increase in permeate conductivity for 15 hours of operation [99]. The permeate conductivity started to increase after 5 hours when feed stream oil concentration was 200 ppm but was less than 5 μS/cm even after 15 hours of operation [99]. So a gradual increase in permeate conductivity was also observed with increasing oil concentration in feed water, possibly through volatilization of hydrocarbons in the

oil from feed stream (operated at elevated temperature) to the permeate stream. Presence of surfactants with oil stabilized the oil emulsion, which reduced membrane fouling but increased permeate conductivity (indicating an increased tendency to membrane wetting) [99]. Combined presence of both surfactants and oil, along with salt, thus creates a severe situation in which both wetting and fouling contributes to MD performance deterioration. As a result, the membrane flux reduced quickly to 50% (due to membrane fouling) and the permeate conductivity dramatically increased (due to membrane wetting) [99]. The PVDF and PTFE membranes have demonstrated different wicking phenomenon to nonpolar materials such as oil, which may be attributed to the differences in hydrophobicity and surface roughness of the two membranes. The in-air oil contact angle of PVDF membrane was not observable as the oil droplet was completely adsorbed on the membrane surface through hydrophobic-hydrophobic interaction [196], while the in-air contact angle of PTFE membrane with mineral oil was dynamic [197]. The mineral oil droplet initially beaded up upon the more hydrophobic PTFE membrane as drops with measurable contact angles but then penetrated into the porous membrane and propagated along the membrane surface with observable wetting fronts in about 6 minutes [197]. PTFE membranes showed higher surface roughness than PVDF membranes [176], which might be responsible for the dynamic wetting nature of PTFE. Higher surface roughness of PTFE membranes might have caused the formation of initial mineral oil droplets on PTFE surface, which eventually adsorbed on the porous membrane due to hydrophobic-hydrophobic interaction. It should be kept in mind that for wastewater containing oil, MD is not a favorable option due to its inclination to higher fouling. If a high-strength wastewater contains oil, its recovery using MD will depend on how well the membrane can resist fouling due to oil in the feed water. Many novel membrane modifications/fabrications have been made to enhance performance of MD in oily wastewater recovery (discussed in a following section). Some pre-treatment is necessary to lower oil, surfactant, or salt concentration before recovery of oily wastewater using MD [99]. For DCMD of oily wastewater, no oil concentration was detected in the permeate of a feed with up to 1000 ppm oil [100]. This observation might be influenced by the high molecular weight of the crude oil derivative compounds in the feed. For oily wastewater consisting of low molecular weight hydrocarbons, the low molecular weight hydrocarbons will easily volatilize into the distillate.

The different studies carried out using synthetic/simulated wastewater facilitate basic understanding of the interaction between specific types of contaminants and the membrane surface. However, for real wastewater (containing a combination of different dissolved charged contaminants, surfactants, salts, biomass, etc.) the interactions between different constituents and the membranes led to a multidimensional fouling and wetting scenario [9,99]. In almost all cases, MD systems were found to be unsuitable for direct treatment of raw wastewater as both fouling and wetting of membranes occurred soon after the process commenced [9,86,87,99]. There is no data in the literature related to the contribution to different types of fouling (inorganic, organic, and bio fouling) that occur in MD during the recovery of real wastewater. This provides an impetus for conducting a systematic study of different types of wastewater to evaluate their association to different types of fouling, which, in turn, will help in the development of effective and optimized mitigation measures in MD. Also, further investigation of different MD configurations for reclamation of different types of pre-treated wastewater should be carried out.

2.4.2 Influence of operating conditions

Operating conditions such as feed and permeate streams temperatures, feed stream flow rate, membrane pore size, and membrane material have demonstrated considerable influence on the performance of different MD processes (i.e., DCMD, AGMD, VMD). The degrees of permeate vacuum also exhibited noteworthy impact on the overall performance of VMD process. The following sections discuss the influence of these parameters on the performances of different MD processes.

Effect of feed/permeate temperatures: Antoine equation, which expresses the relationship between the vapour pressure (as a driving force for MD process) and feed temperature, demonstrates that the vapor pressure increases exponentially with the temperature following the relation [139]:

$$p_i^0(T) = \exp\left(\alpha - \frac{\beta}{\gamma + T}\right)$$

where, p_i^0 is in Pa, T is the absolute temperature in K, and α, β, and γ are constants that are readily available (for water, these constants are 23.1964, 3816.44, and -46.13, respectively).

Hence, the permeate flux of membrane distillation process is enhanced due to increased feed temperature [140]. While treating 18.5 ppm methylene blue dye containing wastewater with polypropylene membrane via vacuum membrane distillation (VMD) with a feed flow rate of 14 mL/s and a 5 mm Hg pressure with varying temperature (40° – 70°C), the temperature increase resulted in an increase in the permeate flux (4.25, 4.8, 5.6, and 6.3 $kg/m^2/h$ in the first hour for 40°C, 50°C, 60°C, and 70°C respectively) due to the exponential relation between the vapor pressure difference and the temperature [112]. The VMD experiment at vacuum pressure of 10 mbar and Reynolds number (Re) of 4341.6 with PP membrane using 50 ppm RBBR (Remazol Brilliant Blue R) dye from Sigma Aldrich showed an 27.3% increase in flux at 50°C from 27.5 $kg/m^2/h$ flux at 40°C and 62.9% increase in 60° from the 35 $kg/m^2/h$ flux of 50°C [180]. Similar finding was observed in another VMD experiment with saline water where temperature variation of 25°C, 40°C, and 55°C showed flux enhancement with increased temperature [198]. Another study conducted with three different (unmodified, plasma modified, and chemically modified) hydrophobic PVDF hollow fiber membranes at varying feed temperatures of 40ºC, 50ºC, 60ºC, and 70ºC and a permeate temperature of 25ºC with synthetic seawater of 3.5 wt% NaCl solution through a DCMD set-up (with feed and permeate flow rates of 2.5 L/m and 0.4 L/m, respectively) [44], observed exponential increase of flux with increase in temperature for all three membranes. At low feed temperatures, all three membranes had similar permeate fluxes. However, temperature increase showed significant variation in the permeate flux of the three membranes, with unmodified membrane having the highest permeate flux and around 20% flux drop of modified membranes at 70ºC feed temperature due to membrane modification that resulted in partial pore closure, loss of large pores as well as overall decrease in porosity [44]. Hollow fiber VMD process with commercial PP membrane was implemented to study the separation efficiency of Co^{2+} ion from a synthetic solution simulating radioactive wastewater with a varying feed temperature of 30-70°C with 41.8 L/h permeate flow rate and 0.98 atm permeate vacuum degree [183]. Highest permeate flux was observed at 70°C temperature with an exponential increase of the flux with an increase in temperature (R^2=0.9845) due to the change in the saturated vapor pressure of the solution. Another study on a full-scale spiral wound module with PTFE membrane with a PP support in a PGMD set up with an evaporator inlet temperature of 80°C, and saline water (0-105 g/kg) as feed at a feed flow rate 500 kg/h varied the a condenser inlet temperature (20°C-40°C) to observe the condenser inlet temperature variation effects on the permeate flux [132]. The result

demonstrated a decrease of output rate with an increase in the condenser inlet temperature rate ranging in between 9 to 25 kg/h for 0-105 g/kg of salinity [132]. The highest flow rates of 25, 24, 22, 20, 17.5, and 15 kg/h were observed for the salinity 0, 13, 35, 50, 75, and 105 g/kg, respectively, when the condenser inlet temperature was the lowest, 20°C. The flow rates observed for the same salinity values were 20.5, 18.2, 16.5, 14.5, 12, and 9 kg/h, respectively, when the condenser inlet temperature was 40°C [132]. Another study conducted with FO draw solute as the feed on DCMD operation observed 250% enhancement in permeate flux (from 10 kg/m^2/h to 35 kg/m^2/h with a cold permeate temperature of 15°C) while increasing feed temperature from 40°C to 70°C [95]. The same study observed enhanced permeate flux through lowering the permeate temperature from 30^{o}C to 15^{o}C with different feed temperatures of 40^{o}C (about 100% permeate flux increased from 5 kg/m^2/h to 10 kg/m^2/h) and 70oC (about 25% permeate flux increased from 28 kg/m^2/h to 35 kg/m^2/h) [95].

Studies also revealed that temperature gradient enhancement between the membrane surfaces positively influence the diffusion resulting in enhanced permeate flux [199,200]. Similarly, increased feed temperatures led towards reduced temperature polarization and hence enhanced the mass transfer across the membrane [95,201]. Also, enhancing the feed temperature demonstrated significant increase in permeate flux compared to reducing the permeate temperature due to low alteration in vapor pressure [70,95]. Table 2.4 summarizes the effect of feed/permeate temperature on the permeate flux performance of various MD configurations (DCMD, VMD, AGMD, etc.).

Effect of feed cross flow rate: The boundary layer resistance minimization at increased flow rate leads towards enhanced mass transfer by increasing the heat transfer coefficient [202]. The enhancement in flow rate results in high permeate flux due to the reduced thermal boundary layer thickness and consequent decreased temperature polarization effects [199]. Elevated flux of 9.22 kg/m^2/h was observed as the boundary layer resistance decreased to 1.74x10^6 m^2s Pa/kg with an increase in cross flow velocity of 0.014 m/s (from 0.005 m/s) at fixed feed temperature of 70^{o}C [195]. An approximate three times increase in cross flow velocity (from 0.005 m/s to 0.014 m/s) decreased the boundary layer and increased the flux by 1.27 times (from 7.22 L/m^2/h to 9.22 L/m^2/h) [195]. The effect of varying feed flow rate (14, 17, 30, 42, and 57 mL/s) was investigated for 18.5 ppm methylene blue dye containing wastewater by vacuum membrane distillation using

a PP membrane at 50°C feed temperature [112]. At Reynolds numbers < 5000, significant flux increase was observed with the increase in the flow rate. This was due to the prevention of the pore blocking by the dye molecules as well as reduced temperature and concentration polarization effect due to enhanced heat and mass transfer [112]. A study with a VMD configuration having 19.1, 26, 34.9, and 41 L/h flow rates with a feed temperature of 50°C and vacuum pressure of 10 mbar for 50 ppm RBBR (Remazol Brilliant Blue R) dye solution observed permeate fluxes of 23.5, 26, 26.5, and 28.5 kg/m^2/h, respectively over a 100 minutes operation period [180]. High flow rate resulted in high heat transfer coefficient leading towards higher permeate flux of the VMD system [180]. Flow rate increase from 15 mL/s to 30 mL/s in a VMD experiment using a PP membrane with saline (NaCl) water reduces both the temperature and concentration boundary layer thicknesses near the membrane interface due to higher turbulence flow leading towards enhanced VMD performance [198]. Flow rate variation along with module size variation also significantly affects the hydrodynamic conditions in the hollow fiber DCMD process [44]. Flow variation from 2 to 7.5 L/m kept the MD flux unchanged in a smaller 9.5-mm housing module as the feed stream reached turbulence within this range. However, for a bigger 19-mm housing module, initial increase of permeate flux was observed with an increase in flow rate and eventually, an asymptotic value was reached at feed side Reynolds number (Re_f) > 2500 [44]. However, the maximum permeate flux was lower in the big module under same operating conditions due to the similar permeate flow rate in both modules that resulted in lower permeate side Reynolds number (Re_p) as well as the larger fiber length of the big module. This study revealed that moderate feed flow rate can be adequate if satisfactory permeate flux is achieved as enhanced flow rate has no additional advantages once the turbulence is reached [44]. The study also demonstrated that lumen side (permeate side) flow rate also has impact on permeate flux as increasing the permeate flow rate can result in improved heat transfer and reduction of temperature polarization effect on the permeate side that can enhance the driving force. However, increasing permeate flow rate resulted in an enhanced permeate flux mostly in the low permeate side Reynolds number (Re_p < 300) [44]. At Reynolds numbers higher than 300 the permeate flux reached a steady asymptotic value, which might have resulted from the enhanced transverse vapor flux causing higher mixing on the membrane surface by breaking down the laminar boundary layer that aided the permeate side heat transfer. This study concluded with the recommendation of using a reasonably low permeate

circulation flow rate to optimize the MD performance with relatively low energy consumption [44].

Feed flow velocity variation of 10.5 to 41.8 L/h was conducted with a feed temperature of 70°C and permeate vacuum degree of 0.98 atm to elucidate the effect of flow velocity while removing cobalt ions from simulated radioactive wastewater [183]. Linear correlation (R=0.9912) was observed between the permeate flux and the feed flow velocity because of the variation in the thickness of the boundary layer formed between the membrane and the bulk solution due to the accumulation of the retained Co(II). The study also observed that permeate flux was more affected by the permeate vacuum and the feed temperature than the feed flow velocity [183]. Full-scale spiral wound module with PTFE membrane (having a PP support) was studied in a PGMD set up, with a condenser inlet temperature of 25°C, an evaporator inlet temperature of 80°C, and the feed flow rates varied to 200, 300, 400, and 500 kg/h [132]. The result demonstrated an increase of output rate with an increase in the feed flow rate ranging in between 2.5 to 25 kg/h for 0 – 105 g/kg salinity. The high flow rates resulted in enhanced flux with the same salinity and parallel curves were detected for different salinity feed [132]. AGMD study with simulated seawater using a 0.45 μm PVDF membrane was carried out at 60°C feed temperature and 20°C cold stream temperature with varying feed flow rate (1 – 5.7 L/m) as well as varying cold stream flow rate (1 – 4.5 L/m) [70]. The hot feed flow rate variation caused a permeate flux increase from 2.7 to 3.4 $kg/m^2/h$ whereas the cold stream flow rate variation resulted in similar permeate flux (around 3.4 $kg/m^2/h$) with a feed flow rate of 5.5 L/min without any significant influence [70]. The negligible effect of cold stream flow rate on permeate flux in AGMD can be explained by the overall heat transfer coefficient, which includes the hot-side, the air-gap, and the cold-side heat transfer coefficients. As the heat transfer coefficient in the air-gap is much smaller than the hot and the cold-side heat transfer coefficients, it will dominate the overall heat transfer coefficient. Hence the change in the cold stream flow rate will have little effect on permeate flow rate. It should be pointed out here that the heat transfer coefficients of the hot-side and cold-side is dependent on geometry of the membrane module and the characteristics of the fluid flow [70]. Table 2.5 summarizes the findings from studies evaluating the impact of varying feed flow rates on permeate flux.

Table 2.4: Effects of feed/permeate stream temperatures on permeate flux for different MD configurations. (*Values obtained from graphs.)

MD Configuration	Membrane/ Module	Pore size/ Mean pore diameter (µm)	Major Feed Constituent	Concentration	Feed flow rate/ velocity	Pressure (for VMD)	Feed Temperature (T_f), Permeate/cold-side Temperature (T_p)	Permeate Flux	Ref.
VMD	PP/ Flat Sheet	0.2	Methylene blue dye	18.5 mg/L	14 mL/s	5 mm Hg	T_f = 40°C, 50°C, 60°C, 70°C	4.25, 4.8, 5.6, 6.3 kg/m^2/h	[112]
VMD	PP/ Flat Sheet	0.2	Remazol Brilliant Blue R (RBBR) dye	50 mg/L	0.78 – 1.67 m/s	10 mbar	T_f = 40°C, 50°C, 60°C	27.5, 35, 57 kg/m^2/h	[180]
VMD	PP/ Flat Sheet	0.2	NaCl	100,200,300 g/L	15 mL/s, 30 mL/s	40 – 120 mbar	T_f = 25°C, 40°C, 55°C	~1.8 – 15 kg/m^2/h *	[198]
DCMD	PTFE/ Flat Sheet	0.1	Tapioca starch based synthetic wastewater	COD (1240±360 mg/L), NH_3-N (512±70 mg/L), VFA (512±112 mg/L), TS (2918±236 mg/L), TDS (3008±172 mg/L)	250 – 1000 mL/min (0.005 – 0.014 m/s)	-	T_f = 40°C, 50°C, 60°C, 70°C T_p = 10°C	1.41, 2.66, 4.51, 7.22 L/m^2/h (for 250 mL/min) 1.67, 2.94, 4.97, 7.35 L/m^2/h (for 500 mL/min) 1.80, 3.09, 5.38, 7.71 L/m^2/h (for 600 mL/min) 1.82, 3.34, 6.4, 8.98 L/m^2/h (for 800 mL/min) 2.09, 3.44, 6.62, 9.22 L/m^2/h (for 800 mL/min)	[195]
DCMD	PVDF/ Hollow Fiber (unmodified, plasma modified, chemically modified)	0.421 (unmodified) 0.191 (plasma modified) 0.189 (chemically modified)	NaCl	3.5 wt%	2.5 L/min	-	T_f = 40°C, 50°C, 60°C, 70°C T_p = 25°C	~6 – 65 kg/m^2/h *	[44]
VMD	PP/ Hollow Fiber	0.18	$Co(NO_3)_2$	10 mg/L	41.8 L/h	0.98 atm	T_f = 30°C - 70°C	~0.65 – 6.1 L/m^2/h *	[183]
PGMD	PTFE/ Spiral wound	0.2	Salinity	0-105 g/kg	500 kg/h	-	T_f = 80°C (Evaporator inlet) T_p = 20°C - 40°C (Condenser inlet)	~9 – 25 kg/h *	[132]
DCMD (in an integrated FO-MD setup)	PP/ Flat Sheet	0.22	NaCl (FO Draw Solution)	0.25 – 2 M	0.4 L/min	-	T_f = 40°C, 50°C, 60°C, 70°C T_p = 15°C T_f = 40°C	~10 – 35 L/m^2/h * ~5 – 10 L/m^2/h *	[95]

MD Configuration	Membrane/ Module	Pore size/ Mean pore diameter (µm)	Major Feed Constituent	Concentration	Feed flow rate/ velocity	Pressure (for VMD)	Feed Temperature (T_f), Permeate/cold-side Temperature (T_p)	Permeate Flux	Ref.
							T_p = 30°C, 25°C, 20°C, 15°C T_f = 70°C T_p = 30°C, 25°C, 20°C, 15°C	~28 – 35 L/m^2/h *	
AGMD	PVDF/ Flat Sheet	0.45	Simulated Seawater (Cl, Na, Mg, Ca, K, Br, B, F)	Cl (18,600 mg/L), Na (10,400 mg/L), Mg (1,290 mg/L), Ca (410 mg/L), K (380 mg/L), Br (62 mg/L), B (4.9 mg/L), F (1.9 mg/L)	5.5 L/min	-	T_f = 40°C – 70°C* T_p = 7°C – 30°C	~1 – 7 kg/m^2/h *	[70]
VMD	PP/ Hollow Fiber	0.18	CsCl, $CsNO_3$, NaCl	10 mg/L	41.8 L/h	5.05 kPa	T_f = 30°C -70°C	~0.7 – 6.4 L/m^2/h	[203]
AGMD	Electrospun PVDF, PVDF (Commercial)/ Flat Sheet	0.37 (Electrospun PVDF) 0.22 (Commercial PVDF)	$Pb(NO_3)_2$	1000 mg/L	1.5 L/min	-	T_f = 30°C,40°C,50°C,60°C, 70°C T_p = 7°C T_p = 7°C,10°C,15°C,20°C,25°C, 30°C T_f = 60°C	~4.5 – 28 L/m^2/h * (Electrospun PVDF) ~3.5 – 24 L/m^2/h * (Commercial PVDF) ~21.8 – 15.7 L/m^2/h * (Electrospun PVDF) ~16 – 11.5 L/m^2/h * (Commercial PVDF)	[76]
DCMD	PVDF/ Flat Sheet	0.20	NaCl	17.76 wt%	0.145 m/s	-	T_f = 79°C T_p = 20.5°C	~0.002 – 0.013 kg/m^2/s *	[204]

Note: DCMD = direct contact membrane distillation (MD), VMD = vacuum MD, AGMD = air gap MD, PGMD = permeate gap MD, PP = Polypropylene, PTFE = polytetrafluoroethylene, PVDF = polyvinylidene fluoride.

Table 2.5: Effects of feed stream flow rate/velocity on permeate flux for different MD configurations. (*Values obtained from graphs.)

MD Configuration	Membrane/ Module	Pore size/ Mean pore diameter (µm)	Major Feed Constituent	Concentration	Feed Temperature (T_f), Permeate/cold-side Temperature (T_p)	Pressure (for VMD)	Feed flow rate/ velocity	Permeate Flux	Ref.
VMD	PP/ Flat Sheet	0.2	Methylene blue dye	18.5 mg/L	T_f = 50°C	5 mm Hg	14, 17, 30, 42, 57 mL/s	4.75, 5, 6, 8.1, 8.2 kg/m^2/h	[112]
VMD	PP/ Flat Sheet	0.2	Remazol Brilliant Blue R (RBBR) dye	50 mg/L	T_f = 50°C	10 mbar	19.1, 26, 34.9, 41 L/h	22.5, 26, 26.5, 28.5 kg/m^2/h	[180]
VMD	PP/ Flat Sheet	0.2	NaCl	100 g/L	T_f = 55°C	40 – 120 mbar	15, 30 mL/s	~5 – 14.5 kg/m^2/h *	[198]
DCMD	PTFE/ Flat Sheet	0.1	Tapioca starch based synthetic wastewater	COD (1240±360 mg/L), NH_3-N (512±70 mg/L), VFA (512±112 mg/L), TS (2918±236 mg/L), TDS (3008±172 mg/L)	T_f = 40°C, 50°C, 60°C, 70°C T_p = 10°C	-	250, 500, 600, 800, 1000 mL/min (0.005, 0.008, 0.01, 0.012, 0.014 m/s)	1.41, 1.67, 1.8, 1.82, 2.09 L/m^2/h (for 40°C) 2.66, 2.94, 3.09, 3.34, 3.44 L/m^2/h (for 50°C) 4.51, 4.97, 5.38, 6.4, 6.62 L/m^2/h (for 60°C) 7.22, 7.35, 7.71, 8.98, 9.22 L/m^2/h (for 70°C)	[195]
DCMD	PVDF/ Hollow Fiber	0.421	NaCl	3.5wt%	T_f = 50°C T_p = 25°C	-	0.82-3.06 m/s (9.5 mm housing) 0.17-1.05 m/s (19.5 mm housing)	~12.5 – 15 kg/m^2/h * (9.5 mm housing) ~6 – 11 kg/m^2/h * (19.5 mm housing)	[44]
VMD	PP/ Hollow Fiber	0.18	$Co(NO_3)_2$	10 mg/L	T_f = 70°C	0.98 atm	10.5-41.8 L/h	~4.5 – 6.1 L/m^2/h *	[183]
AGMD	PVDF/ Flat Sheet	0.45	Simulated Seawater (Cl, Na, Mg, Ca, K, Br, B, F)	Cl (18,600 mg/L), Na (10,400 mg/L), Mg (1,290 mg/L), Ca (410 mg/L), K (380 mg/L), Br (62 mg/L), B (4.9 mg/L), F (1.9 mg/L)	T_f = 60°C T_p = 20°C	-	1-5.7 L/min	~2.7 – 3.4 kg/m^2/h *	[70]

MD Configuration	Membrane/ Module	Pore size/ Mean pore diameter (µm)	Major Feed Constituent	Concentration	Feed Temperature (T_f), Permeate/cold-side Temperature (T_p)	Pressure (for VMD)	Feed flow rate/ velocity	Permeate Flux	Ref.
VMD	PP/ Hollow Fiber	0.18	CsCl, $CsNO_3$, NaCl	10 mg/L	T_f = 70°C	5.05 kPa	10.5-41.8 L/h	~4.8 – 6.8 L/m^2/h *	[203]
PGMD	PTFE/ Spiral wound	0.2	Salinity	0-105 g/kg	T_f = 80°C T_p = 25°C	-	200-500 kg/h	~2.5 – 25 kg/h *	[132]
AGMD	Electrospun PVDF, PVDF (Commercial)/ Flat Sheet	0.37 (Electrospun PVDF) 0.22 (Commercial PVDF)	$Pb(NO_3)_2$	1000 mg/L	T_f = 60°C T_p = 7°C	-	0.5-1.5 L/min	~18.6-22 L/m^2/h * (Electrospun PVDF) ~13.79 – 16 L/m^2/h * (Commercial PVDF)	[76]
DCMD	PVDF/ Flat Sheet	0.20	NaCl	17.76 wt%	T_f = 43.2°C, 68°C T_p = 20.5°C	-	0.08-0.33 m/s *	~0.0019 kg/m^2/s * (T_f = 43.2°C) ~0.007 – 0.008 kg/m^2/s * (T_f = 68°C)	[204]
DCMD	PVDF/ Flat Sheet	0.22	NaCl	35 g/L	T_f = 60°C T_p = 20°C	-	1.85-3.7 m/s	~30 – 38 kg/m^2/h *	[205]
AGMD	PTFE, PTFE with PP support/ Flat Sheet	0.45 (PTFE) 0.20 (PTFE, PTFE-PP)	Sucrose	150 g/L	25°C (Transmembrane Temperature)	-	8-58 L/h	~90 – 156 mL/h * (PTFE 0.45) ~78 – 132 mL/h * (PTFE 0.2) ~67 – 90 mL/h * (PTFE-PP 0.2)	[206]

Note: DCMD = direct contact membrane distillation (MD), VMD = vacuum MD, AGMD = air gap MD, PGMD = permeate gap MD, PP = Polypropylene, PTFE = polytetrafluoroethylene, PVDF = polyvinylidene fluoride.

Effect of membrane pore size: Highly hydrophobic, thermally stable, and chemically resistant commercial PTFE membranes of different pore sizes (1 μm, 0.45 μm, and 0.2 μm) with a feed flow rate of 1.5 L/m and feed temperature of 50°C were investigated in terms of permeate flux, salt rejection, and energy consumption by AGMD module with a varying range of concentrations of different salts, NaCl (5,844 – 180,000 mg/L), $MgCl_2$ (4,760 – 95,210 mg/L), Na_2SO_4 (4,260 – 142,000 mg/L), and Na_2CO_3 (5,300 – 106,000 mg/L) [69]. Permeate flux of the pure water increased with the increase of the membrane pore size irrespective of the salt types due to enhanced mass transfer in the pores, with highest increase with NaCl (39.6% and 56.9% increase for 0.45 μm and 1 μm from 0.2 μm) at 180,000 ppm; and lowest increase with Na_2SO_4 (10.9% and 23.22% increase for 0.45 μm and 1 μm from 0.2 μm) at 142,040 ppm. Also, the study observed correlations among concentration, pore size, and permeate flux. With increasing pore size, the high concentration caused a decrease in the rejection, whereas at 0.2 μm pore size (the lowest pore used in this study), the effect of concentration was insignificant. This results from the decrease in the LEP with an increase in the pore size under higher concentrations [69]. Moreover, high concentration and high pore size results in fouling enhancement. Scale and foulant layers on the membrane surface results in reduced membrane hydrophobicity [207]. The scale formation initiated with largest pores on the membrane surfaces leading towards membrane wetting. The difference in pore sizes did not have a major influence on the energy consumption of the AGMD process, and a slight decrease in the energy consumption was observed with the highest pore sizes due to enhanced mass transfer [69]. Investigating dyeing wastewater treatment efficiency through commercially available PVDF membranes (Durapore HVHP 0.45 μm and GVHP 0.22 μm) exhibited high flux with 0.45 μm membrane compared to 0.22 μm membrane, however, better permeate quality by high rejection of dye was attained through the smaller pore size [176]. The high rejection of dyes with smaller pore size in the PVDF membrane could be attributed to lower partial wetting of the 0.22 μm membrane pores compared to 0.45 μm membrane pores [176].

Effect of membrane material: PVDF (GVHP, 0.22 μm) and PTFE (TF-200, 0.2 μm) membranes were implemented to study a simulated dyeing wastewater treatment via a DCMD application. It was revealed that the PTFE membrane demonstrated 63% higher flux when compared to PVDF membrane [176]. Two possible reasons were attributed for the efficient color rejection by PTFE membranes. It was postulated that the dye molecules could not enter the membrane pores due to

the formation of the dye-dye flake-type foulant (foulant-foulant) on the membrane surface, and this loosely bound dye foulant and high fraction of water had a repulsion effect to the hydrophobic PTFE membrane surface. As a result, the PTFE membrane did not suffer from membrane wetting, and its properties could be recovered through water flushing [176].

Effect of permeate vacuum pressure for VMD: Permeate side vacuum degree (pressure difference between the vacuum and feed side) was varied from 0.1 to 0.98 atm (~10 – 100 kPa) with 70°C feed temperature and 41.8 L/h feed flow rate while removing Cobalt ions in a hollow fiber VMD system [183]. No permeate flux was observed till the permeate side vacuum degree was more than 0.6 atm as positive pressure difference was reached beyond this point. An increase in the permeate side vacuum degree above 0.6 atm resulted in an enhanced permeate flux with a steady value of around 6 $L/m^2/h$ at vacuum degree above 0.9 atm [183]. Another notable observation was that the permeate side pressure was not homogenous all through the shell side and there was a pressure build up in the shell side opposite to the vacuum chamber as it was not stripped away in time resulting in accumulation and reduced driving force. The study suggested instead of having a permeate side vacuum degree as high as possible; it should be optimized so that the pressure buildup can be avoided. For this specific study the optimized value for permeate side vacuum degree was 0.9 atm [183]. Another study using VMD configuration with a PP membrane with sodium chloride as feed to simulate highly saline water observed reduced VMD performance (i.e., reduced permeate flux) with increasing vacuum side pressure from 40, 60, 80, 100 to 120 mbar [198]. Increasing pressure on the vacuum side lowers the pressure difference between the feed and permeate side of the membrane and hence lowers the driving force for passage of water vapor through the membrane pores. The study found vacuum pressure is the most significant contributing factor in VMD performance compared to the temperature, flow rate, and feed concentration [198]. Another study investigated the variations in vacuum side pressure from 5.05 kPa to 90.9 kPa at 70°C feed temperature and with a lumen side flow rate of 41.8 L/h in a hollow fiber VMD setup to observe the efficiency of cesium removal from feed water and had similar findings where nearly zero permeate flux was observed for 40.4 kPa or more vacuum side pressure [203]. For vacuum side pressure less than 40.4 kPa, gradual increases in permeate flux was observed. Decreasing vacuum side pressure from 40.4 kPa to 5.05 kPa resulted in enhanced permeate flux from 0.5 $L/m^2/h$ to 7 $L/m^2/h$ [203].

The influence of different operating conditions on the permeate flux and contaminant rejection performance in different MD configurations is equally important as the feed water composition. While a number of studies have demonstrated the impact of operational parameters on MD performance while recovering selected types of wastewaters (hyper saline wastewater, radioactive wastewater, organic wastewater etc.), there are scopes to comprehensively observe effect of these operational parameters for other challenging wastewater categories (e.g., oily wastewater, textile wastewater, pharmaceutical wastewater, etc.) in different MD configurations. It should be mentioned that the extent of fouling and wetting would change with varying operational conditions when MD is employed for recovery of wastewater. Hence there are great prospects in studying performance of different MD configurations (both traditional and emerging), in terms of permeate flux and contaminant rejection, under different operating conditions. A better understanding on how membrane fouling and wetting is influenced by wastewater compositions and operational conditions in a MD configuration will enable effective selection of mitigation approaches for enhanced treatment and recovery in MD process.

2.5 Mitigation of fouling and wetting in MD

2.5.1 Pre-treatment of feed wastewater

Conventional treatment approaches, such as physicochemical (coagulation-flocculation) and/or biological treatment, have been applied as pre-treatment options for textile/dyeing wastewater [86,87], municipal wastewater [92], and olive mill wastewater [91] prior to MD. Reduction of organic content through biological treatment and particulates through physicochemical (coagulation-flocculation) treatment reduced the fouling potential of different complex wastewaters. In case of textile dyeing wastewater, pre-treatment using physicochemical and biological (anaerobic + aerobic) processes resulted in lower fouling and wetting in PTFE membranes. Over a period of 48 hours the pre-treated wastewater showed only a 14% drop in flux compared to more than 97% drop for the same with raw wastewater and the conductivity observed in the permeate stream for pre-treated wastewater, after 48 hours, was also only about 2.8% of that observed with raw wastewater (Table 2.2) [87]. These pre-treatments yielded stable performance with no significant change in flux during extended bench-scale DCMD operation using PTFE

membrane [86,87]. In addition to enhanced flux, the COD, color, and conductivity rejections of pre-treated textile/dyeing wastewater were enhanced when compared to raw wastewater [87]. Active surface substances were removed from textile/dyeing wastewater using a simple foam fractionation process, which slightly reduced the membrane flux and kept the permeate quality within acceptable levels [86]. The foam-fractionation process is an adsorptive separation technique in which air is sparged to produce bubbles in a separator liquid column and as the air bubbles travel through the continuous phase, surfactant adsorbs at the air-liquid interface [208]. Once emerged from the liquid, the air bubbles form a honeycomb-structured cell in the foam matrix with a surfactant-stabilized thin liquid film between the air bubbles. After separation, the collapsed foam solution offers a highly concentrated solution of surfactants separated from the initial solution [208]. Dow et al. reported a 60% drop in trans-membrane flux in 2.5 hours and immediate occurrence of membrane wetting when raw textile wastewater was used as feed water in a bench-scale DCMD system with PTFE membrane [86]. While, a pilot-scale study carried out with continuous foam fractionation of conventionally (physicochemical-biological) treated textile/dyeing wastewater produced no wetting of membranes over a 3-month trial [86]. The mass transfer coefficient (flux per unit trans-membrane pressure) of the module declined to 40% of its initial value after more than 65 days, and caustic cleaning efficiently restored it to 79% of the original value [86]. In the case of municipal wastewater, biological pre-treatment enhanced DCMD performance for both PTFE and PVDF membranes [92].

Performance of the DCMD process for the reclamation of raw and pre-treated (coagulation/flocculation or microfiltration) olive mill wastewater were carried out using PTFE and PVDF membranes [90,91]. PTFE membranes showed better separation coefficients and olive mill wastewater concentration factors, but permeate flux decreased rapidly in the first 30 hours of treatment for raw olive mill wastewater [91]. Microfiltration pre-treatment was more efficient than coagulation/flocculation in removing total organic carbon (TOC) and total solids from olive mill wastewater. Therefore, of the two pre-treatment processes, the integrated microfiltration-DCMD method was found to be more effective for obtaining clean water from olive mill wastewater [91]. Application of membrane bio-reactor (anoxic, aerobic and ultrafiltration) as a pre-treatment for the landfill leachates demonstrated better effluent quality and higher flux in MD due to reduced organic contaminants in feed water [107].

Other pre-treatment options reported in the literature include thermal pre-treatment of acid rock drainage, granular activated carbon adsorption (GAC) for RO concentrate, and coagulation-precipitation-filtration-acidification-degassing for recirculating cooling water. High variability in membrane scaling and flux of raw acid rock drainage through the membrane has been linked to precipitate formation in this system [104]. 85% water recovery with only a 13-15% decline in flux and a 99% ion rejection were achieved. The high organic content of RO concentrate caused a significant reduction in membrane hydrophobicity and attributed to adhesion of low molecular weight organics onto the membrane. GAC pre-treatment helped reduce organic content of RO concentrate by 46-50% and adsorbed a range of hydrophobic and hydrophilic micro-pollutants, ensuring high-quality water production in the associated MD [10]. About 15-18% improvement in batch recovery was achieved, in a vacuum-enhanced DCMD, by dosing a RO brine feed water with a calcium sulfate scale inhibitor (Pretreat Plus 0400, dosing range 2 – 8 ppm) [209]. With dosing of a scale inhibitor in feed water, the flux declined rapidly at first and was partially recovered afterwards. The unusual flux behavior was attributed to the formation of amorphous silica and silicates, which precipitate in a series of steps generating soft and hard gels [209]. The initial rapid flux decline was attributed to the formation of soft silica gels that form on the membrane surface and further reaction of this silica resulted in hard gels, which were scoured off of the membrane surface [209]. Recirculating cooling water operating at several cycles of differing concentration have high levels of contaminants, and chemicals were added for corrosion, scaling and bio-fouling management of cooling system water [210–213]. Reclamation of recirculating cooling water from a coal-fired power plant (with 2-3 cycles of concentration) by MD requires a series of pre-treatment steps such as coagulation, precipitation, filtration, acidification, and degassing [98]. Incorporation of coagulation at the beginning of the pre-treatment scheme demonstrated a 23% improvement MD flux after 30 days when compared to a pre-treatment scenario with no coagulation. Coagulation removed most of the natural organic matter and chemical additives in recirculating cooling water, resulting in the formation of bigger magnesium-calcite crystal deposits on the membrane surface. The larger sized deposits could not enter the membrane pores and only cause partial wetting of the membrane and hence enhanced trans-membrane flux [98]. pH adjustment of feed water has been studied as an option for prevention and management of silica scaling in MD while recovering cooling tower makeup water of a geothermal

power plant [214]. Silica polymerization and scaling risk in MD was reduced at feed water pH of below 5, or above 10 [214]. Consideration of cost (for pH adjustment to 5.0 using HCl or 11.0 using NaOH) and scaling tendencies of the cooling water indicated that feed water pH adjustment with HCl might provide a viable pre-treatment strategy for recovery of studied power plant cooling water [214]. For each particular type of wastewater, pre-treatment options should be selected to remove target contaminants responsible for fouling and wetting in MD. The pre-treatment options should be selected to remove potential foulants in the wastewater such as particulates, colloids, inorganic salts, organic contaminants, and microorganisms. Application of microfiltration, ultrafiltration, or nanofiltration can effectively remove particulates, colloids, and microorganisms [40,91]. Since MD employs hydrophobic membranes to treat and recover fresh water, feed water with high hydrophobic contaminants (e.g., oil, hydrophobic organic material) can cause serious fouling due to the strong hydrophobic-hydrophobic interaction [16,215,216]. On the other hand contaminants such as low surface tension and water miscible liquids (e.g., alcohols), amphiphilic molecules (e.g., surfactants), or other natural surface active agents can induce wetting in hydrophobic membranes [194,197,217]. Table 2.1 and 2.2 highlights different pre-treatment options used in the studies involving treatment and recovery of different wastewater. While the pre-treatment options like coagulation/flocculation, biological (anaerobic-aerobic) treatment, membrane based (ultrafiltration, microfiltration) processes offer removal of different range of contaminants; some pre-treatment options have been employed at removal of specific contaminants (e.g. foam fractionation used for removal of surfactants, granular activated carbon or ultraviolet treatment for removal of organic contaminants, etc.).

2.5.2 Application of integrated MD processes

MD has been integrated with other separation technologies to enhance the overall water recovery performance in a treatment scheme. It can be integrated easily and inexpensively (as it is not a pressure driven system) to a hybrid system and is one of the most preferred membrane processes for inclusion in a hybrid separation technologies [218]. Having an integrated separation process improves the fouling and wetting scenarios in MD operation, and the hybrid system can generate consistent flux over long term. A number of studies have reported hybrid systems incorporating MD to recover high-strength wastewater.

Integration of MD into other desalination processes like RO, NF, and MED units have been reported to reduce brine discharge, enhance overall fresh water production and energy efficiency [204,219–223]. The MD receives the reject water from the desalination processes as feed and further improves the water recovery performance of the entire process. The scaling of inorganic salt crystals is the main concern when MD is integrated to RO [221,223]. Use of integrated RO-MD system has also been reported for reclamation of wastewater [10,222]. With RO concentrate originating from wastewater recovery, fouling scenario deteriorates as organic fouling adds to the inorganic scaling [10,42].

Application of an integrated FO-MD process, with or without additional pre-treatment processes, has been reported to offer successful treatment and reclamation of different types of wastewaters. The FO process offers the advantage of higher rejection, while using a dense membrane at ambient pressure, and less fouling propensity as compared to other membrane based separation processes (e.g., microfiltration or ultrafiltration) [224–226]. As a result, FO requires less scouring and less frequent backwashing than microfiltration or ultrafiltration [227]. MD can be considered as an economic option for recovery of FO draw solution in wastewater treatment to produce fresh water from the initial wastewater feed, provided that waste or low quality heat source is available [228,229]. In comparison to RO, MD does not require high electrical energy input to recover FO draw solution by application of high hydraulic pressures [230,231]. In an integrated FO-MD process, the FO carries out the initial wastewater treatment as water is separated from dissolved solutes and passes through a semi-permeable FO membrane towards the highly concentrated (relative to feed solution) draw solution. This diluted draw solution then acts as a feed to the MD process, which continuously regenerates the FO draw-solute. Use of a cellulose-triacetate FO membrane and PVDF hollow fiber MD membrane in an integrated FO-MD setup for real domestic wastewater treatment (with 35 g/L NaCl as draw solution and real domestic wastewater as feed solution for FO) yielded less fouling in the MD membrane as compared to the FO membrane, over 120-hours of continuous experiment [96]. The FO membrane being the first barrier in contact with the feed water showed more fouling than MD. Water quality analysis indicated that the FO membrane removed a significant percentage of the contaminants and the integrated FO-MD process removed more than 90% contaminants [96]. Husnain et al. (2015) introduced secondary treated municipal wastewater effluent as the FO feed in an integrated FO-MD system for treatment,

with 1 M NaCl solution used as the FO draw/MD feed, and purified water used as the permeate [94,95]. While the FO membrane showed a gradual flux decline over time, for MD, most of the flux declined in the initial 4-6 hours and remained consistent throughout the 50-hour long experiment. For PP membranes, cleaning with tap water after 48 hours yielded no flux recovery, indicating significant irreversible fouling and wetting due to adsorption of organic foulants on the hydrophobic membrane surface. Long-term (ten day) tests indicated reduced hydrophobicity of the PP membranes due to adsorption of organic foulants, which caused wetting problems and allowed contaminants to pass through after only six days of operation [94]. The reported results from the literature indicate better trans-membrane flux performance of PVDF membranes than PP membranes in the treatment of municipal wastewater in an integrated FO-MD system. The results from two studies (both used similar commercial cellulose triacetate FO membranes, and similar temperatures for feed, draw, and permeate sections) showed that the flux through a PVDF hollow fiber membrane (average pore size 0.073 μm, thickness 186±5 μm) was 17.6 $L/m^2/h$ over a 120-hour operation period [96] and the same through a PP membrane (average pore size 0.22 μm, thickness 150±20 μm) was 14.4 $L/m^2/h$ over a 20-hour operation period [95]. Despite the lower average pore size, the higher flux in PVDF hollow fiber membranes might have resulted from variations in other operational parameters (like lower draw solution concentration, higher flow rate in hot side stream compared to cold side stream, etc.). Incorporation of a third treatment scheme (e.g., GAC treatment or ultraviolet oxidation) to prevent contaminant accumulation in the draw solution has offered further performance enhancement of the integrated FO-MD process in treating raw sewage [232].

Other FO-MD studied processes used seawater [97] or oily wastewater [93] as the draw solution and municipal wastewater as FO feed water. An integrated ultrafiltration-FO-MD (UF-FO-MD) process has been reported for the treatment of real oily wastewater and sewage through utilization of the osmotic and thermal energy of the oily wastewater [93]. Following UF, the highly saline and heated oily wastewater (mixed with FO permeate of sewage) was simultaneously used as a FO draw and MD feed. The FO-MD performance was mostly affected by oil content, while temperature and salt content of the oily wastewater had little influence on the system performance [93]. Use of the integrated FO-MD process also indicated enhanced treatment performance of highly saline landfill leachates than that individual FO or MD could offer [108]. The landfill

leachate treatment performance enhancement depends on the salinity of the feed solution. At a total salt concentration of 25,000 mg/L (calculated as NaCl), the total organic carbon, total nitrogen, ammonia nitrogen, mercury, antimony, and arsenic removal performances of FO were 91%, 94%, 97%, 48%, 99%, and 88%, respectively (over a 250-minute operation). While the same for the integrated FO-MD process were >98%, >98%, ~100%, ~100%, ~100%, ~100%, respectively [108]. Also, the integrated FO-MD process was able to completely remove ammonia nitrogen, which is poorly removed by MD alone due to its volatilization and permeation through the MD membrane pores (as discussed in a previous section).

MD has also been integrated with different forms of bioreactors to form integrated membrane bioreactors (MDBR) for the treatment and recovery of wastewater. An integrated aerobic-anaerobic osmotic membrane bioreactor (OMBR, comprising of a bioreactor and a FO subsystem) with MD was studied for the production of potable water from a synthetic wastewater feed solution designed to stimulate high-strength domestic wastewater [230]. The feed solution was prepared from sucrose and ammonium bicarbonate to achieve a strength of 1350 mg/L COD and 160 mg/L NH_4^+-N. The bioreactor was inoculated with a combination of return activated sludge and biomass from a trickling nitrification filter, and the bioreactor was kept at continuous mixing with a submersible pump maintaining a solid retention time of 30 days [230]. The draw solution concentration and draw solution circulation flow, in the FO subsystem using cellulose triacetate membrane, were 35 g/L NaCl and 100 ml/min.

A cross-flow DCMD module was integrated with the OMBR system. Flat sheet PTFE membranes were used in the DCMD process with counter-current flow between the feed and distillate streams. The MD feed and permeate stream temperatures were maintained around 80ºC and 10ºC, respectively [230]. The MD productivity had an early decrease due to membrane fouling, which caused the average, steady-state MD water flux between hours 15 and 48 to become 0.8 L/m^2/h. The low flux performance in the large-scale MD system was attributed to the reduced driving force in the system resulting from heat transfer from the feed side to the distillate side of the membrane [230]. The FO productivity also declined slightly over 48 hour and the average FO water flux was 5.1 L/m^2/h. The slight decline in FO flux was due to membrane fouling and to some extent, reduction in osmotic pressure driving force due to an increase in bioreactor salinity from reverse

salt flux. The integrated system performance in treatment of wastewater was evaluated by the average NH_4^+-N and COD concentration in the bioreactor and MD permeate solution. NH_4^+-N concentration in the permeate solution was 24.6 ± 6.2 mg/L (corresponding to 84.6% removal from OMBR feed solution). The average COD concentration in the permeate was 21.6 ± 2.8 mg/L (corresponding to 98.4% removal from the OMBR feed solution) [230]. The NH_4^+-N concentration in the bioreactor (229-275 mg/L) was higher than the feed solution during the 48-hour test period, which is indicative of slower acclimation of ammonia-oxidizing bacteria compared to other bacteria in the freshly seeded inoculum. Hence, the system performance is expected to improve over longer duration, as the amount of NH_4^+-N in the bioreactor will decrease with time [230]. The lower rejection of NH_4^+-N can be attributed to a number of factors: (a) biological treatment with aerobic/anoxic cycling (where low dissolved oxygen concentration can lead to higher NH_4^+-N concentration compared to continuously aerobic bioreactors that do not incorporate denitrification process) [233], and (b) high MD feed temperature (80ºC) used in the current study may have caused higher amount of volatile NH_3 to form and pass through the MD membranes [115,234].

Jacob et al. (2015) placed a DCMD module in series following a two-stage thermophilic anaerobic membrane bioreactor [195]. The two-stage thermophilic anaerobic membrane bioreactor used a monolithic tubular ceramic membrane (55 channels, 2.5 mm diameter in each channel, 30 mm diameter, 450 mm length, 0.18 m^2 surface area; NGK Insulators, Japan) with a nominal pore size of 0.1 μm [195]. The treated anaerobic effluent was used as the feed to the DCMD module with and without the addition of biomass. The COD rejection efficiencies were 97.2%-99.5% and 98.4%-99.9% due to the absence and presence of biomass, respectively. The presence of biomass significantly reduced the flux due to organic fouling [195].

A hybrid process was also reported with MD placed in a submerged membrane bioreactor operated at elevated temperatures [154]. Both flat sheet and tubular membrane modules were submerged in the bioreactors and tested for the recovery of a synthetic wastewater [154]. Incorporation of an air sparging mechanism on the sides of the tubular membrane bundles provided more consistent permeate flux performance (approximately 5 $L/m^2/h$) for over 2 weeks of operation at a bioreactor temperature of 56ºC [154]. The system also demonstrated consistent TOC rejection and kept the permeate TOC concentrations lower that 0.7 mg/L [154]. DCMD has been integrated with

photocatalysis processes for degradation and removal of azo dyes (Acid Red 18, Acid Yellow 36, and Direct Green 99) in aqueous solution [235]. TiO_2 Aeroxide® P25 (Degussa, Germany) was used as photocatalyst on the DCMD feed tank and irradiated with an UV-lamp (Philips Cleo, irradiation intensity was 146 W/m^2 on the feed tank). Acid Yellow 36 was most difficult to photo-decompose, among the three azo dyes used in the study, and this has been postulated to its less adsorption capacity to the photocatalyst surface [235]. In general, MD was able to reject the photocatalyst particles at different applied concentrations without major changes in permeate flux over a 5-hour operation period. The MD distillate quality varied with the type of azo dyes rejected, with the highest concentrations of TOC (1.2 mg/L), conductivity (2.2 μS/cm), and TDS (1.4 mg/L) content in distillate observed with Direct Green 99 [235].

Among different reported hybrid systems involving MD, the FO-MD process has been studied most comprehensively concerning occurrences of fouling and wetting. Integration of FO with MD provides the advantage of auto regenerating the FO draw solution on the feed side of MD, and it has been successfully applied to recover high-strength wastewater. The RO-MD, or other desalination processes integrated with MD, as a whole, offers an approach to enhance water recovery efficiency of the entire system. In such hybrid systems, the MD receives the concentrate from the RO process (or other desalination processes like NF or MED) and this creates severe fouling and wetting condition for the MD membrane. Incorporation of MD with different bioreactors or photocatalytic reactors has shown promising results for treatment and recovery of wastewater. However, membrane fouling and wetting in such a MD integrated bioreactor or photocatalytic reactors for synthetic and real wastewater merits further research.

2.5.3 Membrane maintenance

Long-term MD performance has been associated with changes in membrane surface properties (like hydrophobicity, roughness) and the membrane lifetime depends on recoverability of these surface properties [173]. Most of the literature concerning long-term real wastewater treatment and reclamation using MD reported use of PTFE and PVDF commercial MD membranes. The higher hydrophobicity of PTFE membrane surfaces reduced wettability and fouling while reclaiming pre-treated municipal wastewater [92] and landfill leachates [107], and also enabled flux recovery by water flushing in textile/dyeing wastewater recovery over a more extended

operational period [176] compared to PVDF membranes. A pilot scale system treating textile/dyeing wastewater with PTFE membranes demonstrated complete recovery of original flux, and about 79% recovery of membrane mass transfer coefficient (expressed in $L/m^2/h/bar$) through a series of cleaning steps after a operation period of 65 days [86]. This study operated a pilot-scale DCMD system for 65 days using a PTFE membrane and real treated textile wastewater as feed water. The performances of different cleaning options were evaluated on the basis of membrane flux ($L/m^2/h$) and membrane mass transfer coefficient ($L/m^2/h/bar$). The membrane flux and membrane mass transfer coefficient reduced to 72% and 53% of the original clean brine values after 65 days pilot-scale operation. The study performed three different cleaning operations in series and used a clean brine solution as feed to assess the cleaning effectiveness after cleaning operation. The cleaning methods used were: (a) warm caustic clean (1.5% NaOH at 55ºC for about 45 minutes), (b) ambient chlorine cleaning (0.1 wt% NaOCl as free chlorine at ambient temperature for 30 minutes), and (c) DI water cleaning (DI water was pumped through the MD module channels until the electrical conductivity stopped to increase and the DI water was left to soak the membrane overnight) [86]. Among the three different cleaning mechanisms employed, the caustic cleaning was successful in recovering membrane flux and membrane mass transfer coefficient. The hypochlorite cleaning did not enhance the mass transfer coefficient. This was linked to the attachment of the fouling materials on the PTFE membranes or the nature of the textile processing material and their resistance to chlorine degradation. DI water cleaning, which is popularly employed to remove inorganic fouling, did not show any improvement in the membrane performance as most of the fouling was organic in nature [86]. Due to the effectiveness of the first caustic cleaning (which achieved membrane flux and membrane mass transfer coefficient enhanced to 77% and 61% of the original clean brine values), a second caustic cleaning was employed over 60 minutes time period. After the second caustic cleaning, the membrane flux was recovered completely, and the mass transfer coefficient was 79% of the initial value [86]. There is a scope for optimization of the caustic cleaning for a particular type of wastewater in terms of caustic concentration, temperature, and time. Also, the cleaning frequency should be selected appropriately, as the fouling rate increased significantly after the cleaning operation [86]. Hydrophobicity of PTFE membranes was mostly recovered by chemical cleaning (0.1% citric acid) during reclamation of pre-treated wastewater (combination of storm water and biologically treated sewage effluent) RO concentrate in DCMD [10]. The wastewater RO concentrate was pre-

treated by a batch adsorption using 5 g/L GAC (Coal based GAC, MDW4050CB, James Cumming & Sons Pty. Ltd., particle size range: 425-600 µm, average pore diameter 30 Å and 1000 m2/g, respectively) [10]. Whereas, significantly faster loss of hydrophobicity with the PTFE membrane was observed with raw RO concentrate (mainly due to the combined adhesion of hydrophilic organic and inorganic $CaCO_3$ on the membrane), which was not improved through water or acid washing [10]. Although after cleaning, the membrane flux was recovered closely to its initial value but the membrane flux dropped more rapidly with enhanced wetting [10]. Chemical rinsing, using an acid (2% w/w HCl solution) and a base (2% w/w NaOH solution) solution, for 30 min each, enabled recovery of the hydrophobic characteristics of the PVDF hollow-fiber membrane during recovery of recirculating cooling water [98]. A NaOH solution was recirculated (at 60^{o}C feed and 20^{o}C permeate temperatures, with periodic addition of NaOH to maintain a pH above 11 in the feed side) for cleaning a PP membrane, following DI water rinse, between DCMD of a synthetic feed water containing a target concentration of silica (~225 mg/L) [236]. The cleaning with NaOH solution achieved recovery of permeate flux to 23 L/m^2/h when testing with new solution began for the second cycle, which is lower than the initial clean membrane flux of 28 L/m^2/h [236]. The flux decline in the second cycle (i.e., after cleaning) was rapid when compared to the first cycle [236]. Membrane flux recovery scenarios investigated using synthetic water do not necessarily reflect the complexity of real wastewater and usually provide better flux recovery performances. A membrane distillation bioreactor (MDBR) with 6 and 12 g/L MLVSS biomass added to a feed solution from an anaerobic reactor treating high-strength simulated wastewater exhibited permeate flux decreases of 50% and 70%, respectively after 72 hours of operation using a PTFE membrane, most of which were removable fouling [195]. 71–77.5% of the fouling of the membrane surface was observed to be removable (after washing with de-ionized water), while 21.2–25.6% of fouling was reversible (after caustic cleaning) [195]. The PTFE membrane recovered 96% of the initial flux after combined water and caustic cleaning [195]. There is a need to perform a more organized study of membrane flux recovery using a number of different membrane cleaning processes (i.e., water flushing, caustic cleaning, acid cleaning, etc.) for different real wastewaters. For wastewater causing organic fouling in the membrane caustic cleaning showed better performance to recover membrane performance in several studies. However, the fouling rates were enhanced post cleaning operation of the system, which can be associated with the change in membrane characteristics due to the cleaning operation. As a result, there is a need for optimization of the cleaning processes (in

terms of chemical concentration, cleaning duration, frequency or cleaning) for particular types of wastewaters, which can cause inorganic fouling, organic fouling or biofouling. Such analyses will enhance the understanding of the membrane-foulant interaction and help in the design of operational protocol for MD systems when applied in wastewater recovery.

Recovery of wetted membranes has mostly been studied with saline water but holds practical significance in application of MD for wastewater reclamation. Dewetting techniques of MD membranes reported in literature involves (a) chemical/water rinsing and/or drying, and (b) backwashing [160,237]. To remove wetting, membranes must be dried and cleaned to remove the water and solutes deposited in the membrane pores, which usually takes several hours leading to process downtime and potential membrane degradation [170]. Reducing the hydrostatic pressure on the membrane to less than LEP will not achieve recovery of wetted membrane pores to its un-wetted form after wetting initiates after reaching LEP [38]. The decrease of pressure below LEP at this point only reduces the flux linearly [38]. Only drying of a wetted MD membrane do not mitigate the wetting issue completely as the salt deposits inside the membrane pores make an irreversible structural change inside the pores [175,238]. Rinsing of MD membranes with distilled water and solvents to remove scalants have shown some improvements in abating wetting in MD systems, however, the membrane gradually loses its resistance to wetting with time in feed solutions with common foulants, as the cleaning poorly restores performance [239]. Membrane recovery by rinsing with concentrated HCl solution was performed to remove iron dioxide precipitates from the surface and pores of a PP membrane [149]. The membrane flux increased after partial dissolution of deposit from the membrane surface, but partial wetting of membrane took place when all the deposits dissolved (also including that precipitated in the pores) and the permeate flux reduced gradually with time after cleaning [149]. Another approach for recovery of wetted membrane is backwashing. Air backwashing (with an air pressure higher than the liquid entry pressure) of a wetted membrane containing the liquid can force wetting liquid out and prevents the solutes from precipitating inside the pores [237,240,241]. On the other hand, air backwashing to dried membrane has been reported to be effective only for removal of deposits on the pore mouth [242]. Dewetting of wetted MD membranes have also been achieved with high-temperature air backwashing [243,244]. The optimum temperature and time of exposure for dewetting a wetted membrane in VMD was reported to be 60-70 ^{o}C and 8-12.5 min., respectively

[244]. A study was carried out to evaluate the relative effectiveness of a pressurized air backwashing technique to the membrane dryout process in reversing membrane wetting in MD [237]. The pressurized air backwashing system restored the LEP to 75% of the pristine membrane in ~10 s treatment time (for lower salinity feeds) by removing the saline solution from the membrane using a cool air stream and hence did not involve a dryout step or evaporation [237]. Compared to the dryout method, which only evaporates the water from membrane pores and leaves behind trapped crystalline solutes within the membrane to promote rewetting, the pressurized air backwashing system removes saline solution (both water and salts) from the membrane without any vaporization [237]. Analysis of SEM image showed possible superficial tears of membrane in pressurized air backwashing technique [237]. The risk of partial membrane wettability can also be limited by reducing the period between cleaning process to maintain a thin scaling layer on the membrane surface [245]. Removal of scaling from the membrane surface in quick intervals limits the degree of oversaturation inside the wetted pores, which reduces internal scaling [245]. The dissolution of pore deposits can initiate wetting as a result of internal scaling [246][247]. As stated before, the recovery techniques of wetted membranes have been studied mostly for saline water. There is a scope to assess the suitability of these techniques in reclamation of different types of wastewaters using MD. The complex composition of different types of wastewaters might offer a completely different scenario to these recovery options, which might warrant modification or enhancement of recovery techniques for wetted membranes. Nevertheless, the reported wetted membrane recovery techniques will offer key approaches to researchers to develop novel membrane wetting recovery methods when MD is applied for wastewater recovery.

2.5.4 Membrane modification/fabrication

Many studies have reported enhanced MD performance during wastewater recovery by using fabricated novel membranes or modified commercial membranes. Wetting resistance of MD membranes has been enhanced through construction of superhydrophobic and omniphobic surfaces. Self-cleaning membranes have also been developed to reduce fouling in MD, whereas modifications of membrane matrix and surface composition have also been carried out to achieve better fouling and wetting performance in recovery of wastewater. The following sections briefly discuss different modified/novel MD membranes.

Superhydrophobic membrane: Superhydrophobic MD membranes are essentially formed by roughening of hydrophobic surfaces, by using inorganic nanoparticle (e.g., silica, titanium oxide, fluorographite) [47,167,248] or micro-particle [172] coating, which essentially lowers the membrane surface energy. A superhydrophobic polydimethylsiloxane (PDMS)/PVDF hybrid electrospun membrane showed 50% higher flux than that of commercial PVDF membranes without any observable fouling or wetting while treating textile/dyeing wastewater [172]. The superhydrophobic membrane containing PDMS microspheres prevented dye particles from entering into the membrane pores and permitted the formation of a loose fouling layer on the membrane surface. As a result, the hybrid PDMS/PVDF membrane showed excellent flux recovery through intermittent water flushing [172]. A tri-bore PVDF hollow fiber membrane with superhydrophobic Teflon AF2400 coating (optimized to a concentration of 0.025 wt% Teflon AF 2400 for 30 sec.) demonstrated enhanced anti-wetting properties (LEP increased by 109%, membrane surface contact angle 151^{o}) and membrane performance in long-term DCMD experiments with synthetic feed water [249]. The superior anti-wetting properties of the coated membranes could be explained due to the lower surface tension and smaller maximum pore size of the coated surface, which makes it more difficult for the liquid to penetrate into the pores and due to the low-surface-energy of the surface, which reduces possibility of surface nucleation and further scaling [249]. Superhydrophobic MD membranes can offer long-term wetting resistance to water into membrane pores when compared to hydrophobic membranes. However, presence of low surface tension contaminants (e.g., alcohol) and surface-active reagents (e.g., surfactants) in feed water poses critical challenge to reclamation of wastewater using superhydrophobic membranes. Wastewater containing amphiphilic-surfactants or low surface tension contaminants may cause wetting in long-term operation of superhydrophobic membranes.

Omniphobic membranes: Omniphobic membranes, which repel both water and oil, provide enhanced resistance to wetting resulting from low surface tension contaminants. The modification of membrane surface chemistry and morphology to have low surface energy materials and single/multi-level re-entrant structures, respectively on the membrane surface enables development of omniphobic membranes [81,157,158,169,197,250]. The incorporation of single/multi-level re-entrant structures to the membrane surface and attainment of low surface energy, provides added wetting resistance to omniphobic membranes than the superhydrophobic

membranes. The re-entrant structure provides a local energy barrier even to the low surface energy contaminants from transitioning from the meta-stable Cassie-Baster state (in which microscopic air pockets remain trapped below the liquid and membrane pores) to the Wenzel state (in which the solid-liquid interface is maximized) and enable propagation of the liquid-air interface within the membrane pore [81,157,251]. An omniphobic membrane was fabricated by grafting negatively-charged silica nanoparticles in a positively-charged nanofiber mat prepared by electrospinning a polymer-surfactant solution of PVDF-hexafluoropropylene (HFP) and cationic surfactant (benzyltriethylammonium) [157]. DCMD experiments were carried out using a synthetic feed solution containing low surface tension substances, prepared to mimic industrial wastewater generated from shale gas production [157]. To demonstrate the DCMD performance in recovering high salinity and low surface tension water mimicking shale gas wastewater, a 1 M NaCl solution with varying (0.1, 0.2, and 0.3 mM) concentrations of sodium dodecyl sulfate (SDS, an anionic surfactant) was introduces as a feed water [157]. While the control PVDF-HFP nanofiber membrane failed in freshwater reclamation due to low wetting resistance, the fabricated omniphobic membrane exhibited successful freshwater production and stable performance over 8 hours of operation [157]. A number of studies have reported grafting of silica nanoparticle (SiNPs) on MD membranes to achieve single/multi-level re-entrant structures on membrane surface and functionalization of fiber substrate with fluoroalkylsilane (FAS) to achieve lower surface energy of the membrane while fabricating an omniphobic membrane [158,252]. These studies utilized a synthetic recipe similar as given above [158], or a recipe for an emulsion prepared by ultrahigh speed mixing of SDS: hexadecane: NaCl at a concentration ratio of 240: 2400 :10000 (mg/L) in water [252], and used as the feed solution to simulate oily waste water. One study reported, modification of a PVDF membrane to produce an omniphobic membrane by coating the PVDF membrane with SiNPs (following NaOH alkaline treatment and (3-Aminopropyl)- triethoxysilane grafting) and lowering the surface energy of the coated membrane using perfluorodecyltrichlorosilane (FDTS) via vapor- phase silanization [81]. The study observed the flux and salt rejection performance on the omniphobic PVDF membrane and compared it to control PVDF membrane. Synthetic solutions were prepared as feed water with 1 M NaCl and progressively varying SDS concentration (0.05, 0.1, 0.2 mM) or mineral oil concentration (8, 40, 80 mg/L) after every 2 hours [81]. Four-hour long DCMD experiments demonstrated almost complete rejection of salts in the omniphobic PVDF membrane, while the flux showed a very small

gradual decline over this time period. The control PVDF membrane was completely wetted with increasing SDS concentration (>0.1 mM) [81]. Whereas, in case of mineral oil in feed (8 mg/L) the flux rate started to decline due to fouling, and eventually the membrane wetted as the mineral oil concentration was raised above 40 mg/L, and was evident through the rapid increase of flux and decrease of salt rejection [81]. The same study reported DCMD experiments with real shale gas brine (pre-filtered using 16 μm filter, water quality: total dissolved solid 101,000 mg/L, surfactant 3.2 mg/L, oil and grease 2.0 mg/L, total volatile organics <0.14 mg/L, total suspended solids 41 mg/L) as feed water with the modified omniphobic PVDF membrane and control PVDF membrane until 500 mL permeate volume was gathered. The flux decline in the control PVDF and omniphobic PVDF membranes were 50% and 86%, respectively, and the permeate conductivity in case of the control PVDF membrane was about 4 times of that of the omniphobic membrane [81]. The Performance of omniphobic membrane surpasses that of superhydrophobic membrane in repelling low surface tension contaminants [158]. Another fabrication methods for omniphobic membranes involve layer-by-layer assembly of negatively charged silica aerogel and perfluorodecyltriethoxysilane on PVDF membrane and interconnecting them with positively charged poly(diallyldimethyl ammonium chloride) via electro-static interaction [169]. The fabricated omniphobic membrane, demonstrated good wetting resistance in an AGMD with feed water from reverse osmosis brine of coal seam gas produced water (from Gloucester Basin located along the lower north coast of New South Wales, Australia, conductivity ~22.6 mS/cm), which contained externally added surfactants (SDS at an increasing concentration of 0.1, 0.3, and 0.5 mM) [169]. Chung et al. reported fabrication of an omniphobic PVDF hollow-fiber membrane via silica nanoparticle deposition (causing surface roughness and re-entrant structure) followed by a Teflon AF 2400 coating (causing surface energy lowering), which demonstrated good repellency toward different liquids with varying surface tensions and used it successfully in a VMD with synthetic water containing sodium dodecyl sulfate surfactant (at varying concentrations of 0.2, 0.4, and 0.6 mM in a 3.5 wt% NaCl solution) [250]. Observations from different studies indicate that omniphobic membranes demonstrate superior wetting resistance to water, low surface tension contaminants (e.g., alcohol), and surfactants. So, the omniphobic membranes can be used in place of superhydrophobic membranes to prevent wetting in MD. In this sense, the omniphobic membranes can be regarded as a superior version of the superhydrophobic membranes. However, for other types of water (i.e., water without low surface tension contaminants or surfactants)

superhydrophobic membranes can be used with enhanced wetting resistant performance than usual hydrophobic membranes.

Hydrophobic membrane with hydrophilic skin layer: Recent research works demonstrated fabrication of an in air hydrophilic (or underwater oleophobic) coating layer on hydrophobic membranes to prevent adsorption of non-polar contaminants on membranes [168,253]. Lin et al. compared wettability of a PVDF hydrophobic membrane, a composite PVDF membrane with superhydrophilic skin layer, and an omniphobic membrane [196]. The superhydrophilic skin was developed by spray coating a perfluorooctanoate/chitosan/silica nanoparticle (PFO/CTS/SiNP) nanoparticle-polymer composite onto a PVDF membrane. Both hydrophobic PVDF membrane and omniphobic membranes were in-air hydrophobic, while the superhydrophilic coated surface of the composite membrane was in-air hydrophilic. The composite membrane underwent an oleophilic-to-superoleophilic transition with complete adsorption of in-air oil droplet on surface in 10 min. The reconfiguration of surface functional groups on the membrane has been suggested to be a possible mechanism for dynamic wetting by an oil droplet. It was assumed that the oil was initially in contact with the low-surface energy perfluoroalkyl chains in the PFO and after extended contact with the PFO/CTS/SiNP surface coating layer, interaction between oil and CTS became dominant and thus membrane wetting was promoted [196]. Dynamic wetting of membranes has also been reported with commercial PTFE membranes contacting different low-surface-tension liquids where the time required to fully wet the surface varied and depended on the contacting liquids [197]. Both the hydrophobic PVDF membrane and composite membranes were wicked by oil droplet in air, while the omniphobic membrane was not wicked by oil in air due to its combined reentrant surface morphology and low-surface-energy of materials. The under-water oil contact angles were very low for PVDF membrane due to the strong hydrophobic-hydrophobic interaction of membrane surfaces with oil droplet. The composite membrane was highly oleophobic under water due to strong repulsive hydration force experienced by the oil droplet when it endeavored to wet the superhydrophilic PFO/CTS/SiNP surface. The omniphobic membrane also demonstrated oleophobic character under water. But, when compared to the in-water oleophobicity of composite membrane, the omniphobic membranes were relatively less oleophobic under water due to the hydrophobic-hydrophobic interaction between oil and the low-surface-energy membrane materials [196]. Nonetheless, omniphobic membranes have demonstrated larger contact angles towards

hydrophobic and low-surface tension liquids, when compared to hydrophobic membranes [81,157,158,169,197,250].

Fouling and reusability of three different MD membranes were evaluated to study the effect of membrane surface wettability modification on reclamation of shale oil and gas produced water [79]. The concentrations of total dissolved solids, total organic carbon, oil and grease, and total volatile petroleum hydrocarbon in the shale oil and gas produced waters used in this study was 39,650-40,370 mg/L, 700-1,400 mg/L, 6.2-9.2 mg/L, 4.8-4.82 mg/L, respectively [79]. The three membranes were (a) PVDF hydrophobic membrane, (b) superhydrophobic PVDF membrane (with low surface energy material FAS and a re-entrant structure attained by grafting with silica nanoparticle), and (c) composite PVDF membrane with hydrophilic PVA coating (Janus membrane, the PVDF-PVA membrane was in air hydrophilic and underwater oleophobic) [79,254]. The superhydrophobic membrane fabricated in this study featured both low surface energy material and a re-entrant structure, which makes it equivalent to an omniphobic membrane as referred by other researchers. The relation between membrane surface wettability and fouling potential was influenced by feed water composition. The membrane fouling was reversible by physical membrane cleaning in all the membranes studied in reclamation of shale oil and gas produced water [79]. However, the superhydrophobic (equivalent to an omniphobic) membrane exhibited better reusability among the three studied membranes, at the expense of water productivity, in three successive treatment cycles [79].

Self-cleaning membrane: Self-cleaning properties of membranes against inorganic/organic scaling have been reported in several literatures [171,255]. An electrically conducting composite PP membrane with a carbon nanotube-poly(vinyl alcohol) layer demonstrated enhanced cleaning capacity of silicate scaling that developed during MD operation through generation of hydroxide ion by water electrolysis [171]. Incorporation of TiO_2 nanoparticles in a PVDF membrane showed decomposition of gallic acid foulants in the membrane under irradiation of UV light due to photocatalytic activity of TiO_2 nanoparticles blended in the membrane [255].

Other novel composite/surface modified membranes: Apart from the above-mentioned variations, a number of studies have reported modification of membrane matrix/surface layer property to enhance flux and alleviate fouling-wetting scenarios in MD. A carbon nanotube incorporated

PVDF-PP membrane for the MD of pharmaceutical wastewaters demonstrated higher rejection for four active pharmaceutical ingredients (ibuprofen, dibucaine, acetaminophen, diphenhydramine) and improved permeate flux due to the integration of immobilized carbon nanotubes in the membrane matrix [256]. CNTs are highly hydrophobic and are known to have rapid sorption-desorption capacity: as a result it has been postulated that water vapor molecules hop from one site to another by interaction with the CNT surfaces and increase overall vapor transport [256]. The CNTs also provided alternate routes for mass transport via diffusion along their smooth surface and directly through their inner tubes, which enhanced vapor transport [256]. Khayet developed composite hydrophobic/hydrophilic membranes via the phase inversion method using a blend of fluorinated surface modifying macromolecules and host polymers (polysulfone and polyethersulfone), and successfully employed them in DCMD of low-level and medium-level radioactive wastewater with higher LEP of water values, lower permeate fluxes, higher rejection factors, and lower radioactive adsorption to the membrane surface [103]. Some researchers reported fabrication/modification of membranes to enhance wetting resistance at the expense of permeate flux. A fabricated PVDF-Cloisite 15A nanocomposite membrane was able to improve permeate quality significantly while treating textile/dyeing wastewater in DCMD, but the membrane flux rapidly declined to 50% within the first few hours of a 40-hour operation [88]. Lin et al. modified the surface of a hydrophobic porous PTFE membrane by applying a thin layer of agarose hydrogel for textile/dyeing wastewater reclamation [89]. The modified PTFE membrane exhibited no wetting and about 71% of the flux of the bare PTFE membrane while treating textile/dyeing wastewater [89].

Despite the increasing interest in fabrication/modification of MD membranes for enhanced flux and reduced fouling/wetting propensity, most novel studies report short-time performance of the membranes in bench-scale systems using synthetic/simulated wastewater. In order to assess the full potential of the fabricated/modified membranes, long-term pilot-scale performance of these membranes must be evaluated using real wastewaters.

2.6 Energy consumption and economic aspects of MD for wastewater recovery

A number of studies have looked into energy consumption in MD processes, using thermodynamic modeling or pilot-scale operations, while it is applied for desalination of seawater, brackish water

[57,85,117,118,133,238]. Thiel et al. reported energy consumption scenarios in reclamation of shale gas produced water for several desalination technologies through the modeling of produced water properties (i.e., high salinities and diverse compositions commonly encountered in produced water from shale formations) using Pitzer's equation [17]. This study emphasized on how the produced water qualities create differences in system thermodynamics at salinities significantly above the oceanic range. Efficiency models were developed for mechanical vapor compression (MVC), multi-effect distillation (MED), forward osmosis (FO), humidification-dehumidification (HDH), permeate gap membrane distillation (PGMD), and reverse osmosis (single- and double-stage RO) systems [17]. Thermal and electrical energy consumptions (in kWh/m^3 of recovered water) were evaluated for the above-mentioned processes with a feed stream and brine stream salinity of 15% and 26%, respectively. Total energy consumption of RO and MVC was lower among all the processes. However, all of the energy consumption for RO and MVC was electrical energy. For the feed and brine salinity conditions considered, the total energy consumption in single-effect MVC, dual-effect MVC, single-stage RO, and dual-stage RO processes were 26 kWh/m^3, 19 kWh/m^3, 14 kWh/m^3, and 10 kWh/m^3, respectively. The total energy consumption in tri-effect MED, zero-extraction HDH, PGMD, and FO processes were ~200 kWh/m^3, ~360 kWh/m^3, ~510 kWh/m^3, and ~600 kWh/m^3, respectively [17]. Majority of the energy consumption in the MED and FO, and almost all of the energy consumption in HDH and PGMD processes were thermal energy. Shihong Lin et al. (2014) also demonstrated an energy requirement of 27.6 kJ/kg of seawater for recovery of seawater using DCMD at a working temperature of 60°C, which regardless of the mass transfer kinetics will not be able to achieve a single-pass feed water recovery rate higher than 6.4% [57]. When compared to typical seawater desalination using RO process the energy requirement is about 3.18 kJ/kg of seawater (for a typical recovery of 50%) [57]. Fouling comparison study conducted among DCMD, RO, and FO under similar hydrodynamic conditions, observed superior MD performance (with a 14% flux reduction) over RO and FO (with around 48% and 46% flux reductions, respectively) for organic (alginate) fouling after a 18 hour application [257]. Rise of diffusion coefficient of the organic foulants due to high feed temperature of MD resulted in the transport away of contaminants from the membrane surface hence flux enhancement occurs when compared to RO and FO. Also, hydraulic resistance of the membrane-fouling layer in MD has insignificant influence on permeate flux [257]. When inorganic (calcium sulfate) feed solution was used, all three (RO, FO, and MD) systems operated under somewhat

supersaturated condition for 36 h without scaling. FO exhibited the greatest scaling resistance against a feed of 33±2 mM calcium sulfate without significant flux decline. Scaling began to occur at significantly higher concentrations at the membrane and the concentrations were 46-58 mM for FO membrane (cellulose triacetate membrane), 35-38 mM for RO membrane (polyamide thin film composite membranes), and 33-38 mM for MD membrane (PVDF membrane) [257]. The superior inorganic scaling resistance in FO could be explained by the low surface energy of the FO cellulose triacetate membranes and due to enhanced crystallization kinetics of inorganic salt at high temperatures in the MD systems. The flux decline in MD was faster than that of FO and RO after gypsum scaling triggered. So, MD systems should be used with appropriate membrane management schemes when the feed water source contains both organic and inorganic foulants (e.g., municipal wastewater). Furthermore, MD feed stream temperature should also be selected in a way that the solubility of inorganic contaminants does not decline drastically to cause severe fouling and flux decline [257].

The gained output ratio (GOR), which is defined by the ratio between the useful heat (i.e. the heat associated with water vapor transfer) and the total heat input of the system, is used to evaluate the thermal efficiency of MD processes [17,57,85]. For PGMD, the GOR ranges from about 1 to 2 depending on the system size, feed and brine salinity [17]. The low GOR value, due to single-pass application, can be improved by recirculating the brine for high recovery ratio. Also, multi-stage MD configurations can be adopted for better heat recovery in the system and improve GOR. GOR and flux performance of common single stage MD configurations (DCMD, AGMD, CGMD, PGMD) were modeled up to high feed salinity levels (salinity up to 260 g/kg), and AGMD was observed to be more resistant to higher feed salinity levels and can achieve high GOR values than other configurations due to lower heat loss across the low thermal conductivity air gap [117]. The GOR values for a feed salinity of 250 g/kg and a flux of 2 $L/m^2/h$ was observed to be ~ 2.75 (AGMD), ~ 2.1 (for CGMD, thick membrane of 1.2 mm thickness), ~ 1.6 (for CGMD), and ~ 1 (for PGMD) [117]. AGMD systems should be operated without any partial or complete flooding of the air-gap. Any flooding of the air gap will lower the performance of AGMD towards that of PGMD. On the other hand, CGMD and DCMD with a thick membrane (thickness equal to the sum of the membrane and air gap thickness of AGMD) are also resistant to high salinity without having any gap flooding concerns during operation. However, performance of an AGMD system without

gap flooding is better than that of CGMD with a thick membrane since the permeability coefficient of the open air-gap is higher and the thermal conductivity of the air gap is likely to be lower than that of the membrane [117].

In the presence of an alternative waste-heat or low-grade heat source the MD process can compete with different desalination processes. Application of DCMD, coupled with a salt-gradient solar pond (SGSP), for reclamation of terminal lake water demonstrated use of low-grade heat from the lower convective zone of the salt-gradient solar pond [82,84]. The coupled system constructed an SGSP inside a lake for reclamation of terminal lake water and utilized approximately 20 kW/m^2 and 60 kW/m^2 of energy from the solar pond to drive thermal distillation, for two different feed temperatures (33.9ºC and 53.9ºC, respectively) [82]. Water production was on the order of $1.6x10^{-3}$ $m^3/d/m^2$ of SGSP, with membrane areas ranging from 1.0 to $1.3x10^{-3}$ m^2/m^2 of SGSP [82]. Approximately 75-80% of the extracted energy was used to transport water across the membrane (the enthalpy flow), and the remainder was lost by conduction in the membrane [82]. Therefore, improvement of DCMD membranes and modules to reduce conductive heat losses would yield higher water fluxes. The use of an alternative renewable thermal energy source compensated the high thermal energy requirement of MD and only little electrical energy is required to operate MD process [82,84]. Noel Dow et al. (2017) demonstrated use of DCMD in recovering textile wastewater and reported an average specific thermal energy consumption of 1,600 kWh/m^3 until the total permeated water volume was 2 m^3/m^2 of membrane surface area [86]. With increasing fouling in the membranes, the specific thermal energy consumption rose sharply to 4,180 kWh/m^3 before the system was stopped for cleaning [86]. The substantial rise in thermal energy consumption leads to less water treated for the same thermal energy input and justified membrane cleaning. Assessment of waste-heat (generated in the textile plant) integration observed that MD could be applied to the particular textile plant when other treatment strategies (like reverse osmosis or nanofiltration) are introduced for saline-wastewater isolation and pre-concentration of feed stream to reduce waste volume [86].

Woldemariam et al. reported AGMD pilot plant trials with pharmaceutical residues and relevant energy demand analysis with economic evaluations of large scale water recovery systems [106]. The low-temperature district heating return line feasibly supplied the thermal energy requirement

for the MD process. Specific heat demands for the AGMD ranged from 692 to 875 kWh/m^3 without heat recovery and as low as 105 kWh/m^3 when heat recovery is possible [106]. The economic evaluation was performed for three cases: (i) Case 1: specific thermal energy input of 692 kWh/m^3 with no heat recovery and employing 1176 MD modules, (ii) Case 2: specific thermal energy input of 735 kWh/m^3 with no heat recovery and employing 644 MD modules, and (iii) Case 3: specific thermal energy input of 875 kWh/m^3 with recovery of 770 kWh/m^3 (i.e. with a demand of 105 kW/m^3) and employing 1212 MD modules [106]. The capital cost of water treatment was estimated based on five years lifetime for membranes and a twenty-year operational span of other MD equipment in the system (having 10 m^3/h treatment capacity). Case 2 configurations have the least specific capital expenditure (CAPEX) due to the higher permeate flux and so smaller number of modules requirement. Cases 1 and 3 have nearly overlapping specific CAPEX values due to the very close permeate flux, and so closer number of MD modules is required for a particular production capacity. Hence, case 2 specific CAPEX showed a reduction from $50,000 to $20,000 per ($m^3$/h) when the plant capacity increases from 10 to 100 in m^3/h [106]. For a plant capacity of 8000 m^3/h, specific CAPEX will be as low as $9,800 and $16,000 per ($m^3$/h) for Cases 2 and 1, respectively. The annual operational and maintenance expenditure (OPMEX) were also evaluated for the three scenarios. Heat demand had the highest contribution (about 94%) in the total OPMEX for the systems followed by CAPEX (3.4%), service and maintenance (1.2%), and costs of membrane (0.7%). Case 3 and Case 2 registered the lowest and highest cost of heat, which was mostly due to heat recovery in Case 3 and larger heat demand for Case 2. The total unit cost of water was $5.4/$m^3$ for a MD plant having 8,000 m^3/h treatment capacity, and heat requires an amount of $5.1/$m^3$ of water [106]. Heat recovery (Case 3) enabled achievement of lowest unit cost of water treatment, but this scenario also generates least permeate flux (so it will require large membrane area and higher initial investment) [106].

Energy consumption and economic concerns are important for consideration of any technology. MD, which requires very high thermal energy input compared to many desalination processes, shows great potential and competing energy consumption scenarios to other desalination technologies when alternative (waste-heat or low-grade heat) energy sources are available to heat up the feed stream. Pre-treatment of wastewater before MD becomes necessary to reduce fouling and wetting concerns, which otherwise will increase energy consumption and reduce efficiency in

the treatment and recovery process. The contribution of pre-treatment strategies to the overall expenditure of water recovery is an important factor. While a number of studies have looked into incorporation of different pre-treatment and integrated processes with MD, it is important to evaluate the overall increase in capital, operational, and maintenance expenditure due to incorporation of different pre-treatment strategies.

2.7 Outlook on MD for wastewater reclamation

MD for wastewater reclamation differs from saline water desalination mostly due to differences in feed water quality and the interaction between contaminants and the membrane surface. It should be mentioned here that the different fouling and wetting mechanisms in MD remains same in both these applications. It is evident that fouling and wetting scenarios (i.e., occurrence rate, extent, etc.) will significantly vary in MD when used for wastewater reclamation, compared to desalination of saline water. Applicability of MD in desalination has been limited to high-salinity brines due its high-energy requirement compared to pressure-driven RO process. It should be kept in mind that, while various pre-treatments are provided to wastewater to control fouling (inorganic, organic and biofouling) and wetting in MD, the justification of employing MD over RO, in recovering a pre-treated wastewater, is seldom studied in detail. Nevertheless, MD has been highlighted as an economic option for recovery of highly saline pre-treated wastewater provided waste/alternative heat sources are available [230]. A pre-treated wastewater with low/moderate salinity and organic content might still pose significant organic fouling and biofouling problems in RO membranes due to low operational temperature. Such wastewater might necessitate higher degree of pre-treatment before RO or make MD a better option for reclamation. While a number of studies have compared RO and MD based on feed salinity and energy requirement, there is a scope for investigating the impact of organic and microbial quality of feed wastewater in selection of recovery process for a given volume of wastewater.

Successful application of MD for wastewater reclamation will require a comprehensive understanding of membrane fouling and wetting mechanisms and relevant mitigation strategies. As interest grows for wastewater reclamation using MD, the following issues should be kept in mind:

- The interaction between the membrane and wastewater constituents affects MD performance in a complex way, influencing permeate flux, permeate quality, membrane fouling and wetting.
- Pre-treatment of wastewater is essential to achieve consistent performance of MD in wastewater reclamation. For industries with existing wastewater treatment facility, use of MD for wastewater reclamation often becomes feasible due to availability of pre-treated wastewater and waste-heat in close proximity. There is a scope to study different pre-treatment processes integrated with MD for wastewater reclamation.
- Limited systematic research has been conducted into different membrane maintenance approaches. There is significant lack of organized information on cleaning approaches for flux recovery in long-term operation of MD with real wastewater.
- Several novel/modified MD membranes have been reported in the literature. Mostly, these novel/modified membranes have been studied using synthetic wastewater. Only a few of these membranes were examined for reclamation of real wastewater.

Results from the literature indicate that MD is a promising wastewater reclamation process, and it can be effectively used when paired with suitable pre-treatment options. However, systematic, long-term, pilot-scale evaluation of different MD module configurations are required to ensure robust operational processes in industrial-scale wastewater treatment and reclamation. On top of this, combined energy and cost analyses are imperative to compare the applicability of MD with other wastewater recovery processes to further optimize and enhance the economic performance of MD.

Acknowledgements

The Natural Sciences and Engineering Research Council of Canada (NSERC) financially supported this work. The views and opinions of authors expressed herein do not necessarily state or reflect those of NSERC, Canada or any other agency thereof.

Author Contribution

M.R.C. and N.A. contributed equally to this work.

Chapter 3: Membrane desalination processes for water recovery from pre-treated brewery wastewater: Performance and fouling

Abstract

Membrane technologies for water reclamation can be effective for combating water shortages while reducing the wastewater discharge to the environment. Here, we investigated water recovery potential from biologically treated brewery wastewater using membrane distillation (MD), nanofiltration (NF), and reverse osmosis (RO). Both MD and RO achieved high organics (~97% TOC) and nutrients (>99% TN and ~100% TP) removal, whereas NF exhibited lower removal rates of TN (~64%) and TOC (~86%). A relatively lower water flux drop (~53%) was observed for MD compared to NF and RO (~98%). Significantly higher water recovery (~ 86%) was obtained with the MD, compared to NF (~16%) and RO (~12%). The physicochemical characterization of the fouled membranes revealed biofouling along with organic and inorganic fouling for both NF and RO membranes. However, the MD membrane was fouled primarily by organic and inorganic species, with no noticeable biofouling. Though chemical cleaning was effective for water flux recovery of MD, NF, and RO membranes, the repeated operations altered the membrane surface morphology significantly for both NF and RO membranes. Overall, the comparison study revealed that MD has the potential to be directly used for water reclamation from pre-treated brewery wastewater with minimal flux drop, and high organics and nutrient rejection, and flux recovery.

Keywords: Membrane distillation (MD); Nanofiltration (NF); Reverse osmosis (RO); Water Recovery; Fouling.

3.1 Introduction

Water reclamation through advanced wastewater treatment processes can offer effective means to address water shortages while simultaneously reducing the volume of wastewater discharged to the environment [1,28,258]. Membrane-based separation processes are consistently gaining popularity as advanced treatment steps in reclamation of water through wastewater streams, providing a dependable supply of reusable water [1,3–7,259]. Membrane-based separation processes such as thermal-driven membrane distillation (MD), pressure-driven nanofiltration (NF), and reverse osmosis (RO) have been reported as effective and efficient in literature for water recovery [1,3,261,4–7,9,11,259,260]. MD is a vapor-driven thermal membrane-based process where water molecules are transported through a porous and hydrophobic membrane in a vapor phase [12,38,40,262,263]. The porous, hydrophobic membrane is used to separate a hot, highly concentrated feed stream from the cold permeate stream [12,40,162]. The temperature difference between the feed and permeate streams generates a partial vapor pressure difference, which drives the water vapor to pass through the membrane from the feed to the permeate side. This water vapor gets condensed back on the recirculating permeate stream. The hydrophobic membrane prevents the direct permeation of feed water achieving contaminant rejection. Due to reduced sensitivity to concentration polarization and the driving force resulting from the temperature difference, MD can operate at high salinities on the feed side [42]. MD demonstrates several distinct advantages such as: a 100% theoretical non-volatile salt rejection, a lower required operating temperature when compared to conventional thermal desalination processes, the ability to utilize low-grade thermal energy, a lower operating hydrostatic pressure, and less stringent mechanical property requirements for the membranes used when compared to conventional pressure-driven membrane processes [40,46,267,268,47,49–51,162,264–266]. On the other hand, pressure-driven membrane processes (like RO) employ a semi-permeable membrane that rejects dissolved constituents present in feed water primarily due to size exclusion, charge exclusion, and physical-chemical interactions between the solute, solvent, and membrane [269,270]. The RO membranes do not have discrete pore openings across the membrane. Rather, the polymeric RO membrane has a layered web-like structure, which provides a tortuous pathway for water to pass across the membrane to reach the permeate side [271]. RO membranes have an average pore diameter of less than 10^{-9} m, which can reject monovalent ions from the feed stream [271]. Compared to RO, the

NF membranes have larger pore sizes (10^{-9} m to 10^{-8} m), which results in lower rejection of monovalent ions but higher permeate flux in the NF process [272]. MD and RO have been frequently discussed and compared for their desalination application. While RO is considered to be more efficient in terms of energy, MD is considered to perform better in resisting fouling as well in treating highly concentrated wastewater [13,15,17]. NF requires less pressure compared to RO, thus, if the implementation of NF is adequate for a specific type of wastewater, it will be most cost effective than RO. While still being indicative real performance, most research in literature conducted studies focusing on using saline water and synthetic water when comparing thermal and pressure-based membrane performances.

One of the major challenges in adopting membrane-based processes is membrane fouling, which prohibits the widespread implementation of membranes for wastewater treatment and reclamation [4,5,7,13,17]. Foulants (depositing compounds causing fouling) can be inorganic, organic, or biological in nature and they can interact with each other and/or the membrane surfaces. Membrane fouling is affected by the following parameters [40]: i) foulant characteristics (e.g., concentration, size, solubility, diffusivity, hydrophobicity-hydrophilicity, charge); ii) membrane properties (e.g., pore size and its uniformity distribution, membrane structure, surface charge, surface functional groups, surface roughness); iii) operational conditions (e.g., flux, solution temperature, flow velocity, pressure); and iv) feed water characteristics (e.g., pH, ionic strength, presence of organic/inorganic matter, microorganisms). Depending on the type of foulants in the feed solution, membrane fouling is broadly classified as: (i) inorganic fouling (including both colloidal/particulate fouling and inorganic scaling); (ii) organic fouling; or (iii) biological fouling [42,64,149,150,269,272–275]. Inorganic fouling is due to the accumulation of colloidal and particulate inorganic matter on the membrane surface. It can also occur when the solubility product of dissolved inorganic ions exceeds the equilibrium, and the precipitated ions forms a scaling layer on the membrane surface. The organic fouling refers to the deposition or adsorption of dissolved or particulate organic matter on the membrane surface. Biological fouling (or biofouling) refers to the adhesion and growth of microorganisms accompanied with the agglomeration of extracellular materials on the membrane surface. Continuous build-up of different types of foulants leads to membrane pore blocking and surface fouling [4,9,13,257,273,274,276,277]. In order to overcome the fouling issues in membrane-based processes, different wastewater pre-treatment options are

employed [3,5,276,278,279,7,12,40,94,95,98,239,258]. The pre-treatment of wastewater is intended to reduce the waste load from the feed stream, which in turn reduces the fouling propensity of the feed to ensure more stable operation of membrane-based processes for consistent water recovery. The occurrence of fouling introduces additional costs as it requires a higher driving force to generate required permeate flux. The extent of pre-treatment is determined by the quality of the feed water suitable for different membrane-based processes. It is important to study the fouling occurring in different types of membrane-based processes when it is applied for the reclamation of a specific type of wastewater. The fouling characterization will help with the effective selection of membrane-based processes for wastewater recovery.

Beer is one of the most consumed beverages in the world, which is among the top five in beverage sales by world market share [18]. The brewing industries that produce beers have high economic value (estimated at approximately 593 billion USD in 2017) and the global beer market has been projected with a compound annual growth rate of 1.8% between 2019 and 2025 [280]. In Canada, beer is the most popular alcoholic beverage which constitutes about 41.5% of total alcohol sales through the liquor boards and other retail outlets. Interestingly, nearly 85% of the beer sales in 2016 in Canada originated from local breweries [281]. Between 2013 and 2018, the number of breweries in Canada increased by 162% (from 380 breweries in 2013 to 995 breweries in 2018) [282]. The beer economy contributed about 13.6 billion CAD to Canada's gross domestic product in 2016 and has generated many jobs while generating economic activities across other sectors as well [282]. However, the production of beer results in discharging a high quantity of wastewater (~3 to 10 L wastewater for 1 L of beer production) containing sugars, ethanol, soluble starch, total suspended solids, volatile fatty acids, and a low concentration of heavy metals [22–25]. Discharge of brewery wastewater effluent requires adequate treatment to comply with the regulations providing protection to the environment, aquatic life, and to human health. Along with enhanced financial incentive of intake water and wastewater disposal fees, the brewers are inclining towards using sustainable solutions for the regeneration of water from the wastewater effluent for production or non-production purpose. Conventional brewery wastewater treatment approaches include different physico-chemical primary treatment processes followed by secondary biological schemes, like aerobic sequencing batch reactors [283], up-flow anaerobic sludge blanket reactors [284,285], and anaerobic membrane bioreactors [286,287]. Other studies have also explored

electrochemical processes for brewery wastewater treatment [288]. However, the anaerobic membrane bioreactor process has been widely adopted for treating brewery wastewater prior to its disposal [22,286].

Previous studies explored the potential of water reclamation from membrane bioreactor treated wastewater effluents through NF, RO, and MD for different types of wastewaters. The reclaimed water would be for both potable and non-potable reuse applications and the types of wastewater investigated included synthetic water, municipal wastewater, sewage treatment, and more [1,5–7,28,31,259,289,290]. The incorporation of membrane-based separation processes with adequately pre-treated brewery wastewater may inspire the recovery and reuse of water within the brewing facilities to reduce the footprint of beer production. In addition to the water recovery performance (both in terms of quality and quantity of reclaimed water), it is also important to assess the fouling characteristics of different membrane-based processes as they are employed to recover brewery wastewater.

This study employed three different membrane-based technologies, namely MD, RO, and NF for the reclamation of pre-treated brewery wastewater. The high-strength brewery wastewater was pre-treated using a membrane bioreactor (MBR) and the effluent was used as the feed for the membrane-based processes. Commercial membranes were used to evaluate the water recovery in MD, NF, and RO processes through assessing the permeate flux decline and contaminant rejections. The altered surface morphologies and chemical compositions of the membranes before and after water recovery operations were evaluated to elucidate the fouling phenomena in these processes. The outcome of the effective membrane cleaning mechanisms for the processes were also explored for possible flux recovery and membrane reuse. To the best of our knowledge, no other study has directly compared the water recovery performances and fouling characterization of MD, NF, and RO processes distinctly for MBR pre-treated brewery wastewater effluents.

3.2 Materials and method

3.2.1 Membranes and modules

3.2.1.1 Commercial membranes

Commercially available flat sheet highly hydrophobic microporous polytetrafluoroethylene (PTFE, TF-200) membranes with a polypropylene support from Pall Gelman, USA (pore size 0.20 µm, thickness 139 µm, porosity 84%, tensile strength 21.75 MPa, contact angle 139°, and liquid entry pressure (LEP) of 40 psi/2.68 bar) were used for MD applications. PTFE membranes are non-reactive with a high resistance to almost all the chemicals, as well as displaying excellent thermal stability up to 260°C [291]. For the nanofiltration membrane, polyamide thin film composite (TFC) NF-90 (tight nanofiltration membrane) from Dow Filmtec (Minneapolis, MN, USA) (molecular weight cut-off ~200-400 Da, thickness 218±40 nm, and recommended operational pH range 2-11) was used due to its high rejection efficiency in industrial application. The commercial UTC-82C polyamide (TFC) reverse osmosis membrane obtained from Toray Company (Poway, CA, USA) (molecular weight cut-off 0 Da) was implemented due to its enhanced performance and chemical resistance. Table 3.1 represents the commercial membranes used during this research.

Table 3.1: Commercial membranes used in the study for membrane distillation (MD), nanofiltration (NF), and reverse osmosis (RO)

Commercial membrane (Application)	**Manufacturer**	**Pore size/ Molecular weight cut-off**	**Polymer**
PTFE TF-200 (MD)	Pall Gelman	0.20 µm	Polytetrafluoroethylene
NF 90 (NF)	Dow Filmtec	~200-400 Da	Polyamide
UTC-82C (RO)	Toray	0 Da	Polyamide

3.2.1.2 System descriptions and operational conditions

For MD, a direct contact membrane distillation (DCMD) configuration, as shown in Figure 3.1a, was used. A PTFE flat sheet membrane cell (CF042P-FO) from Sterlitech Corporation, USA, was used. The effective membrane surface area of the DCMD cell was 34 cm^2. A constant temperature

of 55˚C (T_f) was maintained for the bulk hot feed using a hot water bath (Cole Parmer). Also, a chiller (Cole Parmer) was used to maintain a constant temperature of 16˚C (T_p) at the bulk cool permeate side. Both the hot feed and the cold permeate were circulated by two gear pumps (Model GH-75211-10, Cole-Parmer, Canada) at around 0.8 psi (Pressure Gauge Model GH-68930-12, Cole-Parmer, Canada) at the same speed across the bottom and the upper face of the membrane cell, respectively. Flow meters (0.1-1 LPM, McMaster-Carr, Canada) were used to observe the constant 0.7 LPM hot feed and the cool permeate circulation rate. The conductivity of the feed and permeate solution was measured with an electric conductivity meter (Okaton Instruments, IL, USA). MD application was continued for 80 hours to achieve considerable recovery (>80%) with nearly 50% flux drop.

A standard laboratory-scale cross flow filtration system, connected by stainless steel tubes and PVC tubes, was used for both NF and RO application. The schematics of the crossflow filtration system is shown in Figure 3.1b. The crossflow system was equipped with a diaphragm pump (1.7 GPM, 230 V, 60 Hz, 3 PH motor, hydra cell, Ca, USA), a stainless-steel water permeation cell, a panel-mount flow meter (0.25~1.5 LPM, purchased from McMaster-Carr, Canada), and a feed solution tank. The effective membrane surface area of the crossflow system was 33 cm^2. For NF and RO, 120 psi (P_{NF}, 8.27 bar) and 400 psi (P_{RO}, 27.58 bar) pressures were employed, respectively, at a feed side circulation rate of 0.7 LPM. A representative 400 psi value is specifically chosen from literature [270] that falls within the range of typical RO pressure (between 10 bar – 70 bar, i.e., 145 psi and 1015 psi) [257]. Also, 120 psi value was chosen for NF that falls within the typical operating pressure range of NF (between 5 bar – 20 bar, i.e., 70 psi – 290 psi) [292]. Low pressure was chosen for NF to study whether lower pressure would have minimal (less compact) fouling and enhance permeate flux and recovery from pre-treated brewery wastewater effluent. During the experiments, the temperature was maintained at 20.0 ± 0.5˚C. Both NF and RO membranes were compacted using DI water for 24 hours prior to water recovery applications. All the experiments were performed three times except for 3% of cases, and the average values were considered and presented.

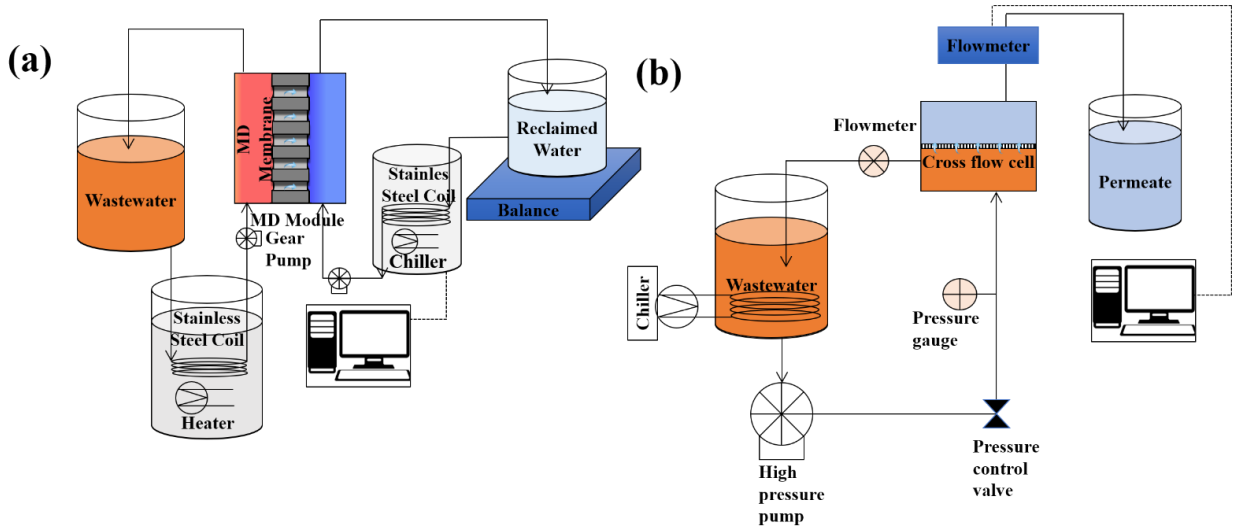

Figure 3.1: (a) Direct contact membrane distillation (DCMD) configuration and (b) Crossflow nanofiltration (NF) and reverse osmosis (RO) configuration used for pre-treated brewery wastewater effluent for 80 hours.

3.2.2 Feed characteristics

Brewery wastewater was obtained from a local brewery, which was pre-treated using a MBR. The wastewater contained a high chemical oxygen demand (COD) of 10,300±730 mg/L, pH 5.3±0.4, and alkalinity of 2.9±1.8 meq/L. A hybrid system using a combination of a Up-flow Anaerobic Sludge Blanket (UASB) reactor and a multi-staged membrane tank using 1.5 µm, 0.45 µm, and 0.04 µm membranes (ultrafiltration) was used to treat the brewery wastewater. Afterwards, air was circulated through the membrane tank effluent, and this effluent was further used as a feed for advanced membrane-based separation processes for possible water reclamation. Table 3.2 provides the characteristics of the pre-treated brewery wastewater. Furthermore, powdered activated carbon (NORIT SAE SUPER, average particle size diameter 15 µm and 965 m^2/gm specific surface area) treated the ultra-filtered (0.04 µm) brewery wastewater effluent, which was then used with RO process to observe the effect of additional pre-treatment on RO permeate flux. The PAC aid dose was 100 mg AC/L of wastewater. Often wastewater treatment processes adopt a pre-treatment utilizing activated carbon (AC) for the removal of organics and micro pollutants through adsorption via powdered (PAC) or granular (GAC) forms. Hence, PAC addition prior to ultrafiltration would reduce the load of the MBR effluent, which consequently improves the RO performance during water recovery. The COD of the PAC treated wastewater effluent was 40±2 mg/L.

Table 3.2: Brewery wastewater effluent characteristics from hybrid membrane bioreactor (MBR). This effluent was used as feed water in different advanced membrane-based separation processes

Parameters	**Unit**	**Concentration in hybrid MBR pre-treated effluent**
Chemical oxygen demand (COD)	mg/L	50 ± 10
Total organic carbon (TOC)	mg/L	30.33 ± 0.78
Total solids (TS)	g/L	1.77 ± 0.1
Turbidity	NTU	0.90 ± 0.05
Alkalinity	meq/L	16.98 ± 2.34
Silt density index (SDI)	--	4.89 ± 0.6
Electrical conductivity (EC)	mS/cm	5.5 ± 0.3
Total nitrogen (TN)	mg/L	34.64 ± 0.32
Total phosphorous (TP)	mg/L	101.41 ± 1.27
Extracellular polymeric substance (EPS)	mg/L	70 ± 20
Ca^{2+}, Mg^{2+}, Na^{+}, K^{+}, Li^{+}	mg/L	26.44±1.19, 32.31±1.51, 490.89±1.56, 28.86±1.3, 2.98±1.27
PO_4^{3-}, SO_4^{2-}, NO_3^{-}, Cl^{-}	mg/L	97.55±2.87, 32.93±1.05, 33.39±1.22, 48.24±1.03

COD and total organic carbon (TOC) concentrations were quantified to reveal the organic concentrations. COD, total nitrogen (TN), and total phosphorous (TP) concentrations were measured using Hach kits (London, Ontario, Canada), along with a Hach DR2800 spectrophotometer (London, Ontario, Canada) to measure absorbance. TOC analysis was conducted using a TOC analyzer (Shimadzu, Tokyo, Japan). Total solids (TS) concentration was measured using Standard Methods (2540 B) [293]. The alkalinity of the pre-treated feed water was measured following the Titration Method of the Standard Methods (2320 A) using an automatic titrator (848 Titrino plus, Metrohm) [294]. Turbidity and electrical conductivity (EC) were measured using a turbidity meter (ORION AQ3010) and a conductivity meter (Oakton Instruments), respectively. Silt density index (SDI) was measured following the ASTM D4189-07 (2014) [295]. Extracellular polymeric substance (EPS) was measured following the method described in Chen et al. (2016) [286]. Finally, cation and anion analyses were conducted using an

ion chromatograph (IC) (930 Compact IC Flex and 858 Professional Sample Processor by Metrohm).

3.2.3 Performance evaluation during water recovery

Performances of the MD, NF, and RO processes were observed primarily by flux reduction with a 5 L feed and concentrating the feed for 80 hrs. An 80-hour time interval was chosen to attain a high water recovery (>80%) and moderate flux drop (~50%). The permeate flux J (L/m^2-h) was measured using Eq.3.1.

$$J = \frac{\Delta M}{A\Delta t} \tag{3.1}$$

where ΔM is the quantity of the permeate (L), A is the effective membrane area (m^2), and Δt is the operational time (h). For NF and RO, the permeate flux was normalized to applied trans-membrane pressure and expressed as L/m^2-h-bar.

The osmotic pressure is the pressure required to stop the osmotic flow, which means that pressure must be applied to the concentrated feed solution to stop the flow of the pure water towards the concentrated solution via a semi-permeable membrane. Osmotic pressure of the wastewater effluent can be measured by using the van Laar equation in Eq. 3.2 [296].

$$\Pi_{0,p,f} = -(\frac{R_1 T}{V_0}) ln a_1 \tag{3.2}$$

where, $\Pi_{0,p,f}$ is the osmotic pressure, R_1 is the ideal gas constant, T is the absolute temperature, V_0 is the molar volume of the solvent, and a_1 is the water activity. For RO and NF, pressure higher than the osmotic pressure is applied in the feed side and hence, water flows through the semi-permeable membrane from the feed side towards the permeate side leaving behind the contaminants.

The concentrations of different water quality parameters in the feed and the permeate solutions were applied in Eq. 3.3 to calculate rejection (R) percentage.

$$R\ (\%) = \left(1 - \frac{C_{permeate}}{C_{feed}}\right) X100 \tag{3.3}$$

where, C_{feed} and $C_{permeate}$ are the concentrations of any water quality parameter in the feed and permeate solutions, respectively.

3.2.4 Membrane fouling characterization

The surface morphologies of the pristine and fouled membranes were observed with a Field Emission Scanning Electron Microscope (FE-SEM, Quanta 450 Environmental, FEI Company, USA). The membrane samples were coated with a 4 nm thick platinum layer prior to the microscopic observations. Energy Dispersive X-ray Spectroscopy (EDS) was employed to measure the elemental compositions on the membrane surfaces. Attenuated Total Reflectance-Fourier Transform Infrared (ATR-FTIR, Nicolet 6700/Smart iTR, Thermo Scientific, USA) spectra was used for qualitative analysis of the chemical changes in the active layer by identifying the changes in the functional groups of the pristine and the fouled membranes. During FTIR analysis, the intensity of the peak at specific wavelengths confirmed the presence of specific functional groups. Surface hydrophobicity and hydrophilicity of the membranes were assessed by DI water contact angle measurements using the sessile drop method (VCA, AST Products, Inc., Billerica, MA, USA). A DI water droplet was placed on the membrane surface and an image of the DI water drop was recorded. The contact angle was then measured by fitting the Young-Laplace equation around the DI water droplet.

3.2.5 Membrane recovery

Two cycles of water recovery (6 hours each) with chemical cleaning were investigated to evaluate recovery performances of different membranes. The 6-hour cycles were chosen to observe the efficacy of membrane cleaning in terms of membrane performance and membrane fouling. Previous studies have observed the efficacy of membrane cleaning during long term operation with 3 hour cleaning intervals [176]. After 6 hours operation, the MD system was cleaned with DI water for 1 hour followed by 30 minutes of caustic (0.1M NaOH) and 30 minutes of acid (0.01M HCl) cleaning for removal of organics and inorganics foulants [297]. The system was then cleaned with deionized (DI) water produced by a Milli-Q ultrapure water purification system to remove any residues. After that, a second 6-hour cycle of operations was observed. The same cleaning protocol was maintained to recover the MD membrane after the second cycle of water recovery. NF and RO systems were cleaned with 0.5 mM EDTA at pH 11 by discarding the initial 30% of the solution and recirculating the remaining 70% of the solution for 2 hours after 6 hours operations of first cycle of water recovery [273,277,298]. Afterwards, the system was cleaned with DI water

to remove any residues followed by the second 6 hours cycle of recovery. The same cleaning protocol was maintained for NF and RO membranes after the second cycle of recovery.

3.3 Results and discussion

3.3.1 Permeate flux of membrane-based separation processes during water recovery

MD application over 80 hours interval resulted in ~86% water recovery from a 5 L feed solution. The initial permeate flux was ~30 L/m^2-h, and it was reduced by ~53% after 80 h. NF of the same feed solution (volume 5 L) for 80 hours could recover around 16% of water with 98% flux drop from an initial permeate flux of 3.8 L/m^2-h-bar. The RO process recovered around 12% of feed water with about 98% flux drop from an initial permeate flux of 1.7 L/m^2-h-bar. Figure 3.2 shows the percent permeate flux drop and percent recovery in MD, NF, and RO processes after 80 hours operation with an initial 5L feed solution. The comparison was carried out based on selecting operational pressures from the typical operating pressure ranges for RO and NF [257,270,292], respectively, as well as same experimental duration of 80 hours, similar crossflow rate of 0.7 LPM, similar feed characteristics, and same initial feed volume of 5 L. Representative pressure values within the operating pressure ranges were chosen to experimentally study the permeate flux drop and recovery performances with different membrane processes while using 5 L pre-treated brewery wastewater effluent as feed at 0.7 LPM crossflow rate for 80 hours.

The permeate flux drop is an indication of the occurrence of membrane fouling. Membrane surface analysis (discussed in later sections) would provide a comprehensive understanding of the fouling phenomena. The SDI value of the pre-treated brewery feed water was 4.89 (i.e., less than 5), which rationalizes its application as feed water in the NF and RO processes [299]. However, the collective influence of inorganic fouling, organic fouling, and biofouling, especially at low operational temperature (20.0 ± 0.5˚C), could have contributed negatively to the NF and RO performances. Further pre-treatment of the MBR effluent might have improved the performance (permeate flux) of the NF and RO processes. To keep the fouling characterization and comparison consistent across MD, NF, and RO processes, the same feed water was used in all three systems in the current study. From the percentages of flux drop and water recovery, it can be concluded that MD performs better

than NF and RO over 80 hours operations when pre-treated brewery wastewater is applied as feed water in these processes. Further analyses of foulants are provided in Section 3.3.3.

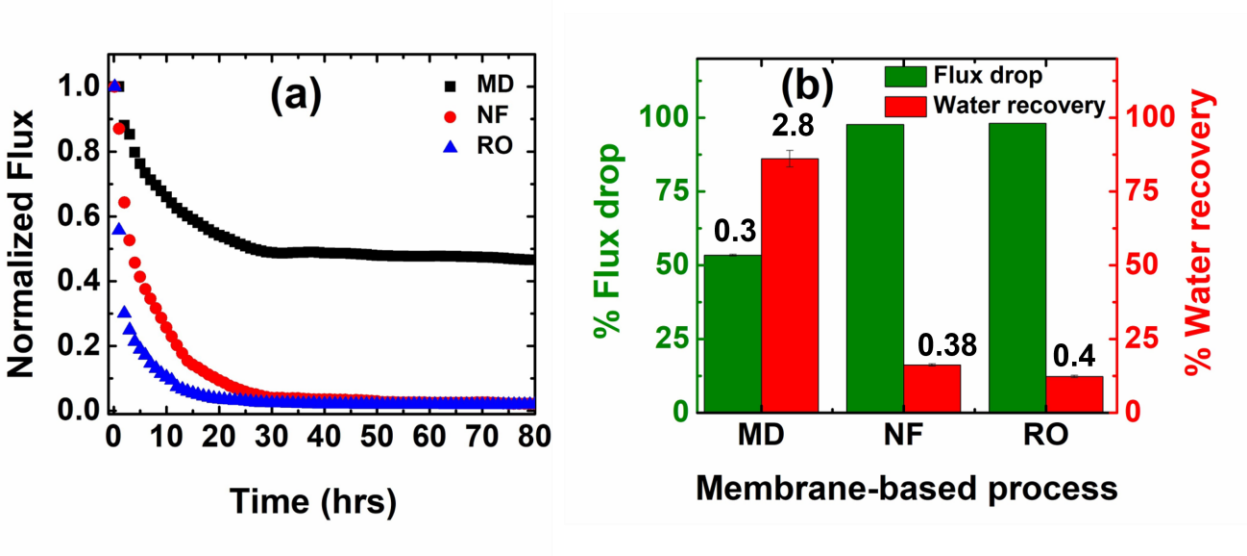

Figure 3.2: (a) Normalized permeate flux and (b) Permeate flux drop and water recovery of DCMD (PTFE), NF (NF90), and RO (Toray) for 80 hours operation with a feed with COD = 50 ± 10 mg/L and a 0.7 LPM flowrate, T_f = 55°C and T_p = 16°C for MD, P_{NF} =120 psi, P_{RO} = 400 psi with a constant temperature of 20.0 ± 0.5˚C. DCMD process has 53% flux drop with 86% water recovery whereas NF and RO membranes have 98% flux drop with 16% and 12% water recovery respectively [All the experiments were performed three times with the exception of 3% of the cases, and the average values were considered and presented; the error bars of (b) represent the standard deviation from the average value].

3.3.2 Membrane rejection

Figure 3.3 shows that around 99%, 86%, and 97% TOC rejections were observed with MD, NF, and RO, respectively. The feed TOC was 30.3±0.78 mg/L and the permeate TOC concentrations were 0.42 mg/l, 4.17 mg/l, and 0.97 mg/l for MD, NF, and RO, respectively. To evaluate membrane wetting, electrical conductivity (EC) of MD permeate was measured. EC of MD permeate was considerably low (around 18±2 µs/cm) ensuring that membrane pores were not wetted. Negligible concentration of sodium (~0.17 mg/L) and chloride (~0.1 mg/L) ions as well as the absence of other ions (potassium, calcium, magnesium, lithium, nitrate, phosphate, sulphate) in the MD permeate also confirmed that MD membrane pore wetting did not occur even after the 80 hours of operation. The conductivity of the RO and NF permeate were 118±2 µS/cm and 714 ±2 µS/cm, respectively. However, as no wetting was observed with MD, the adsorption-desorption mechanism could be responsible for organic permeation through the membrane without pore

wetting [74]. Organics like humic acid initially adsorb on the membrane surface and forms a hydrogen bond with water vapor. The hydrogen bond is formed between the carboxylic group in the humic acid and the oxygen molecule in water vapor. The hydrogen bond fails as the vapor passes through the membrane pores and re-adsorption of humic acid takes place in downstream pore surface. The continuous adsorption-desorption process continues until the humic acid crosses the membrane cross-section and gets dispersed to the permeate side [276,297].

For the pressure-based NF and RO processes, size exclusion was the critical form of organics rejection. As a result, NF achieved lesser TOC rejection than RO. Similar trends were observed for COD rejection. Significant (>98%) COD removal was found in MD, whereas ~94% removal was observed in NF and RO (with RO rejection performance slightly higher than NF). Complete removal of total nitrogen (TN) and total phosphorus (TP) were obtained with MD. RO also demonstrated enhanced removal performance for TP (100% rejection) and TN (99% rejection). However, for NF, only 64% rejection of TN and 95% rejection of TP were observed. The larger pore size of NF membranes, which enabled slightly higher water recovery percentage than RO, contributed to its lower rejection performances. Thus, both MD and RO membranes demonstrated superior rejection performance for TOC, COD, TN, and TP than NF membranes. Furthermore, RO permeate flux performance was investigated with PAC aid treated ultra-filtered wastewater effluent where improved permeate flux was observed with RO membranes (Figure A1.2) along with 97% COD removal. The organics, inorganics, and microbes all can cause significant RO membrane fouling within a very short period. Thus, it can be surmised that RO process can be implemented for water recovery if further load reduction of the feed water is conducted instead of directly implementing MBR treated feed. As NF membrane was inept in terms of contaminant rejection, implementation of NF process for water recovery from MBR treated high strength brewery wastewater would not be ideal.

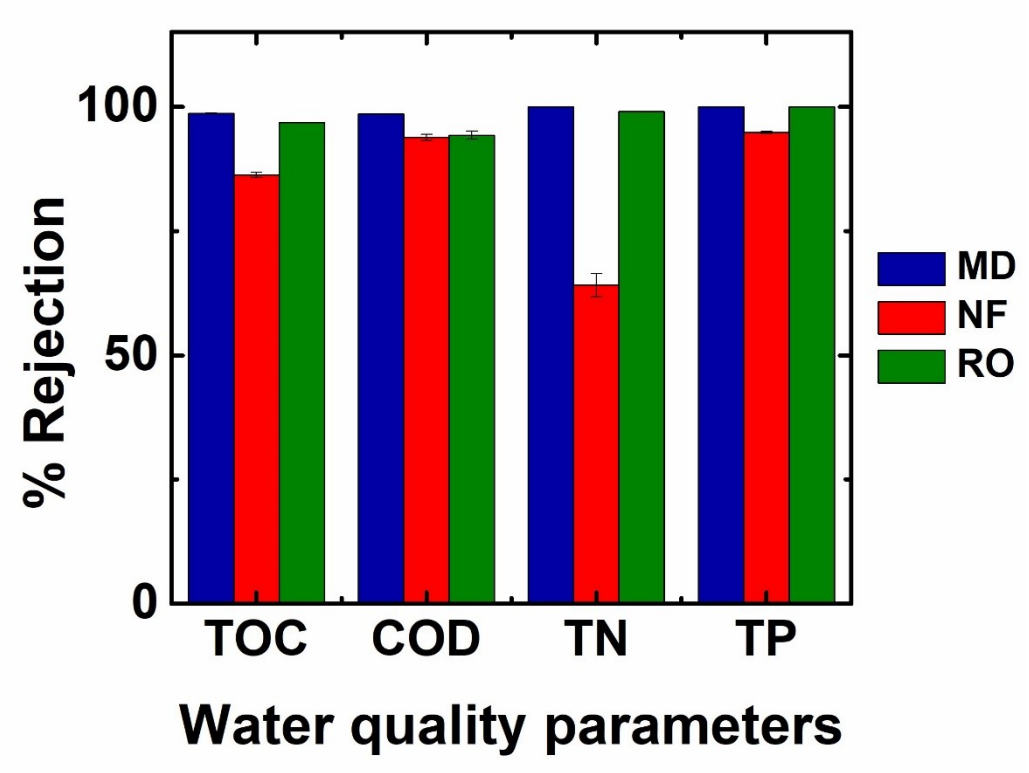

Figure 3.3: Rejection of Total Organic Carbon (TOC), Chemical Oxygen Demand (COD), Total Nitrogen (TN), and Total Phosphorous (TP) of DCMD (PTFE), NF (NF90), and RO (Toray) membranes after 80 hours application with a feed with COD = 50 ± 10 mg/L and a 0.7 LPM flowrate, $T_f = 55^0$C and $T_p = 16^0$C for MD, P_{NF} =120 psi, P_{RO} = 400 psi with a constant temperature of 20.0 ± 0.5˚C. High Rejection of TOC, COD, TN, and TP with DCMD and RO membranes were observed whereas NF membrane was inept in TOC and TN rejection along with lower COD and TP removal than DCMD and RO [All the experiments were performed three times with the exception of 3% of the cases, and the average values were considered and presented; the error bars represent the standard deviation from the average value].

3.3.3 Membrane fouling analysis

The surface morphology of the pristine and fouled membranes was observed through the SEM analysis (Figure 3.4). Figure 3.4a(i) and 3.4a(ii) shows the variation in the surface morphology of the PTFE MD membrane before and after fouling, respectively. The presence of the fouling layer shown in Figure 3.4a(ii) could be attributed to the organics and inorganics present in the feed water. The fouled PTFE MD membrane has a thick foulant layer on the top of the membrane surface which caused the permeate flux decline. No biofouling was observed on the MD membrane surface after 80 hours of operation. For the NF membranes (Figure 3.4b(ii)) and RO membranes (Figure 3.4c(ii)), the significant flux drop could be attributed to the combined effect of organic

fouling, inorganic fouling, and biofouling. Both NF and RO membranes showed presence of organic, inorganic foulants, and microorganisms (Figure 3.4b(ii) and 3.4c(ii)) on the membrane surface after 80 hours of operation. The feed wastewater contained a considerable amount of organics and nutrients. Also, the operating temperature (20.0 ± 0.5˚C) of the RO and NF was favorable for microbial growth. Overall, the combination of organic foulants with a considerable amount of EPS, inorganic scales, and microorganisms drastically reduced the permeate flux within a short time after filtration was initiated.

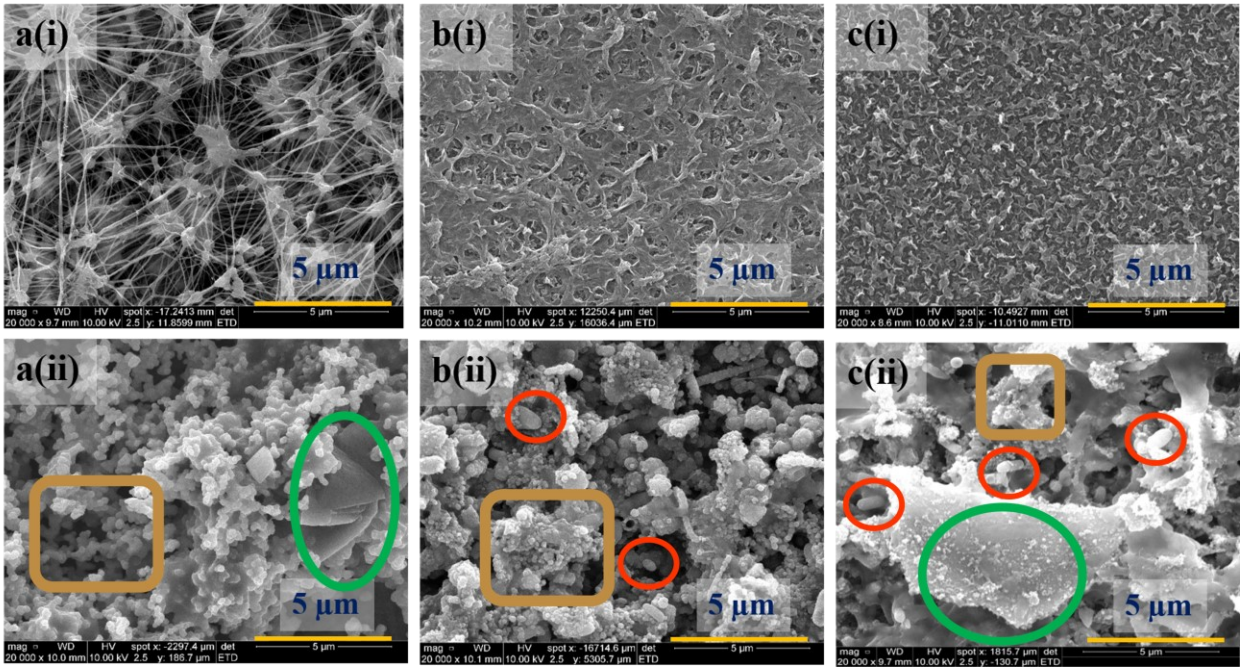

Figure 3.4: SEM images of (a) DCMD (PTFE), (b) NF (NF90), and (c) RO (Toray) membranes to observe the variation of surface fouling morphology of (i) pristine, and (ii) fouled membranes after 80 hours application with MBR treated wastewater with a COD = 50 ± 10 mg/L and a 0.7 LPM flowrate, T_f = 55ºC and T_p = 16ºC for MD, P_{NF} =120 psi, P_{RO} = 400 psi with constant temperature of 20.0 ± 0.5˚C. DCMD membrane surface layer (a) contains organic and inorganic fouling whereas NF (b) and RO (c) membrane surfaces contain microbial cells along with organic and inorganic fouling. The green, brown, and red shapes show the inorganic, organic, and biofouling, respectively, on the membrane surfaces.

Figure 3.5 shows the ATR-FTIR peaks observed on the pristine and fouled membrane surfaces. The peak at 1046.37 cm^{-1} (Figure 3.5a and 3.5b) for the fouled MD and NF, at 1011 cm^{-1} (Figure 3.5b), and 1015 cm^{-1} (Figure 3.5c) for the fouled NF and RO membranes, respectively, are attributed to the presence of C-O, C-O-C from polysaccharides (carbohydrates) or P-OR (esters)

[300–303]. The peak observed near 1234 cm^{-1} (1200 cm^{-1}-1275 cm^{-1}) on the NF membrane is ascribed to phosphoramide ($P(=O)(NH_2)_3$ [303]. The characteristic peaks near 1400 cm^{-1} to 1421 cm^{-1} in all fouled membranes are from carboxylic acids of the humic substances (O-H stretching) [4]. The peaks near 1471 cm^{-1} to 1482 cm^{-1} for all three fouled membranes are associated with calcium carbonate scaling [302]. The peaks at 1575 cm^{-1} and 1541 cm^{-1} for MD membranes corresponds to the vibration of amide from proteins (Amide II, CNH) [4,300,301]. The peaks observed at 1640 cm^{-1} and 1645 cm^{-1} for MD and NF-RO, respectively, is associated with amide I band from proteins (C=O) [4,300,301]. The peaks observed at 2850 cm^{-1} (MD), 2917 cm^{-1} (MD and RO), and 2955 cm^{-1} (MD, NF, and RO) correspond to the cellular lipids (fatty acids, symmetrical and asymmetrical -CH- vibrations) [300,301]. A vibrational band observed at 3000 cm^{-1} to 3600 cm^{-1} with a peak at 3292 cm^{-1} and 3279 cm^{-1} for MD-RO and NF, respectively, are attributed to the O-H and/or N-H from the alcohol and/or amine group [286]. Additional peaks at 684 cm^{-1}, and 870 cm^{-1} for NF and 681 cm^{-1} and 866 cm^{-1} for RO membranes are for calcium phosphate, and calcium carbonate scaling respectively with an additional peak at 828 cm^{-1} for NF membrane due to nitrate [304].

EDS analysis of the membrane surfaces was performed which confirmed the attachment of the foulants by providing the elemental compositional variation of the pristine, fouled, and cleaned membranes (Table 3.3). EDS Analysis confirms the presence of P, N, Ca, Na, Mg, Cl, and O on the fouled membrane surfaces. Thus, SEM-EDS along with FTIR analysis indicates the presence of inorganic Ca, Na, and Mg salts as well as the organic components composed of C, O, N, and P on the fouled membrane surfaces.

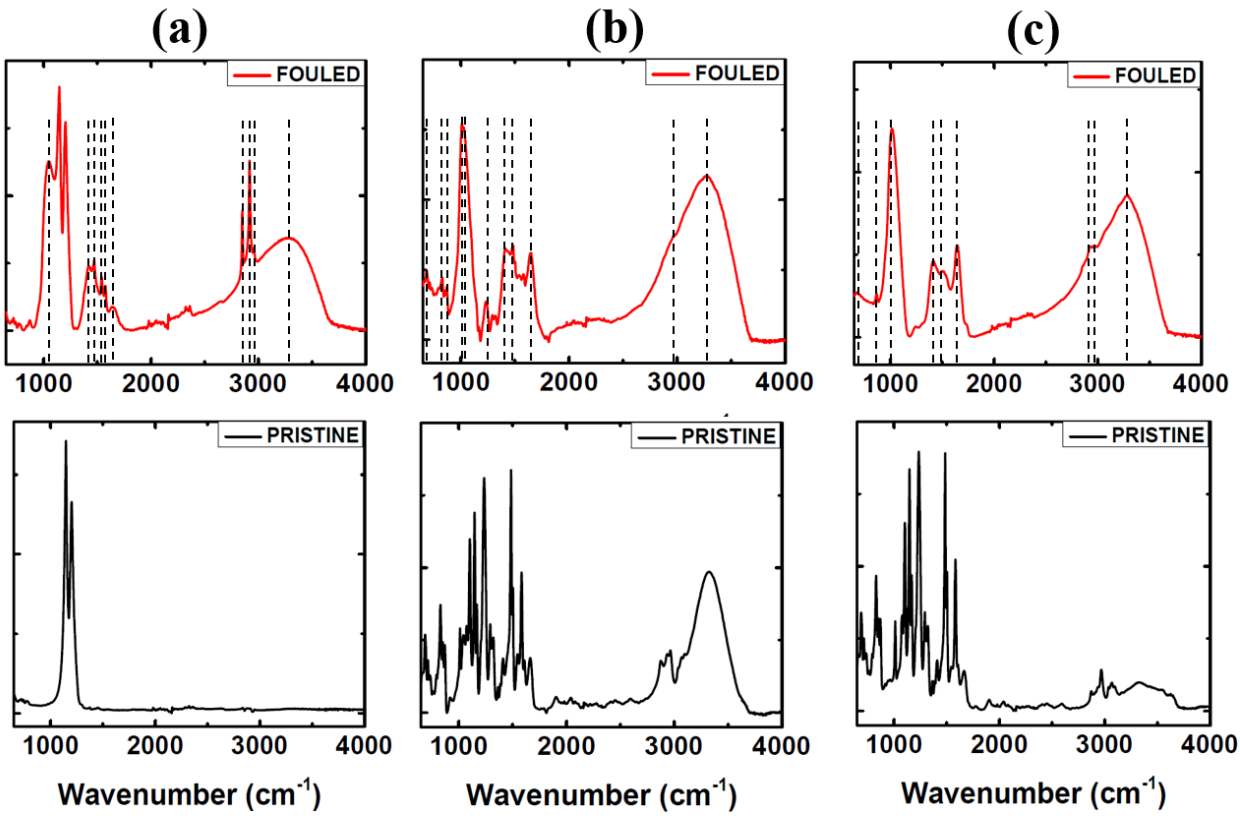

Figure 3.5: Observing chemical changes in the active layers of the (a) DCMD (PTFE), (b) NF (NF90), and (c) RO (Toray) membranes through ATR-FTIR prior to and after 80 hours operation with a feed with COD = 50 ± 10 mg/L and a 0.7 LPM flowrate, $T_f = 55^0C$ and $T_p = 16^0C$ for MD, P_{NF} =120 psi, P_{RO} = 400 psi with a constant temperature of 20.0 ± 0.5˚C.

Table 3.3: Elemental analysis of pristine, and fouled DCMD (PTFE), NF (NF90), and RO (Toray) membrane surfaces through EDS prior to and after 80 hours operation with a feed with COD = 50 ± 10 mg/L and a 0.7 LPM flowrate, $T_f = 55^0C$ and $T_p = 16^0C$ for MD, P_{NF} =120 psi, P_{RO} = 400 psi with a constant temperature of 20.0 ± 0.5˚C

Membrane	**Element percentage observed on membrane surface**										
	C (%)	**O (%)**	**F (%)**	**P (%)**	**N (%)**	**Ca (%)**	**Na (%)**	**Mg (%)**	**Cl (%)**	**S (%)**	**Pt (%)**
MD Pristine	36	-	63.5	-	-	-	-	-	-	-	0.5
MD Fouled	10.3	56.5	-	6.8	2.7	8.6	12.3	1.9	0.7	-	0.2
NF Pristine	81.6	8.6	-	-	7	-	-	-	-	2.6	0.2
NF Fouled	24	48.2	-	7.4	4.6	12.9	-	2.2	-	-	0.7
RO Pristine	82.9	9.7	-	-	4.3	-	-	-	-	2.8	0.3
RO Fouled	29.3	43.7	-	6.7	5.2	11.6	0.9	1.8	-	-	0.8

Figure 3.6 represents the DI water contact angle of the pristine, fouled, and cleaned membranes. The MD membrane experienced the highest drop in contact angle (85.6%), while the contact angle reduction of NF and RO membranes were 50.7% and 34.5%, respectively. With all three membranes, the observed contact angle after 80 hours of application was lowered due to the formation of a hydrophilic fouling layer on the membrane surfaces.

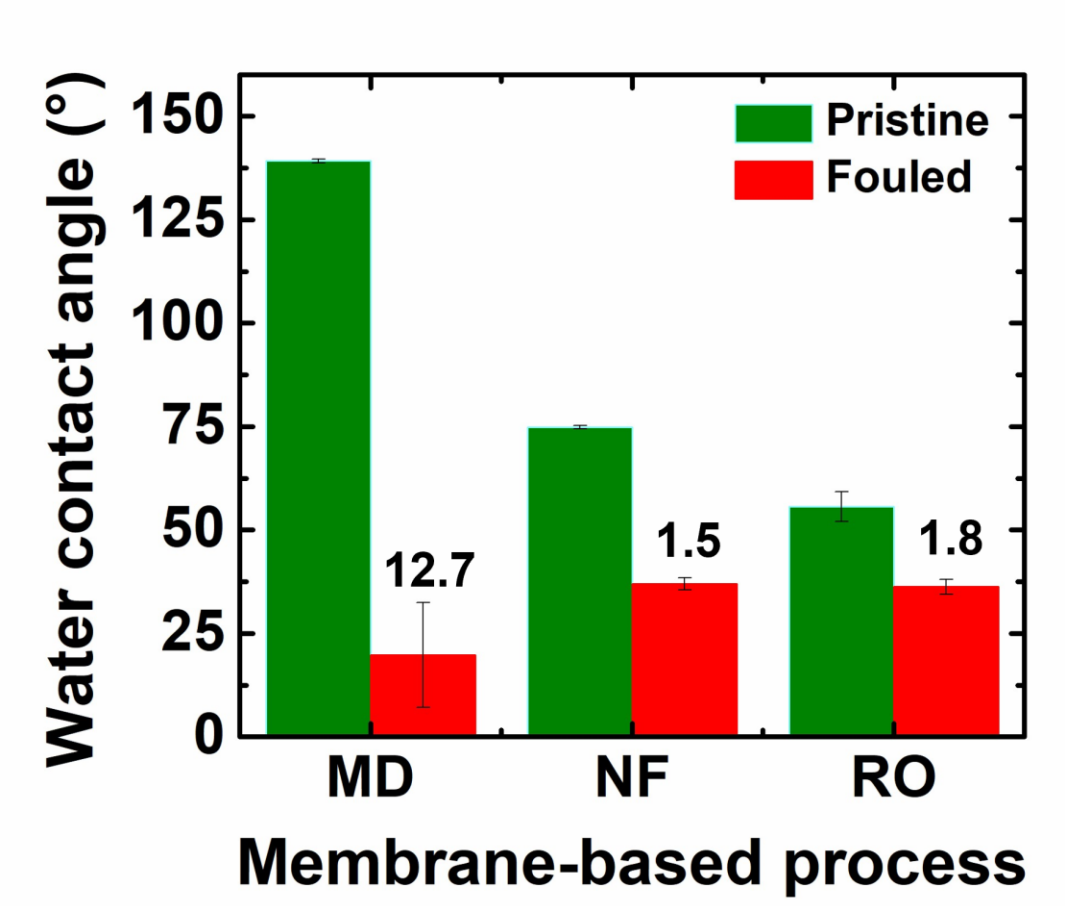

Figure 3.6: Contact angle of pristine, and fouled DCMD (PTFE), NF (NF90), and RO (Toray) membranes prior to and after 80 hours operation with a feed with COD = 50 ± 10 mg/L and a 0.7 LPM flowrate, T_f = 55°C and T_p = 16°C for MD, P_{NF} =120 psi, P_{RO} = 400 psi with a constant temperature of 20.0 ± 0.5˚C. Contact angle reduction of fouled membranes from its pristine conditions are 85.6%, 50.7%, and 34.5% for DCMD, NF, and RO membranes respectively [The contact angle measurements were performed three times with the exception of 3% of the cases, and the average values were considered and presented; the error bars represent the standard deviation from the average value].

The membrane surface morphology through SEM, enhanced elemental composition by EDS analysis, and the functional group through FTIR along with the permeate flux drop confirm the foulants (organic and inorganic) adsorbtion onto the membrane surfaces. EPS present in the feed water containing protein, lipids, polysaccharides, and humic acid were the primary source of the organic constituents of the feed water. All the three membranes showed similar organic foulant adhesion, primarily proteins, lipids, polysaccharides, and humic substances, along with inorganic Ca and Mg carbonate salts. MD (PTFE) membranes demonstrated additional sodium chloride

fouling, while NF and RO displayed additional calcium phosphate fouling. Calcium, the predominant inorganic foulant observed, can form crystal structures by forming calcium carbonates and calcium phosphates (of which hydroxyapatite ($Ca_5(PO_4)OH$) forms crystal structures) [305]. Figures 3.7 and 3.8 depicts the schematic of probable fouling mechanisms of MD and NF/RO membranes, respectively during the water recovery application of pre-treated brewery wastewater effluent.

The high feed temperature in MD process decreased the solubility of the salts in the pre-treated brewery wastewater, which leads to the formation of inorganic salt deposits on the PTFE MD membranes. The amphiprotic organics contain the hydrophobic functional groups like hydrocarbon chain and hydrophilic functional groups like the carboxyl groups that caused an organic foulant layer deposit through the hydrophobic-hydrophobic interaction between the hydrophobic MD membrane surface and the hydrophobic tail of the amphiprotic organics exposing their hydrophilic heads to the feed side [9], which could be responsible for making the MD membrane surface more hydrophilic than other membranes. Previous studies revealed that initiation of the hydrophilic nature of the fouled membrane would enhance membrane fouling due to enhanced adhesion of hydrophilic organics [40]. No biofouling was observed on the MD membrane due to the high temperature, which resisted the microbial cell growth. The thick foulant layer on MD membrane surface could have bacterial endospores as observed by other researchers [152].

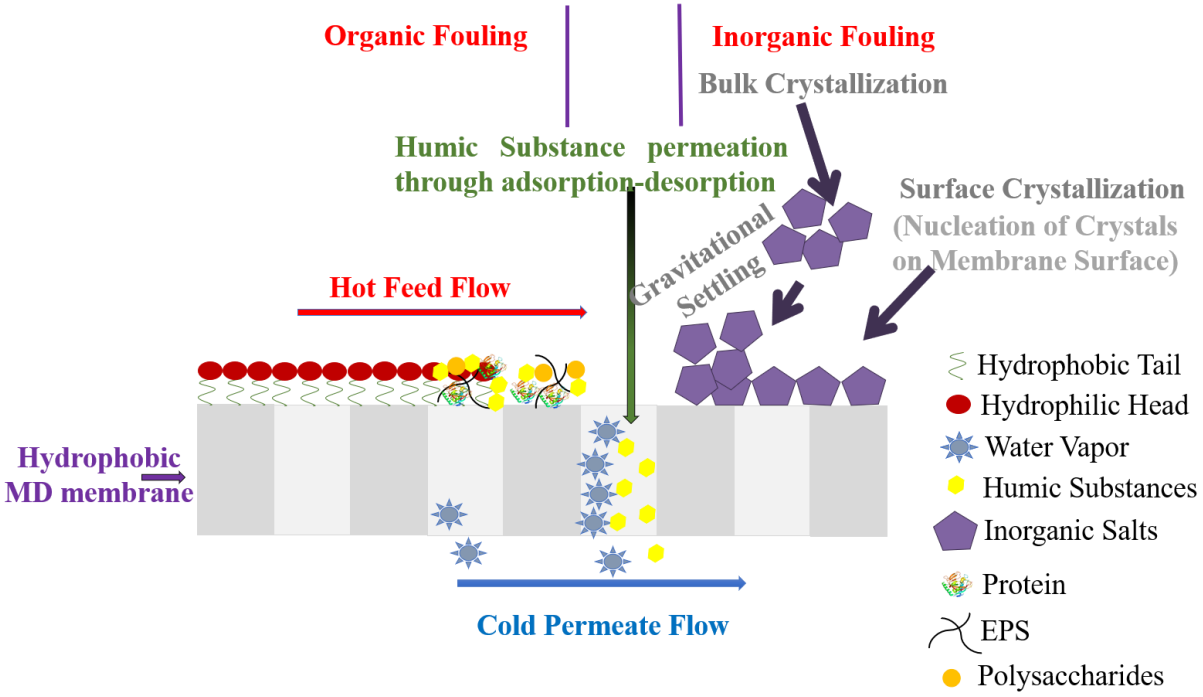

Figure 3.7: Schematic of probable fouling mechanism in the surface layers of the hydrophobic DCMD (PTFE) membrane after 80 hours of operation with a feed with COD = 50 ± 10 mg/L and a 0.7 LPM flowrate, T_f = 55°C and T_p = 16°C including organic fouling and inorganic scales.

NF and RO membranes demonstrated more visible fouling (Figure S2) and a larger percentage flux drops than MD membranes at the end of 80 hours of operation. The high pressure of NF and RO processes additionally contributed to the formation of the cake fouling layer that included complex interaction between the divalent cations (calcium and magnesium) and negatively charged functional groups of the feed organics [306]. The formation of the cake layer and salt crystal precipitations, along with concentration polarization, were the complex phenomena that contributed towards higher membrane fouling and flux decline for the membranes. Commonly found inorganic fouling during pressure-based processes is referred to as scaling, which is caused due to the concentration of sparingly soluble salts of the feed above their saturation limits. In addition to organic and inorganic fouling, the biological foulants were also observed, which collectively caused significant flux decline in these two processes. Also, the hydrophilic functional groups of the organics made the membrane surface hydrophilic, which was confirmed through the reduced contact angle of the fouled membranes. The RO process also had more a compact fouling layer than the NF process (which was visually evident from the darker brown color deposits on the

membrane surface) due to higher pressure and smaller pore sizes (Figure S2). Thus, it was surmised that MBR treatment was not adequate as a pre-treatment for the direct implementation of RO process, with additional pre-treatment clearly necessary to reduce organic, inorganic, and biological foulants of the feed water for RO application.

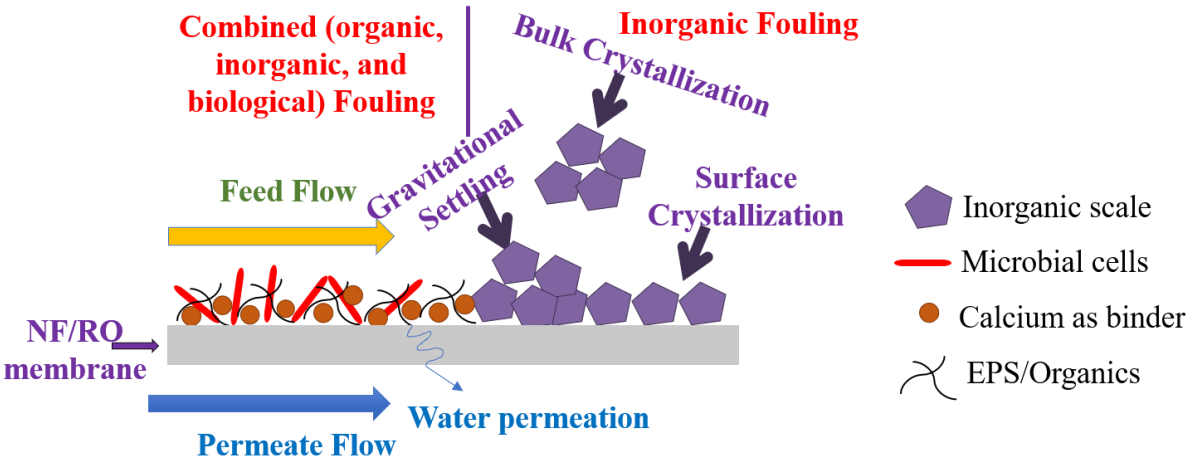

Figure 3.8: Schematic of probable fouling mechanism on the surface layers of the hydrophilic NF and RO membrane after 80 hours operation with a feed with COD = 50 ± 10 mg/L and a 0.7 LPM flowrate, P_{NF} =120 psi, and P_{RO} = 400 psi with a constant temperature of 20.0 ± 0.5˚C including organic fouling and inorganic scales along with microbial cells.

3.3.4 Effect of cleaning on flux recovery

Figure 9 represents the normalized permeate flux (normalized with respect to initial wastewater permeate rate) after membrane recovery for MD, RO, and NF. The SEM images (Figure 3.9) of the fouled membranes after 6 hours of operation showed considerable fouling on the membrane surface. The NF and RO membrane surfaces exhibited biological fouling. On the MD membrane surfaces, no crystalline inorganic foulants were observed, only non-crystalline inorganic and organic fouling layers were present. The spherical deposits after 6 hours of operation might also contain bacterial endospores at the operating temperature (55°C). Membrane cleaning was effective for all three membranes in terms of flux recovery. More than 90% wastewater flux was recovered with all the membranes for two consecutive wastewater application and cleaning operations.

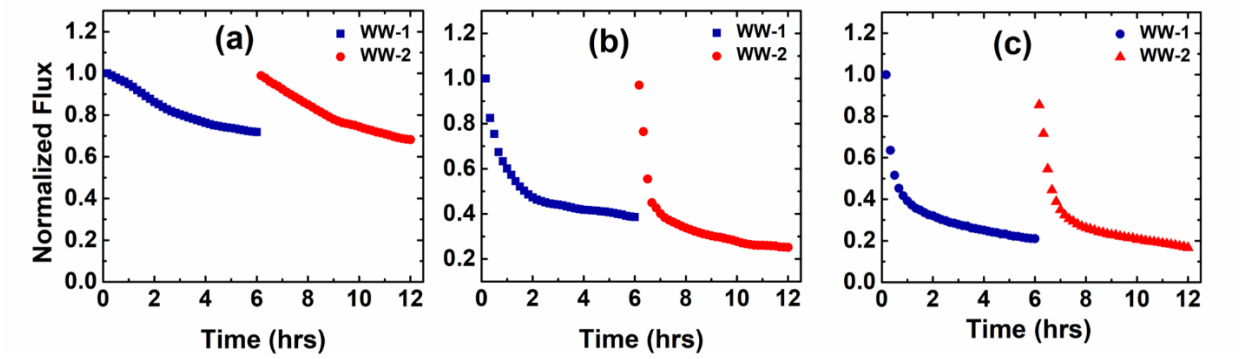

Figure 3.9: Permeate flux recovery after 6 hours application with MBR treated effluent of the (a) DCMD (PTFE) membranes cleaned with 0.1 M NaOH and 0.01 M HCl repeatedly, (b) NF (NF90), and (c) RO (Toray) membranes both cleaned with 0.5 mM EDTA at pH 11 repeatedly followed by DI water rinsing. More than 90% wastewater flux was recovered with all the membranes for two consecutive M application and cleaning operations.

The 6-hour fouling pattern of the MD, NF, and RO membranes was different from the 80 hours fouling layer, displaying a less compact foulant layer without the presence of salt crystals (Figure 3.10). The short operational duration indicates that the lower concentration polarization was the primary cause for reduced fouling. The SEM images of the cleaned MD (PTFE) membrane (FigureA3.S3a) show that the membrane surface morphology after membrane cleaning was similar to that of the pristine membrane. The thick foulant layer previously observed in the fouled MD membrane surface was removed during the cleaning operations and hence, membrane recovery was achieved. However, for the cleaned NF and RO membranes (Figure A1.3b and A1.3c), though the foulants were removed, the membrane surface morphology of the cleaned membrane varied from that of the pristine membranes.

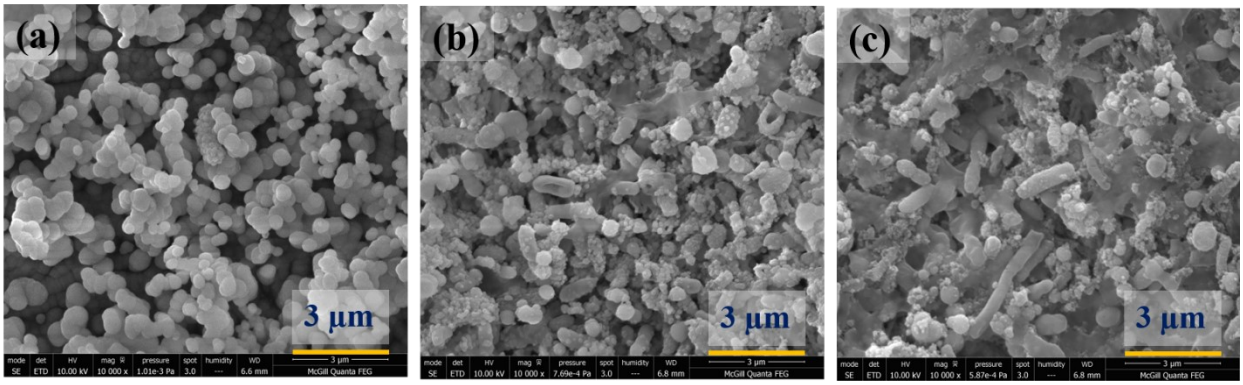

Figure 3.10: SEM images of the fouled (a) DCMD (PTFE) membranes, (b) NF (NF90), and (c) RO (Toray) membranes after 6 hours application with MBR treated effluent with a COD = 50 ±

10 mg/L and a 0.7 LPM flowrate, T_f = 55°C and T_p = 16°C for MD, P_{NF} =120 psi, P_{RO} = 400 psi with a constant temperature of 20.0 ± 0.5˚C.

Furthermore, EDS analysis (Table A1.1) showed that for the MD membrane, the elemental composition of the cleaned membrane (after repeated use and second cleaning) was similar to that of the pristine membrane, which comprised of ~36-37.5% C and ~62-63.5% F. However, for the NF membrane, nearly 5% enhanced elemental N along with ~0.4% increased elemental O was detected. The elemental C and elemental S in the NF membranes decreased by ~4.5% and 0.8%, respectively. For RO membranes, a similar trend to NF was observed, where elemental C and elemental S was decreased by 8.5% and 1.6%, respectively, after cleaning. The elemental N and elemental O content enhanced by 8.3% and 1.7%, respectively, in the RO membrane.

PTFE pristine and cleaned membranes (Figure 3.11a) have similar intensity peaks of -CF_2 and -CF_3 functional groups at 1148 and 1202 cm^{-1}, respectively, which shows that the membrane cleaning was effective by removing foulants and reversing back to the pristine membrane properties. NF membranes (pristine and cleaned, Figure 3.11b) demonstrated similar peaks except at 3302 cm^{-1} for amine group, which might be attributed to the residual of EDTA remaining on the membrane surface after cleaning [307]. RO peaks of the cleaned membrane were altered with decreased intensity except for increased intensity at 3281 cm^{-1}. Thus, it can be surmised that though the membrane cleaning operation could recover more than 90% of the flux, it caused moderate to significant alteration of the NF and RO membrane surfaces due to adsorption of the cleaning chemicals on the membrane surfaces.

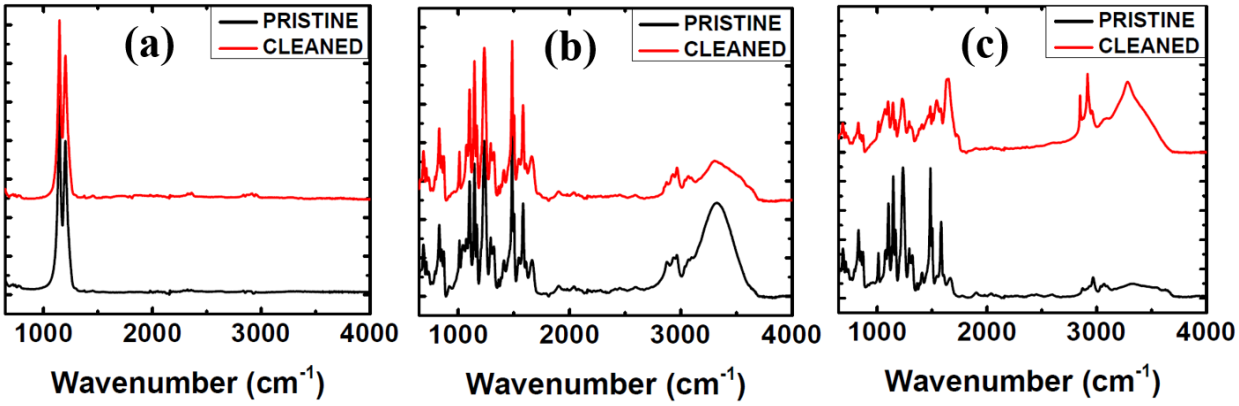

Figure 3.11: ATR-FTIR spectra of surface layers of pristine and cleaned (after repeated 6 hours MBR treated effluent application with a COD = 50 ± 10 mg/L and a 0.7 LPM flowrate, T_f = 55°C and T_p = 16°C for MD, P_{NF} =120 psi, P_{RO} = 400 psi with a constant temperature of 20.0 ± 0.5˚C

and cleaning) (a) DCMD (PTFE) with NaOH (0.1 M) and HCl (0.01 M), (b) NF (NF90), and (c) RO (Toray) membranes with 0.5 mM EDTA at pH 11.

3.4 Conclusions

In this study, the performance, fouling characterization, and contaminant rejection of three membrane-based separation processes (MD, NF, and RO) during water reclamation from MBR treated brewery wastewater effluent were investigated. MD could achieve 86% water recovery with 53% flux reduction after 80 hours application without any membrane wetting. However, NF and RO had significant flux drop rapidly with around 16% and 12% water recovery after 80 hours application with significant flux drop within the first few hours of application. RO performance in terms of permeate flux was enhanced when further powdered activated carbon pre-treatment was implemented. Thus, additional pre-treatment to the MBR effluent prior to NF and RO application can improve the performance of the NF and RO processes, but the same quality feed water was used across all three systems for fouling analysis and characterization. Contaminant rejections were high for both MD and RO, as they could rejected 99% and 97% TOC, respectively, along with high COD, TN, and TP rejection. However, though NF could achieve around 94% COD and ~95% TP rejection, its organic rejection (86%) and nitrogen (64%) rejection was undesirable. All three processes had organic and inorganic fouling. NF and RO membranes showed microbial cells on the membrane surface, whereas the MD membrane did not have any microorganism due to the high feed temperatures resisting microbial growth. EDS and FTIR analysis confirmed the similar absorbance of protein, lipids, polysaccharide, and humic acids on all three membranes with carbonate (MD, NF, and RO) and phosphate scaling (NF and RO). However, the fouling layer was less compact with MD due to the absence of high pressure, when compared to NF and RO. Repeated use and cleaning of the membranes showed MD membranes could be recovered in terms of permeate flux and similar surface morphologies and surface elemental compositions (SEM-EDS analysis). For NF and RO membranes, though significant flux recovery could be achieved, the membrane surfaces were altered. The possible reason for this alteration could be adsorption of chemical cleaning agents on the membrane surface caused by EDTA cleaning at high pH.

This study surmises that MD application has the potential to be implemented for water recovery of MBR treated brewery wastewater directly, without further treatment, due to its notable performance (i.e., high flux recovery, reduced flux decline, and a less compact fouling layer).

However, the optimal condition for specific wastewaters needs to be explored as distinct operational conditions (e.g., feed temperature, membrane materials, membrane opening, etc.) can alter treatment conditions, causing biofouling and deteriorating overall system performance. NF and RO membranes were susceptible to biofouling, which caused a significant flux drop, whereas the high temperature of the MD feed prohibited biofouling by inhibiting the growth of microorganisms. Further treatment of MBR effluents for organic and inorganic load reduction is required prior to RO application, and the implementation of NF would not be adequate due to low rejection capacities.

This study concludes that the implementation of the MD process can possibly be an effective way for water recovery of membrane bioreactor (MBR) treated brewery wastewater effluent as feed water, however, detailed analysis of the MD process with varying membrane materials, temperatures, and pore sizes, as well as varying organic loading of feed water, needs to be investigated for optimized MD implementation and applicability for this specific wastewater. Further studies on the MD retentate to assess the possible nutrient recovery (nitrogen and phosphorous) can also be explored. Moreover, the biofouling potential of the MD membrane needs to be investigated in detail under a wide range of operational conditions. Due to the complex nature of the real wastewater effluent, the interaction among organic foulants with and without the presence of inorganic scale using synthetic feed needs to be assessed for enhanced understanding of the membrane fouling mechanism in MD process. Finally, energy requirements need to be studied for such application as elevating the feed water temperature in MD needs high energy input. However, for micro-breweries with the availability of alternate energy sources (e.g. solar energy and/or process waste heat), MD can provide an effective means for water recovery and reuse within the industry from pretreated brewery wastewater streams.

Appendix A1

The RO permeate flux with and without PAC aid treated wastewater effluent is shown in Figure A1.1. The 80 hour fouled membrane images are provided in Figure A1.2. The SEM images of the membrane after repeated cleaning are shown in Figure A1.3 along with the EDS analysis in Table A1.1. The MD setup with feed and permeate is shown in Figure A1.4. The RO and NF operational setup is shown in Figure A1.5.

Acknowledgements

The authors acknowledge the Ministère de l'Agriculture, des Pêcheries et de l'Alimentation, Québec (MAPAQ) and the Natural Sciences and Engineering Research Council (NSERC) of Canada for providing funding support for this project. We thank Dr. Sheng Chang, Professor, University of Guelph, for his support towards MBR process water and his students (Peter Inns and Han Chen) for collecting and shipping the process water for this project. Nawrin Anwar gratefully acknowledges the support of Alexander Graham Bell Canada Graduate Scholarship (CGSD) for doctoral studies from the Natural Sciences and Engineering Research Council of Canada (NSERC). The authors also acknowledge ongoing support from Concordia University, Canada.

Chapter 4: Direct contact membrane distillation (DCMD) application for water recovery from pre-treated high strength brewery wastewater: A parametric study

Abstract

The optimal membrane performance of direct contact membrane distillation (DCMD) application for membrane bioreactor treated (MBR) brewery wastewater effluent was investigated by assessing the impact of key operational parameters: hot feed temperature, membrane material, and pore sizes as well as varying feed load during DCMD water reclamation application. The study identified 0.45 µm pore size membranes were less prone to fouling compared to 0.2 µm. Moderate hot feed temperature of 55°C was the ideal condition for stable DCMD implementation for water reclamation with low flux drop and moderate recovery with minimal membrane fouling in comparison to 65°C and 45°C. Despite high flux, PTFE membrane was more prone to fouling due to its high hydrophobicity causing hydrophobic-hydrophobic interaction between the membrane and hydrophobic foulant and eventually resulting in low recovery compared to PVDF membrane. Further studies demonstrated considerably high fouling, and low recovery (86%) with high feed load whereas load feed load resulted in high recovery (93%), less membrane fouling, and nearly complete rejection of all contaminants (COD, TN, TP, and other ions (Na^+, K^+, Ca^{+2}, Mg^{+2}, Li^+, Cl^-, NO_3^-, PO_4^{-3}, SO_4^{-2})) over 90 hours of application. The high feed load performed well in terms of rejection for all contaminants and ions except for the volatile NH_4^+ (~78% rejection). Membrane analysis observed salt crystals on the membrane surface along with organic fouling. Protein was identified as the primary organic membrane foulants. Membrane flux could be completely recovered by NaOH-HCl-DI water sequential cleaning. The study identified 0.45 µm PVDF membrane with 55°C hot feed temperature and 10 gCOD/L/d feed load to MBR to be the best condition for stable DCMD implementation for water reclamation with low flux drop and moderate recovery with minimal membrane fouling.

Keywords: Membrane distillation (MD); Water recovery; Membrane fouling; Contaminant rejection; Membrane reversibility.

4.1 Introduction

The shortage of clean water across the globe has led to the development of advanced wastewater treatment and recovery technologies to provide dependable freshwater access to the community. Novel technologies, like membrane separation processes, have gained attention for water reclamation to deliver freshwater as well as to reduce the wastewater load to the environment [1,3–5,259,308,309]. Current membrane separation processes for water reclamation are categorized as pressure-driven, such as reverse osmosis (RO) and thermal-driven membrane distillation MD. Though RO is already an established technology for desalination, the emerging MD process has become as a promising technology for freshwater production. MD is a thermally driven membrane-based separation process where vapor is the primary driving force as the water molecules are transferred from the hot feed towards the cold distillate through a porous hydrophobic membrane in vapor phase [12,37,38,263]. The temperature difference between the hot feed and cold distillate creates a partial vapor pressure difference that drives the water vapor to pass through the porous hydrophobic membrane from the hot feed leaving behind the contaminants and gets condensed to pure water in the cold distillate side as a permeate. MD has distinct advantages over other processes: it theoretically rejects 100% non-volatile salts, operates at higher concentrations/salinities compared to RO, requires lower operating temperature compared to conventional thermal desalination processes, can utilize alternate energy sources like solar/waste heat, and requires less stringent mechanical membrane properties compared to conventional pressure-driven membrane separation processes such as RO [16,38,40,46,162].

Beer is one of the top five in beverage sales by world market share. In Canada, approximately 41.5% of the total alcohol sales constitutes of beer and around 85% of these sales originate from local breweries [22,310]. The number of breweries in Canada has increased nearly 12.9% from 2018 (995 breweries) to 2019 (1123) [282]. The brewing industry has high monetary value and it contributes around 149,000 jobs which generates nearly $5.3 billion income with a $13.6 billion contribution of Canada's GDP [282]. However, nearly 3 to 10 L of wastewater are generated from 1 L of beer production [18,24,25]. This wastewater constitutes of sugars, volatile fatty acids, ethanol, soluble starch, total suspended solids, and a very low concentration of heavy metals [22,23]. For the human health, aquatic life, and environmental safety, the brewery wastewater

effluent requires adequate treatment that adhere to the guidelines and regulations. High wastewater disposal standards as well as enhanced financial incentive associated with the intake water have led the brewers toward sustainable solutions to recover and reuse water from the effluent.

Researchers have explored the potential of thermally driven emerging membrane distillation process for water reclamation from various wastewater streams like fermentation wastewater, textile wastewater, municipal wastewater, industrial wastewater, etc. [9,111,176,308,311,312] . Our previous study investigated probable water reclamation from pre-treated brewery wastewater effluent through pressure-driven and thermally driven membrane separation processes [309], where the thermally driven direct contact membrane distillation (DCMD) process exhibited the prospective of integrated with membrane bioreactor (MBR) treated brewery wastewater effluent without further polishing due to high recovery and excellent rejection. Even with high rejection performance, the extensive membrane fouling causing significant flux drop, and very low recovery caused the RO process to incorporate additional treatment for the MBR effluent. As biological treatment is already a recognized process [22,286] for brewery wastewater treatment prior to disposal, the integration of DCMD with existing processes like MBR can be a promising solution for water reclamation from brewery industries.

Though previous study revealed that the incorporation of DCMD with MBR treated brewery wastewater has the potential to reclaim water [309], there is a need for detailed investigation of membrane performance and membrane fouling based on varying operating conditions prior to large scale implementation to better comprehend the optimal performance. Membrane fouling is a complex phenomenon which hinders the membrane performance. Various parameters, including membrane material, pore sizes, hot feed temperature as well as the feed loading may pose a significant influence on the membrane performance in terms of the flux and membrane fouling [276]. However, it is difficult to predict the exact effects of membrane fouling and membrane performance with varying operating conditions, membrane materials, and feed loading as membrane fouling is a complex phenomenon. For specific wastewater, the effect of all these parameters will be distinct and cannot be predicted from different types of wastewaters. Hence, before process implementation, it is inevitable to assess the impact of operating conditions, membrane materials, and feed loading to evaluate the optimal conditions as well as to avoid

process failure. A better understanding of the interactions between specific feed, operating conditions, membrane materials, and membrane performance can make water recovery sustainable and reduce the water footprint in beer production. The previous research demonstrated that membrane performance and fouling vary with different operational conditions during DCMD application. Researchers observed the permeate flux of the membrane distillation process is enhanced due to increased feed temperature [140]. Three different (unmodified, plasma modified, and chemically modified) hydrophobic PVDF hollow fiber membranes were employed at various feed temperatures of 40°C, 50°C, 60°C, and 70°C and a permeate temperature of 25°C with synthetic seawater of 3.5 wt% NaCl solution in a DCMD set-up (with feed and permeate flow rates of 2.5 L/m and 0.4 L/m, respectively) [265] where the exponential increase of trans-membrane flux with increase in temperature for all three membranes were demonstrated. At low feed temperatures, all three membranes had similar permeate flux. However, enhancing the feed temperature demonstrated substantial variation in the permeate flux of the three membranes, with unmodified membrane having the highest permeate flux and around 20% flux drop of modified membranes at 70°C feed temperature due to membrane modification [265]. Researchers also observed that varying hot feed temperature has a significant impact on membrane performance compared to that of varying cold distillate/permeate temperature [308]. A study conducted with simulated dyeing wastewater treatment via DCMD application with PVDF (0.22 μm) and PTFE (0.2 μm) membranes demonstrated that 63% higher flux was observed with the PTFE membrane compared to PVDF membrane [176]. The influence of feed characteristics on the permeate flux and contaminant rejection performance in MD is equally important as the operating condition and membrane materials. Researchers observed the occurrence of fouling and wetting in direct contact membrane distillation (DCMD) of synthetic solutions prepared using dyes specifically found in textile/dyeing wastewater [176]. Fermentation wastewater, having high organic content, resulted in a 50.5% reduction in flux after 12-hour DCMD treatment without any pre-treatment of feed water [9]. For brewery wastewater treated by MBR, the effluent contains a combination of different contaminants (organic and inorganic) [309]. The interactions between these various constituents and the membranes may lead to multidimensional fouling with varying feed characteristics. This variation in fouling provides an impetus for conducting investigations for the reclamation of pre-treated brewery wastewater under varying operating conditions, membrane materials, and feed characteristics which, in turn, will help in the effective implementation of the membrane-based

technology. To the best of our knowledge, no other study has observed the impact of operating conditions, membrane properties, and feed characteristics for DCMD application of membrane bioreactor treated real brewery wastewater effluent.

Even though our previous research identified DCMD as a potential membrane separation process for water recovery from pre-treated high strength brewery wastewater without further polishing, the major issue during DCMD application with the pre-treated brewery wastewater was the membrane fouling causing significant flux reduction. Membrane fouling can be either of organic, inorganic, or biological resulting in membrane performance degradation which eventually lead towards process failure. The objective of this research was to investigate the effect of major parameters, e.g., operational conditions, membrane properties, and feed characteristics, on membrane performance and membrane fouling to better elucidate the DCMD application for water reclamation from pre-treated brewery wastewater as well as to find the optimal condition for its application. This study employed DCMD for the reclamation of membrane bioreactor (MBR) treated high-strength brewery wastewater with varying feed temperature, membrane materials and pore sizes as well as with varying strength of wastewater. Commercially available hydrophobic membranes were implemented to assess the membrane recovery performance through evaluating the membrane permeate flux and contaminant rejections. In addition to that, membrane surface morphologies and chemical compositions before and after the recovery applications were studied to better comprehend the fouling phenomena. Moreover, membrane recovery through membrane cleaning was implemented for possible membrane reuse.

4.2 Methodology

4.2.1 DCMD configuration

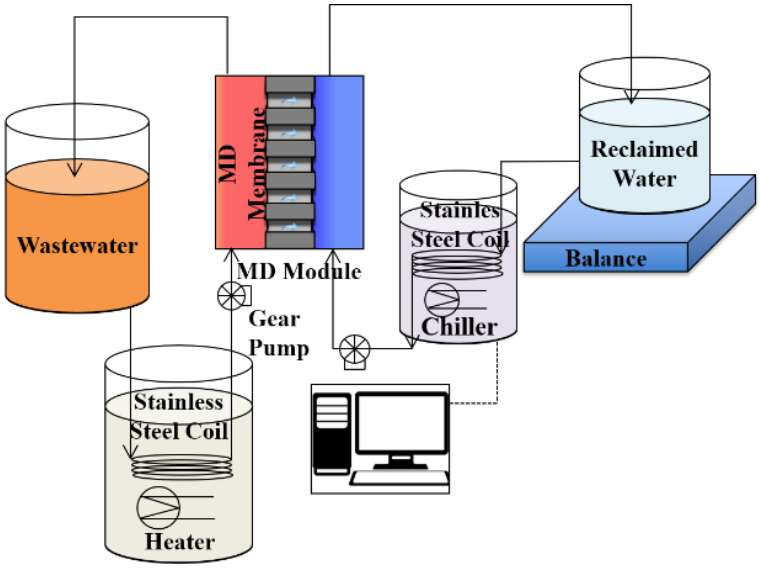

Figure 4.1: Direct Contact Membrane Distillation (DCMD) system for water recovery application from pre-treated brewery wastewater. The hot feed temperature is maintained through a heating unit whereas the cold temperature of the permeate/distillate side is maintained through a cooling unit. A balance is used for the calculation of the permeate flux through the weight difference directly via a computer.

A direct contact membrane distillation (DCMD) configuration as shown in Figure 4.1 was used. A flat sheet membrane cell (CF042P-FO) from Sterlitech Corporation, USA was employed. The effective membrane surface area of the DCMD cell was 34 cm^2. A constant temperature (T_f) was maintained for the bulk hot feed using a hot water bath. Also, a chiller was used to maintain a constant cold temperature (T_p) at the cool permeate side. Both the hot feed and the cold permeate were circulated by two gear pumps (Model GH-75211-10, Cole-Parmer, Canada) at around 0.8 psi (Pressure Gauge Model GH-68930-12, Cole-Parmer, Canada) at the same speed across the bottom and the upper face of the membrane cell, respectively. Flow meters (0.1-1 LPM, McMaster-CARR, Canada) were used to observe the constant 0.7 LPM hot feed and the cool permeate circulation rate. The conductivity of the feed and permeate solution was measured with an electric conductivity meter (Oakton Instruments, IL, USA).

4.2.2 Membrane properties

For MD membranes, commercially available PVDF and PTFE membranes were used as described in Table 4.1. Flat sheet highly hydrophobic microporous polytetrafluoroethylene (PTFE, TF-450 and TF-200) membrane with a polypropylene support from Pall Gelman, USA (pore size 0.45 µm and 0.20 µm, thickness 135 µm and 139 µm, porosity ~84%, tensile strength 21.75 MPa, contact angle 139°, and liquid entry pressure (LEP) of 1.1 bar and 2.68 bar) were used. PTFE membranes are non-reactive with high resistance to almost all the chemicals as well as they have excellent thermal stability up to 260°C [291]. For PVDF membranes, commercially available microporous Polyvinylidene fluoride membranes from Durapore (Millipore) with a 0.45 µm and 0.22 µm pore sizes, porosity of 72.11% and 69.24%, contact angle of 117.9° and 120.2°, LEP of 1.17 bar and 1.95 bar were used.

Table 4.1: Commercial membrane characteristics used in the study of direct contact membrane distillation (DCMD)

Commercial membrane (Application)	**Manufacturer**	**Pore size/ Molecular weight cut-off**	**Porosity (%)**	**Polymer**
PTFE TF-450	Pall Gelman	0.45 µm	84.32	Polytetrafluoroethylene
PTFE TF-200	Pall Gelman	0.20 µm	80	Polytetrafluoroethylene
PVDF (HVHP)	Millipore (Durapore)	0.45 µm	72.11	Polyvinylidenefluoride
PVDF (GVHP)	Millipore (Durapore)	0.22 µm	69.24	Polyvinylidenefluoride

4.2.3 Feed characteristics

The effluent utilized for water reclamation application in this study was obtained from a local brewery industry that was pre-treated using a hybrid membrane bioreactor (MBR). A hybrid membrane bioreactor (MBR) with a combination of Up-flow Anaerobic Sludge Blanket (UASB) reactor and multi-staged membrane tank using 1.5 µm, 0.45 µm, and 0.04 µm filtration

(ultrafiltration) was implemented for brewery wastewater pre-treatment. The MBR was operated at different organic feed loads of 10 gCOD/L/d and 15 gCOD/L/d and air was circulated through the membrane tank effluent. The effluent was used as a feed for direct contact membrane distillation application. Table 4.2 provides the characteristics of the pre-treated brewery wastewater with MBR organic feed loads 10 gCOD/L/d and 15 gCOD/L/d.

Table 4.2: Brewery wastewater effluent characteristics from hybrid membrane bioreactor (MBR). This effluent was used as feed water in direct contact membrane distillation.

Parameters	**Unit**	**Low feed load concentration in hybrid MBR effluent (10 gCOD/L/d to the MBR)**	**High feed load concentration in hybrid MBR effluent (15 gCOD/L/d to the MBR)**
Chemical oxygen demand (COD)	mg/L	77.9 ± 2.8	108 ± 1.4
Turbidity	NTU	0.91 ± 0.5	0.95 ± 0.4
Alkalinity	meq/L	17.7 ± 0.4	39.8 ± 4.23
Electrical conductivity (EC)	mS/cm	7.71 ± 0.4	11.15 ± 0.5
Total nitrogen (TN)	mg/L	323.83±18.6	50.6±2.9
Total phosphorous (TP)	mg/L	188 ± 11.3	292.95 ± 30.4
Extracellular polymeric substance (EPS)	mg/L	160 ± 30	235 ± 25
Na^+, K^+, Ca^{2+}, Mg^{2+}, Li^+, NH_4^+	mg/L	613.83±17.17, 51.43±1.91, 38.03±2.79, 25.24±4.15, 2. 8±1.28,0	989.06±19.86, 70.75±2.79, 54.01±3.61, 61.39±1.42, 0, 26.17±1.46
Cl^-, NO_3^-, PO_4^{3-}, SO_4^{2-}	mg/L	76.01±4.44, 313.83±18.6, 149.72±6.97, 51.41±2.67	96.79±9.16, 15.96±1.94, 292.39 ± 29.76, 40.89±4.23

The organic concentrations of the MBR effluent were measured and expressed as chemical oxygen demand (COD) concentrations. Hach kits (London, Ontario, Canada) were used for quantifying COD, total nitrogen (TN), and total phosphorous (TP) concentrations along with a Hach DR2800

spectrophotometer (London, Ontario, Canada) to measure the absorbance. Standard Method (2540B) [293] was implemented for quantifying the total solids (TS) concentrations. An automatic titrator (848 Titrino plus, Metrohm) [293] was utilized for assessing he alkalinity of the MBR effluent following the Titration Method of the Standard Methods (2320A). A conductivity meter (Oakton Instruments) and a turbidity meter (ORION AQ3010) were used for measuring electrical conductivity and turbidity, respectively. The method described in Chen et al. (2016) was implemented for measuring the extracellular polymeric substance (EPS) [286]. Furthermore, an ion chromatograph (IC) (930 Compact IC Flex and 858 Professional Sample Processor by Metrohm) was employed for conducting the cation and anion analyses.

4.2.4 Parametric Study

This study observed three different operating conditions, namely hot feed temperature, membrane material, and membrane pore sizes. Feed temperatures were varied at 45ºC, 55ºC, and 65ºC with a constant permeate temperature of 18ºC. For this study, commercially available PVDF (0.45 µm and 0.22 µm pore sizes) and PTFE (0.45 µm and 0.20 µm pore sizes) membranes were used from Millipore (Durapore) and Pall Gelman as stated in section 2.2, respectively. The brewery wastewater effluent containing 10 g/L/d organic load pre-treated by a membrane bioreactor was used as a feed and 2 L of this feed was concentrated for each case over 20 hours. Finally, the optimal condition was implemented with varying feed loads condition (10 gCOD/L /d and 15 gCOD/L/d organic load to MBR) as shown in section 4.2.3 to evaluate the DCMD performance in water recovery applications with a 5 L feed and concentrating the feed for 90 hours. The contaminant rejections, water recovery, and flux reductions were evaluated as described in section 4.2.5. Additionally, the transformed surface morphology, as well as the varying chemical and elemental compositions, were assessed as discussed in section 4.2.6 to observe the membrane fouling characteristics with varying temperatures, membrane materials, pore sizes, and feed loads. Moreover, the membrane recovery options were explored to evaluate the prospect of repeated application of MD membranes for water reclamation. All the experiments were conducted performed three times with the exception of 3% of the cases.

4.2.5 Membrane performance evaluation

DCMD performance was observed primarily by flux reduction with a certain volume of feed and concentrating the feed for specific time. The permeate flux J (L/m^2-h) was measured using Eq.4.1.

$$J = \frac{\Delta M}{A\Delta t} \quad (4.1)$$

where ΔM is the quantity of the permeate (L), A is the effective membrane area (m^2), and Δt is the operational time (h). For evaluating the optimal condition, 2 L of feed was concentrated for 20 hours with varying hot feed temperature, membrane materials, and pore sizes. Afterwards, optimal condition was implemented using 5 L of feed with various organic feed load, with a COD of 83 ± 7 mg/L (10gCOD/L/d to MBR) and 102 ± 10 mg/L (15gCOD/L/d to MBR) for 90 hours.

The varying water quality parameter concentrations were measured in the feed and the permeate solutions. Furthermore, Eq. 4.2 was applied to calculate rejection (R) percentage using the feed and permeate concentrations.

$$R\ (\%) = \left(1 - \frac{C_{permeate}}{C_{feed}}\right) X100 \quad (4.2)$$

where, C_{feed} and $C_{permeate}$ are the concentrations of any water quality parameter in the feed and permeate solutions, respectively.

4.2.6 Membrane characterization

The pristine, fouled, and cleaned membranes were characterized to evaluate basic physiochemical properties through advanced membrane characterization techniques. The surface morphologies of the membranes were observed via scanning-electron microscopy (SEM). The Field Emission Scanning Electron Microscope (FE-SEM, Quanta 450 Environmental, FEI Company, USA) was employed to analyze the membrane surfaces. Preceding the microscopic membrane surface morphology observation, a 4 nm thick platinum layer coating was applied to the pristine and fouled membrane samples. To identify the surface functional group, Automated Total Reflectance-Fourier Transform Infrared (ATR-FTIR, Nicolet 6700/Smart iTR, Thermo Scientific, USA) spectra was used. It can qualitatively assess the chemical changes in the active layer by detecting the functional groups of the pristine and the fouled membranes. During FTIR analysis, the intensity

of the peak at specific wavelengths confirmed the presence of specific functional groups. Furthermore, DI water contact angle measurements were conducted using the sessile drop method (VCA, AST Products, Inc., Billerica, MA, USA).

4.2.7 Membrane Reversibility

Membrane reversibility was first studied with optimal feed loading at optimal temperature along with the optimal membrane material and the pore sizes by concentrating the feed volume 2 L over 20 hours. As the wastewater contain both organic and inorganic foulants, individual and sequential acidic and caustic cleaning were performed to identify the effective membrane cleaning mechanism. After 20 hours of operation, the MD system was cleaned with the following 4 different scenarios: (1) DI water cleaning for 2 h, (2) 30 minutes of caustic (0.1M NaOH) cleaning followed by DI water cleaning for 2 h (3) 30 minutes of acid (0.01M HCl) cleaning followed by DI water cleaning for 2 h, and (4) 30 minutes of caustic cleaning followed by 30 minutes of acid cleaning and 2 h DI water cleaning for removal of organics and inorganics foulants [297]. The DCMD setup was then washed with deionized (DI) water produced by a Milli-Q ultrapure water purification system to eliminate any residues. After that, a 2 h DI water permeate flux was measured. Furthermore, a high strength feed was utilized at an elevated temperature (65°C) to enhance membrane fouling and verify the efficacy of the membrane cleaning mechanism in harsh environment. The high strength feed wastewater characteristic is shown in Table A2.1 in the Appendix A2.

4.3 Results and Discussion

4.3.1 Effect of feed temperature, membrane material, and pore sizes

4.3.1.1 Membrane permeability

The application of DCMD for 20 hours resulted in various water recovery by concentrating a 2 L feed solution with varying feed temperature, membrane material, and pore sizes. The MBR treated brewery wastewater effluent was used as the MD feed. Figure 4.2 shows the initial and final permeate flux in DCMD process after 20 hours of operation with an initial 2L feed solution. It is evident from Figure 4.2 that the highest initial permeate flux was achieved with the PTFE membranes with the high temperature difference with a feed temperature of 65°C. The high temperature difference occurring from the high feed temperature (65°C) and constant distillate temperature (18°C) created high vapor pressure resulting in high permeate flux [40]. For all four membranes with various material and pore sizes, the lowest recovery was attained with the lowest feed temperature of 45°C that caused lower vapor pressure. For PTFE membranes, the highest water recovery was achieved with a hot feed temperature of 55°C whereas with PVDF membranes, the highest recovery was attained at 65°C hot feed temperature. However, the highest flux drops for both PTFE and PVDF membranes from their distinct initial fluxes were noticed at 65°C. Moreover, high permeate flux was observed with PTFE and PVDF 0.45 µm membranes compared to that of PTFE 0.2 µm and PVDF 0.22 µm membranes respectively due to higher pore size and higher porosity. The PVDF membranes having lower porosity compared to that of PTFE membranes resulted in lower initial flux than PTFE membranes. Nevertheless, the overall flux drop with the PVDF membranes were lower that was an indication of less membrane fouling of the PVDF membranes which would be discussed later in the surface morphology section. The membrane wetting assessment was conducted by measuring the electrical conductivity of the permeate which was within the range of 18±2 µS/cm. The substantial low electrical conductivity measurements ensured that the membrane pores were not wetted. Moreover, the insignificant concentration of sodium (<0.3 mg/L) and chloride (<0.2 mg/L) ions along with the absence of other ions (potassium, calcium, magnesium, lithium, nitrate, phosphate, and sulphate) in the permeate for all four membranes with varying temperature, membrane material, and pore sizes also established the absence of membrane pore wetting.

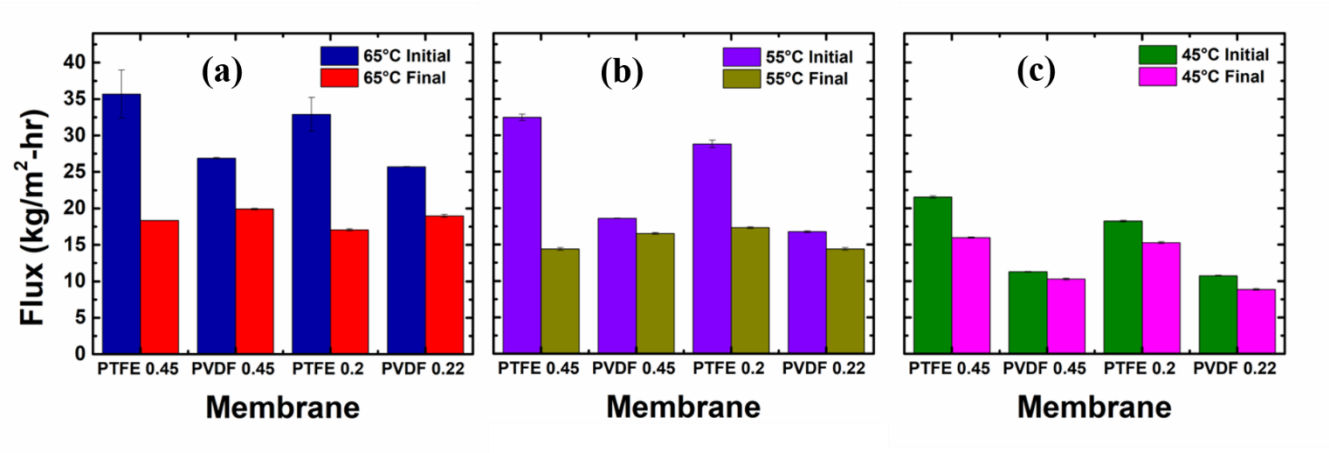

Figure 4.2: Effect of feed temperatures, membrane material, and pore sizes on the permeate flux of a DCMD process. The MBR effluent with a COD = 77.9 ± 2.8 was used as the feed and concentrated for 20 hours with a feed temperature of (a) 65°C, (b) 55°C, and (c) 45°C and permeate temperature of 18°C. The highly hydrophobic PTFE membranes with a pore size of 0.45 µm, and 0.2 µm; and the moderately hydrophobic PVDF membranes with a pore size of 0.45 µm and 0.22 µm were applied with three different hot feed temperatures [All the experiments were performed three times with the exception of 3% of the cases, and the average values were considered and presented; the error bars of (b) represent the standard deviation from the average value].

Despite the initial higher flux of PTFE membranes compared to the PVDF membranes, the highest water recovery of nearly 80% was achieved with PVDF membranes with 0.45µm pore sizes at 65ºC with significant flux drop (~27%) compared to that of 55ºC and 45ºC (~11-12%) from their distinct initial fluxes (Figure A2.1). The permeate flux drop is an indication of the occurrence of membrane fouling. Membrane surface analysis (discussed in later sections) would further provide a broad insight to the fouling phenomena. From the percentages of flux drop and water recovery, it was evident that though high initial permeate flux was achieved with PTFE membranes over 20 hours application, the flux drop was significantly high compared to the PVDF membranes resulting in high recovery. Thus, it was indicative of the occurrence of higher membrane fouling with PTFE membranes compared to the PVDF membranes. Moreover, though the 65°C hot feed temperature provided the highest recovery for PVDF membranes, the high flux drop (~27%) of PVDF membranes with 65°C compared to the 55°C flux drop (~12%) occurred due to membrane fouling (discussed in the later section). Furthermore, the energy requirement of 65°C hot feed would be higher compared to the 55°C hot feed. Thus, from the membrane flux observations including recovery and flux drop, it was determined that PVDF membrane with a pore size of 0.45 µm and

a hot feed temperature of 55°C would provide a stable and optimal long term membrane performance. Analyses of membrane fouling provided in Section 4.3.1.2 would further strengthen this observation.

4.3.1.2 Membrane fouling

The SEM analysis was conducted to elucidate the surface morphology of the pristine and fouled MD membranes. Figure 4.3 illustrates the varying surface morphology of the (a) PVDF and (b) PTFE MD membranes in (i) pristine and fouled condition with varying temperature of (ii) 65°C and (iii) 55°C. The presence of the fouling layer shown in Figure 4.3a(ii), 4.3a(iii), 4.3b(ii), and 4.3b(iii) could be caused by the feed water comprised of organics and inorganics. Scattered and heterogenous fouling layers were observed for PVDF, especially at lower temperatures. However, for PTFE membranes, the fouling layer was homogenous and dense. Higher hydrophobicity of the PTFE membranes (Figure 4.3b(ii) and 4.3b(iii)) compared to that of the PVDF membranes (Figure 4.3a(ii) and 4.3a(iii)) may have ensued in substantial fouling layer leading towards considerable flux decline due to the strong hydrophobic-hydrophobic interaction between the membranes and the hydrophobic tail of the amphiprotic organics present in the MBR treated brewery wastewater effluent. The thick foulant layer of the fouled PTFE MD caused a higher permeate flux decline compared to the PVDF membranes.

It was also revealed that though high temperature will result in high flux, it resulted in higher fouling due to the concentration polarization near the membrane surface. Hence, both for PVDF and PTFE membranes, the membrane fouling was thick for 65°C compared to that of 55°C and 45°C (Figure A2.2 and Figure A2.3). Moreover, the membrane fouling layer was thicker and denser for the 0.22 µm and 0.2 µm PVDF and PTFE membranes, respectively compared to the 0.45 µm pore sizes (Figure A2.4 and A2.5). From the parametric study, it was evident that PVDF membranes with a pore size of 0.45 µm would be optimal for this specific MBR treated brewery wastewater's stable recovery application.

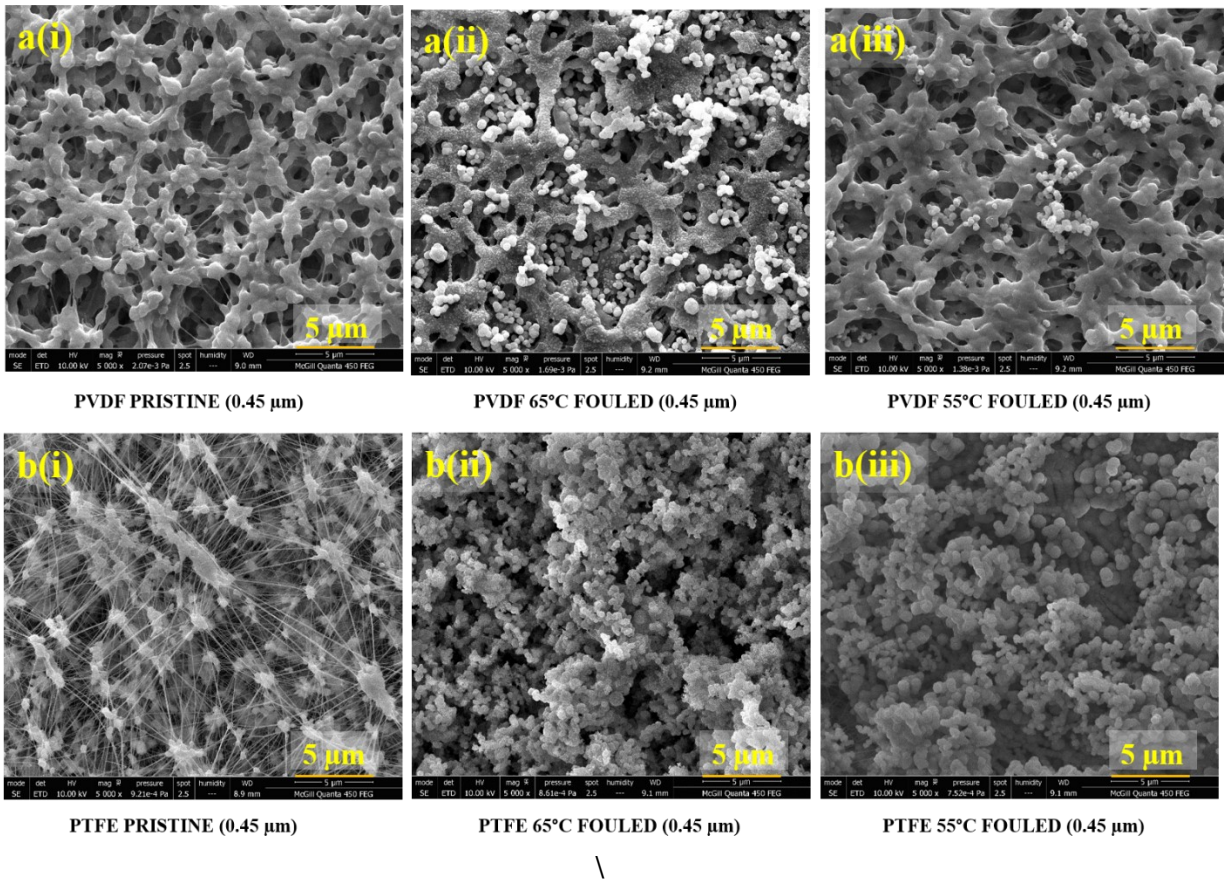

\

Figure 4.3: SEM images of (a) PVDF 0.45 µm, and (b) PTFE 0.45 um during (i) pristine, (ii) 65°C, and (iii) 55°C feed fouled conditions for COD = 77.9 ± 2.8 mg/L after concentrating 2L feed for 20 hours.

4.3.2 Effect of feed loading:

4.3.2.1 Membrane flux and water recovery

Figure 4.4 represents the permeate flux, the flux drop, and water recovery of the DCMD process using a 0.45 µm PVDF membrane and MBR treated brewery wastewater effluent as a feed. Direct contact membrane distillation application for water recovery from MBR treated brewery wastewater effluent over 90 hours using a 0.45 µm PVDF hydrophobic membrane resulted in nearly 93% and 86% water recovery for the low feed load (10 gCOD/L/d to MBR) and high feed load (15 gCOD/L/d), respectively from a 5 L feed solution as shown in Figure 4(b). The flux drop was almost 30% and 45% from their initial fluxes 18.62 kg/m^2-h and 18.31 kg/m^2-h for low feed load and high feed load, respectively.

The permeate flux drop is an indication of the occurrence of membrane fouling. Higher flux drop and lower water recovery of the high feed load are indicative of enhanced membrane fouling compared to the low feed load. Moreover, the gradual flux drop can be attributed to a porous fouling layer on membrane surfaces. However, a broad interpretation of the membrane 1fouling phenomena would be provided by membrane surface analysis discussed in section 3.2.2.

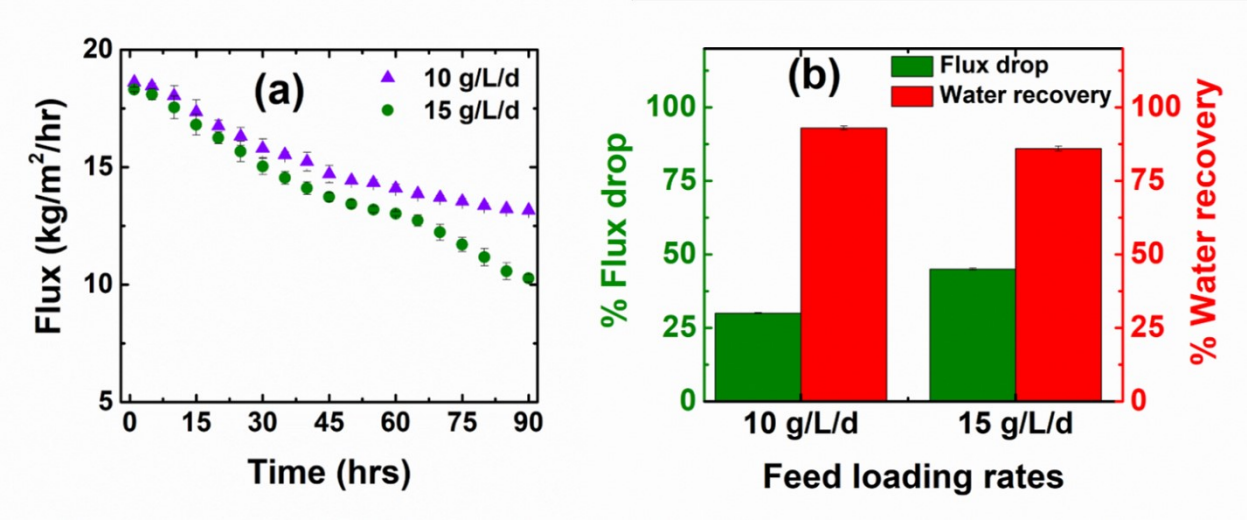

Figure 4.4: (a) Permeate flux, (b) flux drop and water recovery using 0.45 µm PVDF membrane with 55°C feed temperature and with COD = 77.9 ± 2.8 mg/L (10 gCOD/L/d to MBR), and COD = 108 ± 1.4 mg/L (15 gCOD/L/d to MBR) feed water at 0.7 LPM flowrate, and T_p = 18ºC over 90 hours of DCMD application.

4.3.2.2 Membrane surface analysis

The SEM-EDS analysis along with ATR-FTIR analysis were conducted that revealed the membrane surface morphology, elemental, and chemical composition of the pristine and fouled membranes. Figure 4.5 represents the pristine and fouled membrane surface morphology observed through the scanning electron microscopy (SEM) analysis. The variation in the surface morphology of the PVDF 0.45 µm membranes from pristine to fouled conditions are evident in Figure 4.5(a), and 4.5(b) and 4.5(c), respectively. The visible fouling layer and deposits of fouled membranes could be attributed to the organics and inorganics present in the feed water. The fouling layer was scattered and heterogenous for low feed loading (Figure 5(b)) whereas for the high feed loading the fouling layer was homogenous with noticeable salt crystal accumulations on the membrane surface (Figure 4.5(c)). Due to the elevated feed temperature the salt solubility

decreased in the feed water, which eventually lead towards the scale deposition on the membrane surfaces. The formation of visible salt crystals from the high loading feed is due to the concentration polarization of the feed water in addition to the decreased solubility. The high feed temperature of the DCMD process resisted the microbe growth on the membrane surface. Hence, no visible biofouling was detected on the membrane surface. However, other researchers observed bacterial endospores in controlled environment with microbial seeded feed water [152].

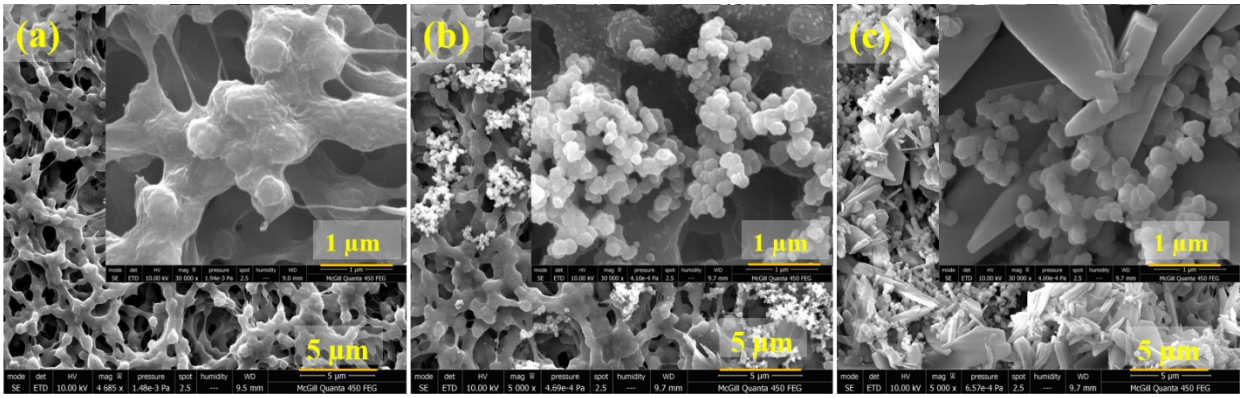

Figure 4.5: Surface morphology of (a) pristine, (b) COD = 77.9 ± 2.8 mg/L (10 gCOD/L/d to MBR), and (c) COD = 108 ± 1.4 mg/L (15 gCOD/L/d to MBR) feed water fouled PVDF 0.45 µm membranes after 90 hours of DCMD application at 0.7 LPM flowrate, and T_f = 55ºC and T_p = 18ºC.

Table 4.3 represents the elemental composition of pristine, low feed load fouled, and high feed load fouled PVDF 0.45 µm membranes. The EDS analysis also confirmed the co-existence of organic and inorganic foulants on the fouled membrane surfaces. The presence of elemental C, O, and P on the fouled membrane surface is an indication of the presence of organic foulants on the membranes. Moreover, the occurrence of elemental Ca, Mg, and Na on the fouled membrane surfaces confirmed the existence of inorganic fouling/scaling (probable presence of carbonate and phosphate salts of Ca, Mg, and Na) observed during the SEM analysis. A considerably high average atomic percentage of elemental Mg (9.2%) was observed on the fouled membrane surfaces with the high feed load compared to the low feed load which was also observed as salt crystals/scales in the SEM images of the high strength feed. ATR-FTIR analysis would further reveal the chemical compositions on the pristine and fouled membrane surfaces.

Table 4.3: Elemental analysis of pristine, and fouled DCMD membrane surfaces through EDS prior to and after 90 hours of operation with a feed with COD = 77.9 ± 2.8 mg/L (10 gCOD/L/d to MBR), and COD = 108 ± 1.4 mg/L (10 gCOD/L/d to MBR) and a 0.7 LPM flowrate, $T_f = 55^0C$ and $T_p = 18^0C$.

Average Atomic %	Pristine 0.45 µm PVDF	Low feed load fouled (COD = 77.9 ± 2.8 mg/L)	High feed load fouled (COD = 108 ± 1.4 mg/L)
C	74.54	43.7	12.99
F	24.95	18.2	6.43
Pt	0.51	0.4	0.25
P	-	4.2	5.4
N	-	0.1	0.01
O	-	30	61.5
Na	-	0.2	1.62
Mg	-	1.1	9.2
Ca	-	2.1	2.6

Figure 4.6 illustrates the ATR-FTIR peaks observed on the pristine and fouled PVDF membrane surfaces. The pristine membrane FTIR spectra observation consisted of the peaks at 833 cm^{-1} relating to the amorphous vibration of PVDF, the peaks at 874 cm^{-1} corresponding to the skeletal vibration of C-C bond, the band at 1070 cm^{-1} relating to the crystalline phase of PVDF, the peaks at 1168 cm^{-1} and 1231 cm^{-1} corresponding to CF_2 stretching, the vibrational band at 1401 cm^{-1} relating to the deformation vibration of the CH_2 group, and the peaks at 3025 cm^{-1} for CH_2 stretching vibration [176]. The FTIR analysis revealed that the pristine PVDF membrane is consisted of several repeating units of CH_2 and CF_2 bonds. The fouled membranes showed reduced peaks of the pristine membrane. The peaks observed at 1647 cm^{-1} and 1656 cm^{-1} for low feed load and high feed load, respectively is associated with the amide I band from proteins (C=O) [300,301]. In addition to that, a vibrational band was observed for both feed loading from 3000 cm^{-1} to 3600 cm^{-1} with peaks at 3025 cm^{-1} and 3254 cm^{-1}, and 3081 cm^{-1} and 3477 cm^{-1} for low feed load and high feed load, respectivly. These peaks are ascribed to the O-H and/or N-H from the alcohol and/or amine group [286].

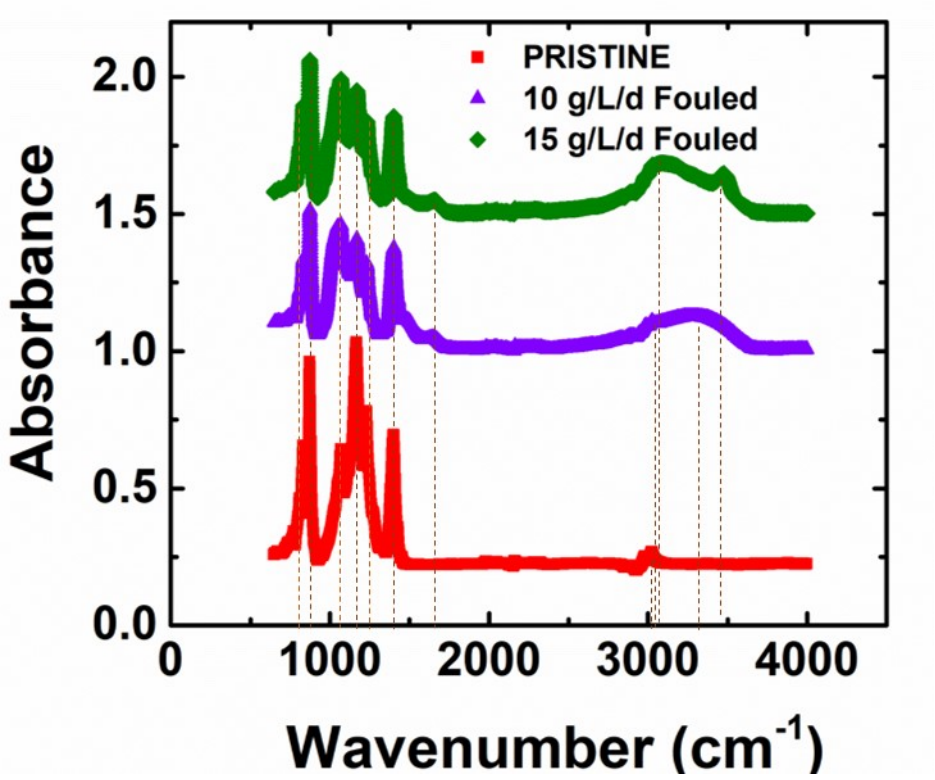

Figure 4.6: FTIR analysis of (a) pristine and fouled PVDF 0.45 µm membranes over 90 hours of DCMD application with MBR treated effluent, (b) COD = 77.9 ± 2.8 mg/L (10 gCOD/L/d to MBR), (d) and COD = 108 ± 1.4 mg/L (15 gCOD/L/d to MBR) with a feed temperature of 55ºC and a permeate temperature of 18ºC at 0.7 LPM flowrate.

From the permeate flux drop and the membrane surface analysis for surface morphology, elemental composition and functional groups through SEM-EDS and, FTIR, it was evident that foulants were adsorbed onto the membrane surfaces which consisted of both organics and inorganics. The high feed loading resulted in high foulant adsorption due to the high concentration polarization of the feed. However, both fouled membranes exhibited similar types of organic foulant adhesion for similar membranes, primarily proteins, along with inorganic Ca, Mg, and Na salts.

4.3.2.3 Contaminant rejection performance

The membrane wetting was evaluated by continuously measuring the electrical conductivity (EC) of the permeate. The EC of the permeate was 21.45±0.1 µS/cm and 305±2.82 µS/cm for low feed load and high feed load, respectively. The EC for the low feed load was considerably low ensuring that the membrane pores were not wetted. However, the EC of the high feed load permeate was

slightly higher, nearly 305 µS/cm. The membrane pores were not wetted for the high loading, but rather, the presence of volatile NH_4^+ in the feed passed through the hydrophobic MD membrane towards the permeate side and increase the EC of the permeate. This statement is further supported by the high electrical conductivity of the concentrate (nearly 33.5 mS/cm) as well as the presence of NH_4^+ in the permeate, and the absence of other ions (sodium, calcium, magnesium, chloride, nitrate, phosphate, sulfate) in the permeate. Moreover, 100% TP rejection and more than 99% COD rejection were observed with DCMD for both feed loading rates as shown in Figure 4.7. However, as no wetting was observed with MD, the adsorption-desorption mechanism could be responsible for organic permeation through the membrane without pore wetting which caused considerably low amount of COD (<1 mg/L) in the permeate [297,309]. 100% TN rejection was observed for low feed load, however, for high feed load the rejection was nearly 78% due to the permeation of volatile NH_4^+. Nearly 11 mg/L NH_4^+ was measured in the permeate for the high feed load. When nitrogen is present in the nitrate/nitrite forms in the feed, it can be retained on the feed side in membrane distillation as it is not volatile and only membrane wetting can allow nitrate to pass to the permeate. However, in an aqueous solution ammonia, nitrogen exists in two forms: volatile ammonia molecules NH_3 and NH_4^+ ions. Increasing the temperature of the feed increases the volatile ammonia in the solution leading to a lower rejection. Thus, it was surmised that DCMD could perform well in terms of contaminant rejection when a low feed load was applied over 90 hours. Only the presence of volatile compounds (NH_4^+ for 15 g/L/d) could lead towards low contaminant rejection for DCMD.

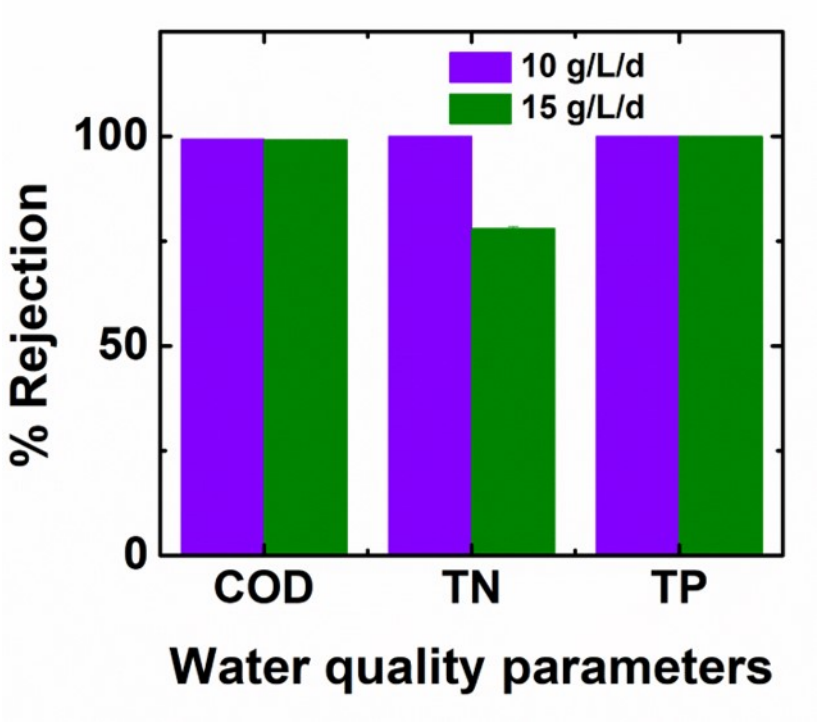

Figure 4.7: Contaminant Rejection of PVDF 0.45 µm membranes for 90 hours of DCMD application with feed COD = 77.9 ± 2.8 mg/L (10 gCOD/L/d to MBR), and COD = 108 ± 1.4 mg/L (15 gCOD/L/d to MBR) with a feed temperature of 55ºC and a permeate temperature of 18ºC at 0.7 LPM flowrate**.**

4.3.4 Membrane Fouling Reversibility

Membrane cleaning operations were conducted with DI water, NaOH, HCl, and sequential NaOH-HCl-DI water cleaning after 20 hours application of 10 gCOD/L/d MBR treated brewery wastewater effluent. Membrane cleaning was most effective for the combined NaOH-HCl-DI water cleaning in terms of flux recovery as complete flux recovery was observed. However, membrane cleaning performance with DI water was not effective for this feed wastewater. Moreover, individual NaOH and HCl cleaning could partially recover the DI water flux. The permeate flux of DI water and pre-treated wastewater effluent for pristine membrane as well as cleaned membranes are demonstrated in Table 4.4.

Table 4.4: Permeate flux during membrane reversibility of DCMD application with a hot feed temperature 55°C and cold permeate temperature 18°C at 0.7 LPM flowrate with 10 g/L/d feed loading.

Membrane Condition	Permeate Flux (kg/m^2-h)	
	DI water Flux	Initial flux for 10 g/L/d
Pristine membrane	19.22	18.67
DI water cleaned membrane after 20 hours of application	16.71	16.47
Caustic cleaned membrane (NaOH) after 20 hours of application	17.04	16.96
Acid cleaned membrane (HCl) after 20 hours of application	17.21	17.13
Caustic cleaned ↓ Acid cleaned ↓ DI water cleaned membrane after 20 hours of application	19.2	18.67

Moreover, membrane recovery was conducted under an extreme condition (high temperature of 65°C and high strength wastewater feed with characteristics in Table A4.1) to enhance fouling for assessing the efficacy of membrane cleaning operations. For high strength wastewater, the membrane flux drop was nearly 73% from the initial flux of 26.56 kg/m^2-h (Figure A2.7) with a 50% water recovery. Almost 89% of the DI water flux could be recovered after the sequential cleaning of the membrane with NaOH, HCl, and DI water. The pristine membrane DI water flux was 27.68 kg/m^2-hr and after the cleaning the DI water flux was 24.64 kg/m^2-h.

4.4 Conclusions

This study evaluated the effect of various operating conditions, e.g., hot feed temperature, membrane material and pore sizes, as well as various feed wastewater load on membrane performance and fouling along with contaminant rejection during water recovery application of DCMD from MBR treated brewery wastewater effluent. Despite enhanced membrane flux with

high hot feed temperature (65°C), the flux drop was significant, whereas with the moderate hot feed temperature (55°C), a comparatively low flux drop was observed. Highest recovery of nearly 80% was achieved with 0.45 µm PVDF membranes at 65ºC hot feed temperature though the flux drop was significant (nearly 27%) compared to that of the lower hot feed temperature of 55ºC and 45ºC (~11%-12%). The flux drops and water recovery observed during the study demonstrated that despite achieving high initial permeate flux with PTFE membranes, the flux drop was significant indicating extensive fouling. On the contrary, PVDF membranes resulted in more steady performance in terms of flux drop and recovery. Moreover, the 55ºC hot feed temperature provided stable performance with considerable water recovery and low flux drop. In addition, membrane surface morphology illustrated that the 0.45 µm PVDF membranes exhibited minimal membrane fouling without any wetting. Thus, the study identified 0.45 µm PVDF membranes utilized with 55ºC hot feed temperature as ideal operating conditions for water recovery from MBR treated brewery wastewater effluent. Furthermore, the energy requirement of the 55°C hot feed would be moderate as well.

The DCMD application with various feed loadings with 0.45 µm PVDF hydrophobic membrane resulted in nearly 93% and 86% water recovery with nearly 30% and 45% flux drops for the low feed load and high feed load, respectively from concentrating a 5 L feed solution for 90 hours. The SEM analysis identified a scattered heterogenous fouling layer for the low feed loading. However, the high feed load exhibited homogenous membrane fouling layer with visible scaling on the membrane surface. Moreover, the presence of elemental C, O, P, Ca, Mg, and Na on the fouled membrane surfaces confirmed the presence of organic and inorganic foulants on the membrane surface. Despite the presence of considerable nitrogen in the feed water, it was not identified on the PVDF membrane surface during EDS analysis whereas our previous studies observed an accumulation of more contaminants including nitrogen on the PTFE membrane surfaces. The ATR-FTIR peaks observed on the fouled PVDF membrane surfaces further established the occurrence of membrane fouling. The organic foulant layer was mostly comprised of proteins (amide I bond, N-H from amine group) and O-H from alcohol group. The consistent low EC of nearly 21.45±0.1 µS/cm and 305±2.82 µS/cm were for the low feed load and high feed loads despite high feed EC, high concentrate EC and the absence of other ions (sodium, calcium, magnesium, chloride, nitrate, phosphate, sulfate) in the permeate ensured the absence of membrane

wetting. Marginally higher EC of nearly 305 µS/cm with high feed load was due to the existence of volatile NH_4^+ in the feed that went through the membrane towards the permeate side increasing its EC. The presence of NH_4^+ in the permeate, and the absence of other ions in the permeate confirmed that membrane pores were not wetted. Nearly complete removal of COD and TP was observed during DCMD application of both feed loads. TN rejection was 100% and nearly 78% for 10 g/L/d, and 15 g/L/d MBR feed load, respectively. Furthermore, sequential membrane cleaning by NaOH and HCl followed by DI water could completely restore the membrane DI water flux for the low feed load. Hence, the DCMD application was successful in terms of contaminant rejection if volatile compounds were not present.

This study concludes that 0.45 µm PVDF membranes with a moderate feed temperature of 55°C could probably be an optimal condition and efficient way for stable water reclamation from membrane bioreactor treated brewery wastewater effluent without the presence of volatile compounds. However, further studies concerning energy requirements for hot feed and hence the economic feasibility of the process need to be conducted for such applications such as elevating the feed water temperature in MD needs high energy input. The alternate energy sources (e.g., solar energy and/or process waste heat), DCMD can offer a sustainable solution for water reclamation application within the industry. Moreover, a pilot scale study needs to be conducted with optimal operating conditions with probable alternate energy sources to study the efficacy of its water reclamation application for a brewery wastewater effluent.

Appendix A2

The permeate flux drop and water recovery for PTFE and PVDF membranes with various pore sizes and varying hot feed temperatures are shown in Figure A2.1. The surface morphology of PVDF and PTFE 0.45 µm membranes in pristine and fouled condition with various hot feed temperatures of 65°C, 55°C, and 45°C are shown in Figure A2.2 and A2.3, respectively. The SEM images of PVDF 0.45 µm and 0.22 µm pristine and fouled membranes with 65°C hot feed temperatures are provided in Figure A2.4. Figure A2.5 represents the SEM images of PTFE 0.45 µm and 0.20 µm membranes in pristine and fouled condition with 65°C hot feed temperature. SEM images along with the EDS analysis are presented in Figure A2.6 for pristine and various feeds fouled PVDF 0.45µm membranes. The MD setup with a feed and permeate is shown in Figure

A2.5. The RO and NF operational setup is shown in Figure A2.6. Table A2.1 shows the high strength feed wastewater characteristics utilized for verifying the membrane cleaning efficacy. Figure A2.7 shows the permeate flux of the raw water with PVDF 0.45 μm with a hot feed temperature of 65°C for 20 hours.

Acknowledgement

The authors acknowledge the Ministre de l'Agriculture, des Pêcheries et de l'Alimentation, Québec (MAPAQ) and the Natural Sciences and Engineering Research Council (NSERC) of Canada for providing funding support for this project. We thank Dr. Sheng Chang, Professor, University of Guelph, for his support towards MBR process water and his students (Peter Inns and Han Chen) for collecting and shipping the process water for this project. Nawrin Anwar gratefully acknowledges the financial support of Fonds de Recherche du Québec-Nature et technologies (FRQNT) and Alexander Graham Bell Canada Graduate Scholarship (CGSD) from the Natural Sciences and Engineering Research Council of Canada (NSERC) for doctoral studies. The authors also acknowledge ongoing support from Concordia University, Canada.

Chapter 5: Techno-economic evaluation of DCMD for water recovery from pre-treated brewery wastewater effluent

Abstract

Membrane distillation (MD) is continuously gaining interest for water recovery application and studies are conducted for water reclamation through MD application for brackish/saline/brine water as well as other types of wastewaters including breweries, textile, fermentation, etc. Nevertheless, researchers have mostly studied the economic aspect of MD for brackish/saline/brine water. This study analytically evaluated the techno-economic aspects of direct contact membrane distillation (DCMD) application for water recovery from pre-treated brewery wastewater. Furthermore, it considered the impact of various sources of energy, like heat recovery within the system as well as solar energy, on the water price. In addition to that, it recognized the effect of major parameters on the water price, e.g., plant capacity, various recovery ratio, and waste heat integration from industries. The study observed a \$2.34/m^3 water price for a 100 m^3/day stand-alone DCMD system, which was reduced to 17.5% and 42% due to heat recovery within the system, and integration of solar energy in addition to heat recovery, respectively. The major cost for a stand-alone DCMD came from the thermal energy requirement (58%) whereas a solar collector cost accounted for the significant portion cost (82%) during integrating solar energy. Results suggested that the source of energy is a key parameter for optimizing cost in the DCMD application, and waste heat incorporation could lead towards a viable, and cost-effective DCMD application.

Keywords: Direct contact membrane distillation; Pre-treated brewery wastewater effluent; Water price; Solar collector; Heat recovery.

5.1 Introduction

With increasing population and continuous enhanced demand for fresh water supply, clean water shortage has become a major concern around the globe resulting in the need of advance processes for fresh water supply [1,2,28]. Recovering water through novel wastewater treatment processes and reusing the recovered water can lead towards efficient technologies to combat the challenges of water scarcity along with wastewater disposal to the natural environment. Membrane separation processes (membrane distillation: MD, nanofiltration: NF, reverse osmosis: RO) can be effective to reclaim water and researchers have investigated the potential of water reclamation from pre-treated wastewater effluents through membrane separation processes for different types of wastewater [1,2,4,5,28,313,314].

Beer, one of the top five in beverage sales by world market share, is the most popular alcoholic beverage in Canada constituting nearly 41.5% of the total alcohol sales and 85% of which originates from local breweries [18,310]. The brewing industries have high economic value, and from 2019 to 2025, the global beer market has a projection of a compound annual growth rate of 1.8% [280]. The number of breweries in Canada has increased nearly 12.9% from 2018 (995 breweries) to 2019 (1123 breweries) [282]. The brewing industry has high economic value, supporting about 149,000 jobs generating $5.3 billion income with a $13.6 billion contribution of Canada's GDP [282]. Nevertheless, beer production generates a large volume of wastewater, nearly 3 to 10 L of wastewater from 1 L of beer production, that contains sugars, volatile fatty acids, ethanol, soluble starch, total suspended solids, and a very low concentration of heavy metals [22–25]. Brewery wastewater effluent discharge needs appropriate treatment to conform with the regulation for human health, aquatic life, and environmental safety. The environmental costs associated with the brewery wastewater disposal include adverse human health effects and negative environmental effects, e.g., excess nutrients (N and P) in the water bodies that may lead to eutrophication. Increasing financial incentive for intake water along with high wastewater disposal standards and fees has led the brewing industries to look for environmentally sustainable ways for recovering water from the brewery wastewater effluent to utilize for production and non-production purpose. The conventional brewery wastewater treatment includes primary (physicochemical) treatment and then secondary (biological) treatment, e.g., UASB (up-flow

anaerobic sludge blanket) reactors and membrane bioreactors [284,286,287]. Some researchers have studied electrochemical processes for treating brewery wastewater [288]. Membrane separation processes are continuously being explored for advanced wastewater treatment to recover reusable water [1–5,7,315]. MD has primarily been implemented for water reclamation from brine/highly saline water. However, the possibility of water recovery from membrane bioreactor treated brewery wastewater effluent via membrane separation processes are investigated in previous studies [309]. The study observed implementation of membrane distillation process has the potential to be integrated in the downstream of membrane bioreactor (MBR) treatment to reclaim water without further polishing whereas RO required additional polishing of MBR effluent due to extensive membrane fouling and very low recovery despite enhanced rejection performance. The MBR provides adequate pre-treatment to the brewery wastewater for MD with high recovery and excellent rejection, and thus incorporation of MD can be promising for recovery and reuse of water within the brewing facilities.

Membrane distillation, a thermally driven emerging membrane separation process, has become a promising and efficient membrane separation technology for water reclamation [9,309,316]. MD is a thermal-based membrane separation process where the temperature difference between the feed and permeate drives the water vapor through hydrophobic microporous membranes from the feed towards the permeate side, and partial vapor pressure difference of the feed and the permeate is the driving force. The hydrophobic membrane is a vital feature of MD which prohibits the direct permeation of feed water towards the permeate and results in contaminant rejection. MD has several advantages, such as: theoretically it rejects 100% non-volatile salt, it requires a lower operating temperature compared to conventional thermal desalination processes, it can use low-grade thermal energy, and it needs a lower operating hydrostatic pressure and less stringent mechanical properties for the membranes when compared to conventional pressure-driven membrane processes [36,38,262,263,316]. Sustainable high quality water reclamation via MD can be possible when low-grade or renewable heat sources and/or waste-heat from industrial processes are available [317,318].

The ability to utilize low-grade waste heat/solar thermal energy along with the viability of integration with other processes have given MD the provision to be explored for water reclamation.

However, prior to real-scale implementation of MD for water reclamation, it is required to assess the economic aspects for better understanding the cost-effectiveness of the process. MD has been broadly explored for the removal of salts from brackish water, seawater, and high-salinity brines [85,319–322]. Therefore, in the literature, the technical analysis for MD has been conducted mostly for brackish/saline/brine water. Researcher studied stand-alone solar-powered desalination for different MD configurations with a 4.4% heat recovery and noted that DCMD is cost effective ($12.7/m^3) compared to AGMD ($18.26/m^3) and VMD ($16.02/m^3) [323]. Another study conducted by Kesieme et al. for freshwater production from brine water observed that with a waste heat source, the water price of MD can be reduced nearly 73% from $2.2/m^3 to $0.6/m^3 for a 30,000 m^3/day capacity plant. Furthermore, to achieve zero liquid discharge via AGMD from a highly saline water, the researchers observed €9/m^3, and €4.4/m^3 as current costs for 10 m^3/day and 1000 m^3/day feed capacity, respectively [322]. A study conducted by Haamid et al. noted that water price for desalination of brackish water with a feed capacity of 100 m^3/h was $6.78/m^3. However, the integration of waste heat and solar power reduced the water price nearly 76% to $1.6/m^3 while considering 40% of the heat energy comes from the alternate sources [320]. However, most of the economic studies are conducted for freshwater production from saline water. There is a need for the economic study for other types of wastewater effluents to better comprehend the implementation of MD process for water reclamation from various types of wastewater effluent. As MD has certain advantages, like concentrating wastewater nearly to saturation (tolerating higher concentrations than RO and requiring less pre-treatment compared to RO) as well as utilizing alternate energy sources directly (the heat can be used directly without converting it into electricity), it has the potential to be implemented for water recovery from wastewater effluent. Hence, it is inevitable to focus on the economic aspect of MD for wastewater effluents in addition to seawater for broader perspective. To the best of our knowledge, no other research has comprehensively studied the economic aspects of MD system for pre-treated brewery wastewater effluent. This study analyzed the water price of water reclamation from a pre-treated brewery wastewater effluent via DCMD.

The objective of this research is to methodically analyze the economic aspect of DCMD system for water reclamation from a pre-treated brewery wastewater effluent. As our previous study observed that MD has the potential to be implemented directly for water recovery from MBR

treated brewery wastewater with nearly 85% recovery [309] which would otherwise be discarded into the environment, it is necessary to evaluate the economic viability of the process as well as to explore the alternate energy resources to improve the cost for better understanding the scope of MD application for water recovery in the real-world. Moreover, to better comprehend the effect of alternate energy sources on the water price, DCMD process was evaluated with heat recovery within the system as well as with solar energy as an alternate source of energy. Furthermore, effect of varying process parameters on the cost of the DCMD, like; plant capacity, water recovery, and waste heat integration from industry were explored. This research provided a basis of the economic aspect of the emerging DCMD process for water recovery from pre-treated brewery wastewater and a perspective to potential implementation of DCMD for water recovery from brewery industries for reuse for environmental sustainability.

5.2 Direct Contact Membrane Distillation system

Figure 5.1 represents the schematics of the stand-alone Direct Contact Membrane Distillation (DCMD) system implemented for water recovery from a pre-treated real brewery wastewater effluent (COD of 50±10 mg/L, TS of 1.77 mg/L, and EC of 5.5±0.3 mS/cm) at a capacity of 100 m^3/day. The pre-treated brewery wastewater effluent was transported through the intake pump from the source and then stored in a feed tank. Afterwards, the water was pumped through the heating unit to attain desired feed temperature required for DCMD (55°C) and then passed through the DCMD module as a hot feed. The permeate tank circulated the cold permeate via another pump and utilized a cooling unit to maintain the desired temperature (20°C) for the cold permeate. The vapor pressure difference between the hot feed and the cold permeates enabled the vapor to pass through the hydrophobic microporous membrane and the cold temperature of the permeate side condensed the permeate. The produced permeate went through further polishing prior to reuse and the concentrate of the feed side was rejected and collected for disposal.

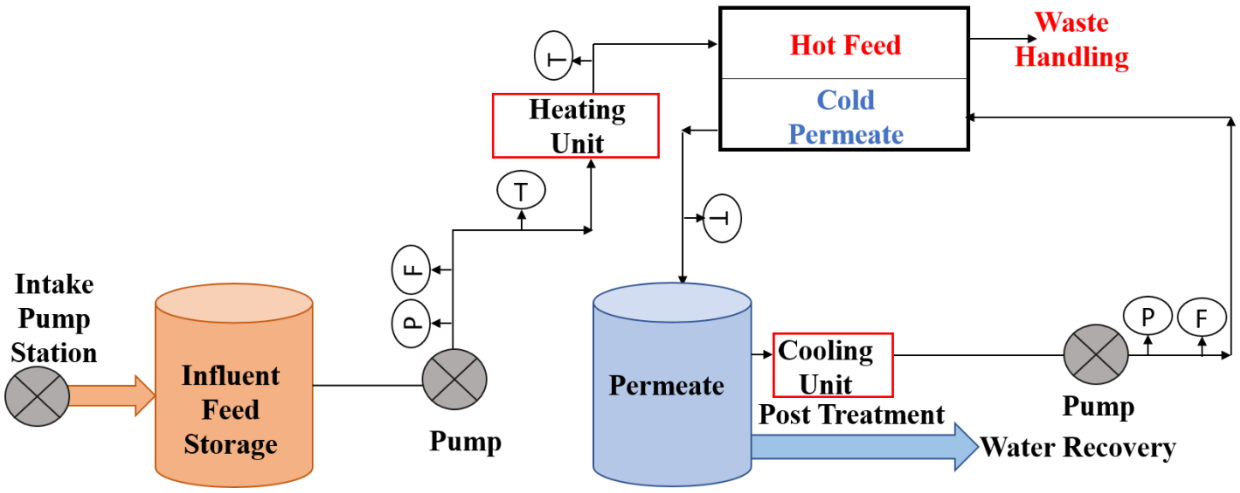

Figure 5.1: Schematic representations of Direct Contact Membrane Distillation (DCMD) system with heating and cooling units for water recovery from pre-treated brewery wastewater. The capacity of the system is 100 m^3/day. The produced permeate undergoes post-treatment and the concentrate reject contributes towards waste handling. The hot feed and the cold permeate temperatures are 55° C and 20° C, respectively. P, F, and T, stands for the pressure gauge, flowmeter, and temperature sensors in the schematic**.**

Figure A3.1 represents the DCMD set-up with a heat exchanger to recover heat within the DCMD system for reclaiming water from pre-treated brewery wastewater effluent. The capacity was 100 m^3/day with a hot feed temperature of 55°C. For heat recovery, a heat exchanger was added within the system to reduce the thermal energy requirement from outside. The heat exchanger transferred heat from the hot stream towards the cold stream, thus raising the feed temperature to a certain extent. To further reach the desired hot feed temperature, thermal energy is added.

Figure 5.2 shows the conceptual DCMD set-up with a heat exchanger and a solar collector. The same concept of DCMD operations occurred, i.e., vapors passed through the hydrophobic membrane from the hot feed towards the cold permeate, and then condensed and went for further post treatment prior to reuse. The heat exchanger transferred heat from the hot stream towards the cold stream, thus raising the feed temperature to a certain extent. To further reach the desired hot feed temperature, a solar collector was used. The direct utilization of solar heat without converting it to electricity is one of the major advantages of the MD system that renders it application promising. Thus, it was considered that a combination of heat exchanger and solar collector can eliminate the complete heating and cooling units using electricity, and substantially contribute towards a cost-effective water recovery system.

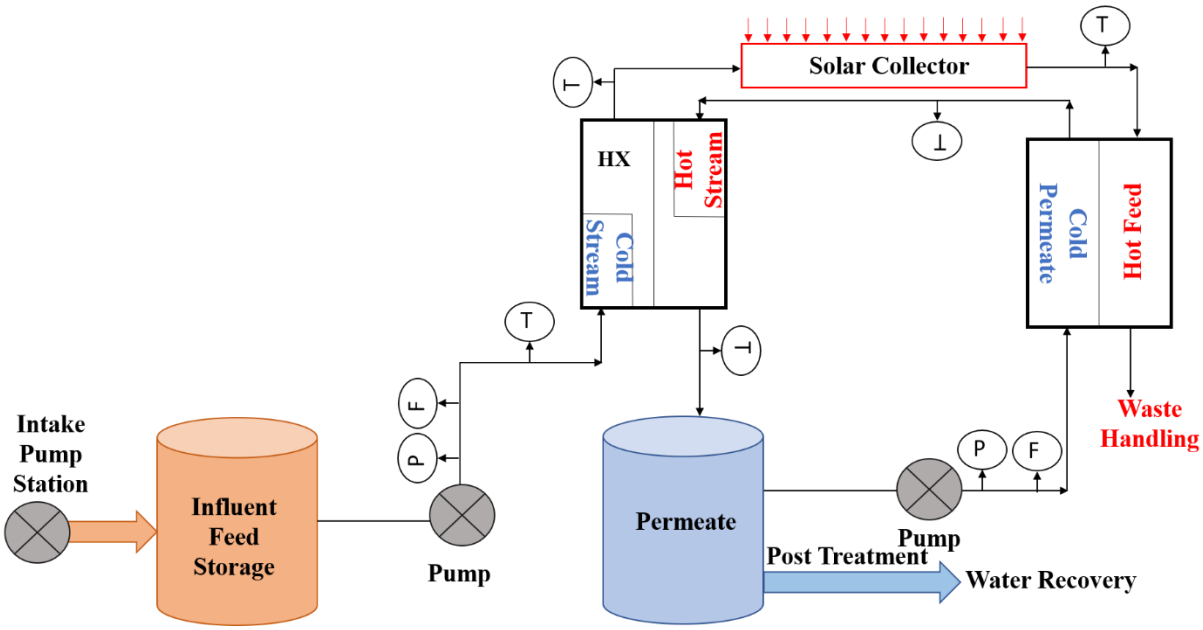

Figure 5.2: Illustration of Direct Contact Membrane Distillation (DCMD) system with heat exchanger and solar collectors for water recovery from pre-treated brewery wastewater with a 100 m^3/day capacity. The permeate product goes through further polishing and the rejected concentrate contributes towards waste handling. The hot feed and the cold permeate temperatures are 55° C and 20° C, respectively. P, F, and T, stands for the pressure gauge, flowmeter, and temperature sensors in the schematic.

5.3 Techno-economic evaluation

The techno-economic evaluation is a required component prior to practical implementation of any system. Previous studies were mostly conducted for cost estimation for brackish/saline/brine water [320–323]. To further develop and employ the emerging MD for water recovery from pre-treated brewery wastewater, assessing the cost of the system is essential. The economic viability of the project would help to determine the large-scale application as well as encourage the researchers to focus on the ways to overcome the challenges through further studies. Many researchers have explored the water recovery from different types of wastewater other than brackish/saline/brine water [9,86,309]. However, there is always a lack of studies on the economic aspects of water recovery from wastewater. Therefore, the techno-economic evaluation would provide an insight on the feasibility of the real-life implementation as well as encourage to explore further sustainable cost-effective applications for water recovery through MD from pre-treated wastewater.

5.3.1 Cost components

The MD system often lacks the cost estimation because of the absence of real-scale large MD plants which hinders the widespread application of MD due to a lack of better comprehension of the economic viability of MD. However, due to the resemblance between different cost components of the reverse osmosis (RO) and MD plants [320], like the site development, land and building construction, post/chemical treatment, intake, outfalls, some parts of the cost modelling of MD can be conducted from the existing RO plants cost estimation formulas. Moreover, the energy cost can be calculated based on the thermal and electrical energy requirements of the MD process as discussed in section 5.3.2 using the energy formula. The operating parameters (like temperature, recovery rates, etc.) can be considered from literature where lab-scale application of MD for water recovery from pre-treated brewery wastewater is implemented [309]. Thus, the operational parameters, cost data and economic formulas from literature were considered to estimate the cost of DCMD plant for water recovery from pre-treated brewery wastewater for reuse [309,320]. The cost computations were conducted based on the capital expenditure (CapEx) and operational expenditure (OpEx) components of the direct membrane distillation system as shown in Figure 5.3.

Since the initiation of the project design concept, approval, the funding/loan (either from investors or banks), and finally acquiring the land and developing the sites as well as constructing the building, all associated costs were considered as capital costs of the project. Moreover, the acceptance testing was also considered as a capital expenditure component as it was required for continuous plant operation. The capital expenditure consists of direct and indirect capital costs. The direct costs associate with the basic structure of the plant, e.g., land acquisition, site development, building construction, intake and outfall structure, post treatment, membrane module, solar collectors, pumps, heat exchanger, pressure vessels, and electrical devices, etc. The indirect capital costs are usually the cost associated with overhead expenses like any rents, administrative expenses, pilot testing, legal services, environmental legislations, and testing, etc. The costs associated with regular activities that are required to operate the plants efficiently are known as operation expenditures (or operation and maintenance cost) of the plant that consist of direct and indirect costs. The direct operational expenditure comprised of the costs of any

maintenance or replacement (like membrane replacement and/or solar collector maintenance) as well as the labor costs, chemical costs, thermal or electrical energy costs, cleaning, repairs, etc. The indirect operational expenditure consisted of staff training and certification, professional developments, etc. Tables 5.1 and 5.2 demonstrate the economic formula, and the operational and economic data that are implemented for the capital expenditures and operational expenditures estimation of the direct contact membrane distillation plant of this study, respectively.

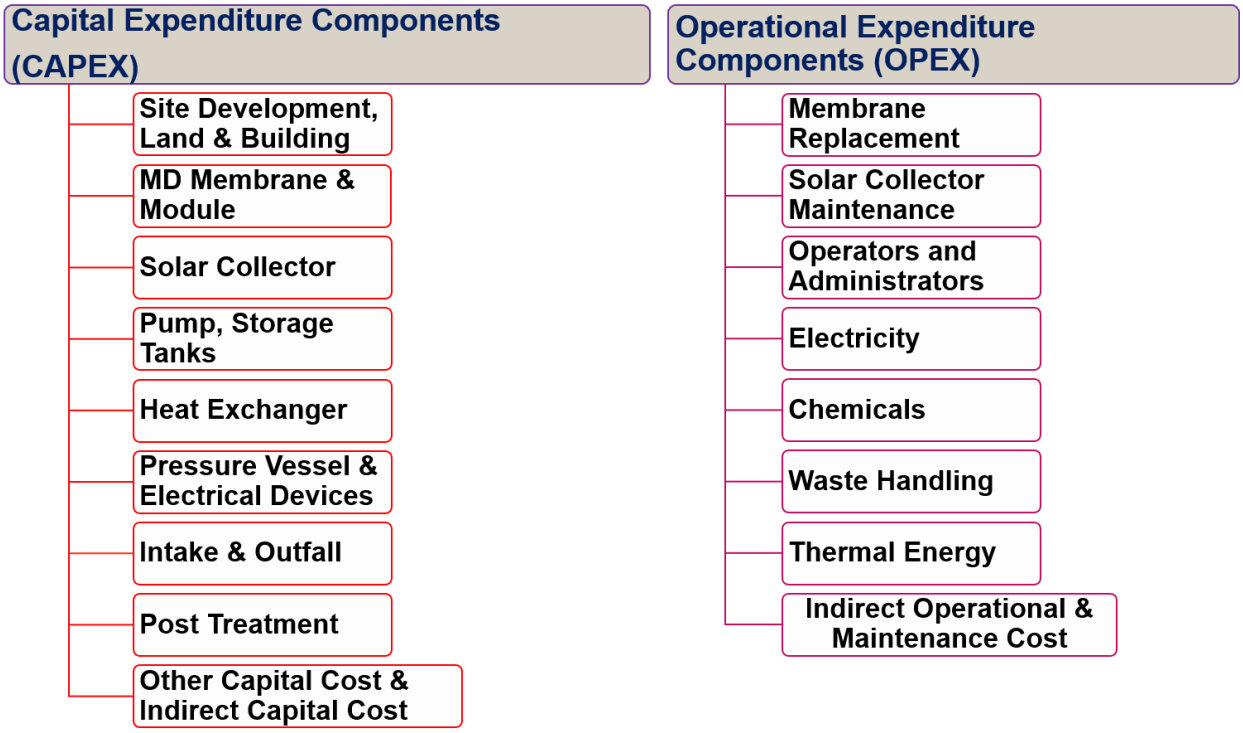

Figure 5.3: Water price component breakdown for membrane distillation plant that includes capital cost, and operational and maintenance cost including both direct and indirect costs.

Table 5.1: Cost estimation of a Membrane Distillation Plants.

Cost Component	**Cost estimation correlation** [319,321,324–327]
Capital expenditure components (CapEx)	
Site development	$C_{Site} = Q_P \times 26.42 \times 1.245$
Land and building	$C_{B-L} = 45 \times Q_P \times t_H \times f$
Intake	$C_I = \frac{Q_f}{t_H \times 450}(393000 + 10710P_P \times 1.01325)$
Outfall	$C_{out} = 50 \times Q_c \times t_H$
Membrane	$C_M^{MD} = C_{MD} \times A_{MD}$
Heat exchanger	$C_{HX} = \{1337\ X[(A_{HX})]^{0.42}\}$
Solar collector	$C_{SC}^{MD} = C_{SCC} \times A_{SC}$
Pressure vessel and electrical devices	$C_{El} = Q_P \times 140 \times 1.245$
Pump	$C_P = \frac{Q_f}{t_H \times 450}(393000 + 10710P_P \times 1.01325)$
Storage tanks	$C_{storage} = Q \times 264.17 \times 0.4 \times 5$
Post treatment	$C_{PT} = 50 \times Q_p \times t_H$
Other capital costs	$C_{Other} = 2 \times 44.9 \times Q_F \times t_H \times 1.245$
Indirect capital costs	1% of direct capital cost
Operational expenditure components (OpEx)	
Module and membrane replacement	$C_{M-r}^{MD} = r_m C_M^{MD}$
Electricity	$C_E = SEEC_E \times C_e \times Q_F \times t_Y$
Labor	$C_L = 0.0275 \times Q_F \times t_Y \times f$
Chemicals	$C_{CH} = t_Y \times (Q_P) \times C_{CH} \times f$
Waste handling	$C_{WS} = 0.025 \times Q_P \times t_Y \times f$
Solar collector maintenance	$C_{SC-r}^{MD} = r_{sc} C_{SC}^{MD}$
Thermal energy	$C_{TH} = 50 \times 0.008 \times STEC_{MD} \times t_Y$
Indirect operational and maintenance	1% of direct operational and maintenance cost

Table 5.2: Economic parameters for DCMD plants.

Parameter	Value
Plant load factor, f	90% [314]
Membrane replacement factor, r_m	20% [323]
Solar collector maintenance factor, r_{sc}	5%
Discount rate in % per year, r	8% [328]
Amortization period, n	20 years [323]
Daily operating hours, t_H	8 h [326,327]
Yearly operating hours, t_Y	2920 h/yr [326,327]
Cost of electricity, C_e	0.104 $/kWh [329]
MD membrane unit price, C_{MD}	199.94 $/m^2 [321]
Solar collector unit cost, C_{SCC}	208 $/m^2 [325]

5.3.2 Energy Requirements of DCMD

The membrane distillation requires a considerable amount of thermal energy for heating the feed as well as some electrical energy for operating the pumps. The specific thermal energy consumption ($STEC_{MD}$) in kWh/m^3 of the MD system was calculated by the following Eq. (5.1) [330]:

$$STEC_{MD} = \left(\frac{Q_m \cdot \rho_f}{J_p \cdot A_m}\right)/3600 \quad \text{(5.1)}$$

Where, Q_m is the total heat flux (in kW) Eq. (5.2) [85]:

$$Q_m = C_p m_f \Delta T \quad \text{(5.2)}$$

In equations (5.1) and (5.2), ρ_f is density of the feed (kg/m^3), J_p is the water permeate flux (kg/m^2-s), A_m is the area of the membrane (m^2), C_p is the specific heat capacity of the feed (J/kg-°C), m_f is the mass flow rate of the feed (kg/s), and ΔT is the temperature difference between the feed and the permeate (°C) .

The specific electrical energy consumption (SEEC) of the MD system in kWh/m^3 was calculated by the following Eq.(5.3) [85]:

$$SEEC_{MD} = \frac{m_f.P}{36.\ \eta.m_{dist.}} \quad (5.3)$$

Where, m_f and m_p are the feed and permeate mass flow rate, respectively (kg/s), η is the efficiency of the circulating pump, and P is the pressure over the membrane distillation system (bar).

For the solar-powered DCMD system, the solar collector area was calculated by the following equation Eq. (5.4) [329]:

$$A_{SC} = \frac{m_f.C_p.\Delta T_s}{\Sigma(I_{glob}).(\eta_c)} \quad (5.4)$$

Where, m_f is the feed mass flow rate (kg/s), C_p is the specific heat capacity of the feed (J/kg-°C), ΔT_s is the water temperature difference between the solar collector inlet and outlet (°C), I_{glob} is the average global solar radiation (W/m^2), and η_c is the efficiency of the solar collector. The annual global average solar radiation for a horizontal surface of Quebec was considered. The solar collector efficiency typically varies within 35%-60% [323]. For this case, 60% solar efficiency was considered which is the maximum efficiency that can so far be attained for the solar collector.

5.3.3 Water Price of DCMD

The water price of the DCMD process was calculated by using equation Eq. (5.5) [331]:

$$Cost_{WP} = \frac{CRF}{Q_p * t_Y * f}(CapEX + \frac{OpEX}{CRF}) \quad (5.5)$$

Where, $Cost_{WP}$ is the water price in \$/m^3 unit, CapEX and OpEX are the total capital cost and total operational cost, respectively, both including direct costs and indirect costs. Q_p is the permeate flow per hour (m^3/h), t_Y is the yearly operational hours (h/yr), f is the plant load factor, and CRF is the capital recovery factor that is expressed by the following equation Eq. (6) [332]:

$$CRF = \frac{r(1+r)^n}{(1+r)^n - 1} \quad (6)$$

Where, r is the annual discount rate (%), and n is the amortization period.

5.3.4 Techno-economic evaluation

The techno-economic assessment of a DCMD system for water recovery from a pre-treated brewery wastewater was conducted. To better comprehend the overall economic feasibility of the

system, various energy sources were considered. For a stand-alone DCMD system, the electrical energy supplied from the grid is the operating energy source whereas for the solar-powered DCMD, solar collector and heat exchangers are the sources of thermal energy required by the system.

5.3.4.1 Stand-alone DCMD

The water price of a stand-alone DCMD system was calculated as \$2.34/m^3 for a 100 m^3/day feed where the feed is a pre-treated brewery wastewater effluent. The cost breakdown is illustrated in Figure 5.4 which shows the contribution of different cost components in the water price.

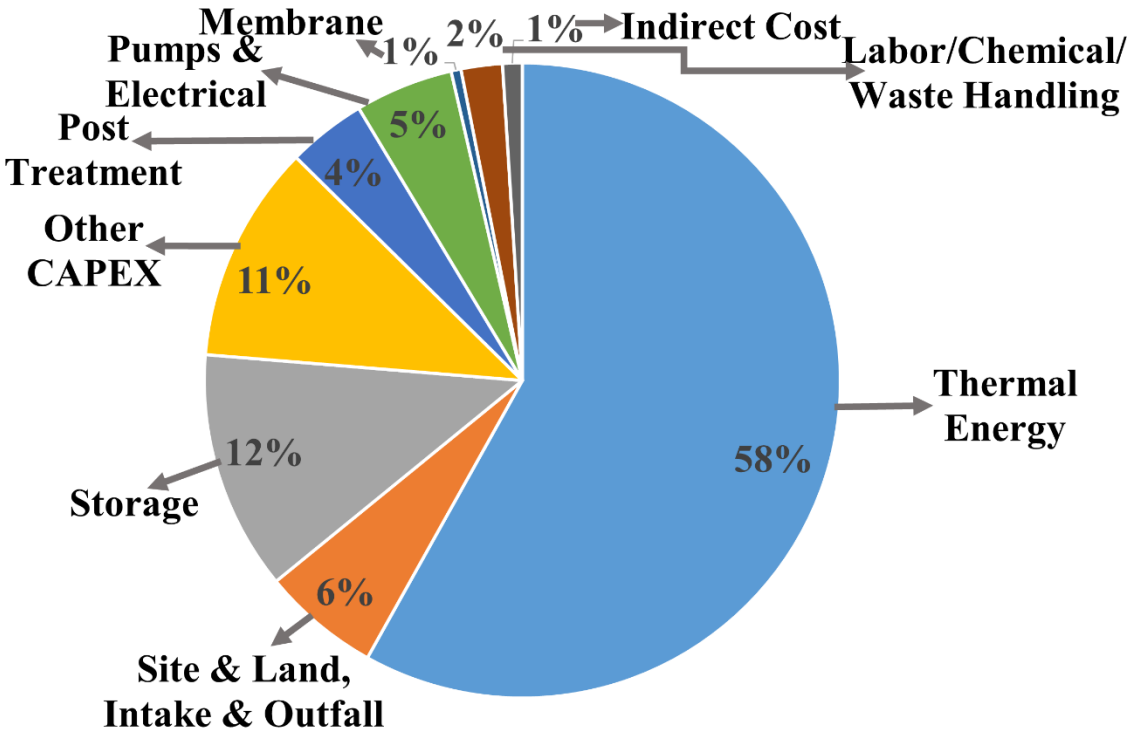

Figure 5.4: Costs of direct contact membrane distillation (DCMD) system for water recovery from pre-treated brewery wastewater with heating and cooling units for hot feed and cold permeate, respectively. The water price for 100 m^3/day feed is \$2.34/m^3. Thermal energy cost contributes to about 58% of the total cost for the DCMD system. The cost components, parameters and correlations considered for the water price estimation are described in Table 5.1, and 5.2.

For a stand-alone DCMD process, thermal energy contributed towards the largest percentage of the water price which is around 58%. This thermal energy was utilized to maintain the hot feed

temperature at 55°C. Other major cost elements for a stand-alone DCMD process consisted of storage (12%), other capital expenditures like service equipment, utilities, commissioning, etc. (11%), site/land development and intake/outfall (6%), and pumps and electrical expenses (5%). The water price obtained from this study fell within the range of \$0.40/m^3 to \$130/m^3 as reported in previous studies conducted on membrane distillation systems [321,333]. However, all these studies were conducted for brackish/saline water and included the pre-treatment costs as well. Furthermore, studies on utilization of low-pressure reverse osmosis followed by an activated carbon post-treatment to reclaim water from flash cooler condensates from the UHT (ultra high temperature) process of dairy factory for reuse as boiler water found the capital and operational expenditure to be €0.45/m^3 and €1.16/m^3. Altogether the water price was €1.61/m^3 (\$2.23/m^3) which is comparable with the water price of \$2.34/m^3 of the stand-alone DCMD application of this research [334]. Our study estimated the cost of water recovery for a pre-treated brewery wastewater effluent that would otherwise be discarded. The high recovery (85%) of MD, as well as high resistance to fouling in addition to the pre-treatment provided further benefit for the enhancement of the overall water recovery application. As the thermal energy contributes to a major part of the cost, alternate sources of energy like, heat recovery might provide a cost-effective water recovery option from pre-treated brewery wastewater effluent.

5.3.4.2 DCMD with heat recovery

The water price of a DCMD system with a heat recovery unit to utilize heat within the system was calculated as \$1.93/m^3 for a 100 m^3/day feed where the feed is a pre-treated brewery wastewater effluent. The cost analysis is exhibited in Figure 5.5 which shows the percentage of various cost components in the water price. Addition of a heat exchanger reduced the water production cost nearly 17.5% from \$2.34/m^3 to \$1.93/ m^3. For the DCMD process along with heat recovery, the thermal energy cost reduced nearly 7% from 58% to 51% of the total expenditure. The cost of heat exchanger was nearly 3% of the total cost. Thus, heat recovery decreased the overall cost of the heat requirements of DCMD system resulting in a reduction of the unit water price. Other major cost elements for a stand-alone DCMD process consisted of storage (13%), other capital expenditure (12%), site/land development and intake/outfall (7%), post treatment (5%), and pumps and electrical expenses (5%). Heat recovery within the system showed that alternate energy sources can be promising to reduce the overall costs. Hence, it encouraged the incorporation of

solar energy in addition to heat recovery within the system to better assess the cost optimization for DCMD application for water recovery from pre-treated brewery wastewater.

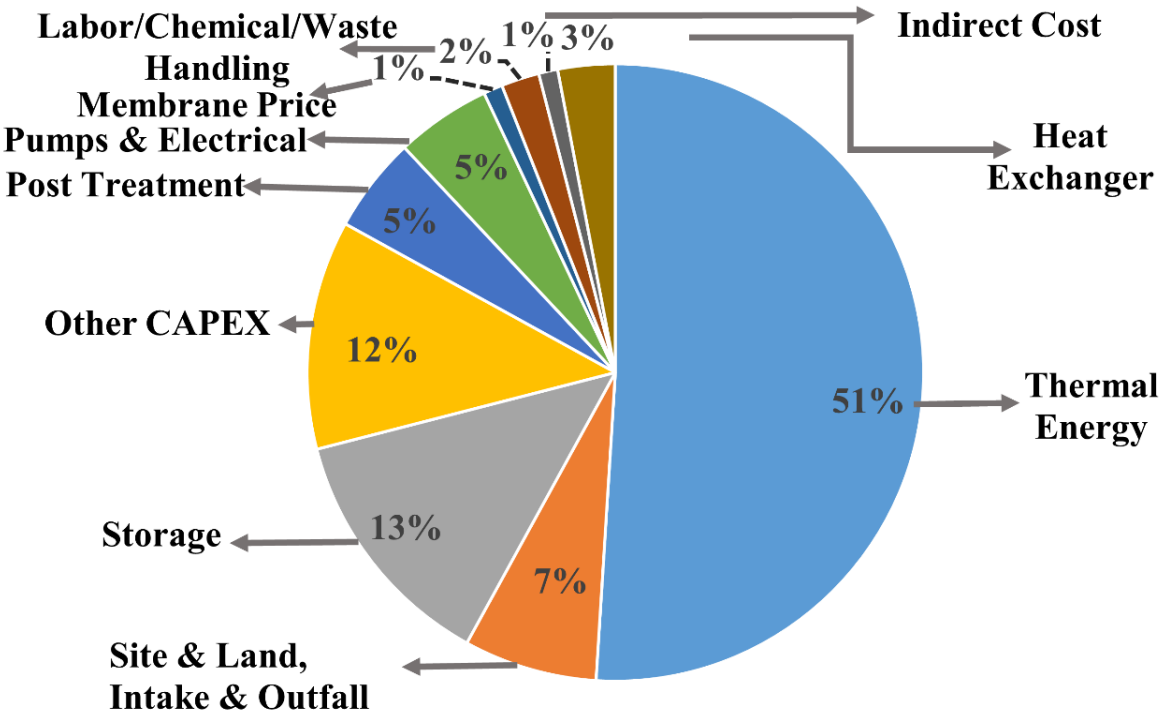

Figure 5.5: Costs of direct contact membrane distillation (DCMD) system for water recovery from pre-treated brewery wastewater with heat recovery through a heat exchanger in addition to the heating and cooling units. The water price for 100 m^3/day feed reduces nearly 17.5% to \$1.93/m^3 compared to that without heat recovery implementation. Addition of heat exchanger reduces the thermal energy cost contribution to about 7%. The cost components, parameters and correlations considered for the water price estimation are described in Table 5.1, and 5.2.

5.3.4.3 Solar powered DCMD with heat-recovery

The water price of a solar-powered DCMD along with a heat exchanger to recover and utilize heat within the system is calculated as \$1.35/m^3 for a 100 m^3/day feed where the feed is a pre-treated brewery wastewater effluent. The cost analysis is demonstrated in Figure 5.6 which represents the impact of various cost components in the water price. For the solar-powered DCMD process along with heat recovery, the largest percentage of the water price came from the solar collectors which is around 82%. The other significant cost components of the solar-powered DCMD process were comprised of storage (5%), other capital expenditure (4%), site/land development and intake/outfall (2%), and labor/chemical/waste Handling/heat exchanger/ pumps and electrical expenses (5%). The membrane price contributed to around 1% of the total cost of the system and

it was consistent irrespective of the energy sources. Inclusion of solar power and a heat exchanger reduced the water production cost nearly 42% from \$2.34/m^3 to \$1.35/m^3. This study considered the solar collector efficiency 60% and solar collector consisted of the major portion of the water price. A sensitivity analysis demonstrated that higher solar collector efficiency of 70% and 80% will result in nearly 12% and 21% reduction in the water price from \$1.35/m^3 to \$1.19/m^3 and \$1.07/m^3. Hence, with further development in a more efficient solar collector, DCMD application will be more economical.

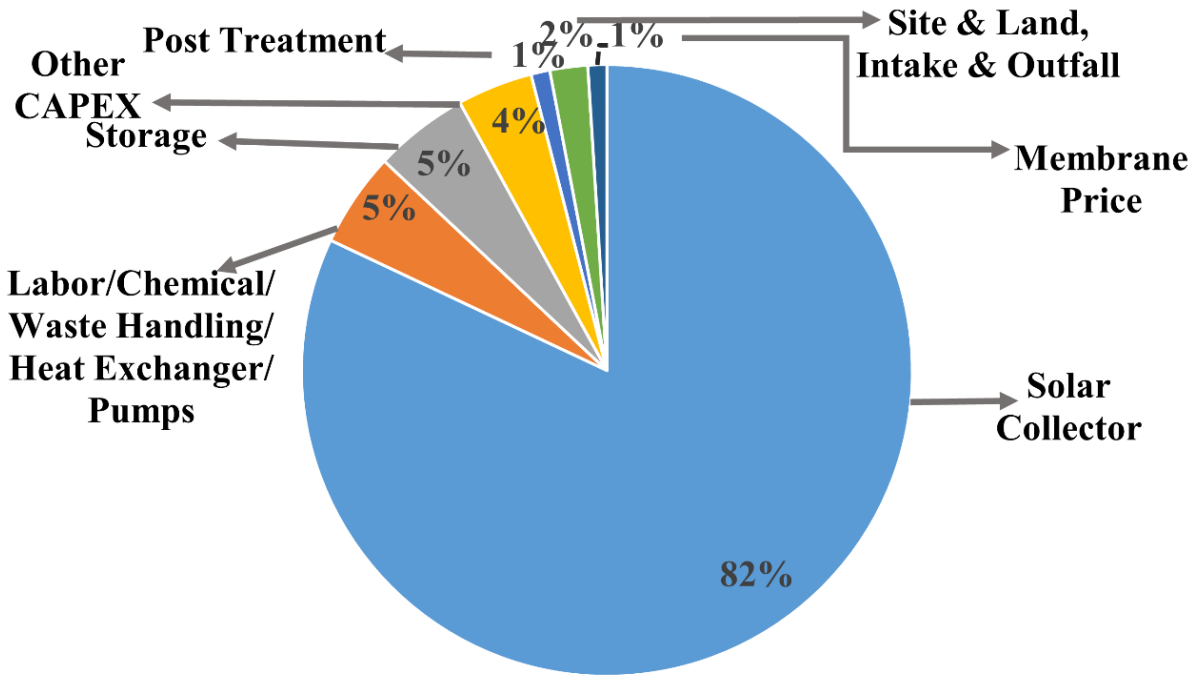

Figure 5.6: Water price distribution for water recovery utilizing Direct contact membrane distillation (DCMD) system from pre-treated brewery wastewater with solar energy utilized as a heating source for the feed in addition to a heat recovery unit within the system. The water production cost for 100 m^3/day feed is 42% reduced from the initial cost where no solar energy was considered for heating and results in \$1.35/m^3 water price. The solar collector cost is the major cost for this system and contributes to nearly 82% of the total cost of the solar-powered DCMD system. The cost components, parameters and correlations considered for the water price estimation are described in Tables 5.1, and 5.2.

5.3.4.4 Effect of varying parameters on water price

The water price from a MD plant depends on various operating parameters associated with the plant, e.g., plant capacity, recovery ratio, waste heat recovery within the industry, etc. To better

comprehend the planning and economic feasibility of the industrial application of a DCMD plant for water recovery, studying the variation of unit water price with these parameters are inevitable. The following sections elaborates the impact of varying parameters on unit water price of a DCMD system for water recovery from a pre-treated brewery wastewater.

5.3.4.4.1 Effect of varying capacity

The impact of varying plant capacity on the unit water price of a stand-alone DCMD and a solar powered-heat recovered (SP-HR) DCMD are illustrated in Figure 5.7. For a stand-alone DCMD system in this study, the unit water price increased nearly 30% and 90% from \$2.34/m^3 for 25% and 50% capacity reduction from 100 m^3/day, respectively. This trend was comparable to previous study where MD was implemented for a zero-liquid discharge from high saline wastewater and the cost analysis for an air gap membrane distillation (AGMD) showed that for a feed capacity of 10 m^3/day and 1000 m^3/day, the specific costs are €9/m^3 (\$10.63/m^3) and €4.4/m^3 (\$5.2/m^3), respectively [322]. This could be attributed to the various fixed capital expenses regardless of plants capacity as well as the high thermal energy requirement for high-capacity plants through electricity grids. However, for the solar powered and heat recovered (SP-HR) DCMD in this study, unit water price varied very insignificantly, with an average price of \$(1.355±0.003)/m^3 and exhibited similar trend of slightly increasing water price with decreasing capacity. The negligible variation of unit water price of a SP-HR DCMD could be explained through the fixed expenses related to the capital costs including the solar collector installation as well as no dependence on electricity for thermal energy. Thus, from the capacity variation of a DCMD system, it was evident that the thermal energy plays a significant role in the unit water price of the overall system. Therefore, the unit water price variation with different sources of energy needs to be further explored to better comprehend the economic feasibility of the MD process and is discussed in the following section.

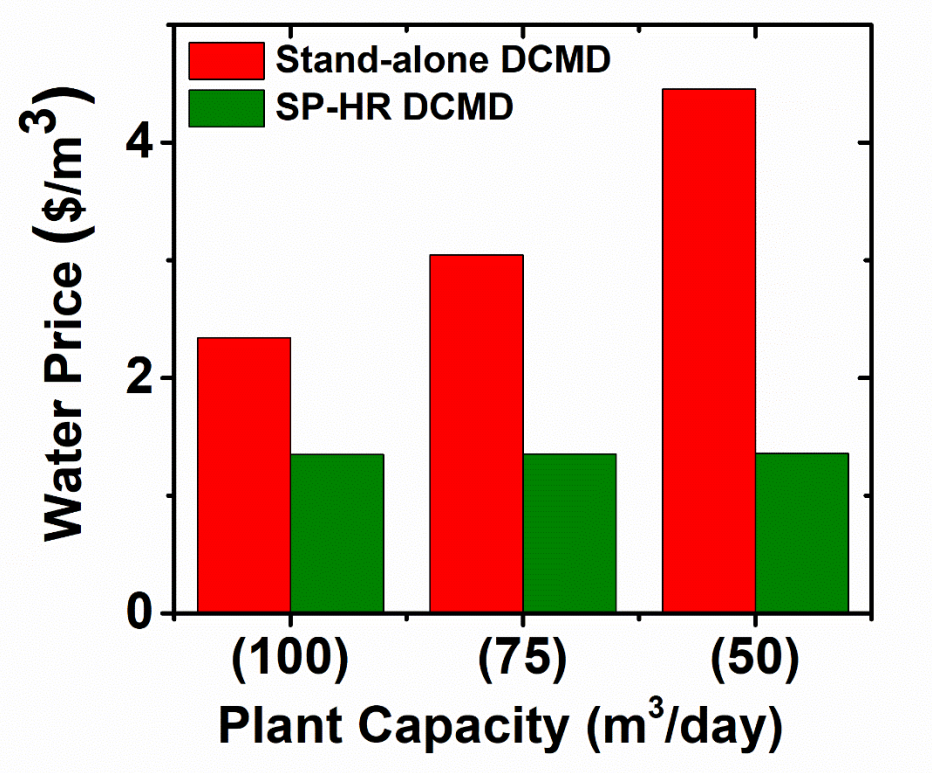

Figure 5.7: Water price variation with varying plant capacities for water recovery utilizing Direct contact membrane distillation (DCMD) system from pre-treated brewery wastewater with a stand-alone DCMD, and a solar powered and heat recovered (SP-HR) DCMD. The unit water price increases with a lower production capacity for a stand-alone DCMD \$2.34/m^3, \$3.05/m^3, and \$4.45/m^3 for 100 m^3/day, 75 m^3/day, and 50 m^3/day plant capacity, respectively. However, the unit water price for a solar powered and heat recovered DCMD with capacity variation is very insignificant with an average cost of \$(1.355±0.003)/m^3 due to the large cost associated with the installation of the solar collector.

5.3.4.4.2 Effect of varying recovery

Varying recovery ratio is related to the quantity of water recovery, that is, high recovery ratio results in higher amount of water recovered through the same system. Thus, the unit water price variation is directly related to the recovery ratio. High water recovery will result in low unit water price and similar trend was observed in our study (Figure 5.8). For a stand-alone DCMD, for 75%, 85%, and 95% water recovery, the unit water price was \$2.91/m^3, \$2.34/m^3, and \$1.86/m^3, respectively. Nearly 24% of the cost increased due to 10% reduction in water recovery from 85% whereas, about 20.5% of the cost decreased for 10% rise in water recovery for a stand-alone DCMD. Nevertheless, for a SP-HR DCMD, though the trend was similar to that of a stand-alone DCMD, the change in the unit price was lower compared to that of the stand-alone DCMD. A 10%

reduction in water recovery from 85% for a SP-HR DCMD demonstrated a 12.5% increase in unit water price, which was nearly half compared to that of the increase of a stand-alone DCMD. Furthermore, a 10% increase in water recovery from 85% resulted in nearly 9.6% unit water price decline. The recovery ratio variation showed that for a SP-HR DCMD, the change (increase/decrease) in water price was less susceptible compared to that of a stand-alone DCMD. The dependence of the fixed capital cost associated with the solar collector installation and less dependence on the operational cost related to the required thermal energy through the electricity were the primary factors that caused these trends.

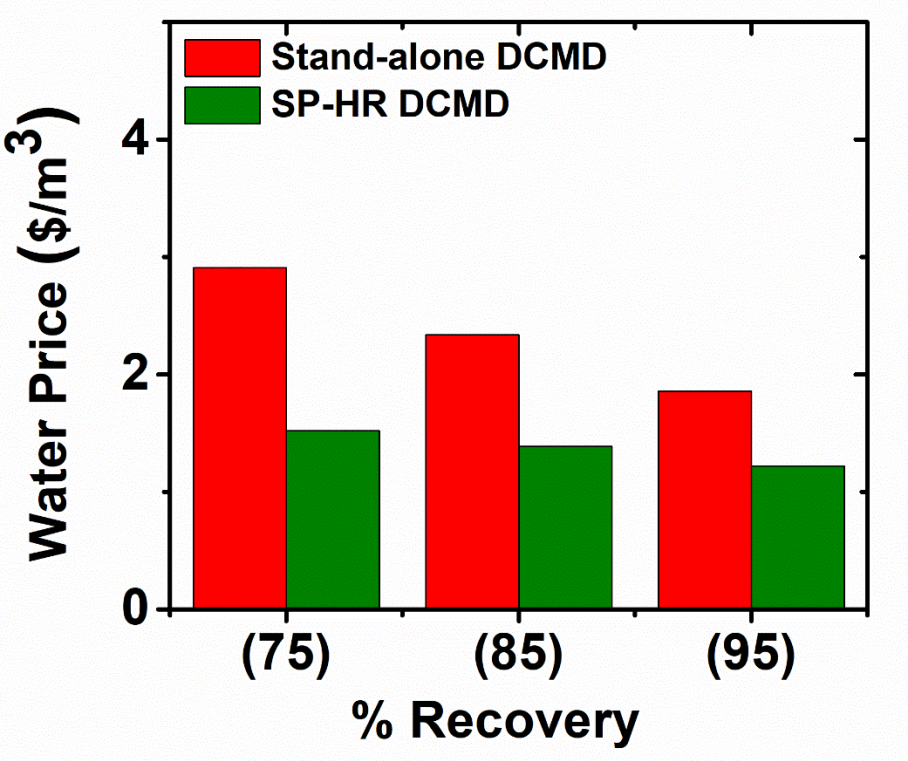

Figure 5.8: Change in water price with varying water recovery through application of direct contact membrane distillation (DCMD) system from pre-treated brewery wastewater with a stand-alone DCMD, and a solar powered and heat recovered (SP-HR) DCMD for 100 m^3/day plant capacity. The unit water price decreases with higher recovery ratios. For a stand-alone DCMD \$2.91/m^3, \$2.34/m^3, and \$1.86/m^3 for 75%, 85%, and 95% water recovery, respectively. However, the unit water price for a solar powered and heat recovered (SP-HR) DCMD follows the similar trend of a stand-alone DCMD with a reduction in unit water price with an increase in water recovery. For a SP-HR DCMD, a decrease in water recovery from 85% to 75% results in 12.5% increase in unit water price from \$1.35/m^3, whereas 10% increase of water recovery from 85% results in a 9.6% unit water price reduction to \$1.22/m^3.

5.3.4.4.3 Effect of addition of waste heat

Researchers have investigated the impact of solar energy for desalination implementing MD as well as emphasized the possibility of integration of waste heat in the MD system [320]. In addition to heat recovery within the system, the addition of waste heat from industry can be a source of thermal energy requirement reduction of the overall MD process, thus causing the unit water price reduction. The techno-economic analysis of impact of waste heat integration to the solar powered-heat recovered (SP-HR) DCMD process in this study demonstrated an encouraging perspective of DCMD application for water recovery which is demonstrated in Figure 9. For a 100 m^3/day capacity solar-powered and heat-recovered DCMD plant,10%, 30%, and 50% waste heat integration from the industry were considered. The water price was reduced by 7.4%, 22.2%, and 38.5%, respectively, from \$1.35/m^3 to \$1.25/m^3, \$1.05/m^3, and \$0.83/m^3 due to the integration of 10%, 30%, and 50% waste heat to the SP-HR DCMD process. The overall of reduction of water price from a stand-alone DCMD process to a 50% waste-heat integrated SP-HR DCMD process was 64.5%, from \$2.34/m^3 to \$0.83/m^3 that provides a tremendous possibility for the further investigation and implementation of the emerging DCMD for water reclamation from other industrial application. The result from this study indicated that the water price of waste heat recovery system was lower than that of the solar collector. However, several factors need to be confirmed, like, the cost and efficiency of the waste heat recovery process that is related to the process design and affects the water price significantly, location and capacity of the plant that may hinder the waste heat recovery utilization etc. However, the hot wastewater of the brewery industry as well as the biogas generated from the pre-treatment (membrane bioreactor), can potentially be a source of waste heat within the brewery industry. Thus, it is imperative to cautiously consider the alternate energy sources and their utilization for membrane distillation system.

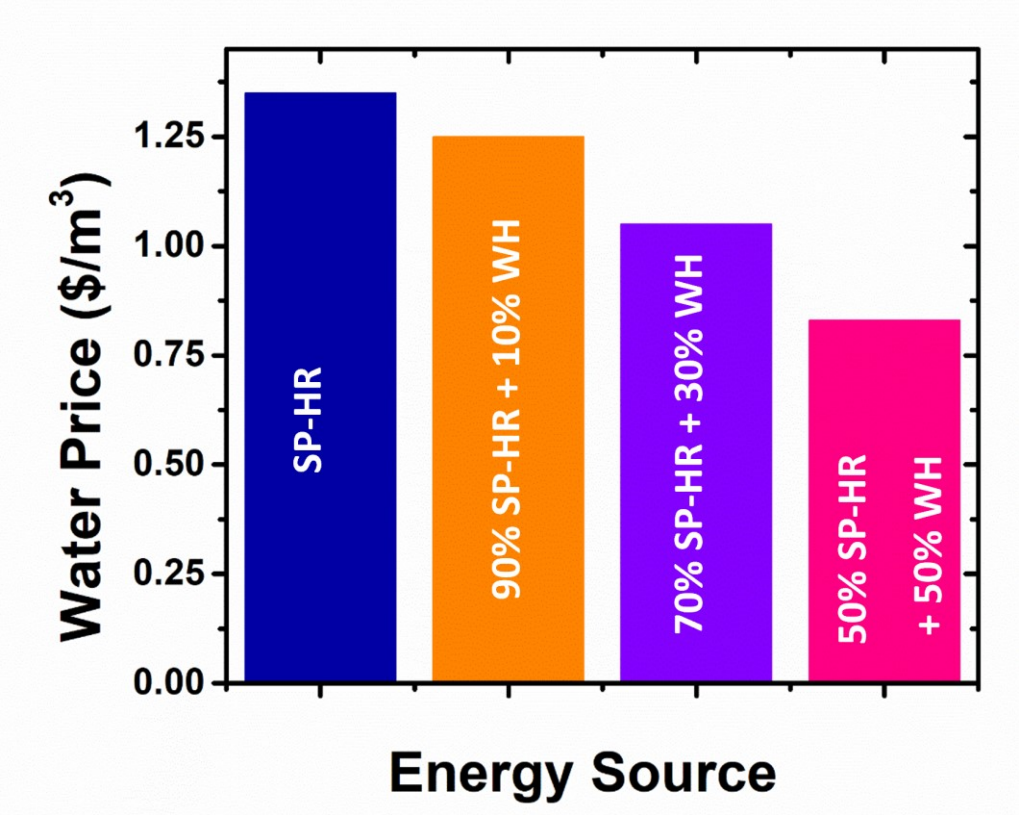

Figure 5.9: Change in water price with varying waste heat recovery through application of direct contact membrane distillation (DCMD) system from pre-treated brewery wastewater with a solar powered and heat recovered (SP-HR) DCMD for 100 m^3/day plant capacity. The unit water price for a solar powered and heat recovered (SP-HR) DCMD follows a decreasing trend of unit water price with an increase in waste heat recovery. Addition of 10%, 30%, and 50% waste heat from the industry results in 7.4%, 22.2%, and 38.5% reduction in unit water price from \$1.35/m^3.

5.4 Conclusions

This study analyzed the techno-economic aspect of a direct contact membrane distillation for water recovery from a pre-treated brewery wastewater effluent. At first, an economic analysis of a 100 m^3/day capacity stand-alone DCMD plant was conducted that revealed that thermal energy contributes to a major portion (nearly 58%) of the total cost of the system. However, the reasonable unit water price \$2.34/m^3 was obtained due to use of moderate hot feed temperature (55°C) as well as the prior pre-treatment of the water. As alternate energy sources integrated with DCMD are a promising feature for its application, a DCMD with a heat recovery unit within the system as well as a DCMD with a solar powered and heat-recovered within the system were further studied for a plant capacity of 100 m^3/day. These studies observed 17.5% and 42% reductions of costs from \$2.34/m^3 for a heat recovered, and a solar-powered and heat-recovered DCMD application,

respectively, from a stand-alone DCMD which encourages the utilization of alternate energy sources as a source of thermal energy for DCMD implementation. Though thermal energy cost was still a major contributor (nearly 51%) for the heat recovered system with a 3% heat exchanger cost, for a solar-powered and heat-recovered DCMD, the major costs was associated with the solar collectors which was nearly 82% of the total cost. The enhancement of the efficiency of the solar collector will further improve the economics of solar-powered DCMD. Overall, the cost of the DCMD application depends on various factors. However, the source of energy is one major factor that can result in significant improvement in the cost of DCMD application. Integration of alternate energy sources, like solar power and waste heat from the industries can cause substantial reduction in the water price making MD application more promising and sustainable. From a stand-alone DCMD process to a 50% waste-heat integrated SP-HR DCMD process, nearly 64.5% of the water price reduction occurred. This provides a great prospect for the researcher for future study and application of the evolving DCMD for water recovery from industrial wastewater effluents. The water recovery is another major factor for industrial applications of MD. High recovery is usually associated with the adequate pre-treatment of the wastewater effluent which also causes less membrane fouling and more membrane life. Low recovery causes an increase in unit water price. This study concluded that practical and optimal application of DCMD can be promising through integration of alternate energy sources as well as using pre-treated wastewater effluent for high recovery.

Considering the future prospect of MD application for water reclamation, pilot application of membrane distillation needs to be conducted for long term assessment. Further developments in the technological aspects, like improved energy sources, advance membrane materials, and modules would be necessary. Also, with more established, commercial, and mass production of MD membranes and modules through dedicated industries, it will be more cost effective. Hence, it will lead towards a sustainable, and economically feasible application of DCMD for water reclamation from industries.

Appendix A3

The MD configuration with heat recovery within the system is shown in Figure A3.1 and the schematic of a DCMD with industrial waste heat integration in addition to solar collector and heat recovery within the system is shown in Figure A3.2.

Acknowledgement

Nawrin Anwar gratefully acknowledges the encouraging support of Fonds de Recherche du Québec-Nature et technologies (FRQNT) and Alexander Graham Bell Canada Graduate Scholarship (CGSD) from the Natural Sciences and Engineering Research Council of Canada (NSERC) for doctoral studies.

Chapter 6: Conclusions and future work

6.1 Conclusions and contributions

Our study concluded that practical and optimal application of DCMD can be promising through integration of alternate energy sources as well as using pre-treated wastewater effluent for high recovery from high strength brewery wastewater. This study identifies the feasible membrane separation process membrane distillation (DCMD) by comparing it with already established reverse osmosis and nanofiltration. The optimal condition for DCMD application along with ensuring the economic feasibility of its application is also recognized. High quality product water was reclaimed through DCMD application without the presence of organics and inorganics, including calcium, sodium, magnesium ions. Hence, prior to consumption, this water will require disinfection and mineralization to achieve drinking water quality standard. This research provides an impetus for pilot scale application of water reclamation application of MBR treated brewery wastewater. The conclusion and contribution of this study can be summarized through three different aspects: (i) identification of effective membrane separation process for water reclamation from MBR treated brewery wastewater effluent, (ii) optimizing the process through recognizing the ideal commercial membrane material, pore size, hot feed temperature as well as feed load for application, and (iii) assessing the economic viability of the DCMD for water reclamation as a stand-alone process as well as with alternate energy sources.

(i) This research identified membrane distillation as an effective membrane separation process with the potential to be integrated with a membrane bioreactor to treat brewery wastewater effluent. While comparing the water reclamation potential with pressure-based membrane separation processes, MD exhibited superior performance with low flux decline, considerably high recovery (~ 86% with MD compared to 12% and 16% with RO and NF, respectively), and less compact reversible membrane fouling during water reclamation from membrane bioreactor treated brewery wastewater effluent.

(ii) Furthermore, the PVDF membrane with 0.45 μm pore size was recognized as an ideal commercially available membrane for water reclamation application. Despite high initial permeate

flux, PTFE membranes were more prone to fouling due to its enhanced hydrophobicity which eventually resulted in low recovery and high flux drop. A moderate temperature of 55°C was detected as optimal hot feed temperature for this specific application. Sequential cleaning of PVDF membrane with NaOH-HCl-DI water was found to be effective, even in a harsh environment (extensive membrane fouling) with enhanced hot feed temperature and high strength wastewater.

(iii) Finally, an economic evaluation of a 100 m^3/day capacity stand-alone DCMD plant identified that thermal energy contributes to major portion (nearly 58%) of the total cost of the system during water reclamation application. However, the reasonable unit water price of \$2.34/m^3 was obtained due to the use of pre-treated wastewater effluent as well as utilization of moderate hot feed temperature (55°C). This research also identified that alternate energy source integration with DCMD can considerably lower the unit water price and thus can make the process application promising and sustainable. Nearly a 42% cost reduction from stand-alone DCMD was observed with the same plant capacity with a solar powered and heat recovered system which is encouraging for DCMD application through the utilization of alternate energy sources as a source of thermal energy. Moreover, 50% waste-heat integration along with a solar powered and heat recovered DCMD process showed a substantial (64.5%) decline of unit water price compared to a stand-alone DCMD process.

6.2 Future work

Membrane distillation is a promising wastewater reclamation process and combining it in downstream of already established MBR techniques can be effective for water recovery and reuse within the brewery facility. This research provides a great prospect for the researcher for future study and application of the evolving DCMD for water recovery from industrial wastewater effluents. The following research can be conducted in the future:

- Implementing the optimal conditions for various membrane distillation configurations to identify the best configuration for this specific wastewater effluent.
- Examining the MD retentate to assess the possible nutrient recovery (nitrogen and phosphorus) can also be explored for agricultural utilization.

- Energy requirements need to be compared with varying conditions for such application to detect the ideal configuration in terms of both performance, fouling, energy, and economy.
- The enhancement of the efficiency of the solar collector will further improve the economics of solar-powered DCMD.
- Systematic, long-term, pilot-scale evaluation of ideal MD configurations is required to ensure robust operational processes in water reclamation from MBR treated brewery wastewater effluent.
- MD can also be studied for other wastewater effluents for water reclamation application, like textile wastewater where waste heat integration has the potential to be utilized from the textile industries.

6.3 Publications

The already published journal/book chapters/ conference papers from September 2016 to the present are given below along with manuscripts in preparation:

Journal publication

- **Anwar, N.**, Rahaman, M.S. "Membrane desalination processes for water recovery from pre-treated brewery wastewater: Performance and fouling", Separation and Purification Technology, Volume 252, December 2020.
- Choudhury, M.R., ***Anwar, N.**, Jassby, D., Rahaman, M.S. "Fouling and wetting in the membrane distillation driven wastewater treatment and reclamation process – A review", Advances in Colloid and Interface Science, Volume 269, July 2019, 370-339. (* M.R.C. and N.A. contributed equally to this work).
- Rajagopal, R., Choudhury, M. R., **Anwar**, **N.**, Goyette,B., Rahaman, M. S. "Influence of Pre-Hydrolysis on Sewage Treatment in an Up-Flow Anaerobic Sludge Blanket (UASB) Reactor: A Review", Water 2019, Volume 11, Issue 2.
- Sultana, S., Choudhury, M. R., Bakr, A. R., **Anwar, N.**, Rahaman, M. S. "Effectiveness of Electro-Oxidation and Electro-Fenton Processes in Removal of Organic Matter from High Strength Brewery Wastewater", Journal of Applied Electrochemistry, March 2018.
- Omi, F. R., Choudhury, M. R., **Anwar, N.**, Bakr, A. R., M. S. Rahaman, "Highly Conductive Ultrafiltration Membrane via Vacuum Filtration Assisted Layer-by-Layer

Deposition of Functionalized Carbon Nanotubes." Industrial & Engineering Chemistry Research, DOI: 10.1021/acs.iecr.7b00847, May 2017.

Book chapter publication

- **Anwar, N.**, Yang, L., Ma, W., Usman, M.S., Rahaman, M. S. (2020) "Biofouling in RO desalination membranes". In: Saji V., Meroufel A., Sorour A. (eds) Corrosion and Fouling Control in Desalination Industry (pp. 269-283). Springer, Cham.
- Touati, K., Usman, M.S., Chen, T., **Anwar, N.**, Choudhury, M.R., M.S., Rahaman, M. S. (2020) "Inorganic scaling in desalination systems", In: Saji V., Meroufel A., Sorour A. (eds) Corrosion and Fouling Control in Desalination Industry (pp. 251-268). Springer, Cham.

Conference proceedings

- **Anwar, N.**; Choudhury, M.R., Rahaman, M.S. "Membrane distillation (MD) and reverse osmosis (RO) processes for water recovery from pre-treated high strength brewery wastewater", North American Membrane Society (NAMS) Meeting, May 11-15, 2019, Pittsburgh, PA, USA
- **Anwar, N.**, Choudhury, M.R., Chen, T., Rahaman, M.S. (2018) "Water Recovery from High Strength Brewery Wastewater via a Membrane Distillation Process" 256th ACS National Meeting, Boston, MA, USA, August 19-23, 2018.
- Chen, T., Ma, W., **Anwar, N.**, Adhikary, S., Rahaman, M.S. Highly hydrophobic, electrospun, reduced graphene oxide (rGO)/PVDF-HFP membranes for use in membrane distillation", North American Membrane Society (NAMS) Meeting, June 9-13, 2018, Lexington, KY, USA.
- **Anwar, N**, Sultana, S., Choudhury, M.R., Chen, T., Rahaman, M.S (2018) "Water Recovery from High Strength Brewery Wastewater Using Integrated Electro Chemical and Reverse Osmosis Process" CSCE Annual Conference and Annual General Meeting, Fredericton, NB, June 13-June 16, 2018.
- Choudhury. M.R., **Anwar, N.**, Rajagopal, R., Rahaman, M.S. "Application of electrochemical advanced oxidation processes (EAOPs) for treatment of concentrate from psychrophilic anaerobic digester units", CSCE Annual Conference, June 13 - June 16, 2018, Fredericton, NB, Canada.

- Sultana, S., **Anwar, N**, Okro, O., and Rahaman, M.S (2017) "Evaluation of Electrocoagulation as a method of Pretreatment for Highly Concentrated Brewery Wastewater" CSCE Annual Conference and Annual General Meeting, Vancouver, BC, May 31-June 3, 2017.

Manuscript in preparation

- "Direct contact membrane distillation (DCMD) application for water recovery from pre-treated brewery wastewater effluent: A parametric study."
- "Techno-economic evaluation of DCMD for water recovery from pre-treated brewery wastewater effluent."

References

[1] L.S. Tam, T.W. Tang, G.N. Lau, K.R. Sharma, G.H. Chen, A pilot study for wastewater reclamation and reuse with MBR/RO and MF/RO systems, Desalination. 202 (2007) 106–113. doi:10.1016/j.desal.2005.12.045.

[2] M. Gündoğdu, Y.A. Jarma, N. Kabay, T. Pek, M. Yüksel, Integration of MBR with NF/RO processes for industrial wastewater reclamation and water reuse-effect of membrane type on product water quality, J. Water Process Eng. 29 (2019) 100574. doi:10.1016/j.jwpe.2018.02.009.

[3] M.F. Tay, C. Liu, E.R. Cornelissen, B. Wu, T.H. Chong, The feasibility of nanofiltration membrane bioreactor (NF-MBR)+reverse osmosis (RO) process for water reclamation: Comparison with ultrafiltration membrane bioreactor (UF-MBR)+RO process, Water Res. 129 (2018) 180–189. doi:10.1016/j.watres.2017.11.013.

[4] K. Chon, J. Cho, H.K. Shon, Fouling characteristics of a membrane bioreactor and nanofiltration hybrid system for municipal wastewater reclamation, Bioresour. Technol. 130 (2013) 239–247. doi:10.1016/j.biortech.2012.12.007.

[5] K. Chon, S. Sarp, S. Lee, J.H. Lee, J.A. Lopez-Ramirez, J. Cho, Evaluation of a membrane bioreactor and nanofiltration for municipal wastewater reclamation: Trace contaminant control and fouling mitigation, Desalination. 272 (2011) 128–134. doi:10.1016/j.desal.2011.01.002.

[6] M. Gündoğdu, N. Kabay, N. Yiğit, M. Kitiş, T. Pek, M. Yüksel, Effect of concentrate recirculation on the product water quality of integrated MBR – NF process for wastewater reclamation and industrial reuse, J. Water Process Eng. 29 (2019) 100485. doi:10.1016/j.jwpe.2017.08.023.

[7] A.A. Alturki, N. Tadkaew, J.A. McDonald, S.J. Khan, W.E. Price, L.D. Nghiem, Combining MBR and NF/RO membrane filtration for the removal of trace organics in indirect potable water reuse applications, J. Memb. Sci. 365 (2010) 206–215. doi:10.1016/j.memsci.2010.09.008.

[8] X. Zhu, A. Dudchenko, X. Gu, D. Jassby, Surfactant-stabilized oil separation from water using ultrafiltration and nanofiltration, J. Memb. Sci. 529 (2017) 159–169. doi:10.1016/j.memsci.2017.02.004.

[9] Y. Wu, Y. Kang, L. Zhang, D. Qu, X. Cheng, L. Feng, Performance and fouling mechanism of direct contact membrane distillation (DCMD) treating fermentation wastewater with high organic concentrations, J. Environ. Sci. (China). 65 (2018) 253–261. doi:10.1016/j.jes.2017.01.015.

[10] G. Naidu, S. Jeong, Y. Choi, S. Vigneswaran, Membrane distillation for wastewater reverse osmosis concentrate treatment with water reuse potential, J. Memb. Sci. 524 (2017) 565–575. doi:10.1016/j.memsci.2016.11.068.

[11] S. Rodriguez-Mozaz, M. Ricart, M. Köck-Schulmeyer, H. Guasch, C. Bonnineau, L. Proia, M.L. de Alda, S. Sabater, D. Barceló, Pharmaceuticals and pesticides in reclaimed water: Efficiency assessment of a microfiltration-reverse osmosis (MF-RO) pilot plant, J. Hazard. Mater. 282 (2015) 165–173. doi:10.1016/j.jhazmat.2014.09.015.

[12] A. Alkhudhiri, N. Darwish, N. Hilal, Membrane distillation: A comprehensive review, Desalination. 287 (2012) 2–18. doi:10.1016/j.desal.2011.08.027.

[13] D.M. Warsinger, J. Swaminathan, E. Guillen-Burrieza, H.A. Arafat, J.H. Lienhard V, Scaling and fouling in membrane distillation for desalination applications: A review, Desalination. 356 (2015) 294–313. doi:10.1016/j.desal.2014.06.031.

[14] L.D. Tijing, Y.C. Woo, J.S. Choi, S. Lee, S.H. Kim, H.K. Shon, Fouling and its control in membrane distillation-A review, J. Memb. Sci. 475 (2015) 215–244. doi:10.1016/j.memsci.2014.09.042.

[15] D.M. Warsinger, K.H. Mistry, K.G. Nayar, H.W. Chung, J.H.V. Lienhard, Entropy generation of desalination powered by variable temperature waste heat, Entropy. 17 (2015) 7530–7566. doi:10.3390/e17117530.

[16] D.M. Warsinger, J. Swaminathan, E. Guillen-Burrieza, H.A. Arafat, J.H. Lienhard V, Scaling and fouling in membrane distillation for desalination applications: A review, Desalination. 356 (2015) 294–313. doi:10.1016/j.desal.2014.06.031.

[17] G.P. Thiel, E.W. Tow, L.D. Banchik, H.W. Chung, J.H. Lienhard V, Energy consumption in desalinating produced water from shale oil and gas extraction, Desalination. 366 (2015) 94–112. doi:10.1016/j.desal.2014.12.038.
[18] L. Fillaudeau, P. Blanpain-Avet, G. Daufin, Water, wastewater and waste management in brewing industries, J. Clean. Prod. 14 (2006) 463–471. doi:10.1016/j.jclepro.2005.01.002.
[19] B. Sinha, Beer Market by Type (Lager, Ale, Stout & Porter, Malt, and Others), Category (Popular-Priced, Premium, and Super Premium), Packaging (Glass, PET Bottle, Metal Can, and Others), and Production (Macro-brewery, Micro-brewery, Craft Brewery, and Others) -, 2018. www.alliedmarketresearch.com.
[20] G. Hermis, Brewing Up Benefits: The Economic Footprint of Canada's Beer Economy - January 2018, 2018.
[21] No Title, (n.d.). https://industry.beercanada.com/national-overview?fbclid=IwAR0QTINPjoGQfgBn1Uyo6_zDXUQbwd_4Q7AxsApt0v69ZFanacwsPGje9ZU, (n.d.).
[22] G.S. Simate, J. Cluett, S.E. Iyuke, E.T. Musapatika, S. Ndlovu, L.F. Walubita, A.E. Alvarez, The treatment of brewery wastewater for reuse: State of the art, Desalination. 273 (2011) 235–247. doi:10.1016/j.desal.2011.02.035.
[23] A. Doubla, S. Laminsi, S. Nzali, E. Njoyim, J. Kamsu-Kom, J.L. Brisset, Organic pollutants abatement and biodecontamination of brewery effluents by a non-thermal quenched plasma at atmospheric pressure, Chemosphere. 69 (2007) 332–337. doi:10.1016/j.chemosphere.2007.04.007.
[24] L. Braeken, B. Van Der Bruggen, C. Vandecasteele, Regeneration of brewery waste water using nanofiltration, Water Res. 38 (2004) 3075–3082. doi:10.1016/j.watres.2004.03.028.
[25] K. Kanagachandran, R. Jayaratne, Utilization potential of brewery waste water sludge as an organic fertilizer, J. Inst. Brew. 112 (2006) 92–96. doi:10.1002/j.2050-0416.2006.tb00236.x.
[26] No Title, (n.d.). https://www.growlermag.com/the-thirsty-business-of-beer-how-breweries-are-confronting-the-industrys-water-problem/.
[27] M. Gryta, K. Karakulski, A.W. Morawski, Purification of oily wastewater by hybrid UF/MD, Water Res. 35 (2001) 3665–3669. doi:10.1016/S0043-1354(01)00083-5.
[28] K. Chon, H. KyongShon, J. Cho, Membrane bioreactor and nanofiltration hybrid system for reclamation of municipal wastewater: Removal of nutrients, organic matter and micropollutants, Bioresour. Technol. 122 (2012) 181–188. doi:10.1016/j.biortech.2012.04.048.
[29] M.C. Hacıfazlıoğlu, H.R. Tomasini, N. Kabay, L. Bertin, T. Pek, M. Kitiş, N. Yiğit, M. Yüksel, Effect of pressure on desalination of MBR effluents with high salinity by using NF and RO processes for reuse in irrigation, J. Water Process Eng. 25 (2018) 22–27. doi:10.1016/j.jwpe.2018.06.001.
[30] I. Parlar, M. Hacıfazlıoğlu, N. Kabay, T. Pek, M. Yüksel, Performance comparison of reverse osmosis (RO) with integrated nanofiltration (NF) and reverse osmosis process for desalination of MBR effluent, J. Water Process Eng. 29 (2019) 100640. doi:10.1016/j.jwpe.2018.06.002.
[31] L. Chen, C. Liu, C. Cao, L. Zhu, Treatment of anaerobic membrane bioreactor (AnMBR) effluent using direct contact membrane distillation, Desalin. Water Treat. 65 (2017) 89–97. doi:10.5004/dwt.2017.20407.
[32] K. Valta, T. Kosanovic, D. Malamis, M. Moustakas, Konstantinos Loizidou, Overview of water usage and wastewater management in the food and beverage industry, Desalin. Water Treat. 53 (2014) 3335–3347. doi:https://doi.org/10.1080/19443994.2014.934100.
[33] Z. Zeng, J. Liu, H.H.G. Savenije, A simple approach to assess water scarcity integrating water quantity and quality, Ecol. Indic. 34 (2013) 441–449. doi:10.1016/j.ecolind.2013.06.012.
[34] L.A. Hoover, W.A. Phillip, A. Tiraferri, N.Y. Yip, M. Elimelech, Forward with osmosis: Emerging applications for greater sustainability, Environ. Sci. Technol. 45 (2011). doi:10.1021/es202576h.
[35] M.A. Shannon, P.W. Bohn, M. Elimelech, J.G. Georgiadis, B.J. Mariñas, A.M. Mayes, Science and technology for water purification in the coming decades, Nature. 452 (2008) 301–310. doi:10.1038/nature06599.

[36] A. Alkhudhiri, N. Darwish, N. Hilal, Membrane distillation: A comprehensive review, Desalination. 287 (2012) 2–18. doi:10.1016/j.desal.2011.08.027.
[37] M. Khayet, T. Matsuura, J.I. Mengual, M. Qtaishat, Design of novel direct contact membrane distillation membranes, Desalination. 192 (2006) 105–111. doi:10.1016/j.desal.2005.06.047.
[38] K.W. Lawson, D.R. Lloyd, Membrane distillation, J. Memb. Sci. 124 (1997) 1–25. doi:10.1016/S0376-7388(96)00236-0.
[39] E. Drioli, A. Ali, F. Macedonio, Membrane distillation: Recent developments and perspectives, Desalination. 356 (2015) 56–84. doi:10.1016/j.desal.2014.10.028.
[40] L.D. Tijing, Y.C. Woo, J.S. Choi, S. Lee, S.H. Kim, H.K. Shon, Fouling and its control in membrane distillation-A review, J. Memb. Sci. 475 (2015) 215–244. doi:10.1016/j.memsci.2014.09.042.
[41] Y. Chen, Z. Wang, K. Jennings, S. Lin, Probing Pore Wetting in Membrane Distillation using Impedance: Early Detection and Mechanism of Surfactant-induced Wetting, Environ. Sci. Technol. Lett. (2017) acs.estlett.7b00372. doi:10.1021/acs.estlett.7b00372.
[42] E. Curcio, X. Ji, G. Di Profio, A.O. Sulaiman, E. Fontananova, E. Drioli, Membrane distillation operated at high seawater concentration factors: Role of the membrane on CaCO3 scaling in presence of humic acid, J. Memb. Sci. 346 (2010) 263–269. doi:10.1016/j.memsci.2009.09.044.
[43] P. Wang, M.M. Teoh, T.S. Chung, Morphological architecture of dual-layer hollow fiber for membrane distillation with higher desalination performance, Water Res. 45 (2011) 5489–5500. doi:10.1016/j.watres.2011.08.012.
[44] X. Yang, R. Wang, L. Shi, A.G. Fane, M. Debowski, Performance improvement of PVDF hollow fiber-based membrane distillation process, J. Memb. Sci. 369 (2011) 437–447. doi:10.1016/j.memsci.2010.12.020.
[45] M. Khayet, T. Matsuura, Preparation and Characterization of Polyvinylidene Fluoride Membranes for Membrane Distillation, Ind. Eng. Chem. Res. 40 (2001) 5710–5718. doi:10.1021/ie010553y.
[46] S. Al-Obaidani, E. Curcio, F. Macedonio, G. Di Profio, H. Al-Hinai, E. Drioli, Potential of membrane distillation in seawater desalination: Thermal efficiency, sensitivity study and cost estimation, J. Memb. Sci. 323 (2008) 85–98. doi:10.1016/j.memsci.2008.06.006.
[47] A. Razmjou, E. Arifin, G. Dong, J. Mansouri, V. Chen, Superhydrophobic modification of TiO 2 nanocomposite PVDF membranes for applications in membrane distillation, J. Memb. Sci. 415–416 (2012) 850–863. doi:10.1016/j.memsci.2012.06.004.
[48] J. Blanco Gálvez, L. García-Rodríguez, I. Martín-Mateos, Seawater desalination by an innovative solar-powered membrane distillation system: the MEDESOL project, Desalination. 246 (2009) 567–576. doi:10.1016/j.desal.2008.12.005.
[49] H. Kurokawa, T. Sawa, Heat recovery characteristics of membrane distillation, Heat Transf. Res. 25 (1996) 135–150.
[50] H.W. Chung, J. Swaminathan, D.M. Warsinger, J.H. Lienhard V, Multistage vacuum membrane distillation (MSVMD) systems for high salinity applications, J. Memb. Sci. 497 (2016) 128–141. doi:10.1016/j.memsci.2015.09.009.
[51] Y. Liao, R. Wang, A.G. Fane, Engineering superhydrophobic surface on poly(vinylidene fluoride) nanofiber membranes for direct contact membrane distillation, J. Memb. Sci. 440 (2013) 77–87. doi:10.1016/j.memsci.2013.04.006.
[52] P.D. Dongare, A. Alabastri, S. Pedersen, K.R. Zodrow, N.J. Hogan, O. Neumann, J. Wu, T. Wang, A. Deshmukh, M. Elimelech, Q. Li, P. Nordlander, N.J. Halas, Nanophotonics-enabled solar membrane distillation for off-grid water purification, Proc. Natl. Acad. Sci. 114 (2017) 6936–6941. doi:10.1073/pnas.1701835114.
[53] D.B. Gingerich, M.S. Mauter, Quantity, Quality, and Availability of Waste Heat from United States Thermal Power Generation, Environ. Sci. Technol. 49 (2015) 8297–8306. doi:10.1021/es5060989.
[54] E. Curcio, E. Drioli, Membrane distillation and related operations - A review, Sep. Purif. Rev. 34 (2005) 35–86. doi:10.1081/SPM-200054951.
[55] K.A. Salls, D. Won, E.P. Kolodziej, A.E. Childress, S.R. Hiibel, Evaluation of semi-volatile

contaminant transport in a novel, gas-tight direct contact membrane distillation system, Desalination. 427 (2018) 35–41. doi:10.1016/j.desal.2017.11.001.
[56] A. Deshmukh, C. Boo, V. Karanikola, S. Lin, A.P. Straub, T. Tong, D.M. Warsinger, M. Elimelech, Membrane distillation at the water-energy nexus: Limits, opportunities, and challenges, Energy Environ. Sci. 11 (2018) 1177–1196. doi:10.1039/c8ee00291f.
[57] S. Lin, N.Y. Yip, M. Elimelech, Direct contact membrane distillation with heat recovery: Thermodynamic insights from module scale modeling, J. Memb. Sci. 453 (2014) 498–515. doi:10.1016/j.memsci.2013.11.016.
[58] A. V. Dudchenko, C. Chen, A. Cardenas, J. Rolf, D. Jassby, Frequency-dependent stability of CNT Joule heaters in ionizable media and desalination processes, Nat. Nanotechnol. 12 (2017) 557–563. doi:10.1038/nnano.2017.102.
[59] E.K. Summers, J.H. Lienhard, Experimental study of thermal performance in air gap membrane distillation systems, including the direct solar heating of membranes, Desalination. 330 (2013) 100–111. doi:10.1016/j.desal.2013.09.023.
[60] M.R. Qtaishat, T. Matsuura, Modelling of pore wetting in membrane distillation compared with pervaporation, Elsevier Ltd, 2015. doi:10.1016/B978-1-78242-246-4.00013-1.
[61] E. Guillen-Burrieza, M.O. Mavukkandy, M.R. Bilad, H.A. Arafat, Understanding wetting phenomena in membrane distillation and how operational parameters can affect it, J. Memb. Sci. 515 (2016) 163–174. doi:10.1016/j.memsci.2016.05.051.
[62] Y. Liao, R. Wang, A.G. Fane, Engineering superhydrophobic surface on poly(vinylidene fluoride) nanofiber membranes for direct contact membrane distillation, J. Memb. Sci. 440 (2013) 77–87. doi:10.1016/j.memsci.2013.04.006.
[63] M. Gryta, Long-term performance of membrane distillation process, J. Memb. Sci. 265 (2005) 153–159. doi:10.1016/j.memsci.2005.04.049.
[64] M.S. El-Bourawi, Z. Ding, R. Ma, M. Khayet, A framework for better understanding membrane distillation separation process, J. Memb. Sci. 285 (2006) 4–29. doi:10.1016/j.memsci.2006.08.002.
[65] A.M. Alklaibi, The potential of membrane distillation as a stand-alone desalination process, Desalination. 223 (2008) 375–385. doi:10.1016/j.desal.2007.01.201.
[66] K.Y. Wang, S.W. Foo, T. Chung, Mixed Matrix PVDF Hollow Fiber Membranes with Nanoscale Pores for Desalination through Direct Contact Membrane Distillation Mixed Matrix PVDF Hollow Fiber Membranes with Nanoscale Pores for Desalination through Direct Contact Membrane Distillation, (2009) 4474–4483. doi:10.1021/ie8009704.
[67] J.-P. Mericq, S. Laborie, C. Cabassud, Vacuum membrane distillation for an integrated seawater desalination process, Desalin. Water Treat. 9 (2009) 287–296. doi:10.5004/dwt.2009.862.
[68] L. Song, Z. Ma, X. Liao, P.B. Kosaraju, J.R. Irish, K.K. Sirkar, Pilot plant studies of novel membranes and devices for direct contact membrane distillation-based desalination, J. Memb. Sci. 323 (2008) 257–270. doi:10.1016/j.memsci.2008.05.079.
[69] A. Alkhudhiri, N. Hilal, Air gap membrane distillation: A detailed study of high saline solution, Desalination. 403 (2017) 179–186. doi:10.1016/j.desal.2016.07.046.
[70] F.A. Banat, J. Simandl, Desalination by Membrane Distillation: A Parametric Study, Sep. Sci. Technol. 33 (1998) 201–226. doi:10.1080/01496399808544764.
[71] G.W. Meindersma, C.M. Guijt, A.B. de Haan, Desalination and water recycling by air gap membrane distillation, Desalination. 187 (2006) 291–301. doi:10.1016/j.desal.2005.04.088.
[72] J. Ge, Y. Peng, Z. Li, P. Chen, S. Wang, Membrane fouling and wetting in a DCMD process for RO brine concentration, Desalination. 344 (2014) 97–107. doi:10.1016/j.desal.2014.03.017.
[73] S.T. Hsu, K.T. Cheng, J.S. Chiou, Seawater desalination by direct contact membrane distillation, Desalination. 143 (2002) 279–287. doi:10.1016/S0011-9164(02)00266-7.
[74] F. He, K.K. Sirkar, J. Gilron, Studies on scaling of membranes in desalination by direct contact membrane distillation: CaCO3 and mixed CaCO3/CaSO4 systems, Chem. Eng. Sci. 64 (2009) 1844–1859. doi:10.1016/j.ces.2008.12.036.

[75] H. Attia, S. Alexander, C.J. Wright, N. Hilal, Superhydrophobic electrospun membrane for heavy metals removal by air gap membrane distillation (AGMD), Desalination. 420 (2017) 318–329. doi:10.1016/j.desal.2017.07.022.
[76] H. Attia, M.S. Osman, D.J. Johnson, C. Wright, N. Hilal, Modelling of air gap membrane distillation and its application in heavy metals removal, Desalination. 424 (2017) 27–36. doi:10.1016/j.desal.2017.09.027.
[77] H. Attia, D.J. Johnson, C.J. Wright, N. Hilal, Comparison between dual-layer (superhydrophobic–hydrophobic) and single superhydrophobic layer electrospun membranes for heavy metal recovery by air-gap membrane distillation, Desalination. 439 (2018) 31–45. doi:10.1016/j.desal.2018.04.003.
[78] D.L. Shaffer, L.H. Arias Chavez, M. Ben-Sasson, S. Romero-Vargas Castrillón, N.Y. Yip, M. Elimelech, Desalination and reuse of high-salinity shale gas produced water: Drivers, technologies, and future directions, Environ. Sci. Technol. 47 (2013) 9569–9583. doi:10.1021/es401966e.
[79] X. Du, Z. Zhang, K.H. Carlson, J. Lee, T. Tong, Membrane fouling and reusability in membrane distillation of shale oil and gas produced water: Effects of membrane surface wettability, J. Memb. Sci. 567 (2018) 199–208. doi:10.1016/j.memsci.2018.09.036.
[80] H. Cho, Y. Shin, Y. Choi, S. Lee, J. Sohn, D. Kim, J. Koo, Fouling behaviors of membrane distillation (MD) in shale gas wastewater treatment, Desalin. Water Treat. 61 (2017) 5004. doi:10.5004/dwt.2017.0070.
[81] C. Boo, J. Lee, M. Elimelech, Omniphobic Polyvinylidene Fluoride (PVDF) Membrane for Desalination of Shale Gas Produced Water by Membrane Distillation, Environ. Sci. Technol. 50 (2016) 12275–12282. doi:10.1021/acs.est.6b03882.
[82] F. Suárez, S.W. Tyler, A.E. Childress, A theoretical study of a direct contact membrane distillation system coupled to a salt-gradient solar pond for terminal lakes reclamation, Water Res. 44 (2010) 4601–4615. doi:10.1016/j.watres.2010.05.050.
[83] R.D. Gustafson, S.R. Hiibel, A.E. Childress, Membrane distillation driven by intermittent and variable-temperature waste heat: System arrangements for water production and heat storage, Desalination. 448 (2018) 49–59. doi:10.1002/1098-1071(2000)11:6<380::AID-HC3>3.0.CO;2-U.
[84] F. Suárez, J.A. Ruskowitz, S.W. Tyler, A.E. Childress, Renewable water: Direct contact membrane distillation coupled with solar ponds, Appl. Energy. 158 (2015) 532–539. doi:10.1016/j.apenergy.2015.08.110.
[85] H.C. Duong, P. Cooper, B. Nelemans, T.Y. Cath, L.D. Nghiem, Evaluating energy consumption of air gap membrane distillation for seawater desalination at pilot scale level, Sep. Purif. Technol. 166 (2016) 55–62. doi:10.1016/j.seppur.2016.04.014.
[86] N. Dow, J. Villalobos García, L. Niadoo, N. Milne, J. Zhang, S. Gray, M. Duke, Demonstration of membrane distillation on textile waste water: assessment of long term performance, membrane cleaning and waste heat integration, Environ. Sci. Water Res. Technol. 3 (2017) 433–449. doi:10.1039/C6EW00290K.
[87] F. Li, J. Huang, Q. Xia, M. Lou, B. Yang, Q. Tian, Y. Liu, Direct contact membrane distillation for the treatment of industrial dyeing wastewater and characteristic pollutants, Sep. Purif. Technol. 195 (2018) 83–91. doi:10.1016/j.seppur.2017.11.058.
[88] N.M. Mokhtar, W.J. Lau, A.F. Ismail, S. Kartohardjono, S.O. Lai, H.C. Teoh, The potential of direct contact membrane distillation for industrial textile wastewater treatment using PVDF-Cloisite 15A nanocomposite membrane, Chem. Eng. Res. Des. 111 (2016) 284–293. doi:10.1016/j.cherd.2016.05.018.
[89] P.J. Lin, M.C. Yang, Y.L. Li, J.H. Chen, Prevention of surfactant wetting with agarose hydrogel layer for direct contact membrane distillation used in dyeing wastewater treatment, J. Memb. Sci. 475 (2015) 511–520. doi:10.1016/j.memsci.2014.11.001.
[90] A. El-Abbassi, A. Hafidi, M.C. García-Payo, M. Khayet, Concentration of olive mill wastewater by membrane distillation for polyphenols recovery, Desalination. 245 (2009) 670–674. doi:10.1016/j.desal.2009.02.035.

[91] A. El-Abbassi, A. Hafidi, M. Khayet, M.C. García-Payo, Integrated direct contact membrane distillation for olive mill wastewater treatment, Desalination. 323 (2013) 31–38. doi:10.1016/j.desal.2012.06.014.
[92] A. Zoungrana, I.H. Zengin, D. Karadag, M. Çakmakci, Treatability of Municipal Wastewater with Direct Contact Membrane Distillation, Sigma J. Eng. Nat. Sci. 8 (2017) 245–254.
[93] D. Lu, Q. Liu, Y. Zhao, H. Liu, J. Ma, Treatment and energy utilization of oily water via integrated ultrafiltration-forward osmosis–membrane distillation (UF-FO-MD) system, J. Memb. Sci. 548 (2018) 275–287. doi:10.1016/j.memsci.2017.11.004.
[94] T. Husnain, R. Riffat, B. Mi, Fouling and long-Term durability of an integrated forward osmosis and membrane distillation system, Water Sci. Technol. 72 (2015) 2000–2005. doi:10.2166/wst.2015.415.
[95] T. Husnain, Y. Liu, R. Riffat, B. Mi, Integration of forward osmosis and membrane distillation for sustainable wastewater reuse, Sep. Purif. Technol. 156 (2015) 424–431. doi:10.1016/j.seppur.2015.10.031.
[96] J. Li, D. Hou, K. Li, Y. Zhang, J. Wang, X. Zhang, Domestic wastewater treatment by forward osmosis-membrane distillation (FO-MD) integrated system, Water Sci. Technol. 77 (2018) 1514–1523. doi:10.2166/wst.2018.031.
[97] W. Luo, H. V. Phan, G. Li, F.I. Hai, W.E. Price, M. Elimelech, L.D. Nghiem, An Osmotic Membrane Bioreactor-Membrane Distillation System for Simultaneous Wastewater Reuse and Seawater Desalination: Performance and Implications, Environ. Sci. Technol. 51 (2017) 14311–14320. doi:10.1021/acs.est.7b02567.
[98] J. Wang, D. Qu, M. Tie, H. Ren, X. Peng, Z. Luan, Effect of coagulation pretreatment on membrane distillation process for desalination of recirculating cooling water, Sep. Purif. Technol. 64 (2008) 108–115. doi:10.1016/j.seppur.2008.07.022.
[99] L. Han, Y.Z. Tan, T. Netke, A.G. Fane, J.W. Chew, Understanding oily wastewater treatment via membrane distillation, J. Memb. Sci. 539 (2017) 284–294. doi:10.1016/j.memsci.2017.06.012.
[100] M. Gryta, K. Karakulski, The application of membrane distillation for the concentration of oil-water emulsions, Desalination. 121 (1999) 23–29. doi:10.1016/S0011-9164(99)00004-1.
[101] H. Liu, J. Wang, Treatment of radioactive wastewater using direct contact membrane distillation, J. Hazard. Mater. 261 (2013) 307–315. doi:10.1016/j.jhazmat.2013.07.045.
[102] G. Zakrzewska-Trznadel, M. Harasimowicz, A.G. Chmielewski, Concentration of radioactive components in liquid low-level radioactive waste by membrane distillation, J. Memb. Sci. 163 (1999) 257–264. doi:10.1016/S0376-7388(99)00171-4.
[103] M. Khayet, Treatment of radioactive wastewater solutions by direct contact membrane distillation using surface modified membranes, Desalination. 321 (2013) 60–66. doi:10.1016/j.desal.2013.02.023.
[104] E.J. Hull, K.R. Zodrow, Acid Rock Drainage Treatment Using Membrane Distillation: Impacts of Chemical-Free Pretreatment on Scale Formation, Pore Wetting, and Product Water Quality, Environ. Sci. Technol. 51 (2017) 11928–11934. doi:10.1021/acs.est.7b02957.
[105] J. Guo, M. Usman, E. Lee, D.Y. Yan, S. Jeong, A. Kyoungjin, M.U. Farid, E. Lee, D.Y. Yan, S. Jeong, A. Kyoungjin AN, Fouling behavior of negatively charged PVDF membrane in membrane distillation for removal of antibiotics from wastewater, J. Memb. Sci. 551 (2018) 12–19. doi:10.1016/j.memsci.2018.01.016.
[106] D. Woldemariam, A. Kullab, U. Fortkamp, J. Magner, H. Royen, A. Martin, Membrane distillation pilot plant trials with pharmaceutical residues and energy demand analysis, Chem. Eng. J. 306 (2016) 471–483. doi:10.1016/j.cej.2016.07.082.
[107] A. Zoungrana, İ.H. Zengin, H. Elcik, B. Özkaya, M. Çakmakci, The treatability of landfill leachate by direct contact membrane distillation and factors influencing the efficiency of the process, Desalin. Water Treat. 71 (2017) 233–243. doi:10.5004/dwt.2017.20494.
[108] Y. Zhou, M. Huang, Q. Deng, T. Cai, Combination and performance of forward osmosis and

membrane distillation (FO-MD) for treatment of high salinity landfill leachate, Desalination. 420 (2017) 99–105. doi:10.1016/j.desal.2017.06.027.
[109] G. Lewandowicz, W. Białas, B. Marczewski, D. Szymanowska, Application of membrane distillation for ethanol recovery during fuel ethanol production, J. Memb. Sci. 375 (2011) 212–219. doi:10.1016/j.memsci.2011.03.045.
[110] R. Thiruvenkatachari, M. Manickam, T.O. Kwon, S. Moon, J.W. Kim, J.W. Kim, Separation of Water and Nitric Acid with Porous Hydrophobic Membrane by Air Gap Membrane Distillation (AGMD), Sep. Sci. Technol. 41 (2006) 3187–3199. doi:10.1080/01496390600854651.
[111] H. Ramlow, R.A.F. Machado, C. Marangoni, Direct contact membrane distillation for textile wastewater treatment: A state of the art review, Water Sci. Technol. 76 (2017) 2565–2579. doi:10.2166/wst.2017.449.
[112] F. Banat, S. Al-Asheh, M. Qtaishat, Treatment of waters colored with methylene blue dye by vacuum membrane distillation, Desalination. 174 (2005) 87–96. doi:10.1016/j.desal.2004.09.004.
[113] C.K. Chiam, R. Sarbatly, Vacuum membrane distillation processes for aqueous solution treatment-A review, Chem. Eng. Process. Process Intensif. 74 (2014) 27–54. doi:10.1016/j.cep.2013.10.002.
[114] M.S. El-bourawi, M. Khayet, R. Ma, Z. Ding, Z. Li, X. Zhang, Application of vacuum membrane distillation for ammonia removal, 301 (2007) 200–209. doi:10.1016/j.memsci.2007.06.021.
[115] Z. Xie, T. Duong, M. Hoang, C. Nguyen, B. Bolto, Ammonia removal by sweep gas membrane distillation, Water Res. 43 (2009) 1693–1699. doi:10.1016/j.watres.2008.12.052.
[116] J. Swaminathan, H.W. Chung, D.M. Warsinger, J.H.L. V, Membrane distillation model based on heat exchanger theory and configuration comparison, Appl. Energy. 184 (2016) 491–505. doi:10.1016/j.apenergy.2016.09.090.
[117] J. Swaminathan, H.W. Chung, D.M. Warsinger, J.H.L. V, Energy efficiency of membrane distillation up to high salinity : Evaluating critical system size and optimal membrane thickness, Appl. Energy. 211 (2018) 715–734. doi:10.1016/j.apenergy.2017.11.043.
[118] J. Swaminathan, H. Won, D.M. Warsinger, F.A. Almarzooqi, H.A. Arafat, J.H.L. V, Energy efficiency of permeate gap and novel conductive gap membrane distillation, J. Memb. Sci. 502 (2016) 171–178. doi:10.1016/j.memsci.2015.12.017.
[119] L. Francis, N. Ghaffour, A.A. Alsaadi, G.L. Amy, Material gap membrane distillation: A new design for water vapor flux enhancement, J. Memb. Sci. 448 (2013) 240–247. doi:10.1016/j.memsci.2013.08.013.
[120] L. Eykens, T. Reyns, K. De Sitter, C. Dotremont, L. Pinoy, B. Van Der Bruggen, How to select a membrane distillation con fi guration ? Process conditions and membrane in fl uence unraveled, Desalination. 399 (2016) 105–115. doi:10.1016/j.desal.2016.08.019.
[121] P. Wang, T.S. Chung, Recent advances in membrane distillation processes: Membrane development, configuration design and application exploring, J. Memb. Sci. 474 (2015) 39–56. doi:10.1016/j.memsci.2014.09.016.
[122] P. Yazgan-birgi, M.I. Hassan, J. Swaminathan, J.H.L. V, Computational fl uid dynamics modeling for performance assessment of permeate gap membrane distillation, J. Memb. Sci. 568 (2018) 55–66. doi:10.1016/j.memsci.2018.09.061.
[123] G. Amy, N. Ghaffour, Z. Li, L. Francis, R. Valladares, T. Missimer, S. Lattemann, Membrane-based seawater desalination : Present and future prospects, Desalination. 401 (2017) 16–21. doi:10.1016/j.desal.2016.10.002.
[124] A.S. Alsaadi, A. Alpatova, J. Lee, L. Francis, N. Gha, Flashed-feed VMD configuration as a novel method for eliminating temperature polarization effect and enhancing water vapor flux, J. Memb. Sci. 563 (2018) 175–182. doi:10.1016/j.memsci.2018.05.060.
[125] P. Wang, T. Chung, A New-Generation Asymmetric Multi-Bore Hollow Fiber Membrane for Sustainable Water Production via Vacuum Membrane Distillation, Environ. Sci. Technol. 47 (2013) 6272–6278. doi:10.1021/es400356z.
[126] E. Drioli, A. Ali, S. Simone, F. Macedonio, S.A. Al-jlil, F.S. Al Shabonah, H.S. Al-romaih, O. Al-

harbi, A. Figoli, A. Criscuoli, Novel PVDF hollow fiber membranes for vacuum and direct contact membrane distillation applications, Sep. Purif. Technol. 115 (2013) 27–38. doi:10.1016/j.seppur.2013.04.040.
[127] M.M. Teoh, S. Bonyadi, T. Chung, Investigation of different hollow fiber module designs for flux enhancement in the membrane distillation process, J. Memb. Sci. 311 (2008) 371–379. doi:10.1016/j.memsci.2007.12.054.
[128] F. Kiefer, M. Spinnler, T. Sattelmayer, Multi-Effect Vacuum Membrane Distillation systems : Model derivation and calibration, Desalination. 438 (2018) 97–111. doi:10.1016/j.desal.2018.03.024.
[129] A.E. Jansen, J.W. Assink, J.H. Hanemaaijer, J. Van Medevoort, E. Van Sonsbeek, Development and pilot testing of full-scale membrane distillation modules for deployment of waste heat, Desalination. 323 (2013) 55–65. doi:10.1016/j.desal.2012.11.030.
[130] J.H. Hanemaaijer, Memstill ® low cost membrane distillation technology for seawater desalination, in: Desalination, 2004: p. 355.
[131] H. Geng, J. Wang, C. Zhang, P. Li, H. Chang, High water recovery of RO brine using multi-stage air gap membrane distillation, Desalination. 355 (2015) 178–185. doi:10.1016/j.desal.2014.10.038.
[132] D. Winter, J. Koschikowski, M. Wieghaus, Desalination using membrane distillation: Experimental studies on full scale spiral wound modules, J. Memb. Sci. 375 (2011) 104–112. doi:10.1016/j.memsci.2011.03.030.
[133] E. Guillén-Burrieza, G. Zaragoza, S. Miralles-Cuevas, J. Blanco, Experimental evaluation of two pilot-scale membrane distillation modules used for solar desalination, J. Memb. Sci. 409–410 (2012) 264–275. doi:10.1016/j.memsci.2012.03.063.
[134] P. Wang, T. Chung, Exploring the Spinning and Operations of Multibore Hollow Fiber Membranes for Vacuum Membrane Distillation, 60 (2014). doi:10.1002/aic.
[135] P. Wang, T. Chung, Design and fabrication of lotus-root-like multi-bore hollow fiber membrane for direct contact membrane distillation, J. Memb. Sci. 421–422 (2012) 361–374. doi:10.1016/j.memsci.2012.08.003.
[136] K. Zhao, W. Heinzl, M. Wenzel, S. Büttner, F. Bollen, G. Lange, S. Heinzl, N. Sarda, Experimental study of the memsys vacuum-multi-effect-membrane-distillation (V-MEMD) module, Desalination. 323 (2013) 150–160. doi:10.1016/j.desal.2012.12.003.
[137] H.B. Park, J. Kamcev, L.M. Robeson, M. Elimelech, B.D. Freeman, Maximizing the right stuff: The trade-off between membrane permeability and selectivity, Science (80-.). 356 (2017) 1138–1148. doi:10.1126/science.aab0530.
[138] J. Vanneste, J.A. Bush, K.L. Hickenbottom, C.A. Marks, D. Jassby, C.S. Turchi, T.Y. Cath, Novel thermal efficiency-based model for determination of thermal conductivity of membrane distillation membranes, J. Memb. Sci. 548 (2018) 298–308. doi:10.1016/j.memsci.2017.11.028.
[139] M. Khayet, Membranes and theoretical modeling of membrane distillation: A review, Adv. Colloid Interface Sci. 164 (2011) 56–88. doi:10.1016/J.CIS.2010.09.005.
[140] A.M. Alklaibi, N. Lior, Membrane-distillation desalination: Status and potential, Desalination. 171 (2005) 111–131. doi:10.1016/j.desal.2004.03.024.
[141] C.J. van Oss, Hydrophobicity of biosurfaces - Origin, quantitative determination and interaction energies, Colloids Surfaces B Biointerfaces. 5 (1995) 91–110. doi:10.1016/0927-7765(95)01217-7.
[142] M. Filella, Colloidal properties of submicronparticles in natural waters, K.J. Wilkinson, J.R.Lead(Eds.), Environ. Sep. Characterisation, John Wiley Sons, England,. (2007) 17–93.
[143] W. Kühnl, A. Piry, V. Kaufmann, T. Grein, S. Ripperger, U. Kulozik, Impact of colloidal interactions on the flux in cross-flow microfiltration of milk at different pH values: A surface energy approach, J. Memb. Sci. 352 (2010) 107–115. doi:10.1016/j.memsci.2010.02.006.
[144] X. Jin, X. Huang, E.M. V Hoek, Role of Specific Ion Interactions in Seawater RO Membrane Fouling by Alginic Acid, Environ. Sci. Technol. 43 (2009) 3580–3587. doi:10.1021/es8036498.
[145] S. Meng, Y. Ye, J. Mansouri, V. Chen, Fouling and crystallisation behaviour of superhydrophobic

nano-composite PVDF membranes in direct contact membrane distillation, J. Memb. Sci. 463 (2014) 102–112. doi:10.1016/j.memsci.2014.03.027.
[146] S. Srisurichan, R. Jiraratananon, A.G. Fane, Humic acid fouling in the membrane distillation process, Desalination. 174 (2005) 63–72. doi:10.1016/j.desal.2004.09.003.
[147] M. Khayet, J.I. Mengual, Effect of salt concentration during the treatment of humic acid solutions by membrane distillation, Desalination. 168 (2004) 373–381. doi:10.1016/j.desal.2004.07.023.
[148] E.E. Meyer, K.J. Rosenberg, J. Israelachvili, Recent progress in understanding hydrophobic interactions., Proc. Natl. Acad. Sci. U. S. A. 103 (2006) 15739–46. doi:10.1073/pnas.0606422103.
[149] M. Gryta, Effect of iron oxides scaling on the MD process performance, Desalination. 216 (2007) 88–102. doi:10.1016/j.desal.2007.01.002.
[150] M. Krivorot, A. Kushmaro, Y. Oren, J. Gilron, Factors affecting biofilm formation and biofouling in membrane distillation of seawater, J. Memb. Sci. 376 (2011) 15–24. doi:10.1016/j.memsci.2011.01.061.
[151] J. Buffle, K.J. Wilkinson, S. Stoll, M. Filella, J. Zhang, A generalized description of aquatic colloidal interactions: The three- culloidal component approach, Environ. Sci. Technol. 32 (1998) 2887–2899. doi:10.1021/es980217h.
[152] A. Bogler, E. Bar-Zeev, Membrane Distillation Biofouling: Impact of Feedwater Temperature on Biofilm Characteristics and Membrane Performance, Environ. Sci. Technol. 52 (2018) 10019–10029. doi:10.1021/acs.est.8b02744.
[153] Q. Zhang, G. Shuwen, J. Zhang, A.G. Fane, S. Kjelleberg, S.A. Rice, D. Mcdougald, Analysis of microbial community composition in a lab-scale membrane distillation bioreactor, J. Appl. Microbiol. 118 (2015) 940–953. doi:10.1111/jam.12759.
[154] J. Phattaranawik, A.G. Fane, A.C.S. Pasquier, W. Bing, F.S. Wong, Experimental study and design of a submerged membrane distillation bioreactor, Chem. Eng. Technol. 32 (2009) 38–44. doi:10.1002/ceat.200800498.
[155] M. Gryta, The assessment of microorganism growth in the membrane distillation system, Desalination. 142 (2002) 79–88. doi:10.1016/S0011-9164(01)00427-1.
[156] K.R. Zodrow, E. Bar-Zeev, M.J. Giannetto, M. Elimelech, Biofouling and Microbial Communities in Membrane Distillation and Reverse Osmosis, Environ. Sci. Technol. 48 (2014) 13155–13164. doi:10.1021/es503051t.
[157] J. Lee, C. Boo, W.H. Ryu, A.D. Taylor, M. Elimelech, Development of Omniphobic Desalination Membranes Using a Charged Electrospun Nanofiber Scaffold, ACS Appl. Mater. Interfaces. 8 (2016) 11154–11161. doi:10.1021/acsami.6b02419.
[158] C. Boo, J. Lee, M. Elimelech, Engineering Surface Energy and Nanostructure of Microporous Films for Expanded Membrane Distillation Applications, Environ. Sci. Technol. 50 (2016) 8112–8119. doi:10.1021/acs.est.6b02316.
[159] M. Gryta, Influence of polypropylene membrane surface porosity on the performance of membrane distillation process, J. Memb. Sci. 287 (2007) 67–78. doi:10.1016/j.memsci.2006.10.011.
[160] M. Rezaei, D.M. Warsinger, J.H. Lienhard V, M.C. Duke, T. Matsuura, W.M. Samhaber, Wetting phenomena in membrane distillation: Mechanisms, reversal, and prevention, Water Res. 139 (2018) 329–352. doi:10.1016/j.watres.2018.03.058.
[161] E. Guillen-Burrieza, M.O. Mavukkandy, M.R. Bilad, H.A. Arafat, Understanding wetting phenomena in membrane distillation and how operational parameters can affect it, J. Memb. Sci. 515 (2016) 163–174. doi:10.1016/j.memsci.2016.05.051.
[162] Y. Chen, Z. Wang, G.K. Jennings, S. Lin, Probing Pore Wetting in Membrane Distillation Using Impedance: Early Detection and Mechanism of Surfactant-Induced Wetting, Environ. Sci. Technol. Lett. 4 (2017) 505–510. doi:10.1021/acs.estlett.7b00372.
[163] Z. Wang, J. Jin, D. Hou, S. Lin, Tailoring surface charge and wetting property for robust oil-fouling mitigation in membrane distillation, J. Memb. Sci. 516 (2016) 113–122. doi:10.1016/j.memsci.2016.06.011.

[164] E. Drioli, A. Ali, F. Macedonio, Membrane distillation: Recent developments and perspectives, Desalination. 356 (2015) 56–84. doi:10.1016/j.desal.2014.10.028.
[165] M. Khayet, J.I. Mengual, T. Matsuura, Porous hydrophobic/hydrophilic composite membranes: Application in desalination using direct contact membrane distillation, J. Memb. Sci. 252 (2005) 101–113. doi:10.1016/j.memsci.2004.11.022.
[166] L. Fortunato, Y. Jang, J. Lee, S. Jeong, S. Lee, T. Leiknes, N. Ghaffour, Fouling development in direct contact membrane distillation : Non-invasive monitoring and destructive analysis, Water Res. 132 (2018) 34–41. doi:10.1016/j.watres.2017.12.059.
[167] D. Zhao, J. Zuo, K.J. Lu, T.S. Chung, Fluorographite modified PVDF membranes for seawater desalination via direct contact membrane distillation, Desalination. 413 (2017) 119–126. doi:10.1016/j.desal.2017.03.012.
[168] D. Hou, C. Ding, K. Li, D. Lin, D. Wang, J. Wang, A novel dual-layer composite membrane with underwater-superoleophobic/hydrophobic asymmetric wettability for robust oil-fouling resistance in membrane distillation desalination, Desalination. 428 (2018) 240–249. doi:10.1016/j.desal.2017.11.039.
[169] Y.C. Woo, Y. Kim, M. Yao, L.D. Tijing, J.S. Choi, S. Lee, S.H. Kim, H.K. Shon, Hierarchical Composite Membranes with Robust Omniphobic Surface Using Layer-By-Layer Assembly Technique, Environ. Sci. Technol. 52 (2018) 2186–2196. doi:10.1021/acs.est.7b05450.
[170] E. Guillen-Burrieza, R. Thomas, B. Mansoor, D. Johnson, N. Hilal, H. Arafat, Effect of dry-out on the fouling of PVDF and PTFE membranes under conditions simulating intermittent seawater membrane distillation (SWMD), J. Memb. Sci. 438 (2013) 126–139. doi:10.1016/j.memsci.2013.03.014.
[171] L. Tang, A. Iddya, X. Zhu, A. V. Dudchenko, W. Duan, C. Turchi, J. Vanneste, T.Y. Cath, D. Jassby, Enhanced Flux and Electrochemical Cleaning of Silicate Scaling on Carbon Nanotube-Coated Membrane Distillation Membranes Treating Geothermal Brines, ACS Appl. Mater. Interfaces. 9 (2017) 38594–38605. doi:10.1021/acsami.7b12615.
[172] A.K. An, J. Guo, E.J. Lee, S. Jeong, Y. Zhao, Z. Wang, T.O. Leiknes, PDMS/PVDF hybrid electrospun membrane with superhydrophobic property and drop impact dynamics for dyeing wastewater treatment using membrane distillation, J. Memb. Sci. 525 (2017) 57–67. doi:10.1016/j.memsci.2016.10.028.
[173] A.L. McGaughey, R.D. Gustafson, A.E. Childress, Effect of long-term operation on membrane surface characteristics and performance in membrane distillation, J. Memb. Sci. 543 (2017) 143–150. doi:10.1016/j.memsci.2017.08.040.
[174] Q.M. Nguyen, S. Jeong, S. Lee, Characteristics of membrane foulants at different degrees of SWRO brine concentration by membrane distillation, Desalination. 409 (2017) 7–20. doi:10.1016/j.desal.2017.01.007.
[175] F. He, J. Gilron, H. Lee, L. Song, K.K. Sirkar, Potential for scaling by sparingly soluble salts in crossflow DCMD, J. Memb. Sci. 311 (2008) 68–80. doi:10.1016/j.memsci.2007.11.056.
[176] A.K. An, J. Guo, S. Jeong, E.J. Lee, S.A.A. Tabatabai, T.O. Leiknes, High flux and antifouling properties of negatively charged membrane for dyeing wastewater treatment by membrane distillation, Water Res. 103 (2016) 362–371. doi:10.1016/j.watres.2016.07.060.
[177] M. Gryta, Fouling in direct contact membrane distillation process, J. Memb. Sci. 325 (2008) 383–394. doi:10.1016/j.memsci.2008.08.001.
[178] A. Bauer, M. Wagner, F. Saravia, S. Bartl, V. Hilgenfeldt, H. Horn, In-situ monitoring and quanti fi cation of fouling development in membrane distillation by means of optical coherence tomography, J. Memb. Sci. 577 (2019) 145–152. doi:10.1016/j.memsci.2019.02.006.
[179] J. Lee, Y. Jang, L. Fortunato, S. Jeong, S. Lee, An advanced online monitoring approach to study the scaling behavior in direct contact membrane distillation, J. Memb. Sci. 546 (2018) 50–60. doi:10.1016/j.memsci.2017.10.009.
[180] A. Criscuoli, J. Zhong, A. Figoli, M.C. Carnevale, R. Huang, E. Drioli, Treatment of dye solutions

by vacuum membrane distillation, Water Res. 42 (2008) 5031–5037. doi:10.1016/j.watres.2008.09.014.
[181] N.M. Mokhtar, W.J. Lau, A.F. Ismail, The potential of membrane distillation in recovering water from hot dyeing solution, J. Water Process Eng. 2 (2014) 71–78. doi:10.1016/j.jwpe.2014.05.006.
[182] C.F. Couto, M.C.S. Amaral, L.C. Lange, L.V. de S. Santos, Effect of humic acid concentration on pharmaceutically active compounds (PhACs) rejection by direct contact membrane distillation (DCMD), Sep. Purif. Technol. 212 (2019) 920–928. doi:10.1016/j.seppur.2018.12.012.
[183] F. Jia, Y. Yin, J. Wang, Removal of cobalt ions from simulated radioactive wastewater by vacuum membrane distillation, Prog. Nucl. Energy. 103 (2018) 20–27. doi:10.1016/j.pnucene.2017.11.008.
[184] F. Jia, J. Li, J. Wang, Y. Sun, Removal of strontium ions from simulated radioactive wastewater by vacuum membrane distillation, Ann. Nucl. Energy. 103 (2017) 363–368. doi:http://dx.doi.org/10.1016/j.anucene.2017.02.003.
[185] G. Zakrzewska-Trznadel, Radioactive Waste Processing: Advancement in Pressure-Driven Processes and Current World Scenario, in: A.K. Pabby, S.S.H. Rizvi, A.M. Sastre (Eds.), Handb. Membr. Sep. Chem. Pharm. Food, Biotechnol. Appl., CRC Press, Taylor & Francis Group, 2009: pp. 843–881. doi:10.1201/9781420009484.ch19.
[186] B. Osuna, G. Ferrero, I. Rodriguez-Roda, N. Collado, J. Comas, J. Sipma, H. Monclús, Comparison of removal of pharmaceuticals in MBR and activated sludge systems, Desalination. 250 (2009) 653–659. doi:10.1016/j.desal.2009.06.073.
[187] S. Zorita, L. Mårtensson, L. Mathiasson, Occurrence and removal of pharmaceuticals in a municipal sewage treatment system in the south of Sweden, Sci. Total Environ. 407 (2009) 2760–2770. doi:10.1016/j.scitotenv.2008.12.030.
[188] X. Jin, J. Shan, C. Wang, J. Wei, C.Y. Tang, Rejection of pharmaceuticals by forward osmosis membranes, J. Hazard. Mater. 227–228 (2012) 55–61. doi:10.1016/j.jhazmat.2012.04.077.
[189] F.X. Kong, H.W. Yang, Y.Q. Wu, X.M. Wang, Y.F. Xie, Rejection of pharmaceuticals during forward osmosis and prediction by using the solution-diffusion model, J. Memb. Sci. 476 (2015) 410–420. doi:10.1016/j.memsci.2014.11.026.
[190] J. Garcia-Ivars, L. Martella, M. Massella, C. Carbonell-Alcaina, M.I. Alcaina-Miranda, M.I. Iborra-Clar, Nanofiltration as tertiary treatment method for removing trace pharmaceutically active compounds in wastewater from wastewater treatment plants, Water Res. 125 (2017) 360–373. doi:10.1016/j.watres.2017.08.070.
[191] S. Gassara, J. Mendret, E. Petit, S. Brosillon, A. Azaïs, A. Deratani, Nanofiltration for wastewater reuse: Counteractive effects of fouling and matrice on the rejection of pharmaceutical active compounds, Sep. Purif. Technol. 133 (2014) 313–327. doi:10.1016/j.seppur.2014.07.007.
[192] K.P.M. Licona, L.R. de O. Geaquinto, J.V. Nicolini, N.G. Figueiredo, S.C. Chiapetta, A.C. Habert, L. Yokoyama, Assessing potential of nanofiltration and reverse osmosis for removal of toxic pharmaceuticals from water, J. Water Process Eng. 25 (2018) 195–204. doi:10.1016/j.jwpe.2018.08.002.
[193] Y.L. Lin, Effects of organic, biological and colloidal fouling on the removal of pharmaceuticals and personal care products by nanofiltration and reverse osmosis membranes, J. Memb. Sci. 542 (2017) 342–351. doi:10.1016/j.memsci.2017.08.023.
[194] G. Naidu, S. Jeong, S. Vigneswaran, Interaction of humic substances on fouling in membrane distillation for seawater desalination, Chem. Eng. J. 262 (2015) 946–957. doi:10.1016/j.cej.2014.10.060.
[195] P. Jacob, P. Phungsai, K. Fukushi, C. Visvanathan, Direct contact membrane distillation for anaerobic effluent treatment, J. Memb. Sci. 475 (2015) 330–339. doi:10.1016/j.memsci.2014.10.021.
[196] Z. Wang, S. Lin, Membrane fouling and wetting in membrane distillation and their mitigation by novel membranes with special wettability, Water Res. 112 (2017) 38–47. doi:10.1016/j.watres.2017.01.022.

[197] S. Lin, S. Nejati, C. Boo, Y. Hu, C.O. Osuji, M. Elimelech, Omniphobic Membrane for Robust Membrane Distillation, Environ. Sci. Technol. Lett. 1 (2014) 443–447. doi:10.1021/ez500267p.
[198] M. Safavi, T. Mohammadi, High-salinity water desalination using VMD, Chem. Eng. J. 149 (2009) 191–195. doi:10.1016/j.cej.2008.10.021.
[199] T.C. Chen, C.D. Ho, H.M. Yeh, Theoretical modeling and experimental analysis of direct contact membrane distillation, J. Memb. Sci. 330 (2009) 279–287. doi:10.1016/j.memsci.2008.12.063.
[200] M. Qtaishat, T. Matsuura, B. Kruczek, M. Khayet, Heat and mass transfer analysis in direct contact membrane distillation, Desalination. 219 (2008) 272–292. doi:10.1016/j.desal.2007.05.019.
[201] S. Gunko, S. Verbych, M. Bryk, N. Hilal, Concentration of apple juice using direct contact membrane distillation, Desalination. 190 (2006) 117–124. doi:10.1016/j.desal.2005.09.001.
[202] S. Srisurichan, R. Jiraratananon, A.G. Fane, Mass transfer mechanisms and transport resistances in direct contact membrane distillation process, J. Memb. Sci. 277 (2006) 186–194. doi:10.1016/j.memsci.2005.10.028.
[203] F. Jia, J. Wang, Separation of cesium ions from aqueous solution by vacuum membrane distillation process, Prog. Nucl. Energy. 98 (2017) 293–300. doi:10.1016/j.pnucene.2017.04.008.
[204] Y. Yun, R. Ma, W. Zhang, A.G. Fane, J. Li, Direct contact membrane distillation mechanism for high concentration NaCl solutions, Desalination. 188 (2006) 251–262. doi:10.1016/j.desal.2005.04.123.
[205] P. Termpiyakul, R. Jiraratananon, S. Srisurichan, Heat and mass transfer characteristics of a direct contact membrane distillation process for desalination, Desalination. 177 (2005) 133–141. doi:10.1016/j.desal.2004.11.019.
[206] M.A. Izquierdo-Gil, M.C. García-Payo, C. Fernández-Pineda, Air gap membrane distillation of sucrose aqueous solutions, J. Memb. Sci. 155 (1999) 291–307. doi:10.1016/S0376-7388(98)00323-8.
[207] M. Gryta, M. Tomaszewska, K. Karakulski, Wastewater treatment by membrane distillation, Desalination. 198 (2006) 67–73. doi:10.1016/j.desal.2006.09.010.
[208] S. Boonyasuwat, S. Chavadej, P. Malakul, J.F. Scamehorn, Anionic and cationic surfactant recovery from water using a multistage foam fractionator, Chem. Eng. J. 93 (2003) 241–252. doi:10.1016/S1385-8947(03)00043-3.
[209] C.R. Martinetti, A.E. Childress, T.Y. Cath, High recovery of concentrated RO brines using forward osmosis and membrane distillation, J. Memb. Sci. 331 (2009) 31–39. doi:10.1016/j.memsci.2009.01.003.
[210] M.R. Choudhury, R.D. Vidic, D.A. Dzombak, Inhibition of Copper Corrosion by Tolyltriazole in Cooling Systems Using Treated Municipal Wastewater as Makeup Water, Arab. J. Sci. Eng. 39 (2014) 7741-. doi:10.1007/s13369-014-1385-z.
[211] M.R. Choudhury, M.A.Z. Siddik, M.Z.E.I. Salam, Use of Shitalakhya River Water as makeup water in power plant cooling system, KSCE J. Civ. Eng. 20 (2016) 571–580. doi:10.1007/s12205-015-1369-x.
[212] M.R. Choudhury, M. Hsieh, R.D. Vidic, D.A. Dzombak, Corrosion management in power plant cooling systems using tertiary-treated municipal wastewater as makeup water, Corros. Sci. 61 (2012) 231–241. doi:10.1016/j.corsci.2012.04.042.
[213] D.A. Dzombak, R.D. Vidic, A.E. Landis, Use of Treated Municipal Wastewater as Power Plant Cooling System Makeup Water : Tertiary Treatment versus Expanded Chemical Regimen for Recirculating Water Quality Management, 2012.
[214] J.A. Bush, J. Vanneste, E.M. Gustafson, C.A. Waechter, D. Jassby, C.S. Turchi, T.Y. Cath, Prevention and management of silica scaling in membrane distillation using pH adjustment, J. Memb. Sci. 554 (2018) 366–377. doi:10.1016/j.memsci.2018.02.059.
[215] Y. Tsao, D.F. Evans, H. Wennerstrom, Long-Range Attractive Force Between Hydrophobic Surfaces Observed by Atomic Force Microscopy, Science (80-.). 262 (1993) 547–550.
[216] J. Israelachvili, R. Pashley, The hydrophobic interaction is long range, decaying exponentially with

distance (Israelachvili and Pashley, 1982).pdf, Nature. 300 (1982) 341–342.
[217] M. Rezaei, D.M. Warsinger, J.H. Lienhard V, W.M. Samhaber, Wetting prevention in membrane distillation through superhydrophobicity and recharging an air layer on the membrane surface, J. Memb. Sci. 530 (2017) 42–52. doi:10.1016/j.memsci.2017.02.013.
[218] D.E. Suk, T. Matsuura, Membrane-based hybrid processes: A review, Sep. Sci. Technol. 41 (2006) 595–626. doi:10.1080/01496390600552347.
[219] M.P. Godino, L. Peña, C. Rincón, J.I. Mengual, Water production from brines by membrane distillation, Desalination. 108 (1997) 91–97. doi:10.1016/S0011-9164(97)00013-1.
[220] M.C. De Andrés, J. Doria, M. Khayet, L. Peñ, J.I. Mengual, Coupling of a membrane distillation module to a multieffect distiller for pure water production, Desalination. 115 (1998) 71–81. doi:10.1016/S0011-9164(98)00028-9.
[221] J.P. Mericq, S. Laborie, C. Cabassud, Vacuum membrane distillation of seawater reverse osmosis brines, Water Res. 44 (2010) 5260–5273. doi:10.1016/j.watres.2010.06.052.
[222] W. Chunrui, J. Yue, C. Huayan, W. Xuan, L. Xiaolong, Membrane distillation and novel integrated membrane process for reverse osmosis drained wastewater treatment, Desalin. Water Treat. 18 (2010) 286–291. doi:10.5004/dwt.2010.1786.
[223] X. Ji, E. Curcio, S. Al Obaidani, G. Di Profio, E. Fontananova, E. Drioli, Membrane distillation-crystallization of seawater reverse osmosis brines, Sep. Purif. Technol. 71 (2009) 76–82. doi:10.1016/j.seppur.2009.11.004.
[224] M. Xie, W.E. Price, L.D. Nghiem, Rejection of pharmaceutically active compounds by forward osmosis: Role of solution pH and membrane orientation, Sep. Purif. Technol. 93 (2012) 107–114. doi:10.1016/j.seppur.2012.03.030.
[225] A.A. Alturki, J.A. McDonald, S.J. Khan, W.E. Price, L.D. Nghiem, M. Elimelech, Removal of trace organic contaminants by the forward osmosis process, Sep. Purif. Technol. 103 (2013) 258–266. doi:10.1016/j.seppur.2012.10.036.
[226] M. Xie, L.D. Nghiem, W.E. Price, M. Elimelech, Comparison of the removal of hydrophobic trace organic contaminants by forward osmosis and reverse osmosis, Water Res. 46 (2012) 2683–2692. doi:10.1016/j.watres.2012.02.023.
[227] W.C.L. Lay, T.H. Chong, C.Y. Tang, A.G. Fane, J. Zhang, Y. Liu, Fouling propensity of forward osmosis: Investigation of the slower flux decline phenomenon, Water Sci. Technol. 61 (2010) 927–936. doi:10.2166/wst.2010.835.
[228] H. Luo, Q. Wang, T.C. Zhang, T. Tao, A. Zhou, L. Chen, X. Bie, A review on the recovery methods of draw solutes in forward osmosis, J. Water Process Eng. 4 (2014) 212–223. doi:10.1016/j.jwpe.2014.10.006.
[229] L. Chekli, S. Phuntsho, J.E. Kim, J. Kim, J.Y. Choi, J.S. Choi, S. Kim, J.H. Kim, S. Hong, J. Sohn, H.K. Shon, A comprehensive review of hybrid forward osmosis systems: Performance, applications and future prospects, J. Memb. Sci. 497 (2016) 430–449. doi:10.1016/j.memsci.2015.09.041.
[230] C.P. Morrow, N.M. Furtaw, J.R. Murphy, A. Achilli, E.A. Marchand, S.R. Hiibel, A.E. Childress, Integrating an aerobic/anoxic osmotic membrane bioreactor with membrane distillation for potable reuse, Desalination. 432 (2018) 46–54. doi:10.1016/j.desal.2017.12.047.
[231] J. Su, R.C. Ong, W. Peng, T. Chung, B.J. Helmer, J.S. de Wit, Advanced FO Membranes from Newly Synthesized CAP Polymer for Wastewater Reclamation through an Integrated FO-MD Hybrid System, AIChE J. 59 (2013) 1245–1254. doi:10.1002/aic.13898.
[232] M. Xie, L.D. Nghiem, W.E. Price, M. Elimelech, A forward osmosis-membrane distillation hybrid process for direct sewer mining: System performance and limitations, Environ. Sci. Technol. 47 (2013) 13486–13493. doi:10.1021/es404056e.
[233] S.M. Hocaoglu, G. Insel, U.U. Cokgor, D. Orhon, Effect of low dissolved oxygen on simultaneous nitrification and denitrification in a membrane bioreactor treating black water, Bioresour. Technol. 102 (2011) 4333–4340. doi:10.1016/j.biortech.2010.11.096.
[234] Z. Ding, L. Liu, Z. Li, R. Ma, Z. Yang, Experimental study of ammonia removal from water by

membrane distillation (MD): The comparison of three configurations, J. Memb. Sci. 286 (2006) 93–103. doi:10.1016/j.memsci.2006.09.015.
[235] S. Mozia, M. Tomaszewska, A.W. Morawski, Photocatalytic membrane reactor (PMR) coupling photocatalysis and membrane distillation-Effectiveness of removal of three azo dyes from water, Catal. Today. 129 (2007) 3–8. doi:10.1016/j.cattod.2007.06.043.
[236] J.A. Bush, J. Vanneste, T.Y. Cath, Comparison of membrane distillation and high-temperature nanofiltration processes for treatment of silica-saturated water, J. Memb. Sci. 570–571 (2019) 258–269. doi:10.1016/j.memsci.2018.10.034.
[237] D.E.M. Warsinger, A. Servi, G.B. Connors, M.O. Mavukkandy, H.A. Arafat, K. Gleason, J.H. Lienhard, Reversing membrane wetting in membrane distillation: comparing dryout to backwashing with pressurized air, Environ. Sci. Water Res. Technol. 3 (2017) 930–939. doi:10.1039/C7EW00085E.
[238] E. Guillén-Burrieza, J. Blanco, G. Zaragoza, D.C. Alarcón, P. Palenzuela, M. Ibarra, W. Gernjak, Experimental analysis of an air gap membrane distillation solar desalination pilot system, J. Memb. Sci. 379 (2011) 386–396. doi:10.1016/j.memsci.2011.06.009.
[239] S. Goh, J. Zhang, Y. Liu, A.G. Fane, Fouling and wetting in membrane distillation (MD) and MD-bioreactor (MDBR) for wastewater reclamation, Desalination. 323 (2013) 39–47. doi:10.1016/j.desal.2012.12.001.
[240] D.M. Warsinger, E.W. Tow, J. Swaminathan, J.H. Lienhard V, Theoretical framework for predicting inorganic fouling in membrane distillation and experimental validation with calcium sulfate, J. Memb. Sci. 528 (2017) 381–390. doi:10.1016/j.memsci.2017.01.031.
[241] D.M. Warsinger, A. Servi, S. Van Belleghem, J. Gonzalez, J. Swaminathan, J. Kharraz, H.W. Chung, H.A. Arafat, K.K. Gleason, J.H. Lienhard V, Combining air recharging and membrane superhydrophobicity for fouling prevention in membrane distillation, J. Memb. Sci. 505 (2016) 241–252. doi:10.1016/j.memsci.2016.01.018.
[242] Y. Choi, G. Naidu, S. Jeong, S. Vigneswaran, S. Lee, R. Wang, A.G. Fane, Experimental comparison of submerged membrane distillation configurations for concentrated brine treatment, Desalination. 420 (2017) 54–62. doi:10.1016/j.desal.2017.06.024.
[243] Y. Shin, H. Cho, J. Choi, Y. Sun Jang, Y.J. Choi, J. Sohn, S. Lee, J. Choi, Application of response surface methodology (RSM) in the optimization of dewetting conditions for flat sheet membrane distillation (MD) membranes, Desalin. Water Treat. 57 (2016) 10020–10030. doi:10.1080/19443994.2015.1038114.
[244] Y. Shin, J. Choi, T. Lee, J. Sohn, S. Lee, Optimization of dewetting conditions for hollow fiber membranes in vacuum membrane distillation, Desalin. Water Treat. 57 (2016) 7582–7592. doi:10.1080/19443994.2015.1044266.
[245] M. Gryta, Water desalination using membrane distillation with acidic stabilization of scaling layer thickness, Desalination. 365 (2015) 160–166. doi:10.1016/j.desal.2015.02.031.
[246] G. Chen, Y. Lu, W.B. Krantz, R. Wang, A.G. Fane, Optimization of operating conditions for a continuous membrane distillation crystallization process with zero salty water discharge, J. Memb. Sci. 450 (2014) 1–11. doi:10.1016/j.memsci.2013.08.034.
[247] M. Gryta, The application of polypropylene membranes for production of fresh water from brines by membrane distillation, Chem. Pap. 71 (2017) 775–784. doi:10.1007/s11696-016-0059-6.
[248] Y. Liao, R. Wang, A.G. Fane, Fabrication of bioinspired composite nanofiber membranes with robust superhydrophobicity for direct contact membrane distillation, Environ. Sci. Technol. 48 (2014) 6335–6341. doi:10.1021/es405795s.
[249] K.J. Lu, J. Zuo, T.S. Chung, Tri-bore PVDF hollow fibers with a super-hydrophobic coating for membrane distillation, J. Memb. Sci. 514 (2016) 165–175. doi:10.1016/j.memsci.2016.04.058.
[250] K.J. Lu, J. Zuo, J. Chang, H.N. Kuan, T.S. Chung, Omniphobic Hollow-Fiber Membranes for Vacuum Membrane Distillation, Environ. Sci. Technol. 52 (2018) 4472–4480. doi:10.1021/acs.est.8b00766.

[251] A. Tuteja, W. Choi, M. Ma, J.M. Mabry, S.A. Mazzella, G.C. Rutledge, G.H. McKinley, R.E. Cohen, Designing superoleophobic surfaces. - Additonal Material, Science (80-.). 318 (2007) 1618–22. doi:10.1126/science.1148326.
[252] R. Zheng, Y. Chen, J. Wang, J. Song, X.M. Li, T. He, Preparation of omniphobic PVDF membrane with hierarchical structure for treating saline oily wastewater using direct contact membrane distillation, J. Memb. Sci. 555 (2018) 197–205. doi:10.1016/j.memsci.2018.03.041.
[253] Z. Wang, D. Hou, S. Lin, Composite Membrane with Underwater-Oleophobic Surface for Anti-Oil-Fouling Membrane Distillation, Environ. Sci. Technol. 50 (2016) 3866–3874. doi:10.1021/acs.est.5b05976.
[254] Y.X. Huang, Z. Wang, J. Jin, S. Lin, Novel Janus Membrane for Membrane Distillation with Simultaneous Fouling and Wetting Resistance, Environ. Sci. Technol. 51 (2017) 13304–13310. doi:10.1021/acs.est.7b02848.
[255] N. Hamzah, C.P. Leo, Membrane distillation of saline with phenolic compound using superhydrophobic PVDF membrane incorporated with TiO2nanoparticles: Separation, fouling and self-cleaning evaluation, Desalination. 418 (2017) 79–88. doi:10.1016/j.desal.2017.05.029.
[256] K. Gethard, O. Sae-Khow, S. Mitra, Carbon nanotube enhanced membrane distillation for simultaneous generation of pure water and concentrating pharmaceutical waste, Sep. Purif. Technol. 90 (2012) 239–245. doi:10.1016/j.seppur.2012.02.042.
[257] E.W. Tow, D.M. Warsinger, A.M. Trueworthy, J. Swaminathan, G.P. Thiel, S.M. Zubair, A.S. Myerson, J.H. Lienhard V, Comparison of fouling propensity between reverse osmosis, forward osmosis, and membrane distillation, J. Memb. Sci. 556 (2018) 352–364. doi:10.1016/j.memsci.2018.03.065.
[258] G.K. Pearce, UF / MF pre-treatment to RO in seawater and wastewater reuse applications : a comparison of energy costs, 222 (2008) 66–73. doi:10.1016/j.desal.2007.05.029.
[259] M. Gündoğdu, Y.A. Jarma, N. Kabay, T. Pek, M. Yüksel, Integration of MBR with NF/RO processes for industrial wastewater reclamation and water reuse-effect of membrane type on product water quality, J. Water Process Eng. 29 (2019) 100574. doi:10.1016/j.jwpe.2018.02.009.
[260] X. Zhu, A. Dudchenko, X. Gu, D. Jassby, Surfactant-stabilized oil separation from water using ultrafiltration and nanofiltration, J. Memb. Sci. 529 (2017) 159–169. doi:10.1016/j.memsci.2017.02.004.
[261] G. Naidu, S. Jeong, Y. Choi, S. Vigneswaran, Membrane distillation for wastewater reverse osmosis concentrate treatment with water reuse potential, J. Memb. Sci. 524 (2017) 565–575. doi:10.1016/j.memsci.2016.11.068.
[262] M. Khayet, T. Matsuura, J.I. Mengual, M. Qtaishat, Design of novel direct contact membrane distillation membranes, Desalination. 192 (2006) 105–111. doi:10.1016/j.desal.2005.06.047.
[263] E. Drioli, A. Ali, F. Macedonio, Membrane distillation: Recent developments and perspectives, Desalination. 356 (2015) 56–84. doi:10.1016/j.desal.2014.10.028.
[264] P. Wang, M.M. Teoh, T.S. Chung, Morphological architecture of dual-layer hollow fiber for membrane distillation with higher desalination performance, Water Res. 45 (2011) 5489–5500. doi:10.1016/j.watres.2011.08.012.
[265] X. Yang, R. Wang, L. Shi, A.G. Fane, M. Debowski, Performance improvement of PVDF hollow fiber-based membrane distillation process, J. Memb. Sci. 369 (2011) 437–447. doi:10.1016/j.memsci.2010.12.020.
[266] M. Khayet, T. Matsuura, Preparation and characterization of polyvinylidene fluoride membranes for membrane distillation, Ind. Eng. Chem. Res. 40 (2001) 5710–5718. doi:10.1021/ie010553y.
[267] J. Blanco Gálvez, L. García-Rodríguez, I. Martín-Mateos, Seawater desalination by an innovative solar-powered membrane distillation system: the MEDESOL project, Desalination. 246 (2009) 567–576. doi:10.1016/j.desal.2008.12.005.
[268] T. Chen, A. Soroush, M.S. Rahaman, Highly Hydrophobic Electrospun Reduced Graphene Oxide/Poly(vinylidene fluoride-co-hexafluoropropylene) Membranes for Use in Membrane

Distillation, Ind. Eng. Chem. Res. 57 (2018) 14535–14543. doi:10.1021/acs.iecr.8b03584.
[269] L. Malaeb, G.M. Ayoub, Reverse osmosis technology for water treatment: State of the art review, Desalination. 267 (2011) 1–8. doi:10.1016/j.desal.2010.09.001.
[270] W. Ma, A. Soroush, T. Van Anh Luong, G. Brennan, M.S. Rahaman, B. Asadishad, N. Tufenkji, Spray- and spin-assisted layer-by-layer assembly of copper nanoparticles on thin-film composite reverse osmosis membrane for biofouling mitigation, Water Res. 99 (2016) 188–199. doi:10.1016/j.watres.2016.04.042.
[271] L.F. Greenlee, D.F. Lawler, B.D. Freeman, B. Marrot, P. Moulin, Reverse osmosis desalination: Water sources, technology, and today's challenges, Water Res. 43 (2009) 2317–2348.
[272] A.W. Mohammad, Y.H. Teow, W.L. Ang, Y.T. Chung, D.L. Oatley-Radcliffe, N. Hilal, Nanofiltration membranes review: Recent advances and future prospects, Desalination. 356 (2015) 226–254. doi:10.1016/j.desal.2014.10.043.
[273] W.S. Ang, A. Tiraferri, K.L. Chen, M. Elimelech, Fouling and cleaning of RO membranes fouled by mixtures of organic foulants simulating wastewater effluent, J. Memb. Sci. 376 (2011) 196–206. doi:10.1016/j.memsci.2011.04.020.
[274] T. Chidambaram, Y. Oren, M. Noel, Fouling of nanofiltration membranes by dyes during brine recovery from textile dye bath wastewater, Chem. Eng. J. 262 (2015) 156–168. doi:10.1016/j.cej.2014.09.062.
[275] J.S. Vrouwenvelder, D.A. Graf von der Schulenburg, J.C. Kruithof, M.L. Johns, M.C.M. van Loosdrecht, Biofouling of spiral-wound nanofiltration and reverse osmosis membranes: A feed spacer problem, Water Res. 43 (2009) 583–594. doi:10.1016/j.watres.2008.11.019.
[276] M.R. Choudhury, N. Anwar, D. Jassby, M. Saifur Rahaman, Fouling and wetting in the membrane distillation driven wastewater reclamation process – A review, Adv. Colloid Interface Sci. (2019). doi:10.1016/j.cis.2019.04.008.
[277] W.S. Ang, N.Y. Yip, A. Tiraferri, M. Elimelech, Chemical cleaning of RO membranes fouled by wastewater effluent: Achieving higher efficiency with dual-step cleaning, J. Memb. Sci. 382 (2011) 100–106. doi:10.1016/j.memsci.2011.07.047.
[278] N.J. Falizi, M.C. Hacıfazlıoğlu, İ. Parlar, N. Kabay, T. Pek, M. Yüksel, Evaluation of MBR treated industrial wastewater quality before and after desalination by NF and RO processes for agricultural reuse, J. Water Process Eng. 22 (2018) 103–108. doi:10.1016/j.jwpe.2018.01.015.
[279] D. Dolar, M. Gros, S. Rodriguez-Mozaz, J. Moreno, J. Comas, I. Rodriguez-Roda, D. Barceló, Removal of emerging contaminants from municipal wastewater with an integrated membrane system, MBR-RO, J. Hazard. Mater. 239–240 (2012) 64–69. doi:10.1016/j.jhazmat.2012.03.029.
[280] B. Sinha, Beer Market by Type (Lager, Ale, Stout & Porter, Malt, and Others), Category (Popular-Priced, Premium, and Super Premium), Packaging (Glass, PET Bottle, Metal Can, and Others), and Production (Macro-brewery, Micro-brewery, Craft Brewery, and Others) -, 2018. www.alliedmarketresearch.com.
[281] G. Hermis, Brewing Up Benefits: The Economic Footprint of Canada's Beer Economy - January 2018, 2018.
[282] Beer Canada, (2019). https://industry.beercanada.com/statistics.
[283] S.G. Wang, X.W. Liu, W.X. Gong, B.Y. Gao, D.H. Zhang, H.Q. Yu, Aerobic granulation with brewery wastewater in a sequencing batch reactor, Bioresour. Technol. 98 (2007) 2142–2147. doi:10.1016/j.biortech.2006.08.018.
[284] K.S. Singh, T. Viraraghavan, Impact of temperature on performance, microbiological, and hydrodynamic aspects of UASB reactors treating municipal wastewater, Water Sci. Technol. 48 (2003) 211–217.
[285] Y. Feng, X. Wang, B.E. Logan, H. Lee, Brewery wastewater treatment using air-cathode microbial fuel cells, Appl. Microbiol. Biotechnol. 78 (2008) 873–880. doi:10.1007/s00253-008-1360-2.
[286] H. Chen, S. Chang, Q. Guo, Y. Hong, P. Wu, Brewery wastewater treatment using an anaerobic membrane bioreactor, Biochem. Eng. J. 105 (2016) 321–331. doi:10.1016/j.bej.2015.10.006.

[287] B.Q. Liao, J.T. Kraemer, D.M. Bagley, Anaerobic membrane bioreactors: Applications and research directions, 2006. doi:10.1080/10643380600678146.
[288] S. Sultana, M. Rahman, C. Ahmed, R. Bakr, N. Anwar, S. Rahaman, Effectiveness of electro-oxidation and electro-Fenton processes in removal of organic matter from high-strength brewery wastewater, J. Appl. Electrochem. 48 (2018) 519–528. doi:10.1007/s10800-018-1185-3.
[289] M.C. Hacıfazlıoğlu, H.R. Tomasini, N. Kabay, L. Bertin, T. Pek, M. Kitiş, N. Yiğit, M. Yüksel, Effect of pressure on desalination of MBR effluents with high salinity by using NF and RO processes for reuse in irrigation, J. Water Process Eng. 25 (2018) 22–27. doi:10.1016/j.jwpe.2018.06.001.
[290] I. Parlar, M. Hacıfazlıoğlu, N. Kabay, T. Pek, M. Yüksel, Performance comparison of reverse osmosis (RO) with integrated nanofiltration (NF) and reverse osmosis process for desalination of MBR effluent, J. Water Process Eng. 29 (2019) 100640. doi:10.1016/j.jwpe.2018.06.002.
[291] T.H. Meltzer, M.W. Jornitz, Filtration and Purification in the Biopharmaceutical Industry, Second, Taylor & Francis, 2008.
[292] L. Wu, H. Wang, T.-W. Xu, Z.-L. Xu, Polymeric Membranes, in: Membr. Sep. Metall. Princ. Appl., Elsevier, 2017: pp. 297–334. doi:https://doi.org/10.1016/B978-0-12-803410-1.00012-8.
[293] 2540 SOLIDS (2017), in: Stand. Methods Exam. Water Wastewater, American Public Health Association, 2018. doi:doi:10.2105/SMWW.2882.030.
[294] 2320 ALKALINITY (2017), in: Stand. Methods Exam. Water Wastewater, American Public Health Association, 2018. doi:doi:10.2105/SMWW.2882.023.
[295] ASTM D4189-07(2014), Standard Test Method for Silt Density Index (SDI) of Water, (2014). doi:10.1520/D4189-07R14.
[296] M.S. Islam, K. Touati, M.S. Rahaman, Feasibility of a hybrid membrane-based process (MF-FO-MD) for fracking wastewater treatment, Sep. Purif. Technol. 229 (2019) 115802. doi:10.1016/j.seppur.2019.115802.
[297] G. Naidu, S. Jeong, S. Vigneswaran, Interaction of humic substances on fouling in membrane distillation for seawater desalination, Chem. Eng. J. 262 (2015) 946–957. doi:10.1016/j.cej.2014.10.060.
[298] L.D. Nghiem, P.J. Coleman, C. Espendiller, Mechanisms underlying the effects of membrane fouling on the nanofiltration of trace organic contaminants, Desalination. 250 (2010) 682–687. doi:10.1016/j.desal.2009.03.025.
[299] P.S. Goh, W.J. Lau, M.H.D. Othman, A.F. Ismail, Membrane fouling in desalination and its mitigation strategies, Desalination. 425 (2018) 130–155. doi:10.1016/j.desal.2017.10.018.
[300] G.P. Sheng, H.Q. Yu, C.M. Wang, FTIR-spectral analysis of two photosynthetic H2-producing strains and their extracellular polymeric substances, Appl. Microbiol. Biotechnol. 73 (2006) 204–210. doi:10.1007/s00253-006-0442-2.
[301] J. Schmitt, H.C. Flemming, FTIR-spectroscopy in microbial and material analysis, Int. Biodeterior. Biodegrad. 41 (1998) 1–11. doi:10.1016/S0964-8305(98)80002-4.
[302] C. Liu, L. Chen, L. Zhu, Application of membrane distillation for the treatment of anaerobic membrane bioreactor effluent: An especial attention to the operating conditions, Chemosphere. 208 (2018) 530–540. doi:10.1016/j.chemosphere.2018.06.013.
[303] A.U. of Beirut, Typical Infared Absorption Frequencies, 1720 (2010). doi:10.1002/9780470944349.
[304] L. Berzina-Cimdina, N. Borodajenko, Research of Calcium Phosphates Using Fourier Transform Infrared Spectroscopy, Infrared Spectrosc. - Mater. Sci. Eng. Technol. (2012). doi:10.5772/36942.
[305] S.P. Chesters, Innovations in the inhibition and cleaning of reverse osmosis membrane scaling and fouling, Desalination. 238 (2009) 22–29. doi:10.1016/j.desal.2008.01.031.
[306] D.C. Sobeck, M.J. Higgins, Examination of three theories for mechanisms of cation-induced bioflocculation., Water Res. 36 (2002) 527–38. http://www.ncbi.nlm.nih.gov/pubmed/11827315.
[307] A. Simon, W.E. Price, L.D. Nghiem, Influence of formulated chemical cleaning reagents on the surface properties and separation efficiency of nanofiltrationmembranes, J. Memb. Sci. 432 (2013) 73–82. doi:10.1016/j.memsci.2012.12.029.

[308] T. Husnain, Y. Liu, R. Riffat, B. Mi, Integration of forward osmosis and membrane distillation for sustainable wastewater reuse, Sep. Purif. Technol. 156 (2015) 424–431. doi:10.1016/j.seppur.2015.10.031.
[309] N. Anwar, M.S. Rahaman, Membrane desalination processes for water recovery from pre-treated brewery wastewater: Performance and fouling, Sep. Purif. Technol. 252 (2020) 117420. doi:10.1016/j.seppur.2020.117420.
[310] G. Hermus, Brewing Up Benefits: The Economic Footprint of Canada's Beer Economy, 2018. https://www.conferenceboard.ca/e-library/abstract.aspx?did=9329.
[311] N. Dow, J. Villalobos García, L. Niadoo, N. Milne, J. Zhang, S. Gray, M. Duke, Demonstration of membrane distillation on textile waste water assessment of long term performance, membrane cleaning and waste heat integration, Environ. Sci. Water Res. Technol. 3 (2017) 433–449. doi:10.1039/c6ew00290k.
[312] M.M. Damtie, B. Kim, Y.C. Woo, J.S. Choi, Membrane distillation for industrial wastewater treatment: Studying the effects of membrane parameters on the wetting performance, Chemosphere. 206 (2018) 793–801. doi:10.1016/j.chemosphere.2018.05.070.
[313] A.H.M.P.S. Energy-efficient, A Hybrid Membrane-Based Process (SWRO-PRO- NF) for Energy-Efficient and High-Water Recovery Desalination System Submitted to, (n.d.).
[314] M. Sarai Atab, A.J. Smallbone, A.P. Roskilly, An operational and economic study of a reverse osmosis desalination system for potable water and land irrigation, Desalination. 397 (2016) 174–184. doi:10.1016/j.desal.2016.06.020.
[315] M. Gündoğdu, N. Kabay, N. Yiğit, M. Kitiş, T. Pek, M. Yüksel, Effect of concentrate recirculation on the product water quality of integrated MBR – NF process for wastewater reclamation and industrial reuse, J. Water Process Eng. 29 (2019) 100485. doi:10.1016/j.jwpe.2017.08.023.
[316] M.R. Choudhury, N. Anwar, D. Jassby, M.S. Rahaman, Fouling and wetting in the membrane distillation driven wastewater reclamation process – A review, Adv. Colloid Interface Sci. 269 (2019) 370–399. doi:10.1016/j.cis.2019.04.008.
[317] P.D. Dongare, A. Alabastri, S. Pedersen, K.R. Zodrow, Nanophotonics-enabled solar membrane distillation for off-grid water purification, (2017) 1–6. doi:10.1073/pnas.1701835114.
[318] D.B. Gingerrich, M.S. Mauter, Quantity, quality, and availability of waste heat from united states thermal power generation, Environ. Sci. Technol. 49 (2015) 8297–8306. doi:https://doi.org/10.1021/es5060989.
[319] R.T. Sataloff, M.M. Johns, K.M. Kost, A techno-economic assessment of membrane distillation for treatment of Marcellus shale produced water, (n.d.).
[320] H.S. Usman, K. Touati, M.S. Rahaman, An economic evaluation of renewable energy-powered membrane distillation for desalination of brackish water, Renew. Energy. 169 (2021) 1294–1304. doi:10.1016/j.renene.2021.01.087.
[321] V. Karanikola, S.E. Moore, A. Deshmukh, R.G. Arnold, M. Elimelech, A.E. Sáez, Economic performance of membrane distillation configurations in optimal solar thermal desalination systems, Desalination. 472 (2019) 114164. doi:10.1016/j.desal.2019.114164.
[322] R. Schwantes, K. Chavan, D. Winter, C. Felsmann, J. Pfafferott, Techno-economic comparison of membrane distillation and MVC in a zero liquid discharge application, Desalination. 428 (2018) 50–68. doi:10.1016/j.desal.2017.11.026.
[323] R.B. Saffarini, E.K. Summers, H.A. Arafat, J.H. Lienhard V, Economic evaluation of stand-alone solar powered membrane distillation systems, Desalination. 299 (2012) 55–62. doi:10.1016/j.desal.2012.05.017.
[324] D. Amaya-Vías, J.A. López-Ramírez, Techno-economic assessment of air and water gap membrane distillation for seawater desalination under different heat source scenarios, Water (Switzerland). 11 (2019). doi:10.3390/w11102117.
[325] F. Banat, N. Jwaied, Economic evaluation of desalination by small-scale autonomous solar-powered membrane distillation units, Desalination. 220 (2008) 566–573.

[326] K. Touati, H.S. Usman, C.N. Mulligan, M.S. Rahaman, Energetic and economic feasibility of a combined membrane-based process for sustainable water and energy systems, Appl. Energy. 264 (2020) 114699. doi:10.1016/j.apenergy.2020.114699.
[327] K. Touati, M.S. Rahaman, Viability of pressure-retarded osmosis for harvesting energy from salinity gradients, Renew. Sustain. Energy Rev. 131 (2020) 109999. doi:10.1016/j.rser.2020.109999.
[328] G. Zuo, R. Wang, R. Field, A.G. Fane, Energy efficiency evaluation and economic analyses of direct contact membrane distillation system using Aspen Plus, Desalination. 283 (2011) 237–244. doi:10.1016/j.desal.2011.04.048.
[329] H.E.. Fath, S.M. Elsherbiny, A.A. Hassan, M. Rommel, M. Wieghaus, J. Koschikowski, M. Vatansever, PV and thermally driven small-scale, stand alone solar desalination systems with very low maintenance needs, Desalination. 225 (2008) 58–69.
[330] I.J. Karrasik, J.P. Messina, P. Cooper, C.C. Heald, Pump Handbook, Third edition, in: 2001: pp. 1–1790.
[331] A. Ghafoor, T. Ahmed, A. Munir, C. Arslan, S.A. Ahmad, Techno-economic feasibility of solar based desalination through reverse osmosis, Desalination. 485 (2020) 114464. doi:10.1016/j.desal.2020.114464.
[332] V.G. Gude, Renewable Energy Powered Desalination Handbook: Application and Thermodynamics, 2018. doi:10.1016/C2017-0-02851-3.
[333] S.E. Moore, S.D. Mirchandani, V. Karanikola, T.M. Nenoff, R.G. Arnold, A. Eduardo Sáez, Process modeling for economic optimization of a solar driven sweeping gas membrane distillation desalination system, Desalination. 437 (2018) 108–120. doi:10.1016/j.desal.2018.03.005.
[334] A. Suárez, P. Fernández, J. Ramón Iglesias, E. Iglesias, F.A. Riera, Cost assessment of membrane processes: A practical example in the dairy wastewater reclamation by reverse osmosis, J. Memb. Sci. 493 (2015) 389–402. doi:10.1016/j.memsci.2015.04.065.

Appendix

Appendix 1

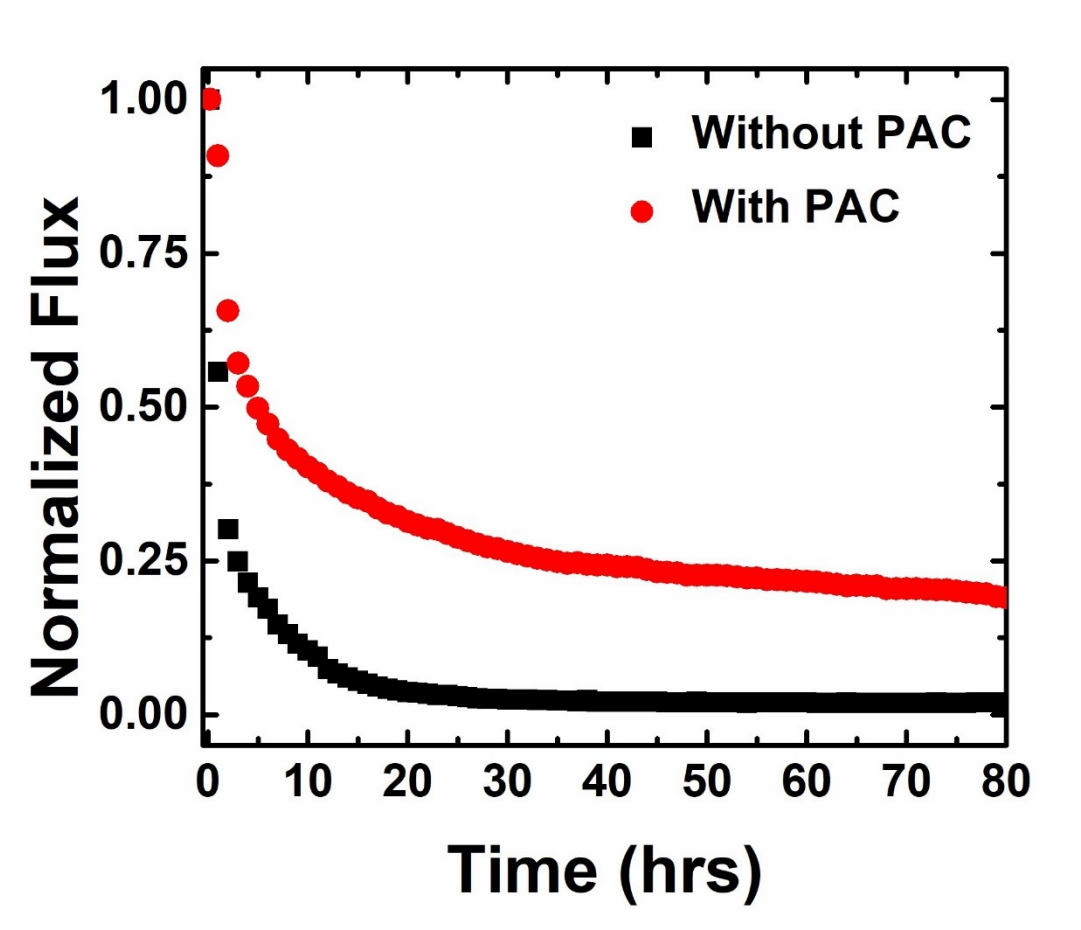

Figure A1.1: Normalized permeate flux for reverse osmosis (RO) Toray membrane for 80 hours operation with MBR treated brewery wastewater effluent without and with powdered activated carbon (PAC) treated ultra-filtered feed at 400 psi with a 0.7 LPM flowrate and a constant temperature of 20.0 ± 0.5˚C.

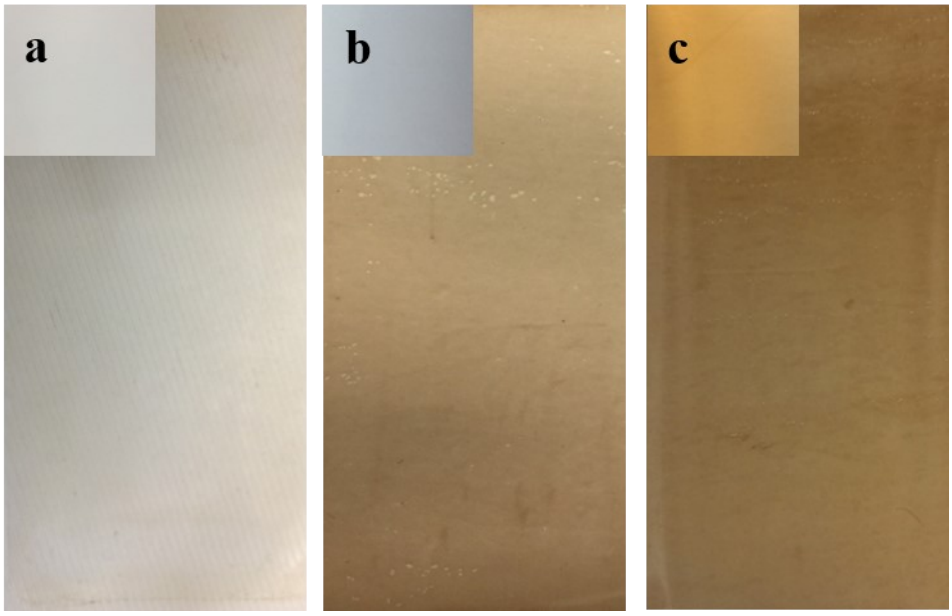

Figure A1.2: Fouled membranes after 80 hours of application (a) DCMD (PTFE), (b) NF (NF90), and (c) RO (Toray) with pristine membranes in the inset with a feed with COD = 50 ± 10 mg/L, T_f = 55°C and T_p = 16°C for MD, P_{NF} =120 psi, P_{RO} = 400 psi with a 0.7 LPM flowrate and a constant temperature of 20.0 ± 0.5˚C.

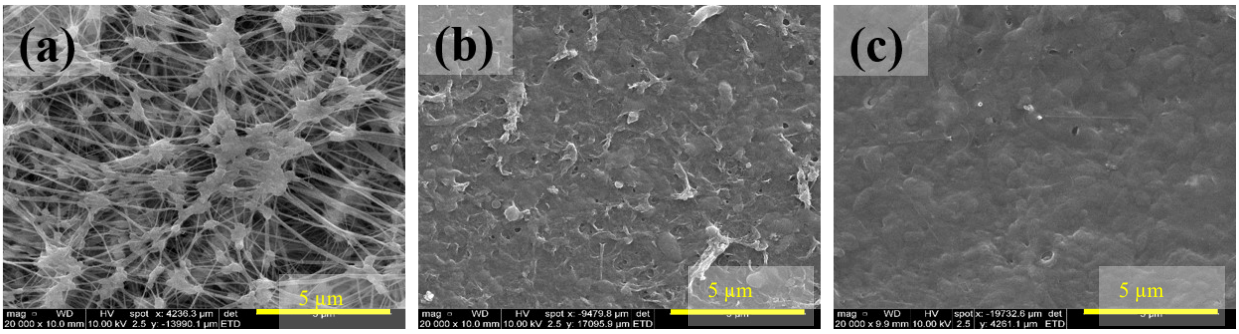

Figure A1.3: SEM images of (a) DCMD (PTFE), (b) NF (NF90), and (c) RO (Toray) membranes after a second cleaning and repeated applications with a feed with COD = 50 ± 10 mg/L, T_f = 55°C and T_p = 16°C for MD, P_{NF} =120 psi, P_{RO} = 400 psi with a 0.7 LPM flowrate and a constant temperature of 20.0 ± 0.5˚C.

Table A1.1: Elemental analysis of pristine, and cleaned DCMD (PTFE), NF (NF90), and RO (Toray) membrane surfaces through EDS after a second cleaning and repeated applications with a feed with COD = 50 ± 10 mg/L, T_f = 55°C and T_p = 16°C for MD, P_{NF} =120 psi, P_{RO} = 400 psi with a 0.7 LPM flowrate and a constant temperature of 20.0 ± 0.5˚C

Membrane	C (%)	O (%)	F (%)	P (%)	N (%)	Ca (%)	Na (%)	Mg (%)	Cl (%)	S (%)	Pt (%)
PTFE Pristine	36	-	63.5	-	-	-	-	-	-	-	0.5
PTFE Cleaned	37.5	-	62	-	-	-	-	-	-	-	0.5
NF Pristine	81.6	8.6	-	-	7	-	-	-	-	2.6	0.2
NF Cleaned	77.1	9	-	-	11.9	-	-	-	-	1.8	0.2
RO Pristine	82.9	9.7	-	-	4.3	-	-	-	-	2.8	0.3
RO Cleaned	74.4	11.4			12.6					1.2	0.4

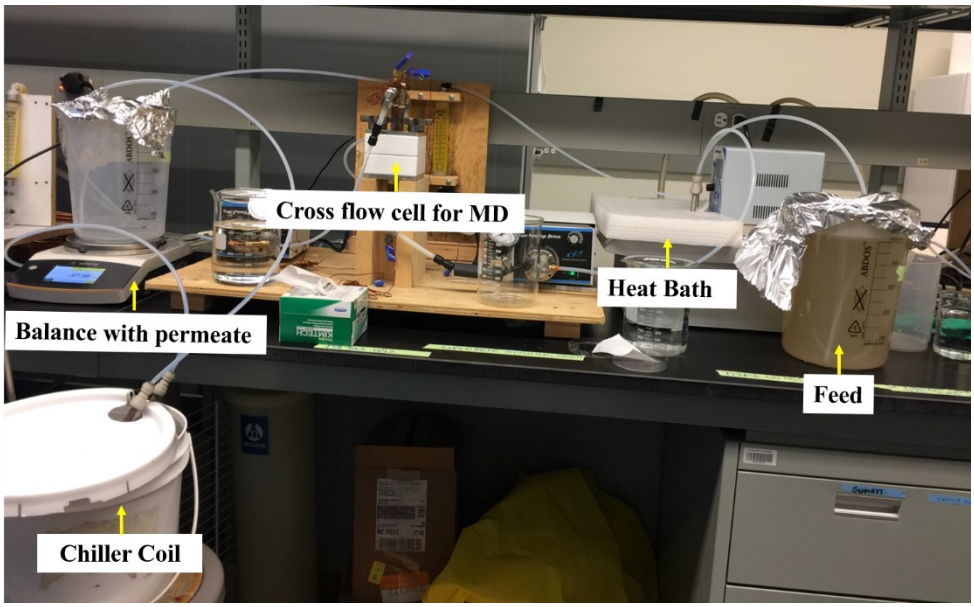

Figure A1.4: Lab scale Direct Contact Membrane Distillation (DCMD) during operation

Figure A1.4 illustrates the bench-scale direct contact membrane distillation (DCMD) configuration that was used in this research. A PTFE flat sheet membrane cell (CF042P-FO) from Sterlitech Corporation, USA, was utilized. The crossflow cell was connected with the feed side and the permeate side with tubes and water circulation was conducted by two gear pumps (Model GH-75211-10, Cole-Parmer, Canada) at around 0.8 psi (Pressure Gauge Model GH-68930-12, Cole-Parmer, Canada) at the same speed across the bottom and the upper face of the membrane cell, respectively. Flow meters (0.1-1 LPM, McMaster-Carr, Canada) were used to observe the constant 0.7 LPM hot feed and the cool permeate circulation rate. The effective membrane surface area of the DCMD cell was 34 cm^2. A constant hot feed temperature (T_f) was maintained for the bulk hot feed using a hot water bath (Cole Parmer). Also, a chiller (Cole Parmer) was attached with the bulk permeate side to maintain a constant cold permeate temperature (T_p). A balance was implemented to automatically record the weight of the permeate side at certain intervals in a computer.

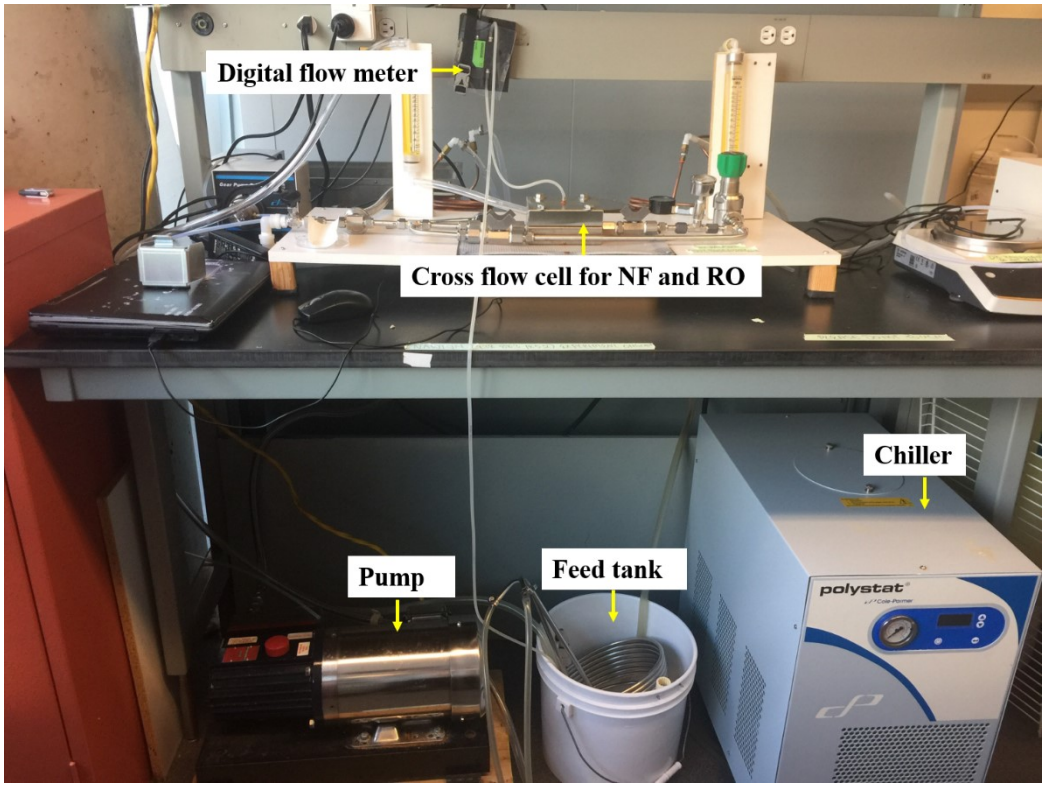

Figure A1.5: Lab scale nanofiltration and reverse osmosis cross flow filtration setup

For NF and RO application, a standard bench-scale cross flow filtration system, connected by stainless steel tubes and PVC tubes was used as shown in Figure A1.5. The crossflow system was equipped with a high-pressure pump (1.7 GPM, 230 V, 60 Hz, 3 PH motor, hydra cell, Ca, USA) that was used to apply the required high pressure on the feed side. The crossflow cell was a stainless-steel water permeation cell and attached to a panel-mount flow meter (0.25~1.5 LPM, purchased from McMaster-Carr, Canada), and a feed solution tank. The effective membrane surface area of the crossflow system was 33 cm^2. The feed tank was connected with a chiller (Cole Parmer) to maintain a constant feed temperature (~20˚C). A digital flow meter connected to the system was automatically recording the flow data at a certain interval into the computer.

Appendix A2

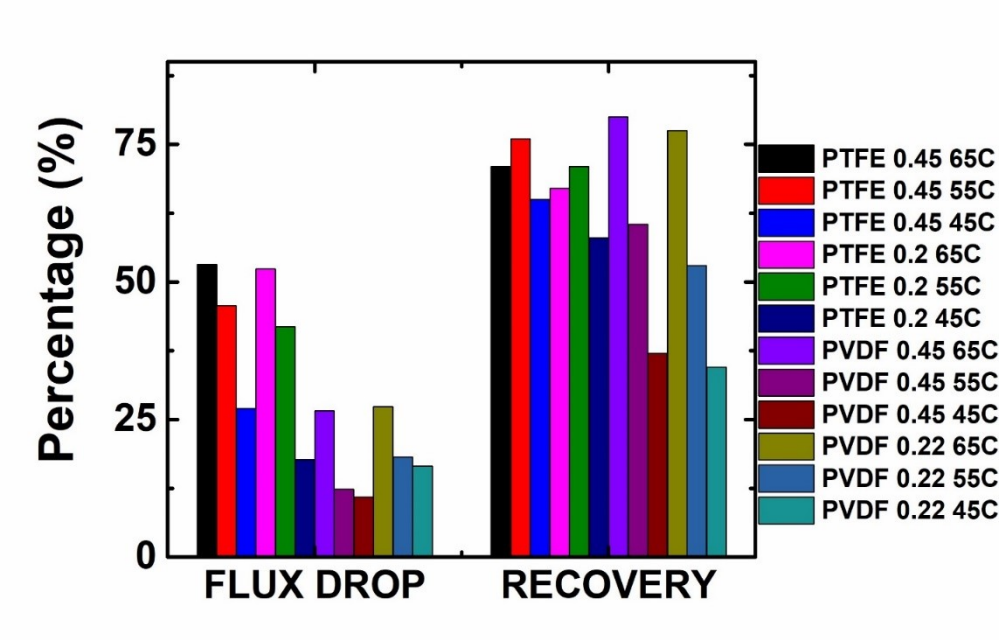

Figure A2.1: Permeate flux drop and water recovery of DCMD PTFE 0.45 µm, and 0.20 µm; and PVDF 0.45 µm, and 0.22 µm for 20 hours of operation with a feed with COD = 77.9 ± 2.8 mg/L and a 0.7 LPM flowrate, T_f = 65ºC, 55ºC, and 45ºC and T_p = 18ºC for MD. PTFE membranes had highest flux drop compared to that of PVDF membranes. However, despite the initial higher flux of PTFE membranes compared to the PVDF membranes, the highest water recovery of nearly 80% was achieved with PVDF membranes with 0.45µm pore sizes at 65ºC with significant flux drop (~27%) compared to 55ºC and 45ºC (~16-18%) from their distinct initial fluxes [All the experiments were replicated at least thrice, and the average values were considered and presented; the error bars of (b) represent the standard deviation from the average value].

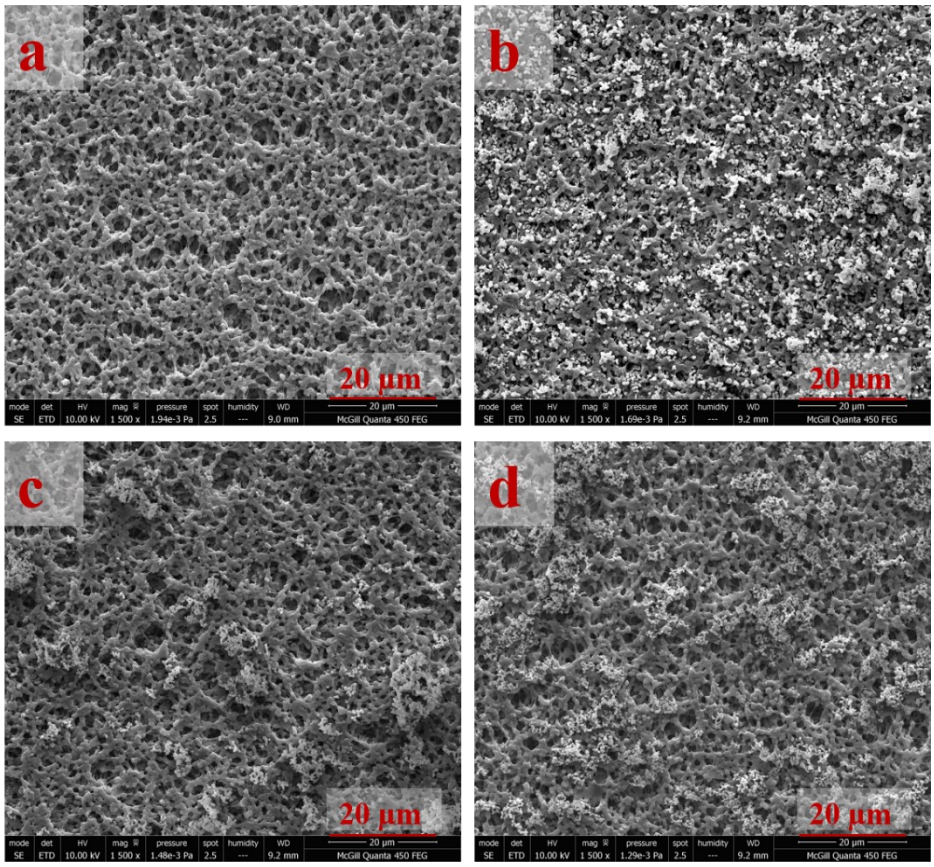

Figure A2.2: Surface morphology of DCMD PVDF 0.45 µm (a) pristine membrane and fouled membranes after 20 hours operation with a feed with COD = 77.9 ± 2.8 mg/L and a 0.7 LPM flowrate with the hot feed temperature (b) T_f = 65ºC, (c) T_f = 55ºC, and (d) (b) T_f = 45ºC and a permeate temperature T_p = 18ºC for MD. Extensive fouling was observed with the highest temperature of 65ºC.

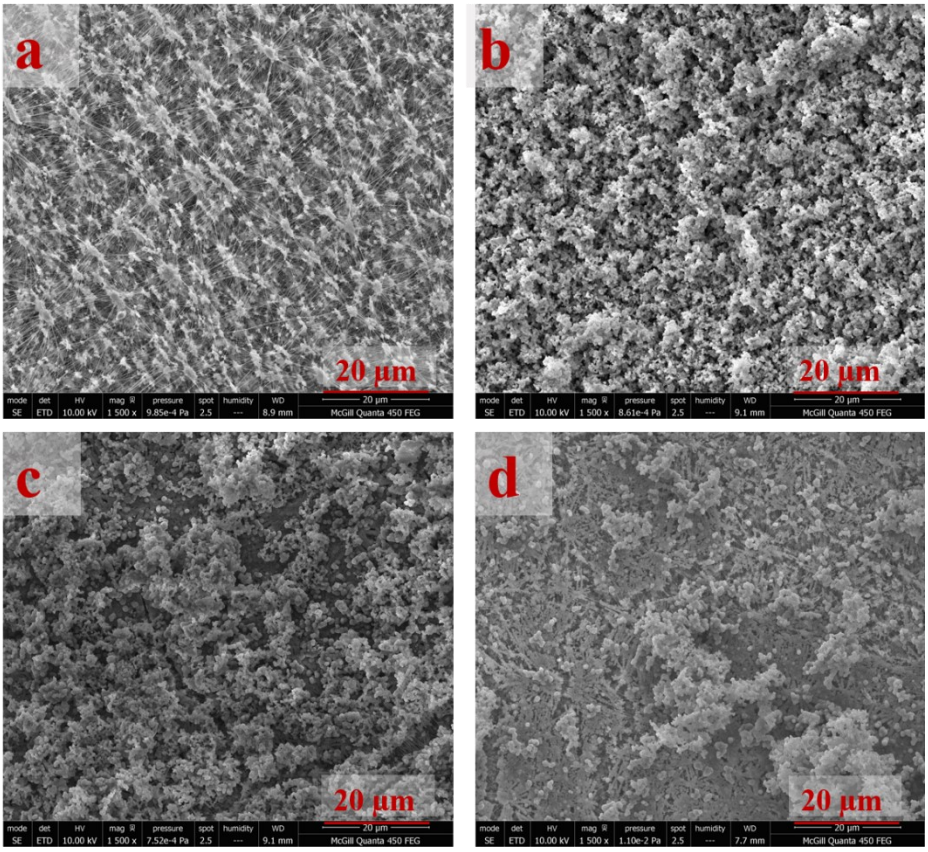

Figure A2.3: Surface morphology of DCMD PTFE 0.45 µm (a) pristine membrane and fouled membranes after 20 hours operation with a feed with COD = 77.9 ± 2.8 mg/L and a 0.7 LPM flowrate with the hot feed temperature (b) T_f = 65ºC, (c) T_f = 55ºC, and (d) (b) T_f = 45ºC and a permeate temperature T_p = 18ºC for MD. Extensive fouling was observed with the highest temperature of 65ºC.

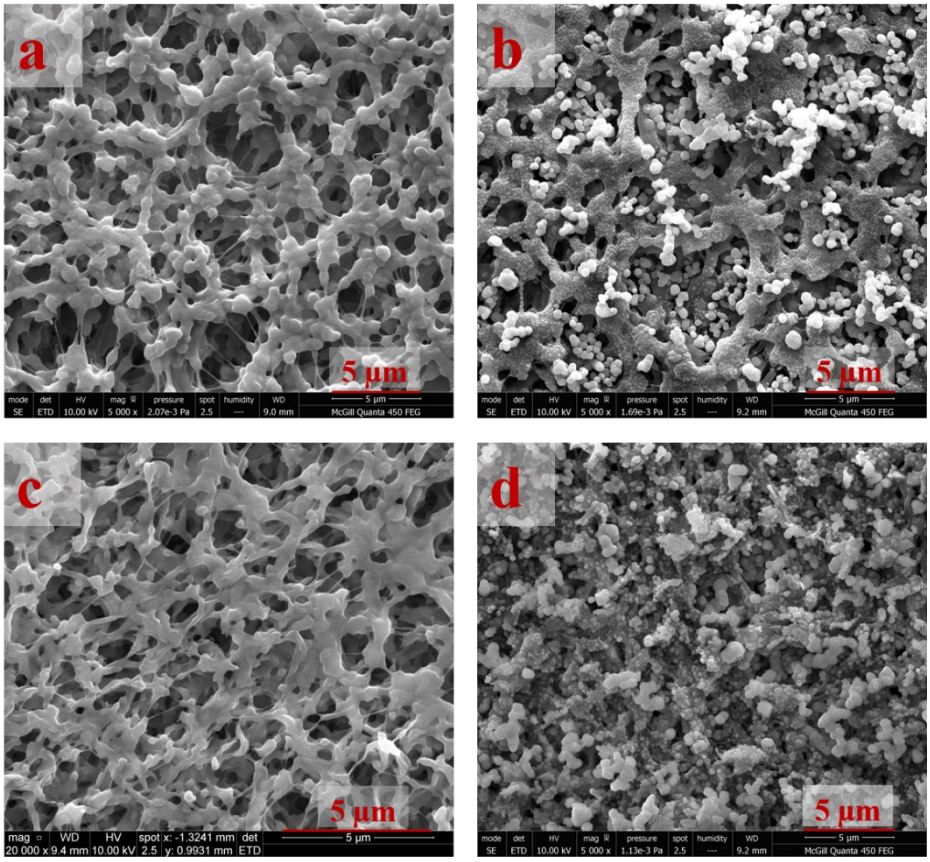

Figure A2.4: Surface morphology of DCMD PVDF 0.45 µm (a) pristine membrane and (b) fouled membranes of the hot feed temperature (b) T_f = 65ºC; and PVDF 0.22 µm (c) pristine membrane and (d) fouled membranes of the hot feed temperature (b) T_f = 65ºC. The DCMD process was operated for 20 hours with a MBR effluent as a feed with COD = 77.9 ± 2.8 mg/L, a 0.7 LPM flowrate, and constant permeate temperature of 18ºC. It is evident from the surface morphology that the membranes with a lower pore size was prone to higher fouling compared to that of the higher pore sizes.

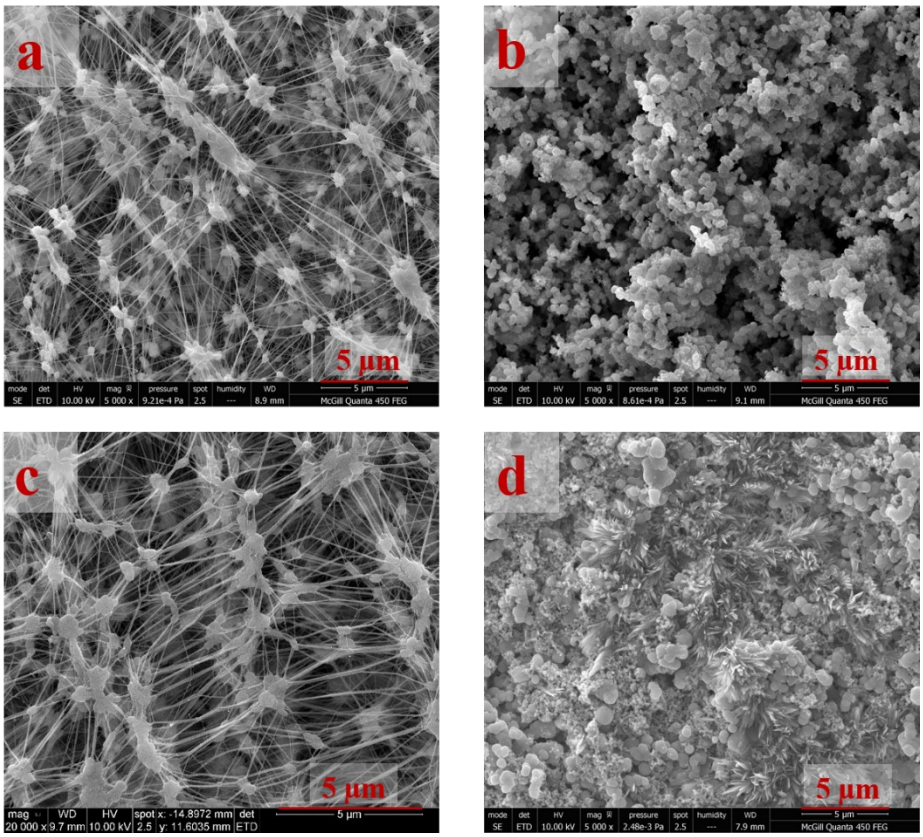

Figure A2.5: Surface morphology of DCMD PTFE 0.45 µm (a) pristine membrane and (b) fouled membranes of the hot feed temperature (b) T_f = 65ºC; and PTFE 0.2 µm (c) pristine membrane and (d) fouled membranes of the hot feed temperature (b) T_f = 65ºC. The DCMD process was operated for 20 hours with a MBR effluent as a feed with COD = 77.9 ± 2.8 mg/L, a 0.7 LPM flowrate, and constant permeate temperature of 18ºC. It is evident from the surface morphology that the membranes with a lower pore size was prone to higher fouling compared to that of the higher pore sizes.

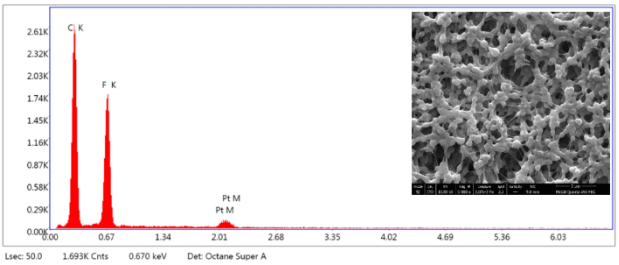

PVDF Pristine 0.45 µm

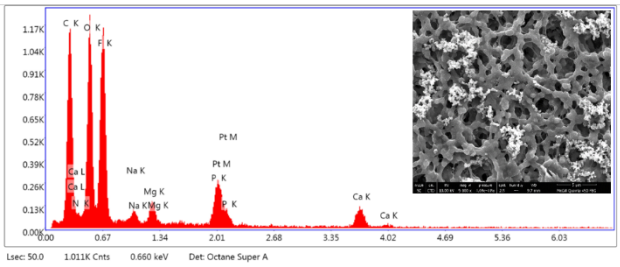

PVDF 10 g/L Fouled 0.45 µm

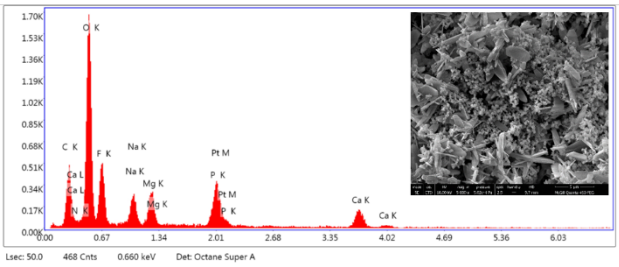

PVDF 15 g/L Fouled 0.45 µm

Figure A2.6: EDS analysis of DCMD PVDF 0.45 µm (a) pristine membrane and fouled membranes with a feed COD (b) 77.9 ± 2.8 mg/L, and (c) 108 ± 1.4 mg/L. The DCMD process was operated at a 0.7 LPM flowrate, hot feed temperature 55ºC, and permeate temperature of 18ºC.

Table A2.1: Pre-treated (UASB) high strength brewery wastewater effluent passed through 1.5 µm filtration was employed as feed at an elevated temperature (65°C) for DCMD application to create extensive membrane fouling to study the efficacy of membrane cleaning mechanism at harsh fouling condition. This effluent was concentrated for 20 hours as a feed water in direct contact membrane distillation with 18°C cold distillate temperature at 0.7 LPM flowrate. The characteristics of the feed are given below.

Parameters	Unit	Concentration
Chemical oxygen demand (COD)	mg/L	137.5 ± 10
Turbidity	NTU	0.98 ± 0.5
Electrical conductivity (EC)	mS/cm	14.95 ± 0.6

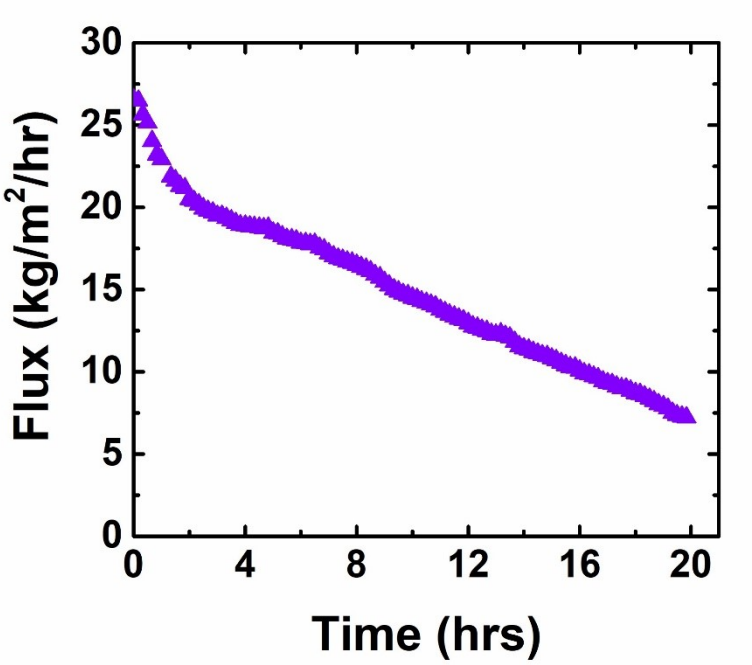

Figure A2.7: Permeate flux of 0.45 μm PVDF membrane with 65°C feed temperature and with COD = 137.5 ± 10 mg/L feed water at 0.7 LPM flowrate, and T_p = 18ºC concentrating over 20 hours during DCMD application.

Appendix A3

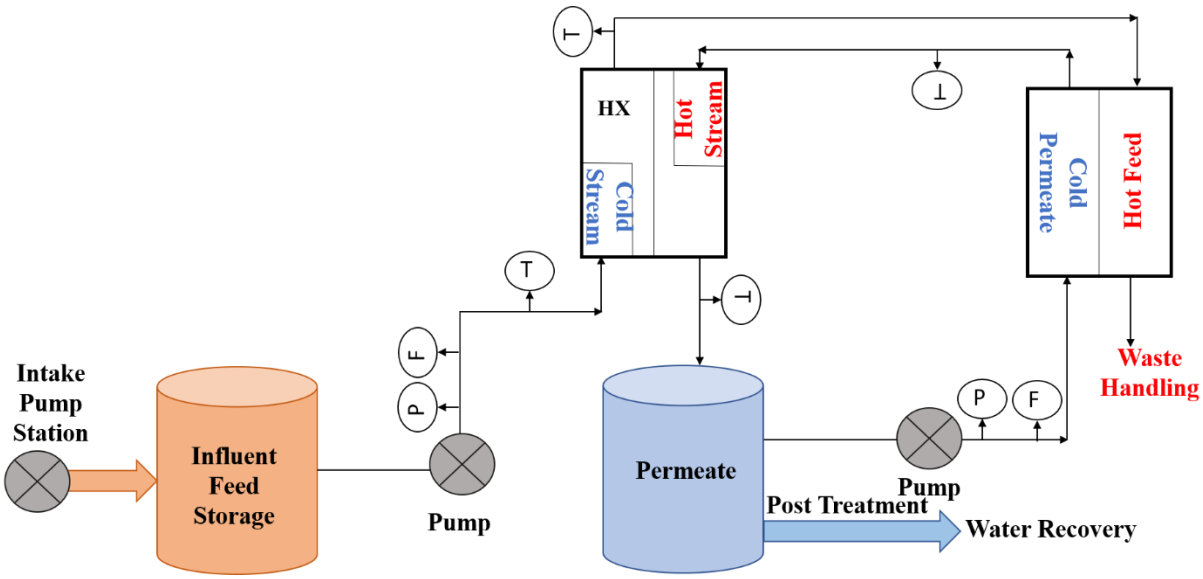

Figure A3.1: Diagram of Direct Contact Membrane Distillation (DCMD) system with heat recovery system (heat exchanger) to reclaim water from pre-treated brewery wastewater with a 100 m^3/day capacity. The permeate product goes through further polishing and the rejected concentrate contributes towards waste handling. The hot feed and the cold permeate temperatures are 55° C and 20° C, respectively. P, F, and T, stands for the pressure gauge, flowmeter, and temperature sensors in the schematic.

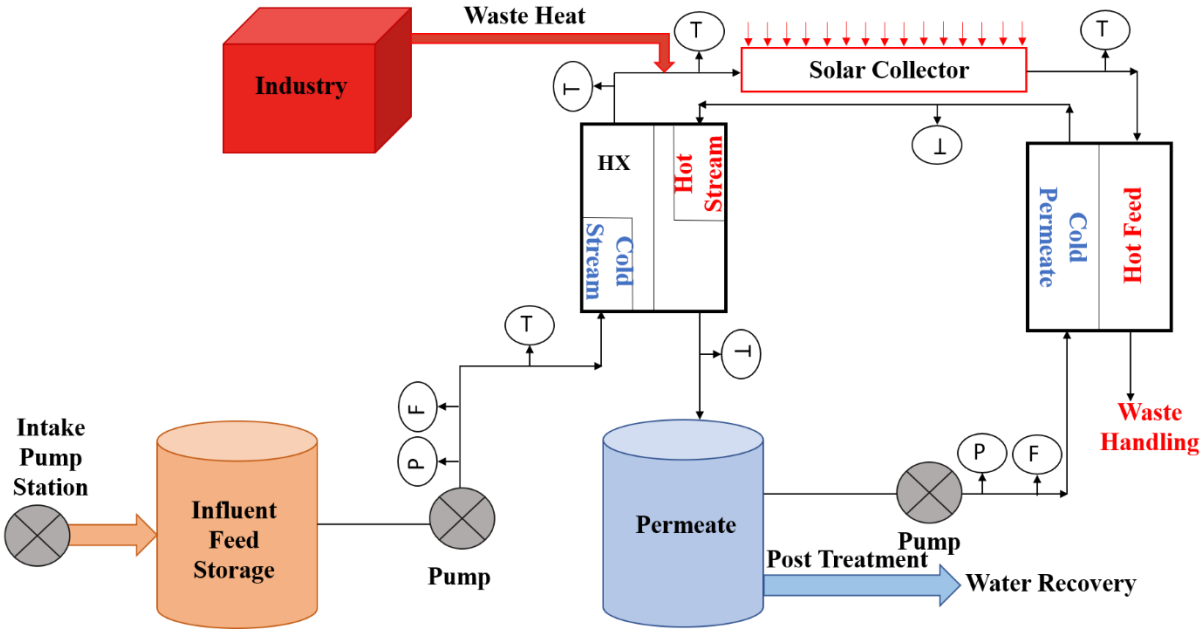

Figure A3.2: DCMD configuration with waste heat (WH) and solar power (SP) integration as a source of thermal energy required for the system to operate at 55°C hot feed temperature for a 100 m^3/day pre-treated brewery wastewater effluent as a feed.